

**Development and Application of an
In vitro Physicochemical Upper
Gastrointestinal System (IPUGS) Simulating
the Human Digestive Processes**

Ji Yeon Yoo

PhD

**Department of Chemical Engineering
Monash University**

September 2008

Declaration

In accordance with Monash University doctorate Regulation 17/ Doctor of Philosophy regulations the following declarations are made:

I hereby declare that this thesis contains no material which has been accepted for the award of any other degree or diploma at any university or equivalent institution and that to the best of my knowledge and belief, this thesis contains no material previously published or written by another person, except where due reference is made in the text of the thesis.

This thesis contains two papers published in peer reviewed journals, three papers published in peer reviewed conference proceedings and 7 unpublished publications. The core theme of the thesis is the development of an *in vitro* physicochemical upper gastrointestinal system and subsequent processes of validation and application of the system. The ideas, development and writing up of all the papers in the thesis were the principal responsibility of myself, the candidate, working within the Department of Chemical Engineering (Monash University) under the supervision of Professor Xiao Dong Chen.

The inclusion of a co-author, my supervisor Professor Xiao Dong Chen, reflects the fact that the works came from active supervision, collaboration and acknowledge inputs into research. In the case of Chapters 2 and 3, my contribution to the work involved the following:

Thesis Chapter	Publication Title (Refer to the List of Publications)	Publication Status	Nature and Extent of Candidate's Contribution
2 (sections 2.2 & 2.3)	GIT Physicochemical Modelling – Critical Review	Published	80%
	GIT Physicochemical Modelling – Critical Review	Published	80%
3 (section 3.2.3, 3.2.4 and 3.3.1)	A soft physicochemical stomach (SPS) model for simulating the human stomach	Published	80%
	<i>In vitro</i> physico-chemical modelling of the human upper gastrointestinal tract	Published	80%
	Physicochemical modelling of the human stomach	Published	80%

Signature of the Candidate: M. J. Yoo Date: 19/Sep/2008

Table of Contents

1. Abstract of the thesis.....	5
2. Acknowledgements.....	6
3. List of Figures.....	7
4. List of Tables.....	11
5. List of Publications.....	12
6. Introduction.....	13
7. Chapter 1. Literature Review on the Human Upper Gastrointestinal Tract.....	15
1.1. Mouth.....	16
1.2. Esophagus.....	18
1.3. Stomach.....	21
1.3.1. Gastric Emptying.....	23
1.3.2. Gastric Secretion.....	25
1.3.3. Gastric Motility.....	27
1.4. References.....	29
8. Chapter 2. Literature review on the <i>in vitro</i> digestion models of the human gastrointestinal tract.....	33
2.1 Introduction.....	33
2.2 Simulator of the Human Intestinal Microbial Ecosystem (SHIME).....	34
2.3. TNO's gastrointestinal model (TIM).....	36
2.4. Other <i>in vitro</i> digestion models in the literature.....	38
2.4.1. <i>In vitro</i> digestion models used in microecological studies.....	38
2.4.2. <i>In vitro</i> digestion models used in toxicological studies and risk assessments.....	39
2.4.3. <i>In vitro</i> digestion models used in the studies of pharmaceuticals.....	41
2.4.4. <i>In vitro</i> digestion models used in the studies of bioavailability of nutrients.....	43
2.4.5. <i>In vitro</i> digestion experimental models for the studies of animal GIT.....	44
2.4.6. <i>In vitro</i> experimental models of mouth.....	45
2.5. Improvements required by the existing <i>in vitro</i> digestion models.....	46
2.6. References.....	49
9. Chapter 3. Modeling of the <i>In vitro</i> Physicochemical Upper Gastrointestinal System (IPUGS) and the Modified <i>In vitro</i> Stomach Stir Tank (MISST).....	57
3.1. Introduction to simulation of the human gastrointestinal functions.....	58
3.1.1. Selection criteria of the test meal – Baby Foods vs Rice.....	60
3.1.2. Introduction to Dietary Carbohydrates and Starch Hydrolysis.....	64
3.2. Building Materials and Methods used in development of the IPUGS.....	65
3.2.1. Development of the Mouth Compartment in the IPUGS.....	66
3.2.2. Development of Esophagus and Stomach Compartments in the IPUGS.....	67
3.2.3. Building Materials and Methods used in MISST.....	74
3.2.4. Recording of pH and temperature.....	75
3.2.5. Observation of samples with a light microscope.....	76
3.3 Results and Discussions.....	76
3.3.1. Recording of the pH and temperature.....	76
3.3.2. Observation of samples with a light microscope.....	80
3.4. Concluding remarks and future works.....	83
3.5. References.....	85

10. Chapter 4 Validation of the Motility used in the <i>In vitro</i> Physicochemical Upper Gastrointestinal System (IPUGS).....	89
4.1. Introduction.....	89
4.2. Materials and Methods.....	93
4.2.1. The new <i>In vitro</i> Physicochemical Upper Gastrointestinal System (IPUGS).....	93
4.2.2 Modified <i>In vitro</i> Stomach Stir Tank (MISST).....	99
4.2.3. Phenol-Sulfuric Acid Assay.....	101
4.2.4. Somogyi-Nelson Method.....	101
4.2.5. High Performance Liquid Chromatography (HPLC).....	102
4.2.6. Recording of pH.....	103
4.3. Results and Discussions.....	103
4.3.1. Phenol-Sulfuric Acid Assay.....	103
4.3.2. Somogyi-Nelson Method.....	110
4.3.3. HPLC.....	117
4.3.4. Recording of the pH.....	119
4.4. Concluding Remarks and Future Works.....	124
4.5. References.....	125
11. Chapter 5. Clinical Application of the IPUGS to Study Motility Disorders.....	130
5.1. Introduction.....	130
5.2 Materials and Methods.....	133
5.2.1. The new <i>In vitro</i> Physicochemical Upper Gastrointestinal System (IPUGS).....	133
5.2.2. Phenol-Sulfuric Acid Assay.....	139
5.2.3. Somogyi-Nelson Method.....	140
5.2.4. High Performance Liquid Chromatography (HPLC).....	141
5.2.5. Recording of pH.....	141
5.3 Results and Discussion.....	142
5.3.1 Phenol-Sulfuric Acid Assay.....	142
5.3.2. Somogyi-Nelson Method.....	147
5.3.3. HPLC.....	153
5.3.4. Recording of the pH.....	155
5.4. Concluding Remarks and Future Works.....	159
5.5. References.....	160
12. Chapter 6. Validation of the Secretion used in the <i>In vitro</i> Physicochemical Upper Gastrointestinal System (IPUGS).....	163
6.1. Introduction.....	163
6.2 Materials and Methods.....	166
6.2.1. <i>In vitro</i> Physicochemical Upper Gastrointestinal System (IPUGS).....	166
6.2.2. Comprehensive compositions of the GI secretions used in the IPUGS.....	171
6.2.2.1. Saliva.....	171
6.2.2.2. Mucosal secretions for the compartments of esophagus and stomach of the IPUGS	175
6.2.2.3. Gastric Secretion.....	177
6.2.3. Phenol-Sulfuric Acid Assay.....	179
6.2.4. Somogyi-Nelson Method.....	180
6.2.5. High Performance Liquid Chromatography (HPLC).....	181
6.2.6. Recording of pH.....	181

6.3. Results and Discussions.....	182
6.3.1 Phenol-Sulfuric Acid Assay.....	182
6.3.2. Somogyi-Nelson Method.....	187
6.3.3. High Performance Liquid Chromatography (HPLC).....	194
6.3.4. Recording of pH profile.....	196
6.4. Conclusions.....	201
6.5. References.....	202
13. Chapter 7. Clinical Application of the IPUGS to Study Secretory Disorders.....	208
7.1. Introduction.....	208
7.2 Materials and Methods.....	210
7.2.1. <i>In vitro</i> Physicochemical Upper Gastrointestinal System (IPUGS).....	210
7.2.2. Compositions of the GI secretions used in the IPUGS.....	214
7.2.2.1. Saliva.....	214
7.2.2.2. Mucosal secretions for the compartments of esophagus and stomach of the IPUGS	215
7.2.2.3. Gastric Secretion.....	215
7.2.3. Phenol-Sulfuric Acid Assay.....	216
7.2.4. Somogyi-Nelson Method.....	217
7.2.5. High Performance Liquid Chromatography (HPLC).....	218
7.2.6. Recording of pH.....	218
7.3. Results and Discussions.....	219
7.3.1. Phenol-Sulfuric Acid Assay.....	219
7.3.2. Somogyi-Nelson Method.....	224
7.3.3. HPLC.....	228
7.3.4. Recording of the pH.....	231
7.4. Concluding Remarks and Future Works.....	233
7.5. References.....	234
14. Chapter 8. Mathematical Modeling of the <i>In vitro</i> Physicochemical Upper Gastrointestinal System (IPUGS).....	238
8.1. Introduction to mathematical and computational modeling of the human gastrointestinal tract (GIT).....	238
8.2. Mathematical modelling of the rice starch hydrolysis.....	240
8.2.1. Materials and Methods Used for the Control Experiments.....	241
8.2.2. Phenol-Sulfuric Acid Assay.....	243
8.2.3. Somogyi-Nelson Method.....	243
8.3. Results and Discussion.....	244
8.3.1. Phenol-Sulfuric Acid Assay.....	244
8.3.2. Somogyi-Nelson Method.....	246
8.4. Conclusions.....	256
8.5. References.....	256
15. Conclusions and Future Works.....	260

Abstract

Increased and combined knowledge of food processing, molecular biology, health and nutrition has triggered production of many different types of functional foods and pharmaceuticals recently. The efficacy and safety of such products are being assessed prior to marketing by *in vivo* and/or *in vitro* studies. Traditional *in vivo* studies require excessive time, cost and labour, as well as ethical approvals with subject to humans or animals in some instances. Therefore excessive number of runs may be avoided if reliable *in vitro* system is available. During the course of this study, an *in vitro* physicochemical upper gastrointestinal tract system (IPUGS), the first of its kind in literature, has been developed to simulate the relevant conditions of the gastrointestinal tract (GIT) as closely as possible to the human physiology with multi-disciplinary approach, combining biology, physiology, gastroenterology, process technology, chemical engineering and automation. The IPUGS is aimed at having a high predictive capability towards the real digestion processes occurring in the human upper GIT which allows for examining of the bioavailability of nutrients and drugs, drug-nutrient interactions, viability of probiotics and case studies of gastrointestinal disorders. Digestion of rice and baby foods have been studied with the IPUGS by UV-spectrophotometer, HPLC, light microscope and pH meter under the conditions of normal state and common gastric disorders, such as gastroparesis, dumping syndrome, Zollinger-Ellison syndrome and hypochlorhydria. By comparing the data from many physiological and clinical sources in the literature, it would seem that the IPUGS was able to generate more reliable data compared to the existing *in vitro* digestion (mechanical) models in the literature. In future, computer-controlled and computer-recorded data by possibly designing a new software or equations would be desirable to implicate a better understanding of the digestive processes.

Acknowledgements

I would like to express my gratitude to all those who gave me the possibility to complete this thesis. I am deeply grateful to my supervisor Professor Xiao Dong Chen from Monash University whose suggestion of this new subject, help, stimulating discussions and encouragements helped me in all the time of research for and writing of this thesis. I acknowledge Professor Chen once again for giving me a great opportunity to initiate research on emerging fields of knowledge and for providing me with inspirational, valuable and prompt feed-backs on my work to facilitate the level of research to one step further. Thank you for your kindness, support and guidance.

I would like to give my special thanks to my family whose patient love and supports enabled me to complete this work.

I want to thank MRGS of Monash University and Australian government for the Australian Postgraduate Award scholarship which enabled me to focus on research. I also would like to thank the Department of Chemical Engineering of Monash University for giving me the permission to commence my candidature and to use the departmental facilities. I would like to thank Mrs. J. Crisfield, Mrs. L. Price, Mr. G. Thunder, Mrs. T. Wall and Ms. W. Schoppe for great assistance in administrative works and friendship.

Especially I am obliged to the technicians in the Department of Chemical Engineering of Monash University, Mr. R. Graham, Mr. J. Barnard and Mr. R. Harrip for always kindly providing help in ordering and organizing laboratory equipments and chemicals.

I also would like to acknowledge Mrs. D. Li (Sales Manager of Danisco Ltd., China) and Dr. S. Kar for offering valuable materials for my experiments. I would like to thank Mr. Joshi (APPI) for training and helping me with Instron, Dr. Y. Jin and Lawrence Quek with providing help for drawing 3D graph. I have furthermore to thank my colleagues in our Biotechnology and Food Engineering (BFE) group, Saptarshi Kar, Sean Lin, Carrie Chen, Lawrence Quek, Eric Wong, Winston Duo, Heng Jin Tham, Kamlesh Patel, Sam Rogers, Yuan Fang, Dylan Zhu and Nada Hamid for friendship and sharing of laboratory space and equipments. I would like to thank my colleagues in our department, Tri Pham, Wei Lit Choo and Margarita Vagas for great friendship and valuable advice. Special thanks to the former PhD students of Professor Chen, Jinah Yoo and Esther Kim for great advices, support, interest and friendship.

List of Figures

Figure 1-1. A figure illustrating the human gastrointestinal tract (GIT)

Figure 1-2. A detailed anatomical diagram of the human mouth

Figure 1-3. A diagram showing the human esophagus

Figure 1-4. An anatomical diagram of a human adult stomach

Figure 1-5. Summary of the gastric secretions in the stomach

Figure 3-1. Stomach mold made with the platinum cure silicon rubber (A) and Equinox™ (B)

Figure 3-2. Tygon® Microbore secretion tubing implanted into the stomach wall

Figure 3-3. A schematic diagram of the tubing linkage set

Figure 3-4. A Diagram of the motility of the esophageal compartment of the IPUGS.

Figure 3-5. A diagram of the first peristaltic wave applied to the IPUGS

Figure 3-6. A diagram of the second peristaltic wave applied to the IPUGS

Figure 3-7. A schematic diagram of the IPUGS

Figure 3-8. A schematic diagram of the MISST

Figure 3-9. The pH profile of the MISST and the IPUGS with baby foods and rice

Figure 3-10. pH profile of the MISST with different stirring speeds of 150rpm and 500rpm.

Figure 3-11. Temperature profile of the MISST and the IPUGS

Figure 3-12. Images of the samples taken from the MISST and the IPUGS at time 0

Figure 3-13. Images of the samples taken from the MISST and the IPUGS at time 30min

Figure 3-14. Images of the samples taken from the MISST and the IPUGS at time 60min

Figure 3-15. Images of the samples taken from the MISST and the IPUGS at time 90min

Figure 3-16. Images of the samples taken from the MISST and the IPUGS at time 180min

Figure 4-1. A diagram showing the apparatus used by other *in vitro* digestion models

Figure 4-2. Tygon® Microbore secretion tubings inserted into the stomach wall for secretion

Figure 4-3. Diagram showing the motility of the esophageal compartment of the IPUGS

Figure 4-4. A diagram of the first peristaltic wave applied to the stomach compartment

Figure 4-5. A diagram of the second peristaltic wave applied to the stomach compartment

Figure 4-6. A schematic diagram of the IPUGS

Figure 4-7. A schematic diagram of the MISST

Figure 4-8. A graph of the concentration of total water soluble carbohydrates (g.L^{-1}) in MISST, IPUGS-1 and 2

Figure 4-9. A graph of the mass of total water soluble carbohydrates (g) during in MISST, IPUGS-1 and 2

Figure 4-10. A graph of the concentration of maltose (g.L^{-1}) in MISST, IPUGS-1 and 2

Figure 4-11. A graph of the mass of maltose (g) in MISST, IPUGS-1 and 2

Figure 4-12. A graph of the derivative of maltose mass over time in MISST, IPUGS-1 and 2

Figure 4-13. A graph of the mass of unconverted starch (g) in MISST, IPUGS-1 and 2

Figure 4-14. A graph of the ratio of the mass of the maltose to the mass of the unconverted starch in MISST, IPUGS-1 and 2

Figure 4-15. A graph showing the mass of maltose over time which was measured by the HPLC in MISST, IPUGS-1 and 2

Figure 4-16. A graph showing the mass of maltotriose over time which was measured by the HPLC in MISST, IPUGS-1 and 2

Figure 4-17. The pH profile of the pH probe 1 (fundus) of MISST, IPUGS-1 and 2

Figure 4-18. A diagram of the arrangement of tubings and probes used in the MISST

Figure 4-19. The pH profile of the pH probe 2 (antrum) of MISST, IPUGS-1 and 2

Figure 5-1. Diagram of the secretion tubings inserted into the stomach wall of the IPUGS

Figure 5-2. Diagram of the motility of the esophageal compartment of the IPUGS

Figure 5-3. A diagram of the first peristaltic wave applied to the stomach of the IPUGS

Figure 5-4. A diagram of the second peristaltic wave applied to the stomach of the IPUGS

Figure 5-5. A schematic diagram of the IPUGS

Figure 5-6. A graph of the concentration of total water soluble carbohydrates (g.L^{-1}) for dumping syndrome, normal state and gastroparesis conditions

Figure 5-7. A graph of the mass of total water soluble carbohydrates (g) for dumping syndrome, normal state and gastroparesis conditions

Figure 5-8. A graph of the concentration of maltose (g.L^{-1}) for dumping syndrome, normal state and gastroparesis conditions

Figure 5-9. A graph of the mass of maltose (g) for dumping syndrome, normal state and gastroparesis conditions

Figure 5-10. A graph of the mass of the unconverted starch (g) for dumping syndrome, normal state and gastroparesis conditions

Figure 5-11. A graph of the ratio of the mass of the maltose (g) to the mass of the unconverted starch (g) for dumping syndrome, normal state and gastroparesis conditions

Figure 5-12. A graph of the natural log (ln) of the ratio of the mass of the maltose (g) to the mass of the unconverted starch (g) for dumping syndrome, normal state and gastroparesis conditions

Figure 5-13. A graph of the mass of maltose (g) measured by HPLC for dumping syndrome, normal state and gastroparesis conditions

Figure 5-14. A graph showing the mass of maltotriose (g) measured by HPLC for dumping syndrome, normal state and gastroparesis conditions

Figure 5-15. pH profile of the pH probe 1 (fundus) for dumping syndrome, normal state and gastroparesis conditions

Figure 5-16. The pH profile of the pH probe 2 (antrum) for dumping syndrome, normal state and gastroparesis conditions

Figure 6-1. A diagram of secretion tubings in the stomach wall of the IPUGS

Figure 6-2. A diagram showing the motility of the esophageal compartment of the IPUGS. Figure

6-3. A diagram of the first peristaltic wave applied to the stomach of the IPUGS. Figure 6-4. A diagram of the second peristaltic wave applied to the stomach of the IPUGS.

Figure 6-5. A graph of the concentration of total carbohydrates ($\text{g}\cdot\text{L}^{-1}$) of the IPUGS with simplified and complex GI secretions and the MISST with simplified GI secretions

Figure 6-6. A graph of the concentration of total carbohydrates ($\text{g}\cdot\text{L}^{-1}$) of the IPUGS with simplified and complex GI secretions and the MISST with simplified GI secretions

Figure 6-7. A graph of the concentration of maltose ($\text{g}\cdot\text{L}^{-1}$) of the IPUGS with simplified and complex GI secretions and the MISST with simplified GI secretions

Figure 6-8. A graph of the mass of maltose (g) of the IPUGS with simplified and complex GI secretions and the MISST with simplified GI secretions

Figure 6-9. A graph of the mass of unconverted starch (g) of the IPUGS with simplified and complex GI secretions and the MISST with simplified GI secretions

Figure 6-10. A graph of the ratio of the mass of maltose to the mass of the unconverted starch of the IPUGS with simplified and complex GI secretions and the MISST with simplified GI secretions

Figure 6-11. A graph of the mass of maltose measured by HPLC for the IPUGS with simplified and complex GI secretions and the MISST with simplified GI secretions

Figure 6-12. A graph of the mass of maltotriose measured by HPLC for the IPUGS with simplified and complex GI secretions and the MISST with simplified GI secretions

Figure 6-13. pH profile of the pH probe 1 (fundus) for the IPUGS with simplified and complex GI secretions and the MISST with simplified GI secretions

Figure 6-14. pH profile of the pH probe 2 (antrum) for the IPUGS with simplified and complex GI secretions and the MISST with simplified GI secretions

Figure 7-1. A graph of the concentration of total carbohydrates ($\text{g}\cdot\text{L}^{-1}$) for the conditions of Zollinger-Ellison Syndrome, normal state and Hypochlorhydria

Figure 7-2. A graph of the mass of total carbohydrates (g) for the conditions of Zollinger-Ellison Syndrome, normal state and Hypochlorhydria

Figure 7-3. A graph of the concentration of maltose (g) for the conditions of Zollinger-Ellison Syndrome, normal state and Hypochlorhydria

Figure 7-4. A graph of the mass of maltose (g) for the conditions of Zollinger-Ellison Syndrome, normal state and Hypochlorhydria

Figure 7-5. A graph of the mass of unconverted starch (g) for the conditions of Zollinger-Ellison Syndrome, normal state and Hypochlorhydria

Figure 7-6. A graph of the ratio of the mass of the maltose to the mass of the unconverted starch with respect to time for the conditions of Zollinger-Ellison Syndrome, normal state and Hypochlorhydria

Figure 7-7. A graph of the mass of maltose (g) in the stomach compartment measured by the HPLC for the conditions of Zollinger-Ellison Syndrome, normal state and Hypochlorhydria

Figure 7-8. A graph of the mass of maltotriose (g) in the stomach compartment measured by the HPLC for the conditions of Zollinger-Ellison Syndrome, normal state and Hypochlorhydria

Figure 7-9. pH profile of the pH probe 1 (fundus) of the conditions of Zollinger-Ellison Syndrome, normal state and Hypochlorhydria

Figure 7-10. The pH profile of the pH probe 2 (antrum) of the conditions of Zollinger-Ellison Syndrome, normal state and Hypochlorhydria

Figure 8-1. A diagram of the apparatus set up for the control experiments

Figure 8-2. A graph of the mass of total carbohydrates (g) of 5 different digestion conditions

Figure 8-3. A graph of the mass of maltose (g) of 5 different digestion conditions

Figure 8-4. A plot of the ratio of the mass of maltose (g) to the mass of total carbohydrates (g) with respect to time (min) for 5 different digestion conditions

Figure 8-5. A graph illustrating the ratio of the mass of maltose (g) to the mass of undigested starch (g) with respect to time (min) under 5 different digestion conditions

Figure 8-6. A plot of the fractional mass of the undigested rice starch (g) over time

Figure 8-7. A plot of the concentrations of HCl (N) and amylase (g.L^{-1}) raised to the powers of 0.13 and 0.04, respectively, against the rate constant of maltose (k_{maltose}), respectively

Figure 8-8. A plot of the rate constant of HCl against the concentration of HCl (N)

Figure 8-9. A plot of the rate constant of HCl against the concentration of amylase (g.L^{-1})

Figure 8-10. A 3-D plot of the k_{maltose} with respect to the concentrations of amylase and HCl, generated by Tecplot.

List of Tables

Table 3-1. Selective criteria to be considered when making a physicochemical model.

Table 3-2. A summary of the composition the HEINZ Little Kids baby foods used.

Table 3-3. A table of the nutritional information of the HEINZ Little Kids

Table 3-4. Nutritional information of the Sun Rice® Japanese style Sushi Rice

Table 3-5. A table of results showing an average value of 10 runs of the volume of the collected distilled water (ml) from the tip of the Tygon Microbore tubings through the tubing linkage set for 10min.

Table 3-6. Key points of improvements required for *in vitro* digestion systems

Table 6-1. Composition of the Shellis synthetic saliva (Shellis, 1978).

Table 6-2. Composition of mixture of amino acids (Shellis, 1978).

Table 6-3. Composition of mixture of vitamins (Shellis, 1978).

Table 6-4. The composition of the gastric secretion used

Table 8-1. A table summarizing the rate of change in maltose mass with respect to the digestive conditions

List of Publications

Michelle Ji Yeon Yoo and Dong Chen (2008) A soft physicochemical stomach (SPS) model for simulating the human stomach. *Annual Australasian Conference of Chemical Engineering (Chemeca 2008), Biotechnology and Nanotechnology*, 127

Michelle Ji Yeon Yoo and Dong Chen (2007) *In vitro* physico-chemical modelling of the human upper gastrointestinal tract (GIT). *Journal of Clinical Biochemistry and Nutrition*, Supplement, Vol. 41, DFP2-6, pg. 64. [Conference Abstract].

Michelle Ji Yeon Yoo and Dong Chen (2007) Physicochemical modelling of the human stomach. *Annual Australasian Conference of Chemical Engineering (Chemeca 2007), Biotechnology and Nanotechnology*, 329, 223-230

Ji Yeon Yoo and Xiao Dong Chen (2006) GIT physico-chemical modeling – A critical review. *International Journal of Food Engineering*, 2 (4), article 4

Xiao Dong Chen and Ji Yeon Yoo (2006) Food engineering as an advancing branch of chemical engineering. *International Journal of Food Engineering*, 2 (2), article 1.

Ji Yeon Yoo and Xiao Dong Chen (2006) GIT physiochemical modeling – critical review. *Annual Australasian Conference of Chemical Engineering (Chemeca 2006), Food and Beverage*, 210

Introduction

Increased and combined knowledge of food processing, molecular biology, health and nutrition has triggered production of many different types of functional foods and pharmaceuticals recently. The establishment of efficacy and safety of such products should be assessed prior to marketing. Traditional *in vivo* studies require excessive time, cost and labour, as well as ethical approvals in some instances. Therefore excessive number of runs may be avoided if reliable *in vitro* system is available. In this thesis, the development and applications of an *in vitro* physicochemical upper gastrointestinal tract system (IPUGS) is described. The current model developed can be explored to replace the more simplified systems in the literature and can operate under controlled conditions. The *in vitro* digestion models of the human gastrointestinal tract (GIT) to date do not successfully simulate the dynamic conditions in the lumen of the GIT, therefore carrying the risk of oversimplification. The IPUGS was used to simulate the relevant conditions of the GIT as closely as possible to the human physiology, for example; examining the bioavailability of nutrients and drugs, drug-nutrient interactions, viability of probiotics and case studies of gastrointestinal disorders. The IPUGS introduced in this thesis is aimed at having a high predictive capability towards the real digestion processes occurring in the human upper GIT. The comprehensive development of such a model involves a multi-disciplinary approach, combining biology, physiology, gastroenterology, process technology, chemical engineering and automation.

The thesis is divided into eight chapters. The first chapter illustrates a detailed overview of the human upper GIT. The second chapter proposes a review on the existing *in vitro* digestion models found in the literature. The third chapter specifies the development of the IPUGS with justifications of the materials and methods used. Another model called modified *in vitro* stomach stir tank (MISST), which was modified from the existing *in vitro* digestion models, is also described, along with preliminary results of using baby foods as a test material. The fourth chapter compares the motility associated with MISST and IPUGS. Mastication and gastric motility of each model are compared, with a detailed discussion on the motility used in other existing *in vitro* digestion models. The fifth chapter shows a case study of the upper GI motility disorders where the results obtained from the IPUGS are compared with *in vivo* physiological data found in the literatures. The sixth chapter describes the composition of the GI secretions as well as the sequential methods of delivering these secretions into the IPUGS. A detailed review on the enzyme

replacements (non-human sources) used as the GI secretions is provided and compared with the outcomes of the other existing *in vitro* digestion models in the literature. The seventh chapter presents a case study of the upper GI secretion disorders where the results obtained from the IPUGS are compared with that of the *in vivo* data in the literature. The last chapter shows a simple mathematical and/or computational modeling of the IPUGS using the data obtained from the IPUGS. Stoichiometry of a rice grain breakdown as well as the rate of rice digestion is established for the analysis.

Chapter 1

Literature Review on the Human Upper Gastrointestinal Tract

The human gastrointestinal tract (GIT) system is composed of mouth, esophagus, stomach, small intestine and large intestine where anatomically it can be divided into the upper (mouth to the stomach) and the lower (small and large intestines) parts (Figure 1-1). The main functions of the GIT are to breakdown foods, to absorb and to transport nutrients into the blood streams in order to maintain body functions. In this section the organs of the human upper GIT, i.e. mouth, esophagus and stomach, are discussed.

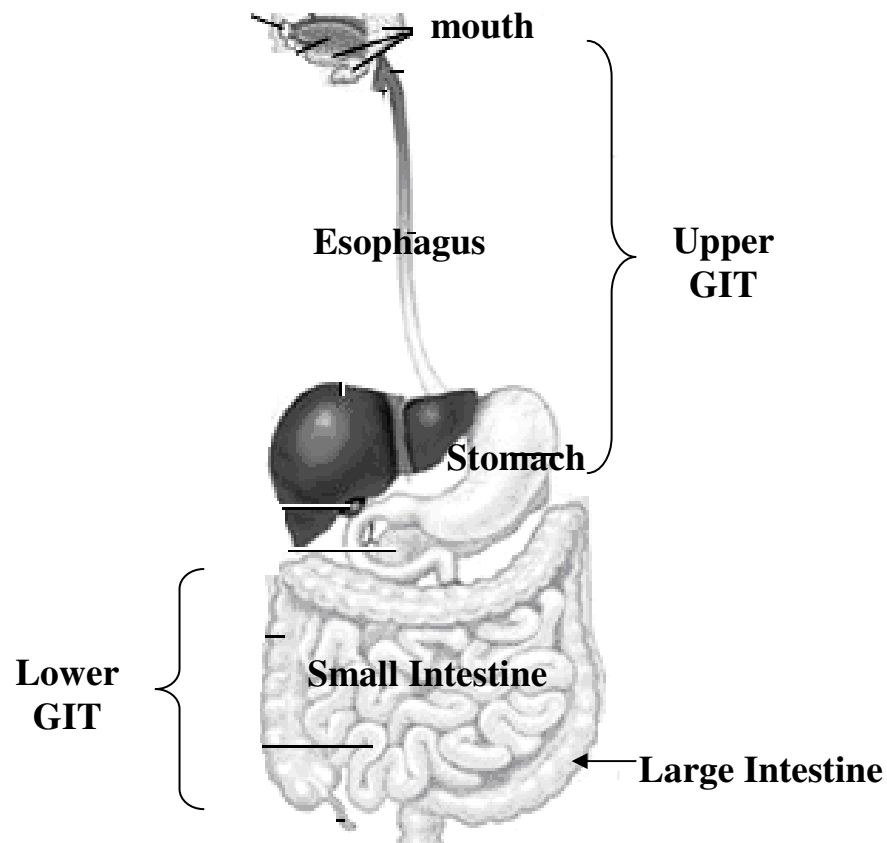


Figure 1-1. A figure illustrating the human gastrointestinal tract (GIT). Upper GIT include mouth, esophagus and stomach, and lower GIT refers to small and large intestines with accessory organs of liver, pancreas and gallbladder. [Figure was modified from 2003 Encyclopaedia Britannica, Inc. <http://www.britannica.com/eb/art-1087/The-human-digestive-system-as-seen-from-the-front>].

The overall digestion processes in the upper GIT can be divided into five basic functions;

Ingestion – taking foods and liquids into the mouth for mastication and swallowing

Secretion – saliva, gastric juice and mucus secreted to assist digestion

Motility – alternating contraction and relaxing of smooth muscle linings in the walls of the esophagus and the stomach for peristaltic propulsion and mixing

Digestion – mechanical (grinding, swallowing and churning) and chemical processes (digestive enzymes) breakdown ingested food into small molecules (chyme).

Absorption – absorption of small molecules and ions via active transport or passive diffusion into blood or lymph in the stomach

1.1. Mouth

Mouth (Figure 1-2) can be classified as an accessory organ to the upper GIT system. It is also known as oral or buccal cavity with average length of 15-20cm and average diameter of 10cm in adults (Kararli, 1995). The mouth is the site of food ingestion where mechanical and limited chemical digestion by saliva occurs.

Mechanical digestion results from mastication (chewing). The ingested food is manipulated by the tongue, ground by the teeth and mixed with saliva to form soft, flexible, paste-like bolus which can be easily swallowed. Swallowing is estimated to have shear rate as high as 60s^{-1} (Briedis *et al*, 1980), and it is a sequentially programmed process with three phases - buccal phase, pharyngeal phase and esophageal phase.

Buccal phase occurs in the mouth under voluntary control. It begins with the tongue compressing the food bolus against the hard palate. The tongue retracts, the soft palate lifts and the bolus is forced into the pharynx. In pharyngeal phase, food enters the pharynx and activates tactile receptors to initiate involuntary reflex activities controlled by swallowing centres in medulla and lower pons. Motor impulses sent to muscles of pharynx via vagus nerves, the epiglottis folds over the larynx, and the larynx is elevated, enabling the pharyngeal muscles squeeze the bolus into the esophagus. Esophageal phase is an involuntary reflex phase where food is squeezed from pharynx into esophagus by peristalsis. The upper esophageal sphincter opens to let the bolus through and peristaltic wave pushes the bolus to the stomach (Mosher, 1927).

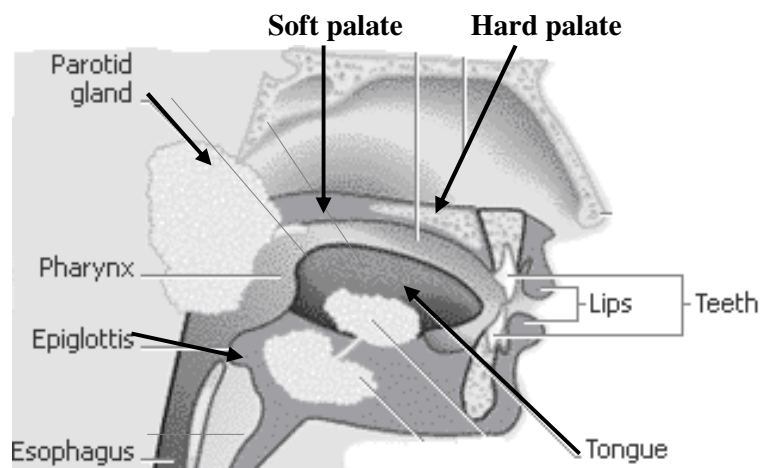


Figure 1-2. A detailed anatomical diagram of the human mouth [modified from <http://images.encarta.msn.com/xrefmedia/aencmed/targets/illus/ilt/0007760a.gif>].

Olfactory, visual, auditory, touch, taste and thought of food are potent stimulators of saliva secretions. Chemicals in the food stimulate receptors in taste buds of the tongue and impulses are conveyed from the taste buds to the brain stem for the saliva to be secreted from three pairs of extrinsic glands which are located outside oral cavity and small buccal glands inside oral cavity mucosa (Sarosiek and McCallum, 2000).

Saliva is produced approximately 1-1.5L daily (Humphrey and Williamson, 2001). It is mainly composed of water (99.5wt%) which acts as a medium for dissolving food, enables the ingested food to be tasted and to initiate digestion process. 0.5wt% of saliva is composed of solutes including ions (such as sodium, potassium, chloride, bicarbonate and phosphates), dissolved gases, various organic substances (such as urea, uric acid, mucus, immunoglobulin A, lysozyme (E.C 3.2.1.17)) and digestive enzymes – salivary amylase (E.C 3.2.1.1) and lingual lipase (E.C 3.1.1.3) (Tortora and Grabowski, 2000). Chloride ions activate the salivary amylase, where bicarbonate and phosphate ions act to buffer the acidity of certain food materials (Helm *et al*, 1982). Urea and uric acid helps to remove waste molecules from the body and mucus is used to lubricate the food for easier movement within the mouth. Immunoglobulin A is an antibody which inhibits pathogenic bacterial growth, and lysozyme act to kill bacteria. Salivary amylase digests long chain polysaccharides (e.g. starch) to disaccharide (e.g. maltose), trisaccharide (e.g. maltotriose) or short chain glucose polymers (α -dextrins). As long as a suitable buffering capacity is supplied, salivary amylase is able to continuously digest carbohydrates. However it is inactivated by acidic pH in the stomach. Lingual lipase digests triglycerides to fatty acids

and monoglycerides. It is able to work in the acidic pH, and therefore is still active even after the food has been swallowed (Tortora and Grabowski, 2000).

On average, 16 hrs of non-stimulated flow of saliva with the flow rate of $0.3\text{ml}\cdot\text{min}^{-1}$ constitute 300ml in total volume of the saliva secretion. Stimulated flow rate ranges from 5.3 to $7.8\text{ml}\cdot\text{min}^{-1}$, contributing 80-90wt% of the average daily salivary secretion (Edgar 1990; Humphrey and Williamson, 2001). Jensdottir *et al* (2005) showed that the concentrations of sodium, chloride and bicarbonate ions increased with increasing saliva flow rate and the concentrations of potassium and phosphate decreased with flow rate. Saliva continues to be heavily secreted for some time after food is swallowed to wash out the mouth and dilute and/or buffer the remnants of irritating chemicals from the foods. Typically, the pH of the saliva falls in the range of 6.35-6.85. The pH rises during the first 5min after the ingestion of foods, reestablishing its lowest pH of 6.1 by 15min after food consumption (Humphrey and Williamson, 2001).

1.2. Esophagus

Esophagus is a hollow tube which links the throat (pharynx) and the stomach to facilitate food transport into the stomach and to prevent the escape of gastric contents into the pharynx. Its length ranges from 18 to 26 cm (Meyer *et al*, 1986; Staiano *et al*, 1991) with average diameter of 2.5cm (Kararli, 1995) and has a wall thickness of 0.3cm with 0.008cm thick mucosa membrane in normal adults (Al-Zaben and Chandrasekar, 2005). Anatomically, the esophagus can be divided into three parts (Figure 1-3) - the upper third of the esophagus, esophageal body and the lower third of the esophagus. The upper third of the esophagus (up to approximately 4cm from the upper esophageal sphincter) is composed entirely of striated muscle. The esophageal body is composed of an outer longitudinal (smooth) muscle layer and an inner circular (striated) muscle layer (Clouse *et al*, 1991). The lower third of the esophagus is entirely made of smooth muscle (Meyer *et al*, 1986) where the peak pressure does not normally exceed 200mmHg (Johnson, 2006). The mean of normal esophageal potential difference pressure was found to be -14 ± 5 mV in the lower 1-6cm of esophagus and -12 ± 6 mV in the upper 14cm of the esophagus (Orlando *et al*, 1982).

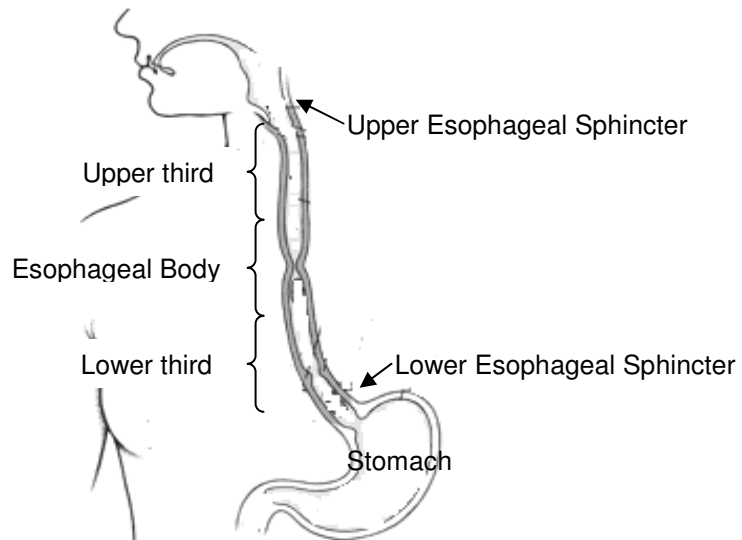


Figure 1-3. A diagram showing the human esophagus. The esophagus is divided into three parts; upper third, esophageal body (middle) and lower third, with two sphincters at each end, called upper and lower esophageal sphincters. [Modified from http://www.merck.com/media/mmhe2/figures/MMHE_09_120_01_eps.gif]

The esophagus has two sphincters on each end, upper esophageal sphincter near the pharynx and lower esophageal sphincter near the stomach, for controlling entry and exit of bolus into and out of the esophagus. The lower esophageal sphincter is a thickened segment of 2.5 to 3.5cm in length and 1.92 to 2.54mm in thickness (Pehlivanov *et al*, 2002) which is part of the circular muscle layer in the lower third of the esophagus (Christensen and Roberts, 1983) and angles upward from the lesser to the greater gastric curvatures (Libermann *et al*, 1981) with a high resting pressure where the pressure decreases with swallowing (Drewes *et al*, 2005). Mean basal pressure of the lower esophageal sphincter in normal subjects has been reported as 25 ± 4 cmH₂O (Corazziari *et al*, 1982) and the contraction amplitudes during induced swallowing ranged from 16.9 to 267mmHg (mean 120 ± 50 mmHg) (Pehlivanov *et al*, 2002; Wu *et al*, 2007). The gastroesophageal pressure gradient for normal human has been reported as 4.5 ± 1.2 mmHg by Wu *et al* (2007).

The mucosa of the esophagus consists of epithelium, lamina propria and muscularis mucosa (smooth muscle). Near the stomach, the mucosa of the esophagus contains mucous glands. The stratified squamous epithelium in the esophagus protects against abrasion and wear-and-tear from swallowing the bolus. The submucosa contains areolar connective tissues, blood vessels and mucous glands. The muscularis of the upper third of

the esophagus is skeletal muscle, the intermediate third is skeletal and smooth muscle, and the lower third is smooth muscle (Tortora and Grabowski, 2000). Submucosal mucous glands are present in the submucosa of all regions but only the upper and the lower thirds have mucosal glands in the lamina propria (Junqueira *et al*, 1998).

The upper esophageal sphincter and the lower esophageal sphincter are tonically closed at rest. These are composed of ring of muscle which regulate the entrance and the exit of the bolus into and out of the esophagus. At the pharyngeal phase of swallowing, the elevation of the larynx causes the upper esophageal sphincter to relax allowing the bolus to enter the esophagus. However during the esophageal phase of swallowing, a progression of coordinated contractions and relaxations of the circular and longitudinal muscle layers in the esophageal body push the bolus towards the stomach by squeezing the wall of the esophagus. The series of simultaneous contractions and relaxations of the esophagus is called peristalsis. The peristaltic sequence traversing the esophageal body is a three distinct contraction segments when separated by pressure difference (Clouse and Staiano, 1993).

When the coordinated esophageal movement is initiated by swallowing, it is called primary peristalsis. Progressive contraction in the esophageal body induced by distention from poorly cleared food or refluxed gastric contents is called secondary peristalsis which begins at or above the location of the inter-luminal stimulus and closely resembles primary peristalsis (Marieb, 1998). During the inter-swallow period, both of the upper and the lower sphincters remain closed to prevent movement of esophageal and/or gastric contents upward (toward the mouth). The pressure of the lower esophageal sphincter decreases within 1.5 to 2.5s of the swallow, and remains decreased until the peristalsis reaches the low esophageal sphincter and increases with an after contraction that is separated from the peristaltic complex. Both central and intramural neural mechanisms in the smooth muscle of the esophageal body are able to influence the motor function of the lower esophageal sphincter (Wu *et al*, 2007). Average duration of contraction in the distal esophagus is less than 6s, and propagation velocity varies through the esophageal body in bimodal fashion. Propagation velocity along the smooth muscle region averages less than $5\text{cm}\cdot\text{s}^{-1}$ and velocity greater than $6.25\text{cm}\cdot\text{s}^{-1}$ is associated with disrupted bolus transit (Pehlivanov *et al*, 2002). In order to assist the peristalsis of the esophagus, mucus is secreted by the esophageal glands to lubricate the bolus and reduce friction. Apart from mucosal secretions, there are neither digestive secretions nor absorption take place in the esophagus (Tortora and Grabowski, 2000).

1.3. Stomach

Stomach is a J-shaped organ (Figure 1-4) with average length of 20cm and average diameter of 15cm in adults (Kararli, 1995) where partially digested bolus from the mouth is passed down through the esophagus via peristalsis for further chemical breakdown by the gastric juice containing pepsin, lipase and hydrochloric acid, as well as mechanical breakdown by gastric motility. It acts as a barrier to ingested pathogenic microorganisms and also operates as a reservoir for temporary storing of the digested food in the form of yellow greenish chyme which can easily be absorbed through the linings of the small intestine. The size and shape varies with the volume of food/fluid it contains, position of body and phase of respiration. The stomach can be anatomically divided into 4 parts (Figure 1-4). Cardia refers to the uppermost region which is connected to the esophagus. Cardiac sphincter (1.5-3cm in width) controls the feed to the stomach (Junqueira *et al*, 1998). Fundus is a storage area where highly elastic smooth muscles line the stomach wall. Together with anatomical modifications (rugae), this enables large amount of bolus to be stored straight after a meal. Body is the largest region located in the centre of the stomach where most of the chemical digestion occurs and the majority of gastric secretions are produced. Pylorus refers to the area connecting the duodenum. Pyloric sphincter controls only small volumes of chyme to pass through to the duodenum via tonic contraction (Tortora and Grabowski, 2000).

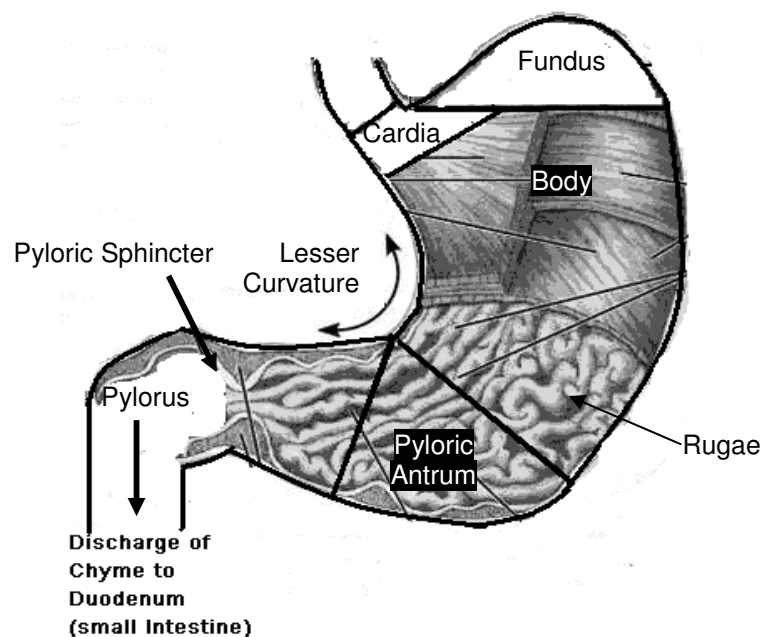


Figure 1-4. An anatomical diagram of a human adult stomach (modified from Marieb (1998)).

The stomach lining is composed of four basic layers - mucosa, sub-mucosa and muscularis externa and serosa, from the lumen outward (Figure 1-4). Mucosa is a moist epithelial membrane, which secretes mucus, digestive enzymes and hormones, protects against infectious diseases and allows absorption of the digested products into the blood stream. In the mucosa, gastric juice is secreted from the gastric glands via narrow channels called gastric pits (Rosse and Gaddum-Rosse, 1997).

The gastric glands contain three types of exocrine gland cells that secrete their products into the stomach lumen via the gastric pits. Both mucous surface cells and mucous neck cells secrete mucus. The chief (zymogenic cells) secrete pepsinogen and gastric lipase. Pepsinogen is converted to pepsin by hydrochloric acid to initiate the digestion of proteins to amino acids. Parietal cells produce hydrochloric acid and intrinsic factor. Hydrochloric acid is an important factor for maintaining acidic pH which enables activation and optimal activity of pepsin, digestion of proteins, and acidic hydrolysis of carbohydrates and killing of pathogenic bacteria in the ingested foods (Marteau, 1993; DeSesso and Jacobson, 2001). Intrinsic factor is a glycoprotein required for normal absorption of ingested vitamin B₁₂ in the small intestine. The secretions from these cells form gastric juice which is produced 2-3L daily. G cell is located in the pyloric antrum which secretes the hormone gastrin into the blood stream to stimulate the gastric secretion and motility. Bicarbonate ions and mucus form a 100µm thick unstirred layer called mucosal barrier. The mucosal barrier protects the stomach from being digested by hydrochloric acid and pepsin, and mucus lubricates food passage along the stomach.

Gastric mucus consists of 95wt% water and ~5wt% glycoprotein and slows down the rate of diffusion of hydrogen ions, pepsin and other large molecules to prevent further injury (Tortora and Grabowski, 2000). Sub-mucosa contains blood vessels, lymphatic vessels, lymph nodules, nerve fibers and elastic fibers. Elastic fibers enable the stomach to regain its shape after a meal. Muscularis externa is a thick smooth muscular layer with circular inner layer and longitudinal outer layer, responsible for peristalsis (Junqueira *et al*, 1998). The circular inner layer thickens to form sphincters which act as valves to prevent backflow and control the food passage from the stomach to the duodenum. Serosa is a protective outermost layer covered with mesothelium (Junqueira *et al*, 1998).

The dimensions and the volumes of the stomach are yet in controversy due to its highly elasticity and the presence of an anatomical modification called rugae. The stomach capacity of the human adults typically lays in the range of 1-1.6L (Karrarli, 1995) and the

basal volume of 0.024L (Kararli, 1995). When the stomach is empty, the walls of the stomach collapse inwards, and the mucosa and the sub-mucosa folds into large longitudinal folds called rugae, as illustrated in Figure 1-4. The rugae unfold and the stomach wall expands when the stomach is full (up to 4L), though the absorptive area remains the same, 0.11m^2 (Hörter and Dressman, 1997). Absorption from the GIT in general can be described using Fick's laws of diffusion (Norris et al, 1998). However the stomach is capable of absorbing non-ionized and lipophilic molecules of moderate size although the absorption is limited by its relatively small absorptive surface area (DeSesso and Jacobson, 2001). Compared to the small intestine, the absorption of nutrients on the surface of the stomach is extremely small and the duration of the food materials in contact with the stomach epithelium is relatively short.

Typical pH range of the empty stomach falls in the range of 1-1.5. However just after ingestion of food, the buffering capacity of food increases the pH to 5.0 to accommodate the activities of the salivary amylase and gastric lipase (Marteau, 1993). After digestion takes place, the pH of the stomach falls back to its empty state due to continuous secretion of the acidic gastric juice and this facilitates the proteolytic activity by the pepsin to reach its optimum activity at pH 2.5 (Marteau, 1993; Hörter and Dressman 1997; Takumi *et al*, 2000). Due to the low gastric pH, the number of resident microorganisms in the stomach is considered low compared to other parts of the GIT - $0-5 \log_{10} \text{CFU.g}^{-1}$ wet weight) (Kararli, 1995). However, many microorganisms are able to pass the stomach with the food depending on the buffering capacity of the foods and associated gastric pH as well as their acid tolerance (Marteau, 1993). The mean osmolarity of the fluids from the stomach is 244mosmol.kg^{-1} , however, this is largely influenced by the osmolarity of the ingested food. The ionic composition of gastric secretion is of 40-102 mM of hydrogen ions, 107-140mMof chloride ions, 19-51mM of sodium ions and 14-17mM ions (Kararli, 1995). The surface tension of human gastric juice is nearly independent of pH and secretion rate, lying normally in the range from $35-45 \text{mNm}^{-1}$ (Hörter and Dressman 1997).

1.3.1. Gastric Emptying

Ingestion takes place in a relatively short time for complete digestion to occur (Scarpignato, 1990). Thus the bolus which entered the stomach is initially stored in the fundus and slowly released into the antrum by peristalsis, which are also known as mixing waves. These waves pass over the stomach every 15-20 seconds to grind and mix the

bolus with digestive gastric secretions and reduce it to soup-like chyme (Fone *et al*, 1990; Houghton *et al*, 1988). As digestion proceeds in the stomach, more vigorous mixing waves begin at the body of the stomach and intensify as they reach the pylorus. This is due to the secretion of gastrin in response to food and acidic pH to stimulate the gastric emptying. The pyloric sphincter normally remains almost, but not completely, closed. As the chyme reaches the pylorus, the pyloric sphincter opens and each mixing wave forces 2-5mL of chyme to the duodenum (small intestine) before the pyloric sphincter closes again (Kararli, 1995). This sequential process is called gastric emptying. Only small particles (up to 7mm) and fluid are emptied and the caloric density of the chyme entering the duodenum is carefully controlled (Hunt, 1980). Most of the chyme is forced back into the body of the stomach for the next mixing wave. Opening and closing of the pyloric sphincter and the coordination of these forward and backward movements of the gastric contents regulate the mixing pattern and the delivery of chyme to the duodenum (Hausken, 1992). The bolus is able to remain in the fundus for about an hour without becoming mixed with gastric juice. During this time, digestion by salivary amylase continues. However the churning action mixes the chyme with acidic gastric juice and thereby inactivating the salivary amylase but activating pepsin and lipases (Tortora and Grabowski, 2000).

Gastric emptying is a non-continuous process which is strongly dependent on the conditions of the stomach and the duodenum. Depending primarily on the volume and secondarily on the composition of the gastric content, the transit time of the ingested meal can vary from 30min (e.g. saline) to 4hr (Granger *et al*, 1985). Consumption of a typical solid meal requires a lag time of 20 to 30min in the fundus, allowing fluids only to pass through the stomach. After the lag phase, the rate of gastric emptying accelerates, establishing almost a linear relationship between the volume of the gastric content and the rate of gastric emptying. Generally, the carbohydrate portion of the ingested meal empties first, protein at an intermediate time and the fats at last (Granger *et al*, 1985; Tortora and Grabowski, 2000). Liquids drunk during a meal frequently bypass the solid portions of the meal and enter the duodenum quickly. Liquids with low nutrient (e.g. water) generally take much less time to pass through, which results in an exponential relationship between the volume of the gastric content and the rate of gastric emptying (Firmer and Cutler, 1988). However when the consumed liquid is hypertonic, acidic or rich in nutrients, the rate of gastric emptying is considerably slower and non-exponential relationship between the volume of the gastric content and the rate of gastric emptying exists. Firmer and

Cutler (1988) concluded that the rate of gastric emptying of any meal can be predicted accurately by knowing its exact nutrient density.

The rate of gastric emptying can also be slowed by a high amount of fats in the duodenum which results in relaxation of the proximal stomach and diminishes the contractions of the distal stomach. Also the presence of free acid, increased tonicity and distension of the duodenum (maximum 30ml chyme) are able to slow the gastric emptying (Firmer and Cutler, 1988). As the chyme enters the duodenum, sensory receptors in the wall are stimulated, causing reflexes to feed-back onto the stomach activity and inhibit gastric emptying. Such receptors are stimulated by distension as well as the fat content of the foods (Tortora and Grabowski, 2000). The size of the stomach can be a limiting factor to the rate of gastric emptying as the non-digestible particles can be retained in the stomach for more than 12hr (Firmer and Cutler, 1988).

1.3.2. Gastric Secretion

The gastric secretion depends upon the intrinsic activity of gastric glands, autonomic innervation, GI hormones, blood flow in the gastric mucosa and stimulants of the gastric juice induced by the food (Kwiecień and Konturek, 2003) (Figure 1-5). The dual control via vagus nerves and gastrin ensures optimal postprandial (after-meal) stimulation of gastric secretion. The digestive phase of gastric secretion can be divided into three phases. Initially, cephalic (reflex) phase is triggered by aroma, taste, sight, touch, sound and thought of food, which may induce up to 50wt% of the total secretion. The phase occurs before the food enters the stomach as to prepare the stomach to be ready for digestive work ahead (Schiller *et al*, 1982; Tortora and Grabowski, 2000).

The next phase is called gastric phase which occurs during the presence of bolus in the stomach. Stomach distension activates stretch receptors and initiates both local reflexes and the long vagovagal reflexes. Impulses travel to the medulla of the brain and then back to the stomach via vagal fibers. Both types of reflexes lead to acetylcholine release, which in turn stimulates the output of more gastric juice. Ingestion of food and distention of the stomach induce remaining secretion. Increase in food amount (especially the protein content because of its buffering effect) triggers the secretion of gastric juices. Gastrin plays the major role in stimulating the parietal cells to secrete hydrochloric acid during the gastric phase. Gastrin increases contraction of the smooth muscle and mucosal blood

flow, and stimulates protein synthesis and growth of certain GI tissues - such as the mucosal lining of the stomach. Highly acidic gastric contents inhibit gastrin secretion. It is predicted that H^+ is actively pumped into the stomach lumen against a concentration gradient. As H^+ is secreted, Cl^- is also pumped into the lumen to maintain an electrical balance in the stomach. The Cl^- is obtained from blood plasma, while the H^+ appear to come from the breakdown of carbonic acid within the parietal cell (Tortora and Grabowski, 2000).

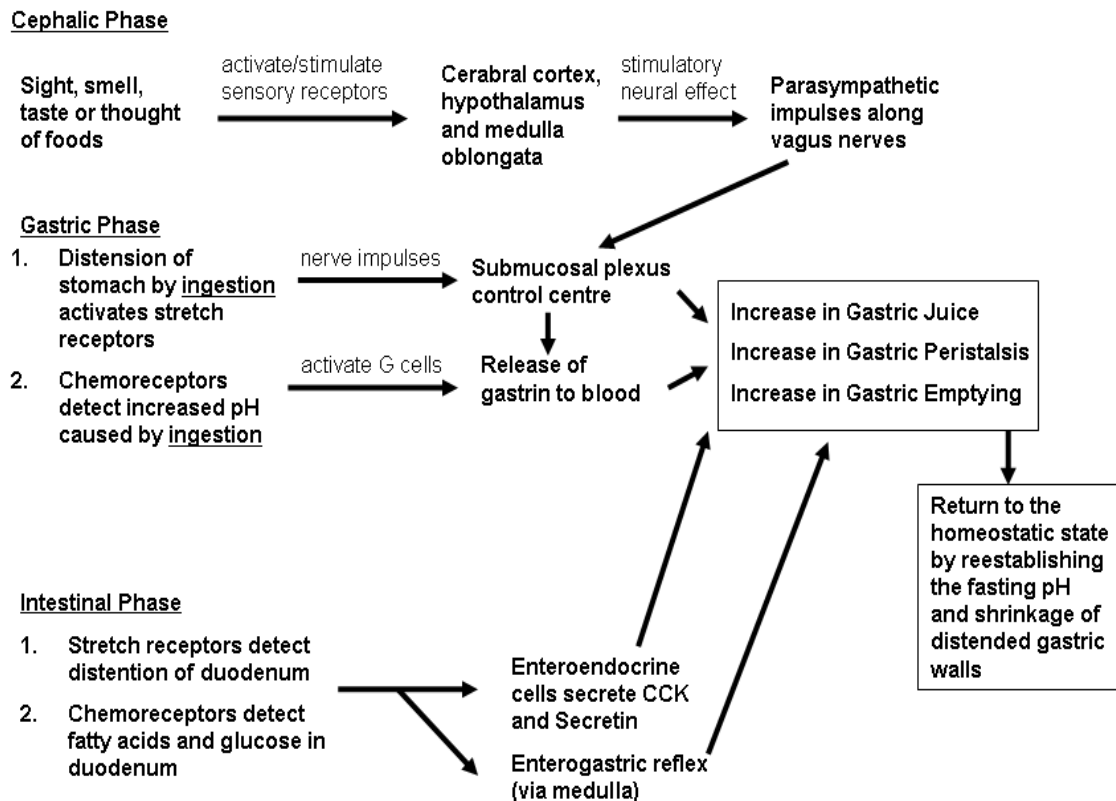


Figure 1-5. Summary of the gastric secretions in the stomach

Intestinal phase takes place with excitatory stimulants when the partially digested chyme reaches the duodenum. This in turn stimulates the intestinal mucosal cells to release two hormones that promote the gastric glands to continue their secretory activity. Secretin stimulates pancreas to secrete bicarbonate ions to neutralize acidity of the chyme and inhibits the gastric secretion and the gastric motility. Cholecystokinin (CCK) stimulates production and release of pancreatic enzymes, stimulating bile release from gall bladder and inhibits gastric secretion and motility of the stomach (Akin and Sun, 2002). The effects of these hormones reflect those of gastrin, and therefore called intestinal (enteric) gastrin. However, intestinal mechanisms stimulate gastric secretion only briefly. As the intestine distends with chyme containing large amounts of hydrogen ions, fats and partially digested proteins, the inhibitory component is triggered in the form of the

enterogastric reflex. The enterogastric reflex inhibits local reflexes and activates sympathetic fibers which cause the pyloric sphincter to tighten and prevent further gastric emptying, hence decrease in the gastric secretion. Enterogastrones (secretin, cholecystokinin, vasoactive intestinal peptide and gastric inhibitory peptide) inhibit gastric recreation when the stomach is very active (Tortora and Grabowski, 2000).

1.3.3. Gastric Motility

The pattern of the gastric motility varies between the fed and the fasted states of the stomach. The gastric motility is controlled by a very complex set of neural and hormonal signals to maximize digestion and absorption of the ingested food. In the stomach, layers of a single smooth muscle unit are present. Groups of these muscle cell units are electrically coupled by gap junctions to create a contracting segment, which has oscillating resting potentials called slow wave potentials. The resting potential difference of the smooth muscle is very small, 5~15mV. When a slow wave potential reaches its threshold level, an action potential is generated causing the muscle to contract (Tortora and Grabowski, 2000; Akin and Sun, 2002). Duration and force of the smooth muscle contraction are dependent on hormones and neural input. The force of the contraction increases with vagal activity, gastrin and motilin. It decreases with gastric juice secretion (Akin and Sun, 2002).

There are two types of electrical activity in the gastric smooth muscle cells – slow wave activity and electrical response activity. Stimulatory and inhibitory effectors on the smooth muscle cells generate a rhythmic depolarization, resulting a generation of slow wave activity (Wang and Chen, 2000). Slow wave activity is also known as Electrical Control Activity (ECA) and Basic Electrical Rhythm (BER). It is the main rhythm generated at all times and is responsible for timing of contractions. It can be detected on the greater curvature of the stomach, with aboral contractions passing from the greater to the lesser curvature. Slow waves are low frequency oscillations of smooth muscle membrane potentials. In the absence of external stimuli, an excised smooth muscle cell will produce an electrical rhythm characteristic of its anatomical position. Higher frequency and lower amplitude potentials are responsible for the contractions via electrical response activity (ERA), which is also known as Spike Like Potential (SLP) and Spike Activity (SP). It is responsible for triggering peristaltic contractions (Chen, 1998; Wang and Chen 2000; Akin and Sun, 2002).

On the basis of the motility patterns of the fed state, the stomach can be divided into two parts. The fundus and upper body of the stomach applies constant pressure on the lumen and acts as a contractile grinder, generating low frequency sustained contractions that are responsible for generating a basal pressure within the stomach. Upon ingestion, the stomach distends to inhibit the fundus contraction, allowing the stomach to expand by five-fold increase in the volume and form a large reservoir without a significant increase in pressure. However the reservoir pressure forcefully pushes the liquids of the gastric content out of the stomach first. Contractions in the fundus are infrequent but of large amplitude with duration of 45s. The lower body and antrum develop strong peristaltic waves of contraction which increase in amplitude as they propagate toward the pylorus. These contractions are stimulated by the presence of the food in the stomach causing distension. The contractions move fractions of the stored bolus towards the pylorus and mix with the gastric secretions by retro-pulsion - contractions of the antrum crush the food against the closed pyloric sphincter. This results in very small amounts of liquid portion of the chyme to be squirted through the pyloric sphincter. However a large fraction of the remaining bolus squeezes back into the stomach. Antral contractions occur only in response to neural stimulation and therefore the gastric smooth muscle contracts only when a slow wave occurs. About 20% of the digestion time, the contractions in the stomach get stronger and sweep the chyme through the pylorus into the duodenum in a short time. For slow waves, contraction strength is moderate (15-22 mmHg) with a typical rate of 3 contractions per minute. These contractions initiate without the need for action potentials (Akin 1998; Luiking *et al*, 1998; Akin and Sun, 1999; Nguyen *et al*, 1999).

Isolated interstitial cells of Cajal (ICC) are electrically active pacemaker cells which create ion currents to control the phasic contraction frequency and direction of the propagated contractions to modify the smooth muscle contractions in the stomach (Hirst, 2001; Čamborová *et al*, 2003) though in the absence of the ICCs lead to failure in generating slow waves (Delvaux, 2004). The ICCs have morphological and biochemical characteristics of both fibroblasts and smooth muscle cells (Akin and Sun, 2002) which form a 3-D network of cells placed between and in the smooth muscle layers of the proximal portion of the stomach body (Čamborová *et al*, 2003). Each part of the stomach with the exception of fundus includes the pacemaker mechanism, a dense network of myenteric ICC, with an increasing number of these cells towards the antrum (Čamborová *et al*, 2003).

At fasted state, Migrating Motor Complex (MMC) is initiated by the secretion of motilin. It is not proven that motilin causes the MMC but its secretion coincides with the motor complex and occurs at about the same frequency in the fasting state and eating inhibits its release. MMC is a distinct pattern of electrochemical activity observed during the periods between meals which originates in the stomach and serves a housekeeper to periodically sweep out the fasted stomach. The total cycle duration of MMC in normal healthy subjects is 84 ± 10.6 min (Tack *et al*, 1998) which consists of 4 phases. Quiescence phase of 45 to 60 min only has rare action potentials and contractions. Peristaltic contractions originate from the stomach and progressively increase in frequency (~ 40 mmHg) for 20.5 ± 4.8 min. The third phase is composed of rapid (propagation velocity of 5.9 ± 1.1 cm.min⁻¹, (Tack *et al*, 1998)), evenly spaced peristaltic contractions (3 contractions per min) for 5.2 ± 0.7 min. Pylorus remains open during these peristaltic contractions, allowing many indigestible materials to pass into the small intestine. The highest contraction strength (~ 80 mmHg) is necessary at this phase to empty large indigestible particles to the small intestine. The last phase is a short transition period between phase 3 and phase 1, which typically lasts for 15 to 30 min. The functional importance of the MMC is not fully understood but the motor components of MMC show an intimate interaction with secretion and absorption in the stomach. Ingestion of food will abolish a MMC and restore a digestive pattern of motility. An increase in gastric, biliary and pancreatic secretion is seen with MMC. These secretions aid in the cleansing activity of MMC and assist in preventing a build-up of bacterial populations in the small and the large intestines. MMC is affected by a various factors. Increase in the gastric osmolarity, increase in the viscosity of the gastric contents and ageing lead to decrease in gastric emptying, body temperature, viscosity and age (Akin 1998; Tack *et al*, 1998; Marieb, 1998).

1.4. References

2003 Encyclopaedia Britannica, Inc.

<http://www.britannica.com/eb/art-1087/The-human-digestive-system-as-seen-from-the-front>

<http://images.encarta.msn.com/xrefmedia/aencmed/targets/illus/ilt/0007760a.gif>

http://www.merck.com/media/mmhe2/figures/MMHE_09_120_01_eps.gif

Akin, A. (1998) Non-invasive detection of spike activity of the stomach from cutaneous EGG. *PhD Thesis* Drexel University, Philadelphia

Akin, A., Sun, H. H. (1999) Time-frequency methods for detecting spike activity of stomach. *Med. Biol. Eng. Comput.*, 37, 381–90

Akin, A., Sun, H. H. (2002). Non-invasive gastric motility monitor: fast electrogastragram (fEGG). *Physiol. Meas.*, 23, 505-519

Al-Zaben, A., Chandrasekar, V. (2005). Effect of esophagus status and catheter configuration on multiple intraluminal impedance measurements. *Physiol. Meas.*, 26, 229-238

- Briedis, D., Moutrie, M. F. M., Balmer, R. T. (1980). A study of the shear viscosity of human whole saliva. *Rheol. Acta.*, 19, 365-374
- Čamborová, P., Hubka, P., Šulková, I., Hulín, I. (2003). The pacemaker activity of interstitial cells of Cajal and gastric electrical activity. *Physiol. Res.*, 52, 275-284
- Chen, J. D. Z. (1998). Non-invasive measurement of gastric myoelectrical activity and its analysis and applications. *Proceedings of the 20th Annual International Conference of the IEE Engineering in Medicine and Biology Society*, 20 (6), 2802-2807
- Christensen, J., Roberts, R. L. (1983). Differences between esophageal body and lower esophageal sphincter in mitochondria of smooth muscle in opossum. *Gastroenterology*, 85, 650-656
- Clouse, R. E., Staiano, A. (1991). Topography of the esophageal peristaltic pressure wave. *Am. J. Physiol.*, 261, G677-G684
- Clouse, R. E., Staiano, A. (1993). Topography of esophageal motility in patients with normal and high amplitude esophageal peristalsis. *Am. J. Physiol.*, 265, G1098-G1107
- Corazzari, E., Fave, G. D., Pozzessere, C., Kohn, A., De Magistris, L., Anzini, F., Torsoli, A. (1982). Effect of bombesin on lower esophageal sphincter pressure in humans. *Gastroenterology*, 83 (1), 10-14
- Delvaux, M. (2004) Alterations of sensori-motor functions of the digestive tract in the pathophysiology of irritable bowel syndrome. *Best Practice & Research Clinical Gastroenterology*, 18 (4), 747-771
- DeSesso, J. M., Jacobson, C. F. (2001). Review: Anatomical and physiological parameters affecting gastrointestinal absorption in humans and rats. *Food & Chem. Toxicology*, 39, 209-228
- Drewes, A. M., Reddy, H., Staahl, C., Funch-Jensen, P., Arendt, L., Gregersen, H., Lundbye-Edgar, W. M. (1990). Saliva and dental health. *British Dental Journal*, 169 (3-4), 96-98
- Firmer, S.J., Cutler, D.J. (1988) Simulation of gastrointestinal drug absorption I. Longitudinal transport in the small intestine. *International Journal of Pharmaceutics*, 48, 231-246
- Fone, D. R., Akkermans, L. M. A., Dent, J., Horowitz, M., Van der Schee, E. J. 1990. Evaluation of patterns of human antral and pyloric motility with antral wall motion detector. *Am. J. Physiol.*, 258, G616-623
- Granger, D. N., Barrowman, J. A., Kvietys, P. R. (1985). *Clinical Gastrointestinal Physiology*. W. B. Saunders, Philadelphia.
- Hausken, T., Odegaard, S., Matre, K., Berstad, A. (1992) Antralduodenal motility and movements of luminal contents studied by duplex sonography. *Gastroenterology*, 102, 1583-1590
- Helm, J. F., Dodds, W. J., Hogan, W. J., Soergel, K. H., Egide, M. S., Wood, C. M. (1982). Acid neutralizing capacity of human saliva. *Gastroenterology*, 83, 69-74
- Hirst, G. D. S. (2001). An additional role for ICC in the control of gastrointestinal motility. *J. Physiol.*, 537, 1
- Hörter, D., Dressman, J.B. (1997) Influence of physicochemical properties on dissolution of drugs in the gastrointestinal tract. *Advanced Drug Delivery Reviews* 25, 3-14
- Houghton, L. A., Read, N. W., Heddle, R., Maddern, G. J., Downton, J., Toouli, J., Dent, J. (1988) Motor activity of the gastric antrum, pylorus and duodenum under fasted conditions and after a liquid meal. *Gastroenterology*, 94, 1276-1284
- Humphrey, S. P., Williamson, R. (2001). A review of saliva: Normal composition, flow and function. *The Journal of Prosthetic Dentistry*, 85 (2), 162-169
- Hunt, J. N. (1980). A possible relation between the regulation of gastric emptying and food intake. *Am. J. Physiol.*, 239 (Gastrointest. Liver Physiol. 2), G1-G4
- Jensdottir, T., Nauntofte, B., Buchwald, C., Bardow, A. (2005). Effects of sucking acidic candy on whole-mouth saliva composition. *Carries Res.*, 39, 468-474
- Junqueira, L., Carneiro, J., Kelly, R.O. (1998) *Basic Histology*. 9th Ed., Publisher: Stamford, Conn: Appleton & Lange, c1986. Chapter 15, 272-302
- Kararli, T. T. (1995). Review article: Comparison of the gastrointestinal anatomy, physiology and biochemistry of humans and commonly used laboratory animals. *Pharmaceutics & Drug Disposition*, 16, 351-380
- Kwiecień, S., Konturek, S. J. (2003). Gastric analysis with fractional test meals (ethanol, caffeine, and peptone meal), augmented histamine or pentagastrin tests, and gastric pH recording. *Journal of Physiology and Pharmacology*, 54 (S3), 69-82
- Libermann, M. D., Heberer, M., Martinoli, S. (1981). Are there muscular structures which may contribute to closure of the gastro-esophageal junction? *Scand. J. Gastroenterol.*, 67, S123

- Luiking, Y. C., Peeters, T. L., Stolk, M. F., Nieuwenhuijs, V. B., Portincasa, P., Depoortere, I., van Berge Henegouwen, G. P., Akkermans, L. M. A. (1998). Motilin induces gall bladder emptying and antral contractions in the fasted state in humans. *Gut*, 42, 830-835
- Marieb, E. N. (1998) *Human Anatomy and Physiology*. 4th Edition. The Benjamin/Cummings Publishing Company, Inc., an Imprint of Addison Wesley Longman, Inc. Chapter 24. The digestive system. pp. 848-907
- Marteau, P., Pochart, P., Bouhnik, Y., Rambaud, J. C. (1993) Fate and effects of some transiting microorganisms in the human gastrointestinal tract. *World Rev. Nutr. Diet*, 74: 1-21
- Meyer, G. W., Austin, R. M., Brady, C. E., Castell, D. O. (1986). Muscle anatomy of the human esophagus. *J. Clin. Gastroenterol.*, 8, 131-134
- Mosher, H. P. (1927) X-ray study of the movements of the tongue, epiglottis and hyoid bone in swallowing, followed by a discussion of difficulty in swallowing caused by retropharyngeal diverticulum, postcricoid webs and exostoses of cervical vertebrae. *Laryngoscope*, 37 (4), 235-262
- Nguyen, H. N., Silny, J., Matern, S. (1999). Multiple intraluminal electrical impedanceometry for recording of upper gastrointestinal motility: current results and further implications. *Am. J. Gastroenterology*, 94 (2), 306-317
- Norris, D.A., Puri, N, Sinko, P.J. (1998) The effect of physical barriers and properties on the oral absorption of particulates. *Advanced Drug Delivery Reviews*, 34, 135-154
- Orlando, R. C., Powell, D. W., Bryson, J. C., Kinard III, H. B., Carney, C. N., Jones, J. D., Bozyski, E. M. (1982). Esophageal potential difference measurements in esophageal disease. *Gastroenterology*, 83(5), 1026-1032
- Pehlivanov, N., Liu, J., Kassab, G. S., Beaumont, C., Mital, R. K. (2002). Relationship between esophageal muscle thickness and intraluminal pressure in patients with esophageal spasm. *Am. J. Physiol. Gastrointest. Liver Physiol.*, 282, 1016-1023
- Rosse, C., Gaddum-Rosse, P. (1997) *Hollinshead's Textbook of Anatomy*. Fifth Ed., Publisher: Philadelphia, PA: Lippincott-Raven Publishers, c1997.pg.88-90
- Sarosiek, J., McCallum, R. W. (2002). Mechanisms of oesophageal mucosal defence. *Baillière's Clinical Gastroenterology*, 14 (5), 701-717
- Scarpignato, C. (1990). Gastric emptying measurement in man. pg. 198-246 In: C.Scarpignato and G. Bianchi Porro (Eds) *Clinical investigations of gastric function*. Front Gastrointest. Res. Basel, Karger
- Schiller, L. R., Walsh, J. H., Feldman, M. (1982) Effect of atropine on gastrin release stimulated by an amino acid meal in humans. *Gastroenterology*, 83, 267-272
- Staiano, A., Clouse, R. E. (1991). Value of subject height in predicting lower esophageal sphincter location in children and adults. *Am. J. Dis. Child*, 145, 1424-1427
- Tack, J., Coulie, B., Wilmer, A., Peeters, T., Janssens, J. (1998). Actions of the 5-hydroxytryptamine 1 receptor agonist sumatriptan on interdigestive gastrointestinal motility in man. *Gut*, 42, 36-41
- Takumi, K., de Jonge, R., Havenaar, A. (2000). Modelling inactivation of *Escherichia coli* by low pH: application to passage through the stomach of young and elderly people. *Journal of Applied Microbiology*, 89, 935-943
- Tortora, G. J., Grabowski, S. R. (2000) *Principles of anatomy and physiology*. 9th Edition. John Wiley and Sons, Inc., Chapter 24, The Digestive System. pp.818-870
- Wang, Z. S., Chen, J. D. Z. (2000). Mathematical modelling of nonlinear coupling mechanisms of gastric slow wave propagation and its SIMULINK simulation for investigating gastric dysrhythmias and pacing. *Computer-Based Medical Systems, 2000. CBMS 2000. Proceedings. 13th IEEE Symposium*. 89-94
- Wu, J. C-Y., Mui, L-M., Cheung, C. M-Y., Chan, Y., Sung, J, J-Y. (2007). Obesity is associated with increased transient lower esophageal sphincter relaxation. *Gastroenterology*, 132(3), 883-889

Declaration of Thesis Chapter 2

In the case of Chapter 2, sections 2.2 and 2.3, the nature and extent of my contribution to the work was the following

Nature of Contribution	Extent of contribution (%)
Development of ideas to write	80%
Writing of the findings	80%

The following co-author contributed the work.

Name	Nature of Contribution	Extent of contribution (%)
Professor Xiao	Development of ideas to write	20%
Dong Chen (Supervisor)	Writing of the findings	20%

*The co-author (supervisor) provided proof reading of my writing

Candidate's Signature M. J. Yoo Date 19/ Sep/ 2008

Declaration by co-author

The undersigned hereby certify that:

1. the above declaration correctly reflects the nature and extent of the candidate's contribution to this work, and the nature of the contribution of each of the co-author
2. they meet the criteria for authorship in that they have participated in the conception, execution or interpretation of at least that part of the publication in their field of expertise
3. they take public responsibility for their part of the publication, except for the responsible author who accepts overall responsibility for the publication
4. there are no other authors of the publication according to these criteria
5. potential conflicts of interest have been disclosed to (a) granting bodies, (b) the editor or publisher of journals or other publications, and (c) the head of the responsible academic unit; and
6. the original data are stored at the following location(s) and will be held for at least five years from the date indicated below:

Location(s): Hard and soft copies of each paper are available to each author's PC and other storage devices under the Department of Chemical Engineering, Monash University (Clayton campus)

Signature of the co-author: X. D. Chen Date 19/ Sep/ 2008

Chapter 2

Review on the available *in vitro* digestion models of the human gastrointestinal tract (GIT) in the literature

This chapter reviews the *in vitro* digestion models (experimental) found in the literature, which simulate the conditions of the human gastrointestinal tract (GIT). Mainly upper GIT part of the *in vitro* digestion models are discussed with some aspects to the continuity to the small and the large intestines.

2.1 Introduction

In vitro digestion models refer to physicochemical (mechanical) models simulating the conditions of the human gastrointestinal (GI) system. Recently there have been intensive researches in the development of such *in vitro* digestion models with aspects of attaining an alternative to traditional approaches of *in vivo* clinical studies with humans and laboratory animals. Such *in vivo* studies can be of necessity in gaining the knowledge of the dynamic nature of living organisms, however, ethical constraints, costs and the time required by these studies often obstruct to amend for new direction of studies. Variations among a species due to gender, age groups and the records of associated disorders also complicate in analysing the obtained results, and thus require a large number of individuals to be tested in order to generate reliable results. Rapid generations of massive results with robustness and high accuracy are in strong demand to meet the fast developing industries of pharmaceuticals and nutraceuticals, as well as in examining novel, toxic or unfamiliar compounds which yet have not been addressed to fully investigate the causes on the well-being of humans.

Currently available *in vitro* digestion models can be classified via different ways. For example, static or dynamic, simulation of one or more GI organs, or dependency on the test materials and the aim of research such as the study of microecology of the lower GIT and bioavailability of drugs, trace elements and toxic compounds. As this is a relatively new area of research, there are only two representative *in vitro* digestion models, called Simulator of the Human Intestinal Microbial Ecosystem (SHIME) and TNO's Intestinal Microsystems (TIM) 1 and 2, which imply various applications via utilizing such models.

Although a large number of *in vitro* digestion models exist in the literature, most of them have been designed to focus on one type of study rather than covering broad aspects of the dynamic human GI conditions. Nevertheless, the use of such *in vitro* digestions can be of great assistance as intensive labour, lengthy timeframe (Castela-Papin *et al*, 1999), ethical constraints can be avoided, and once the model is validated with its ability to simulate the human GI conditions, it can be used as an economic alternative (Allison *et al*, 1989) to the *in vivo* studies to produce large amounts of results with high reproducibility and robustness with capability of selecting certain parameters (Van de Wiele *et al*, 2004a and 2004b), for example the conditions of the weaned infants (De Boever *et al*, 2001).

2.2 Simulator of the Human Intestinal Microbial Ecosystem (SHIME)

Simulator of the human intestinal microbial ecosystem (SHIME) was developed by Molly *et al* (1993) in Belgium which claims to be the first multi-stage simulator in the literature (Molly *et al*, 1993). Initially, five of computer controlled multi-chamber reactors simulating the conditions of the human duodenum/jejunum, ileum, cecum/ascending colon, transverse colon and descending colon were connected in a series to study the heterogenic microbiota of the colon. Later on, the sixth reactor representing the stomach has been added (De Boever *et al*, 2001). Key features of the SHIME include the simulation of the kinetics of the chyme passage through the GIT by controlling of the concentrations and the pump flow rate of the artificial GI digestive enzymes and bile, sequential control of the pH and temperature, feed compositions representing the meal to be ingested and the nutrient medium for the culturing of the colon microbiota, study of probiotic strains, use of physiological GI residence times, inoculation of fecal suspension, simulation of GI motility and anaerobic environment (Molly *et al*, 1993; Kontula *et al*, 1998; Alander *et al*, 1999; De Boever *et al*, 2000; Possemiers *et al*, 2004). The SHIME has been applied for various studies such as nutritional studies (Kontula *et al*, 1998; Alander *et al*, 1999), micro-ecological studies (De Boever *et al*, 2000; Gmeiner *et al*, 2000; De Boever *et al*, 2001; Possemiers *et al*, 2004) and the studies of bioavailability and bioaccessibility of environmental contaminants (Van de Wiele *et al*, 2004a) and antimicrobial agents (Possemiers *et al*, 2005).

As the SHIME is one of the early *in vitro* digestion models, the model excluded many key features, over-simplifying the dynamic nature of the human GIT thus producing contradictory results with limited scope of analyses. Two of the important features

missing in the SHIME include absorption mechanism and buffering capacity. Absorption mechanism is crucial in the small and the large intestines, where the majority of the metabolites and water are absorbed through the GI membrane via either active or passive diffusion processes (Alander *et al*, 1999; Vasiluk *et al*, 2007). However in the SHIME, no such membranes are present, which may convey the situation of diarrhoea rather than the normal digestive condition (De Boever *et al*, 2000) and the interactions between the metabolites and the microbiota cannot be therefore studied. Buffering capacity of ingested meal is another omitted component of the SHIME, which plays a key role in selecting for a wide range of probiotic strains. The stomach compartment of the SHIME has average pH of 3.8 to 4.1 (De Boever *et al*, 2001) in which the probiotic strains that are highly acid-resistant (e.g. lactic acid bacteria) may survive, thus resulting inconsistency in the probiotic strains that are clinically proven to survive in humans (Mattila-Sandholm *et al*, 1999).

Other uncertainties have risen from the inoculation of fecal suspensions which are not representative of the different parts of the human colon microbiota (Possemiers *et al*, 2004; Van de Wiele *et al*, 2004a and 2004b), allowing limited extent of prediction caused by the absence of the interactions between the microbiota with the host, specific absorption and/or adsorption and non-dynamic biochemical activity levels (Gmeiner *et al*, 2000; Van de Wiele *et al*, 2004a). Conflicting results were also caused by variations of individual strain in pre-treatment parameters showed high noise level in the SHIME (Alander *et al*, 1999), adhesion of microorganisms to the reactor vessels and tubing resulting biased growth of particular strains and measuring of average values in log CFU/ml or log CFU/g instead of significantly counted number of bacteria (Molly *et al*, 1993). Establishment of a representative and stabilized microbiota is a pre-requisite for the use of the SHIME where at least 2 weeks were required (Possemiers *et al*, 2004; Paramithiotis *et al*, 2006), though the consistency remains to be answered (Mattila-Sandholm *et al*, 1999). Immune effects (Alander *et al*, 1999) and feed-back mechanisms (Mainville *et al*, 2005) are also missing, which seemed negligible compared to other missing features. Thus only the general effects of probiotics on the microbiota can be examined via the SHIME and further validations in relation to *in vivo* clinical studies are required to gain higher predictive outcomes.

2.3. TNO's gastrointestinal model (TIM)

TNO's gastrointestinal model (TIM) is another widely used *in vitro* digestion model, created by Havenaar and Minekus (1996) in Netherlands. Four computer-controlled chambers simulating the conditions of stomach, duodenum, jejunum and ileum for TIM-1 and large intestines for TIM-2 were developed to simulate the GIT of humans and pigs. Key features of the TIM-1 and 2 include simulation of peristaltic movements, absorption of nutrients and water in the small intestine compartments, simulations of gastric emptying rates and intestinal transit times, pre-set computer controls of pH, body temperature and rates and compositions of the gastric, bile and pancreatic secretions with physiological relevance (Havenaar and Minekus, 1996). The TIM has been used for various applications including the studies of bioavailability and bioconversions of environmental toxins and mutagens (Krul *et al*, 2000; Avantaggiato *et al*, 2003; Dominy *et al*, 2004; Krul *et al*, 2004), absorption and interactions of pharmaceutical products (Blanquet *et al*, 2004; Blanquet *et al*, 2005; Souliman *et al*, 2006), microecology of probiotic strains (Marteau *et al*, 1997; Minekus *et al*, 1999; Blanquet *et al*, 2006) and nutrition of digestibility and absorption (Minekus *et al*, 1995; Havenaar and Minekus, 1996; Haraldsson *et al*, 2005; Maisonnier-Grenier *et al*, 2006).

Though the TIM included more complex features in simulating the digestive activities of the human GIT compared to that of the SHIME, over-simplification and non-effective complexities have resulted in contradictory outcomes with limited extent of analyses. Irrespective of the feeding material, the pH of each compartment was pre-set. For the stomach compartment, either HCl or NaOH was added to adjust the pH to 4.5, 4.2, 2.1 and 1.7 at 5, 20, 60 and 90min respectively (Minekus *et al*, 1995). As different types of ingested materials provide the buffering capacity to various extents, the pre-set pH curve does not seem to simulate the closest possible human conditions. A rapid drop of pH does not mimic the *in vivo* conditions postprandial (Mainville *et al*, 2005), which resulted in a very low viability of probiotic strains with proven clinical survival, such as *Streptococcus thermophilus* and *Lactobacillus bulgaricus* (Marteau *et al*, 1997; Mattila-Sandholm *et al*, 1999).

Fecal inoculations were used to build the colon microbiota in the compartments of the TIM-2, where 48hrs of the microbiota stabilization period was allowed before introducing bacteria and/or food to be studied (Minekus *et al*, 1999). Fecal inoculations used cannot fully represent the microbiota of the human colon (Possemiers *et al*, 2004; Van de Wiele

et al, 2004a) thus the interactions between the microbiota with the host, colonization and adsorption of specific strains of interest, availability of nutrients and competitive interactions within the microbiota could not be studied (Gmeiner *et al*, 2000; Van de Wiele *et al*, 2004b), resulting in diarrhoea in the model (Spratt *et al*, 2005).

Absorption of water soluble amino acids and carbohydrates was simulated in the small intestinal compartments of the TIM-1 by the use of semi-permeable hollow-fiber membrane units with cut off size of up to 5kDa (Havenaar and Minekus, 1996). However the fate of water insoluble compounds could not be predicted (Krul *et al*, 2000) and only passive diffusion of the water soluble compounds was able to be studied (Avantaggiato *et al*, 2003) due to the absence of the mucosal cells which allow active transport of such compounds (Souliman *et al*, 2006), hence the overall absorption process does not mimic the natural absorption processes in the humans.

Transit time with physiological relevance is a very important factor in simulating the human conditions as it determines the distribution of substrates and microorganisms through the GIT and therefore influence the wall growth and inoculation of growth media (Spratt *et al*, 2005). Though the removal of the chyme at $2\text{ml}\cdot\text{hr}^{-1}$ provided the half time of large intestinal content renewal of 36hr which matched with the human physiological transit time (Minekus *et al*, 1999; Blanquet *et al*, 2003; Dominy *et al*, 2004), it should be noted that liquid feed material was used in the TIM, in which the transit time should have been faster compared to the solid and/or semi-solid meals used by clinical studies for measuring the gastric emptying and GI transit times. The transit time is determined by the central nervous system, feed-back (hormonal) controls as well as the nature of the ingested meal. Feed-back controls also determine the GI motility and secretion, thus using of relevant *in vivo* data may provide realistic results (Havenaar and Minekus, 1996). The digestion processes examined by the TIM has been known to be very difficult to mathematically model (Spratt *et al*, 2005) due to the complexities induced by combination of various biological factors. Thus some features of the TIM require reconstruction and further validations in relation to *in vivo* clinical studies to accomplish a closer view to the human GIT.

2.4. Other *in vitro* digestion models in the literature

Numerous *in vitro* digestion experimental models exist in the literature in which compared to the SHIME and the TIM, the value as a tool for possibly replacing the *in vivo* trials is somewhat insignificant due to over-simplification. Such models can be divided into the aim of the studies such, as microecological or bioavailability of toxic, pharmaceutical or nutritional compounds. Alternatively, these experimental models can also be categorized into either single versus multi-compartmental experimentally simulating one or more GI organs, or static versus dynamic conditions. Static models refer to exposure of the test material to secretion at a fixed pH and temperature during a fixed period of time (Boisen and Eggum, 1991; Savoie, 1994) whereas dynamic models include flows of GI secretions and variable pH with respect to time (Savalle *et al*, 1989).

2.4.1. *In vitro* digestion models used in microecological studies

In vitro digestion models of microecological studies have been extensively developed in the late 1990's, where the viability of probiotics in the colon was of interest to many authors. Miller and Wolin (1981) have used an *in vitro* semi-continuous culture fermenter system to study the microbial community in the colon, which has become a bench mark of incorporating *in vitro* digestion (fermenter) models to microecological studies. In some ways, the SHIME seemed to have been modified from the multi-chamber system (MCS) built by Gibson *et al* (1988). The MCS was the first three-stage continuous culture system designed to study microbial populations of the colon. In 1989, Allison *et al* (1989) developed a five-stage continuous culture system which seemed also to be derived from the MCS. The continuous culture system contained five continuously stirred glass vessels to investigate the effects of nutrient availability and the rate of dilution of the microbial populations of the human colon. Allison *et al* (1989) proposed that such model would be of value to the ecological studies of the human gut bacteria. In 1998, a three-stage compound continuous culture system has been developed by Macfarlane *et al* (1998a). The model was used to study the effect of retention time and the metabolism of human gut bacteria (Macfarlane *et al*, 1998a) as well as the degradation of polysaccharides during the growth of the gut bacteria under multi-substrate limiting conditions (Macfarlane *et al*, 1998b). Later on in 2005, a model of simulating the human upper gastrointestinal tract has been developed by Mainville *et al* (2005). It is composed of two

glass reactors representing the stomach and the duodenum, to study the viability of probiotics with kefir. Such multi-compartmental models do have advantages against the batch culture systems as they are able to mimic more complex and dynamic conditions to allow for spatial and temporal heterogeneity (Marteau *et al*, 1997; Brück *et al*, 2002). However the batch culture systems can be of interests for the studies of the fermentability of various substrates (Brück *et al*, 2002) and the viability of the selected probiotic strains under a particular condition for examining the resistances to acidity (HCl), bile or salt (NaCl) for a short period of time, less than 24hrs (Lee and Heo, 2000). Although the predictive value of the batch culture systems would be very limiting as they do not simulate the continuously changing sequential processes *in vivo*, the procedures of conducting such studies can be much simpler, economic and may suit preliminary testing better than the continuous multi-compartmental models.

2.4.2. *In vitro* digestion models used in toxicological studies and risk assessments

Studies of environmental toxins, mutagenic compounds and food allergens have been conducted extensively via the *in vitro* digestion models. However, these models are very similar to each other since dissolution and extraction of the chemical constituents from the test material are the key components for toxicological studies (Trombetta *et al*, 2005). In general, the models are composed glass vessels and a shaking water bath, with two sequential digestion processes. The test material is firstly incubated for pepsin-HCl digestion for simulating the conditions of the stomach, followed by adjustment of pH to near neutral, pH range of 6.5 to 7. Incubation of the pH adjusted sample then undergoes pancreatin-bile digestion for simulation of the small intestine. This method has been used for examining the bioavailability of inorganics in soil (Ruby *et al*, 1999), lead (Ruby *et al*, 1992; Ruby *et al*, 1996; Schroder *et al*, 2004), arsenic (Ruby *et al*, 1996; Rodriguez *et al*, 1999), polycyclic aromatic hydrocarbons (PAH) (Hack and Selenka, 1996), polychlorinated biphenyls (PCB) (Hack and Selenka, 1996; Oomen *et al*, 2000), lindane (Oomen *et al*, 2000), Cadmium (Schroder *et al*, 2003), mycotoxins (Versantvoort *et al*, 2005) and food allergens (Vassilopoulou *et al*, 2006; Moreno, 2007). Such methods seemed to have derived from nutritional studies of assessing the bioavailability of iron from food source (Ruby *et al*, 1999). Such method has also been used in confirming the findings of *in vivo* allergen studies with animals (Kopper *et al*, 2006). Alternatively,

simulated gastric fluid and simulated intestinal fluid have been used by Takagi *et al* (2003) for examining the digestibility of food proteins and effect of preheating on the digestion, and Herman *et al* (2005) and (2006) to study the resistance of transgenic proteins for allergenicity assessments. There is a growing evidence of reproducibility, robustness and the relevance of using the simulated gastric and the intestinal fluids to *in vivo* digestion, however, the potential of allergenicity remains uncertain (Herman *et al*, 2006). Colon has never been included as part of the *in vitro* digestion models designed for toxicological studies as it is a site of water absorption. This is quite contradictory to the *in vitro* digestion models of the microecological studies as those models are mainly focused on the colon. However, very few models contained the mouth part, which seemed necessary especially when examining the children's toys. Although the method seemed simple, Hack and Selenka (1996) claims that it is a suitable technique to measure the quantity of contaminants that may be mobilized under physiological conditions in the human GIT.

Physiologically based extraction test (PBET) developed by Ruby *et al* (1996) used purging of argon gas through the polyethylene separatory funnel (reactor) to study the bioavailability of metals from a solid matrix. The concept of the two sequential digestive incubations remains the same, but with different mixing mechanism. The *in vitro* digestion model developed by Oomen *et al* (2000) used test tubes with head-over-heels method for mixing the soil contaminants with the saliva, gastric juice and intestinal juice. This was used by Oomen *et al* (2003) and Versantvoort *et al* (2005) for estimation of the bioaccessibility of soil contaminants and to study bioaccessibility of mycotoxins from food, respectively. The model was further developed by Brandon *et al* (2006) with the use of stimulated saliva to simulate the conditions of sucking and swallowing to study the bioaccessibility of contaminants and its application in risk assessment. Savage and Catherwood (2007) have also used the same model to determine oxalates in Japanese taro corms.

It would seem that the use of two sequential digestive incubations is able to demonstrate low extraction and dissolution of the chemical constituents, which can be toxic or even carcinogenic. As of ethical concerns, the use of *in vitro* digestion models is in need especially for such type of studies. Although the correlation between the *in vivo* studies using animals and the *in vitro* studies is yet uncertain, development of more comprehensive models is required to increase the predictive value of such *in vitro* digestion models.

2.4.3. *In vitro* digestion models used in the studies of pharmaceuticals

Examining of the behavior of pharmaceuticals via the *in vitro* digestion models has been conducted to study the interactions of drugs to drugs, drugs to meals or nutrients, drugs to the GI secretions, screening of drug formulations during the development of drug dosage forms and quality control tests for batch-to-batch reproducibility. Traditionally, bioavailability of drug administration has been determined by measuring of the plasma/blood concentration *in vivo* (Norris *et al*, 1998). However *in vivo* clinical studies with either humans or laboratory animals such as rodents, rabbits, canine and porcine, can be difficult due to ethical constraints and often the exposure to high doses of drugs such as verapamil and nifedipine, led to the death of the testing subjects (Herling *et al*, 1988). With the use of animals, Herling *et al* (1988) and Tuleu *et al* (1999) reported that administration of drugs itself was very difficult, especially if a specific position in the GIT was to be targeted. They also experienced difficulties in administering enough doses to inhibit the gastric secretion and often the low concentrations used were incompatible with the normal functioning of the drugs. Furthermore, rodents, which are the most commonly used animals (Harrison *et al*, 2004), have different properties of the GIT such as absence of a gall bladder, different gut flora and less efficient in drug binding ability in plasma, when compared to that of the humans. However, piglets are known to be suitable models for the human infant as for having a similar zone of thermal neutrality, similar endocrine status around birth and exhibit very immature intestinal motility patterns (Harrison *et al*, 2004). With ethical concerns, *in vitro* digestion models would assist pharmaceutical studies if validated for use.

The three important elements of *in vitro* digestion models for the study of pharmaceuticals are the control of pH (McGinity and Lach, 1976), dissolution (Blanquet *et al*, 2004) and absorption of the test drugs into the lymph and blood vessels in the stomach (Herling *et al*, 1998) and small intestinal linings (Stops *et al*, 2006). The pHs of the GI secretions largely influence the saturation solubility of ionisable drugs (i.e. as the pH increases, the solubility of the acid increases due to the contribution from the ionized form (Hörter and Dressman, 2001), disintegration of coating materials (Herling *et al*, 1988; Sugawara *et al*, 2005), sustained release of microencapsulated particles (Herling *et al*, 1998; Sugawara *et al*, 2005), physical adsorption of drugs (McGinity and Lach, 1976; Porubcan *et al*, 1978). Gastric pH is subject to change by the presence of foods (Fordtran and Walsh, 1973; Malagelada *et al*, 1976), aging (Ogata *et al*, 1984), disorders such as AIDS (Lake-Bakaar *et al*, 1988) and administration of antacids (Deering and Malagelada, 1979). Thus a

careful control of pH profile is essential for the study of pharmaceuticals. Often simple laboratory equipments, such as a glass beaker and a hot plate magnetic stirrer with a computer control of pH profile by delivering of acidic gastric secretions via a peristaltic pump or auto-burette (Vatier *et al*, 1998a and 1998b; Fatouros *et al*, 2007) have been used for the study of pharmaceuticals.

Dissolution is another critical parameter of pharmaceutical dosage forms (Blanquet *et al*, 2004) which has been studied using static *in vitro* digestion models as described in the European and US Pharmacopoeia (USP). These models are also known as USP apparatus, which have been used to examine sustained release of ofloxacin (Chavanpatil *et al*, 2005), absorption of albendazole formulation (Galia *et al*, 1999) and the impact of food intake on acetaminophen release (Souliman *et al*, 2006). However the USP apparatus are unable to identify the possible risks of specific GI conditions such as fed state, dose dumping and interaction with other drugs (Blanquet *et al*, 2004). Thus the dynamic nature of the GIT is unable to be simulated, providing very limited information on passive diffusion of the test materials.

A number of models contained mucosal lining such as hog mucosa (Castela-Papin *et al*, 1999), rabbit gastric mucosa (Herling *et al*, 1988) and Caco-2 cells (Kobayashi *et al*, 2001) to simulate the absorption mechanisms of the drugs. Such models enable better predictions of the therapeutic impacts of the drugs of interest as the interactions between the drugs, including neutral, acidic, basic or amphoteric, interactions with physiologically relevant pH and absorption can be studied together. Lately, Sugawara *et al* (2005) modified the *in vitro* system built by Kobayashi *et al* (2001) for prediction of drug dissolution and absorption with change of pHs in the GIT after oral administration. Monolayer of Caco-2 cells derived from colonic carcinoma of humans was included in the *in vitro* system, in which Caco-2 cells express most of the enzymatic, functional and morphological characteristics of the intestinal mucosa and thus generally accepted for use in drug transport studies (Hidalgo *et al*, 1989; Hilgers *et al*, 1990; Gan *et al*, 1994). However with these *in vitro* digestion models, it has been assumed that an instantaneous distribution of equilibrium is to be reached upon drug administration via perfect mixing in the microenvironment of the drugs and their receptors, which is contrary to the anatomical and physiological complexities of the human GIT (Dokoumetzidis *et al*, 2004). Despite simplification of the complex absorptive mechanisms, *in vitro* digestion models have been used as a screening tool widely in the pharmaceutical studies.

2.4.4. *In vitro* digestion models used in the studies of bioavailability of nutrients

The study of bioavailability of nutrients has been very much focused on iron compared to other nutrients. Lately, polyphenols and antioxidants have also gained interests of many authors with regard to the health benefits. The procedures of *in vitro* digestion methods are very similar to that of the toxicological studies, where pepsin-HCl digestion was followed by pH adjustment with NaHCO₃ to near neutral pH of 6.5 to 7.5, and pancreatin-bile digestion followed. Typically glass vessels with a shaking water bath were used as well. Applications of such assays include examining of bioavailability of iron (Miller *et al*, 1981; Gangloff *et al*, 1996), vitamin B6 (Ekanayake and Nelson, 1986), cholesterol (Fouad *et al*, 1991), phosphorus (Liu *et al*, 1998), amino acids (Lindberg *et al*, 1998), carotenoid bioavailability from meals (Garrett *et al*, 1999), lipid digestion (Sek *et al*, 2001), angiotensin I converting enzyme inhibitory activity of soy protein digests (Lo *et al*, 2006), dietary fiber and oil-in-water emulsions (Beysseriat *et al*, 2006), digestibility assay of bovine and caprine milk (Almaas *et al*, 2006), bioaccessibility of carotenes from carrots, and the effects of cooking and addition of oil (Hornero-Méndez and Mínguez-Mosquera, 2007), stability of anthocyanins from red cabbage (McDougall *et al*, 2007), effects of baking on protein digestibility of organic spelt products (Abdel-Aal, 2008), bioaccessibility of some essential elements from wheatgrass (Kulkarni *et al*, 2007), behaviour and susceptibility to degradation of barley β -glucan in wheat bread (Cleary *et al*, 2007), nutritional evaluation of β -glucan enrichment in breads (Brennan and Cleary, 2007).

However with nutritional studies, the use of dialysis bag has been noticed often to accomplish a gradual pH change at the early stage of dialysis and continuous removal of dialyzable components during the digestion period (Gauthier *et al*, 1986; Shiowata *et al*, 2006). Such dialysis method has been used to study the influence of amla fruits on the bioavailability of iron from staple cereals and pulses (Gowri *et al*, 2001) and bioaccessibility of total phenols from diet (Saura-Calixto *et al*, 2007). Cámara *et al* (2005) used dialysis method with homogenized meal and deionized distilled water. Cámara *et al* (2005) also used solubility method, with homogenized meal and deionized distilled water placed for pepsin-HCl digestion, followed by adjustment of pH to 5 by adding NaHCO₃, then pancreatin-bile salt mixture incubation, then ice bath to stop intestinal digestion. Shiowatana *et al* (2006) used dynamic continuous-flow dialysis method to simulate

intestinal digestion for *in vitro* estimation of mineral bioavailability of foods. Alexandropoulou *et al* (2006) studied effects of iron, ascorbate, meat and casein on the antioxidant capacity of green tea under conditions of *in vitro* digestion. For *in vitro* digestion, Alexandropoulou *et al* (2006) used 4.5hrs of shaking water bath incubation at 37°C, at different pHs, in the presence of pepsin, pancreatin and bile extract and by fractionating digests through a dialysis membrane, as used by Kapsokoufalou and Miller (1991) who studied the iron availability. Similarly, the methods of Kapsokoufalou and Miller (1991) has been used for the studies of iron availability from plant foods (Hazell and Johnson, 1987), iron absorption in humans, comparing the bovine serum albumin with beef muscle and egg whites (Hurrell *et al*, 1988), the formation of dialyzable iron during *in vitro* digestion and extraction of mycoproteins (Karava *et al*, 2007) and the iron availability from milk-based formulas and fruit juices containing milk and cereals (Perales *et al*, 2007).

The absorption of nutrients such as coenzyme Q10 (Bhagavan *et al*, 2007) and polyphenols in chokeberry (Bermúdez-Soto *et al*, 2007), has been studied with *in vitro* digestion models containing Caco-2 cells. The study of nutrient absorption was not as widely used as dialysis bag methods, however, the initial steps of enzymatic digestions were exactly the same. Sanz and Luyten (2007) incorporated mouth part into their *in vitro* digestion model to further investigate the digestion by salivary amylase in evaluating genistein bioaccessibility from enriched custard. However the procedures were typically the same compared to the enzymatic incubations used by other studies.

With the growing interests of polyphenols and intake of balanced nutrients, advanced *in vitro* digestion models that are specifically designed for the study of nutrient bioavailability must be developed. As some nutrients require specific targeting of tissue or location in the GIT to enhance the extent of benefits, innovative absorption mechanisms would be of a demand in the future developments.

2.4.5. *In vitro* digestion experimental models for the studies of animal GIT

A number of *in vitro* digestion models have been developed to study the animal feed and nutrition. Unlike other types of studies, such models were quite distinctive from one

another owing to the absence and/or presence of GI organ(s) among different animals targeted. Pond and Ellis (1988) developed single compartment and two-compartmental models for estimating attributes of digesta flow in cattle, with age-dependent and/or age-independent residence times. Porcine seemed to be the most frequently modeled animal for the *in vitro* studies. The influence of gastric conditions on the efficacy of phytase has been studied with the TIM-2, which represents porcine stomach (Minekus *et al*, 1995). Alternatively, a model ileum of the porcine GI microflora has been used to investigate the effects of vancomycin (Blake *et al*, 2003) and a three-step enzymatic hydrolysis model simulating the stomach, the small and the large intestines, has been developed to determine the kinetics of enzymatic digestion of feeds in pigs (Wilfart *et al*, 2008). Smeets-Peeters *et al* (1999) developed a dynamic *in vitro* model of the canine GIT which seemed to be similar to the TIM-1 and 2, to study the effects of vitamin D on the absorption of calcium in dogs (Smeets-Peeters *et al*, 2000).

Estimation of digestibility of equine feeds by simulating the digestion processes of pre-caecal and hind gut has been conducted by Abdouli and Attia (2007). In their two-stage *in vitro* technique, horse faeces were inoculated as a source of microbiota, which has been used by the studies of the SHIME. With a neonatal rabbit model developed by Mehall *et al* (2001), bacterial translocation and gut colonization with respect to the acidification of the feed formula (Mehall *et al*, 2001) and effects of condensed tannins in white clover flowers on their digestion (Burggraaf *et al*, 2007) have been studied. However with these animal models, the extent of simulating the conditions of the GIT is relatively insignificant, and yet remains with lack of interest when compared to the human *in vitro* digestion models.

2.4.6. *In vitro* experimental models of mouth

Recently, assessments of oral processing (Prinz and Lucas, 1997; Daumas *et al*, 2005; Grgic *et al*, 2006; Prinz *et al*, 2007), flavor release (Van Ruth and Roozen, 2000; Sanz and Luyten, 2006a; Sanz and Luyten, 2006b; Salles *et al*, 2007) and sensory studies (Tang *et al*, 2003; Terpstra *et al*, 2005) have been conducted via *in vitro* mouth reactors. The development of the *in vitro* mouth reactors has yet been extensively studied unlike other types of mechanical *in vitro* digestion models (Dean and Ma, 2007). Sanz and Luyten (2006a) and (2006b) have used a series of incubation steps to combine the mouth part

with the stomach and the intestine. In order to fully exert the simulation of the human conditions, it would be very useful to incorporate mouth part into the *in vitro* digestion models. However the level of oral processing required, such as the time and force of chewing, achieving a high level of simulating the human conditions yet remains to be answered.

2.5. Improvements required by the existing *in vitro* digestion models

Despite the development of numerous *in vitro* digestion models to suit for various types of studies as discussed, the extent of simulations provided by such models is yet primitive as the correlations between the *in vivo* and *in vitro* studies and the consistency of the predictive values remain uncertain. Many of the available *in vitro* digestion models are suited to routine laboratory applications due to completion without the need of specialised materials, equipments or technicians (Coles *et al*, 2005). Alternatives to the building materials of the *in vitro* digestion models can be suggested as the existing models are mostly composed of glass reactors. Random adhesion, adsorption and colonization of bacteria and nutrients on the glass wall surfaces may result biased sampling, causing inevitable errors in enumeration for determining the viability of microbial strains and alterations to the competitive interactions in the microflora (Alander *et al*, 1999; Mainville *et al*, 2005; Spratt *et al*, 2005). Dominy *et al* (2004) modeled clay adhesion to the GI epithelium which resulted in low analytes recoveries, with unclear reasons.

Use of a magnetic stirrer or a shaking water bath to simulate the peristaltic mixing of the GIT may be simple but is inappropriate as the mixing patterns cannot reproduce the fluid mechanics and the shear forces encountered at the walls of human GIT (Spratt *et al*, 2005). Food emulsions generally exhibit non-Newtonian viscoelastic behavior (Malone *et al*, 2003) which may result in constipation (blockage) in the model if the applied motility is not effective. However, many of the existing models did not mention the rate of stirring speeds for each compartment (Macfarlane *et al*, 1998a and 1998b; Vatier *et al*, 1998a and 1998b). Failure in the simulation of the peristaltic motility often leads to alterations in the transit time, modifying the distributions of substrates and microbes throughout the GIT. This in turn may influence the wall growth, the inoculation of growth media and the breakdown of food and novel compounds (Spratt *et al*, 2005).

GI secretions with comprehensive compositions including appropriate amounts of digestive enzymes such as salivary α -amylase, lingual lipase, pepsin, gastric lipase, pancreatic lipase and bile salts, can be considered as relatively a straightforward improvement to the existing method. Due to the expenses and lack of availability of the human digestive enzymes, porcine, plant or bacterial sources of enzymes have been replacing the human enzymes. However considering the biochemical properties and gene ontology functional annotations, the replacement enzymes are often very similar to that of the humans. Sequential use of such enzymes, ionic components and metabolites of the GI secretions at physiological levels have been constantly neglected by the existing *in vitro* models though these can be of a great importance for the lubrication of the mucosa, intraluminal microbial defence and for appropriate functioning of the GIT (Bengmark, 1998; Vatier *et al*, 1998a). Methods of delivering the GI secretions were either via peristaltic pumps (Havenaar and Minekus, 1996) or via auto-burettes (Vatier *et al*, 1998b; Fatouros *et al*, 2007) with computer control for punctual delivery to each compartment. However, this is analogous to using pipettes and thus do not mimic the secretions from the wall of the GIT *in vivo*. Differences of substrate concentrations along the compartments have been observed (Ballyk *et al*, 2001) which caused bias in substrate availability, thereby reducing the growth of some bacterial strains due to repression of enzyme synthesis. Rate of the GI secretions should also be carefully controlled and maintained to simulate the pH of different parts of the GIT with respect to time. This would be of a great importance especially for the pharmaceutical *in vitro* digestion models as drug compounds are ionic (anionic or cationic) and surface interactions involving electrostatic repulsions may occur due to unnecessary fluctuations in the pH. Highly acidic environment may induce lethality of certain bacteria, side effects of drug compounds and abnormal patterns of food breakdown. Also, variations in pH between the fed and the fasted state may contribute complexity to the model especially in terms of absorption (Hörter and Dressman 1997; Castela-Papin *et al*, 1999). Thus a careful control of the pH is necessary.

Absorption mechanisms for metabolites and water are absent which allows only for the principal interactions of the microbial community to be studied (Molly *et al*, 1993; Mattila-Sandholm *et al*, 1999; De Boever *et al*, 2000). The absence of mucosal cells limits the study of absorption to passive diffusion only (Avantaggiato *et al*, 2003; Souliman *et al*, 2006), which is dependent on the rate of release of the compound of interest, digestive degradation, solubilisation and interaction with other components in the chyme. However the efficiency of intestinal absorption arises from whether the stomach

is in fasted or fed state as well (Stops *et al*, 2006). Thus the models designed for pharmaceutical studies in particular, should develop new absorption mechanisms for more accurate outcomes.

Inoculation of human faecal bacteria, which is not representative of the human colon microbial community (Boisseau, 1993), should be avoided for the future studies. Strictly anaerobic environment with exclusion of any gas release during the digestion are also essential with microecological studies. A stabilization period must be provided for the ingested microbes to establish and colonize in the *in vitro* digestion models. Control of the microbial community distribution along the different parts of the GIT would be desirable as it would allow selecting for the bacterial strains of interest and gain control over the saturation of unwanted bacterial strains. Use of selective medium and controlled release of the culture medium may also contribute to the control of the microbial community (Macfarlane *et al*, 1998a and 1998b; Vatier *et al*, 1998a and 1998b).

Application of hormonal controls, which is also known as feed-back mechanisms of the central nervous system, is an important perspective missing in the existing *in vitro* digestion models. Inadequate assumptions of steady equilibrium state neglected the fasting and the fed states. This led to continuous GI secretions at maximum rate and steady-state motility via peristaltic pumps or magnetic stirring, hence simulating incompetent physiological conditions of the humans. Immunological aspects of the human GIT have also been completely omitted in the existing *in vitro* digestion models. Studies of the potential allergenicity of food proteins require immunological assays where the influence of the food matrix on the GI absorption, subsequent stimulation of the immune system and specific immunoglobulin-binding role of the allergens can be monitored (Moreno, 2007).

Addition of the mouth compartment to the existing *in vitro* digestion models can be an extension for the future models as it would be useful to assist the studies of sensory perceived during the ingestion period. The mouth compartment would enable a range of quantity and quality of different foods and different ratio of solid to liquid meals with variable ingestion rates to be controlled easily without the use of a homogenizer or liquidized test meals, thus the conditions of the imperfect non-equilibrium states can be studied in less ambiguous ways. Lack of justification/validation, repeatability, robustness and testing with a range of substrates can also be improved for the forthcoming *in vitro* digestion models.

Considering the recommended improvements to the existing *in vitro* digestion models, a building material of non-reactive, transparent and flexible properties with the visual aids of realistic physical geometry and dimensions can be expected. Better understanding of the GI secretions and motility would facilitate the modeling process to provide a closer view to the dynamic interactions within the human GI system. With a series of computer-controlled validated compartments of mouth, esophagus, stomach, duodenum, jejunum, ileum and the colon, more accurate and reliable predictions could be expected, and mathematical and/or computational modeling can be integrated to enhance the overall analytical predictions. Therefore time-consuming and costly *in vivo* studies can be minimized or even replaced by the *in vitro* digestion models.

2.6. References

- Abdel-Aal, E. S. M. (2008) Effects of baking on protein digestibility of organic spelt products determined by two *in vitro* digestion methods. *LWT-Food Science and Technology*, 41 (7), 1282-1288
- Abdouli, H., Attia, S. B. (2007) Evaluation of a two-stage *in vitro* technique for estimating digestibility of equine feeds using horse faeces as the source of microbial inoculum. *Animal Feed Science and Technology*, 132, 155-162
- Alander, M., De Smet, I., Nollet, L., Verstraete, W., Von Wright, A., Mattila-Sandholm, T. (1999) The effect of probiotic strains on the microbiota of the simulator of the human intestinal microbial ecosystem (SHIME). *International Journal of Food Microbiology*, 46, 71-79
- Alexandropoulou, I., Komaitis, M., Kapsokefalou, M. (2006) Effects of iron ascorbate, meat and casein on the antioxidant capacity of green tea under conditions of *in vitro* digestion. *Food Chemistry*, 94, 359-365
- Allison, C., McFarlan, C., Macfarlane, G.T. (1989) Studies on mixed populations of human intestinal bacteria grown in single-stage and multistage continuous culture system. *Applied and Environmental Microbiology*, 55 (3), 672-678
- Almaas, H., Cases, A-L., Devold, T. G., Holm, H., Langsrud, T., Aabakken, L., Aadnoey, T., Vegarud, G. E. (2006) *In vitro* digestion of bovine and caprine milk by human gastric and duodenal enzymes. *Int. Dairy J.*, 16, 961-968
- Avantaggiato, G., Havenaar, R., Visconti, A. (2003) Assessing the zearalenone-binding activity of adsorbent materials during passage through a dynamic *in vitro* gastrointestinal model. *Food and Chemical Toxicology*, 41, 1283-1290
- Ballyk, M. M., Jones, D.A., Smith, H.L. (2001) Microbial competition in reactors with wall attachment: a mathematical comparison of chemostat and plug flow models. *Microbial Ecology*, 41, 210-221
- Bengmark, S. (1998) Leading article: Ecological control of the gastrointestinal tract. The role of probiotic flora. *Gut*, 42, 2-7
- Bermúdez-Soto, M. J., Tomas-Barberan, F. A., Garcia-Conesa, M. T. (2007) Stability of polyphenols in chokeberry (*aronia melanocarpa*) subjected to *in vitro* gastric and pancreatic digestion. *Food Chemistry*, 102, 865-874
- Beysseriat, M., Decker, E. A., McClements, D. J. (2006) Preliminary study of the influence of dietary fiber on the properties of oil-in-water emulsions passing through an *in vitro* human digestion model *Food Hydrocolloids*, 20, 800-809

- Bhagavan, H. N., Chopra, R. K., Craft, N. E., Chitchumroonchokchai, C., Failla, M. L. (2007) Assessment of coenzyme Q10 absorption using an *in vitro* digestion caco-2 cell model. *Int. J. Pharma.*, 333, 112-117
- Blake, D.P., Hillman, K., Fenlon, D.R. (2003) The use of a model ileum to investigate the effects of novel and existing antimicrobials on indigenous porcine gastrointestinal microflora: using vancomycin as an example. *Animal Feed Science and Technology*, 103, 123-139
- Blanquet, S., Meunier, J.P., Minekus, M., Marol-Bonnin, S., Alric, M. (2003) Recombinant *Saccharomyces cerevisiae* expressing P450 in artificial digestive systems: a model for biotransformation in the human digestive environment. *Applied and Environmental Microbiology*, 69(5), 2884-2892
- Blanquet, S., Evelijn, Z., Beyssac, E., Meunier, J-P., Denis, S., Havenaar, R., Alric, M. (2004). A dynamic artificial gastrointestinal system for studying the behavior of orally administered drug dosage forms under various physiological conditions. *Pharmaceutical Research*, 21 (4), 585-591
- Blanquet, S., Garrat, G., Beyssac, E., Perrier, C., Denis, S., Hébrad, G., Alric, M. (2005). Effects of cryoprotectants on the viability and activity of freeze dried recombinant yeasts as novel oral drug delivery systems assessed by an artificial digestion system. *Euro. J. Pharm. Biopharm.*, 61, 32-39
- Boisen, S., Eggum, B. O. 1991. Critical evaluation of *in vitro* methods for estimation of digestibility in simple stomach animals. *Nutrition Research Reviews*, 4, 141-162
- Boisseau J. (1993) Basis for the evaluation of the microbiological risks due to veterinary drug residues in food. *Veterinary Microbiology*, 35, 187-192
- Brandon, E. A., Oomen, A. G., Rompelberg, C. J. M., Versantvoort, C. H. M., Van Engelen, J. G. M., Sips, A. J. A. M. (2006) Consumer product *in vitro* digestion model: bioaccessibility of contaminants and its application in risk assessment. *Regulatory Toxicology and Pharmacology*, 44, 161-171
- Brennan, C. S., Cleary, L. J. (2007) Utilisation Glucagel® in the β -glucan enrichment of breads: a physicochemical and nutritional evaluation. *Food Res. Int.*, 40, 291-296
- Brück, W.M., Graverholt, G., Gibson, G.R. (2002) Use of batch culture and a two-stage continuous culture system to study the effect of supplemental α -lactalbumin and glycomacropeptide on mixed populations of human gut bacteria. *FEMS Microbiology Ecology*, 41, 231-237
- Burggraaf, V., Waghorn, G., Woodward, S., Thom, E. (2007) Effects of condensed tannins in white clover flowers on their digestion *in vitro*. *Animal Feed Science and Technology*, 142 (1-2), 44-58
- Cámara, F., Amaro, M. A., Barberá, R., Clemente, G. (2005) Bioaccessibility of minerals in school meals: comparison between dialysis and solubility methods. *Food Chemistry*, 92, 481-489
- Castela-Papin, N., Cai, S., Vatier, J., Keller, F., Souleau, C.H., Farinotti, R. (1999) Drug interactions with diosmectite: a study using the artificial stomach-duodenum model. *International Journal of Pharmaceutics*, 182, 111-119
- Chavanpatil, M., Jain, P., Chaudhari, S., Shear, R., Vavia, P. (2005) Development of sustained release gastroretentive drug delivery system for ofloxacin: *in vitro* and *in vivo* evaluation. *International Journal of Pharmaceutics*, 304, 178-184
- Cleary, L. J., Andersson, R., Brennan, C. S. (2007) The behavior and susceptibility to degradation of high and low molecular weight barley β -glucan in wheat bread during baking and *in vitro* digestion. *Food Chemistry*, 102, 889-897
- Coles, L. T., Moughan, P. J., Darragh, A. J. (2005) *In vitro* digestion and fermentation methods, including gas production techniques, as applied to nutritive evaluation of foods in the hindgut of humans and other simple-stomached animals. *Animal Feed Science and Technology*, 123-124, 421-444
- Daumas, B., Xu, W. L., Bronlund, J. (2005) Jaw mechanism modelling and simulation. *Mechanism and Machine Theory*, 40, 821-833
- Dean, J. R., Ma, R. (2007) Approaches to assess the oral bioaccessibility of persistent organic pollutants: A critical review. *Chemosphere*, 68, 1399-1407
- De Boever, P., Deplancke, B., Verstraete, W. (2000) Fermentation by gut microbiota cultured in a simulator of the human intestinal microbial ecosystem is improved by supplementing a soy germ powder. *The Journal of Nutrition* 130 (10), 2599-2606

- De Boever, P., Wouters, R., Vermeirssen, V., Boon, N., Verstraete, W. (2001) Development of a six-stage culture system for simulating the gastrointestinal microbiota of weaned infants. *Microbial Ecology in Health and Disease*, 13, 111-123
- Deering, T. B., Carlson, G. L., Malagelada, U. R., Dunes, J. A., McCall, J. T. (1979) Fate of oral neutralizing antacid and its effect on postprandial gastric secretion and emptying. *Gastroenterology*, 77, 986-990
- Dokoumetzidis, A., Karalis, V., Iliadis, A., Macheras, P. (2004) The heterogeneous course of drug transit through the body. *Trends in Pharmacological Sciences*, 25 (3), 140-146
- Dominy, N.J., Davoust, E., Minekus, M. (2004) Adaptive function of soil consumption: an *in vitro* study modeling the human stomach and small intestine. *The Journal of Experimental Biology*, 207, 319-324
- Ekanayake, A., Nelson, P. E. (1986) An *in vitro* method for estimating biologically available vitamin B6 in processed foods. *Br. J. Nutr.*, 55, 235-244
- Fatouros, D. G., Bergenstahl, B., Mullertz, A. (2007). Morphological observations on a lipid-based drug delivery system during *in vitro* digestion. *European J. Pharm. Sci.*, 31, 85-94
- Fordtran, J. S., Walsh, J. H. (1973) Gastric acid secretion rate and buffer content of the stomach after eating. Results in normal subjects and in patients with duodenal ulcer. *J. Clin. Investigations*, 52, 645-657
- Fouad, M. F., Farrell, O. G., Marshall, W. D., Van der Voort, F. R. (1991) *In vitro* model for lipase-catalyzed lipophile release from fats. *J. Agric. Food Chem.*, 39, 150-153
- Galia, E., Horton, J., Dressman, J. B. (1999) Albendazole generics - a comparative *in vivo* study. *Pharm. Res.*, 16, 1871-1875
- Gan, L. S., Eads, C., Niederer, T., Bridgers, A., Yanni, S., Hsyu, P. H., Pritchard, F. J., Thakker, D. (1994) Use of caco-2 cells as an *in vitro* intestinal absorption and metabolism model. *Drug Develop. Ind. Pharm.*, 20, 615-631
- Gangloff, M. B., Glahn, R. P., Miller, D. D., Van Campen, D. R. (1996) Assessment of iron availability using combined *in vitro* digestion and caco-2 cell culture. *Nutr. Res.*, 16, 479-487
- Garrett, D.A., Failla, M.L., Sarama, R.J. (1999) Development of an *in vitro* digestion method to assess carotenoid bioavailability from meals. *J. Agric. Food Chem.*, 47, 4301-4309
- Gauthier, S. F., Vachon, C., Savoie, I. (1986) Enzymatic conditions of an *in vitro* method to study protein digestion. *Journal of Food Science*, 51, 960-964
- Gibson, G.R., Cummings, J.H., Macfarlane, G.T. (1988) Use of a three-stage continuous culture system to study the effect of mucin on dissimilatory sulfate reduction and methanogenesis by mixed populations of human gut bacteria. *Applied and Environmental Microbiology* 54(11), 2750-2755
- Gmeiner, M., Kneifel, W., Kulbe, K.D., Wouters, R., De Boever, P., Nollet, L., Verstraete, W. (2000) Influence of a symbiotic mixture consisting of *Lactobacillus acidophilus* 74-2 and a fructooligosaccharide preparation on the microbial ecology sustained in a simulation of the human intestinal microbial ecosystem (SHIME reactor). *Applied Microbiology & Biotechnology*, 53, 219-223
- Gowri, B. S., Platel, K., Prakash, J., Srinivasan, K. (2001) Influence of amla fruits (*Embllica officinalis*) on the bioavailability of iron from stable cereals and pulses. *Nutrition Research*, 21, 1483-1492
- Grgic, B., Martin, A. R., Finlay, W. H. (2006) The effect of unsteady flow rate increase on *in vitro* mouth-throat deposition of inhaled boluses. *Aerosol Science*, 37, 1222-1233
- Hack, A., Selenka, F. (1996) Mobilization of PAH and PCB from contaminated soil using a digestive tract model. *Toxicology Letters*, 88, 199-210
- Haraldsson, A-K., Rimsten, L., Alminger, M., Andersson, R., Aman, P., Sandberg, A-S. (2005). Digestion of barley malt porridges in a gastrointestinal model: Iron dialysability, iron uptake by Caco-2 cells and degradation of β -glucan. *J. Cereal Sci.*, 42, 243-254
- Harrison, A. P., Erlwanger, K. H., Elbrond, V. S., Andersen, N. K., Unmack, M. A. (2004). Gastrointestinal tract models and techniques for use in safety pharmacology. *J. Pharma. Toxic. Methods.*, 49, 187-199
- Havenaar, R., Minekus, M. (1996) Simulated Assimilation. *Dairy Industries International*, 61(9), 17-20
- Hazell, T., Johnson, I. T. (1987) *In vitro* estimation of iron availability from a range of plant foods: influence of phytate, ascorbate and citrate. *British Journal of Nutrition*, 57, 223-233

- Herling, A.W., Ljungström, M. (1988) Effects of verapamil on gastric acid secretion in vitro and in vivo. *European Journal of Pharmacology*, 156, 341-350
- Herman, R. A., Korjagin, V. A., Schafer, B. W. (2005) Quantitative measurement of protein digestion in simulated gastric fluid. *Regulatory Toxicology and Pharmacology*, 41, 175-184
- Herman, R. A., Storer, N. P., Gao, Y. (2006) Digestion assays in allergenicity assessment of transgenic proteins. *Environmental Health Perspectives*, 114 (8), 1154-1157
- Hidalgo, I. J., Raub, T. J., Borchardt, R. T. (1989) Characterization of the human colon carcinoma cell line (Caco-2) as a model system for intestinal epithelial permeability. *Gastroenterology*, 96, 736-749
- Hilgers, A. R., conradi, R. A., Burton, P. S. (1990) Caco-2 cell monolayers as a model for drug transport across the intestinal mucosa. *Pharm. Res.*, 7, 902-910
- Hornero-Méndez, D., Mínguez-Mosquera, M. I. (2007) Bioaccessibility of carotenes from carrots: effect of coking and addition of oil. *Innovative Food Science and Emerging Technologies*, 8 (3), 407-412
- Hörter, D., Dressman, J.B. (1997) Influence of physicochemical properties on dissolution of drugs in the gastrointestinal tract. *Advanced Drug Delivery Reviews*, 25, 3-14
- Hörter, D., Dressman, J.B. (2001) Influence of physicochemical properties on dissolution of drugs in the gastrointestinal tract. *Advanced Drug Delivery Reviews*, 46, 75-87
- Hurrell, R. F., Lynch, S. R., Trinidad, T. P., Dassenko, S. A., Cook, J. D. (1988) Iron absorption in humans: bovine serum albumin compared with beef muscle and egg white. *Am. J. Clin. Nutr.*, 47, 102-107
- Kapsokefalou, M., Miller, D. D. (1991) Effects of meat and selected food components on the valence of nonheme iron during in vitro digestion. *J. Food Sci.*, 56 (2), 352-358
- Karava, N. B., Shinde, R. M., Mahoney, R. R. (2007) Formation of dialyzable iron during in vitro digestion and extraction of mycoprotein. *Food Chemistry*, 105 (4), 1630-1635
- Kobayashi, M., Sada, N., Sugawara, M., Iseki, K., Miyazaki, K. (2001) Development of a new system for prediction of drug absorption that takes into account drug dissolution and pH change in the gastrointestinal tract. *Int. J. Phar.*, 221, 87-94
- Kontula, P., Jaskari, J., Nollet, L., De Smet, I., Von Wright, A., Poutanen, K., Mattila-Sandholm, T. (1998) The colonization of a simulator of the human intestinal microbial ecosystem by a probiotic strain fed on a fermented oat bran product: effects on the gastrointestinal microbiota. *Appl. Microbiol. Biotechnol.*, 50, 246-252
- Kopper, R. A., West, C. M., Helm, R. M. (2006) Comparison of physiological and *in vitro* porcine gastric fluid digestion. *Int. Arch. Allergy Immunol.*, 141, 217-222
- Krul, C., Luiten-Schuite, A., Baan, R., Verhagen, H., Mohn, G., Feron, V., Havenaar, R. (2000) Research Section: Application of a dynamic in vitro gastrointestinal tract model to study the availability of food mutagens, using heterocyclic aromatic amines as model compounds. *Food and Chemical Toxicology*, 38, 783-792
- Krul, C. A. M., Zeilmaker, M. J., Schothorst, R. C., Havenaar, R. (2004) Intra-gastric formation and modulation of N-nitrosodimethylamine in a dynamic in vitro gastrointestinal model under human physiological conditions. *Food and Chemical Toxicology*, 42, 51-63
- Kulkarni, S. D., Acharya, R., Rajurkar, N. S., Reddy, A. V. R. (2007) Evaluation of bioaccessibility of some essential elements from wheatgrass (*Triticum aestivum* L.) by in vitro digestion method. *Food Chemistry*, 103, 681-688
- Lake-Bakaar, G., Tom, W., Lake-Bakaar, D., Gupta, N., Beidas, S., Elaskr, M., Straus, E. (1988) Gastropathy and ketoconazole malabsorption in the acquired immunodeficiency syndrome (AIDS). *Ann. Intern. Med.*, 109, 471-473
- Liu, J., Leodoux, D. R., Veum, T. L. (1998) In vitro prediction of phosphorous availability in feed ingredients for swine. *J. Agric. Chem.*, 46, 2678-2681
- Lee, K.Y., Heo, T.R. (2000) Survival of *Bifidobacterium longum* immobilized in calcium alginate beads in simulated gastric juices and bile salt solution. *Applied and Environmental Microbiology*, 66 (2), 869-873
- Lindberg, T., Engberg, S., Sjoberg, L. B., Lonnerdal, B. (1998) In vitro digestion of proteins in human milk fortifiers and in preterm formula. *J. Pediatric Gastroenterol. Nutr.*, 27, 30-36
- Lo, W. M. Y., Farnworth, E. R., Li-Chan, E. C. Y. (2006) Angiotensin I - converting enzyme inhibitory activity of soy protein digests in a dynamic model system simulating the upper gastrointestinal tract. *J. Food Sci.*, 71 (3), S231-S237

- Macfarlane, G.T., Macfarlane, S., Gibson, G.R. (1998a) Validation of a three-stage compound continuous culture system for investigating the effect of retention time on the ecology and metabolism of bacteria in the human colon. *Microb. Ecol.*, 35, 180-187
- Macfarlane, S., Quigley, M.E., Hopkins, M.J., Newton, D.F., Macfarlane, G.T. (1998b) Polysaccharide degradation by human intestinal bacteria during growth under multi-substrate limiting conditions in a three-stage continuous culture system. *FEMS Microbiology Ecology*, 26, 231-243
- Mainville, I., Arcand, Y., Farnworth, E.R. (2005) A dynamic model that simulates the human upper gastrointestinal tract for the study of probiotics. *International Journal of Food Microbiology*, 99, 287-296
- Maisonnier-Grenier, S., Clavurier, K., Saulnier, L., Bonnin, E., Geraert, P. (2006) Biochemical characteristics of wheat and their relation with apparent metabolisable energy value in broilers with or without non-starch polysaccharide enzyme. *J. Sci. Food Agric.*, 86, 1714-1721
- Malagelada, J. R., Longstreth, G. F., Summerskill, W. H. J., Go, V. L. W. (1976) Measurement of gastric functions during digestion of ordinary solid meals in man. *Gastroenterology*, 70, 203-210
- Malone, M.E., Appelqvist, I.A.M., Norton, I.T. (2003) Oral behavior of food hydrocolloids and emulsions. Part 1. Lubrication and deposition considerations. *Food Hydrocolloids* 17, 763-773
- Marteau, P., Minekus, M., Havenaar, R., Huis in't Veld, J.H.J. (1997) Survival of Lactic Acid Bacteria in a dynamic model of the stomach and small intestine: validation and the effects of bile. *J. Dairy Science*, 80, 1031-1037
- Mattila-Sandholm, T., Mättö, J., Saarela, M. (1999) Lactic acid bacteria with health claims-interactions and interference with gastrointestinal flora. *International Dairy Journal*, 9, 25-35
- McDougall, G. J., Fyffe, S., Dobson, P., Stewart, D. (2007) Anthocyanins from red wine – their stability under simulated gastrointestinal digestion. *Phytochemistry*, 66, 2540-2548
- McGinity, J., Lach, J. (1976). In vitro adsorption of various pharmaceuticals to montmorillonite. *J. Pharm. Sci.*, 65, 896-902
- Mehall, J. R., Northrop, R., Saltzman, D. A., Jackson, R. J., Smith, S. D. (2001) Acidification of formula reduces bacterial translocation and gut colonization in a neonatal rabbit model. *J. Pediatric Surgery*, 36 (1), 56-62
- Miller, D. D., Schriker, B. R., Rasmussen, R. R., Van Campen, D. (1981). An *in vitro* method for the estimation of iron from meals. *Am. J. Clin. Nutr.*, 34, 2248-2256
- Miller, T.L., Wolin, M.J. (1981) Fermentation by the human large intestine microbial community in an in vitro semi continuous culture system. *Applied and Environmental Microbiology*, 42 (3), 400-407
- Minekus, M., Marteau, P., Havenaar, R., Huis in't Veld, J. H. J. (1995). A multicompartmental dynamic computer-controlled model simulating the stomach and small intestine. *Alternatives to Laboratory Animals*, 23, 197-209
- Minekus, M., Smeets-Peeters, M., Bernalier, A., Marol-Bonnin, S., Havenaar, R., Marteau, P., Alric, M., Fonty, G., Huis in't Veld, J.H.J. (1999) A computer-controlled system to simulate conditions of the large intestine with peristaltic mixing, water absorption and absorption of fermentation products. *Appl. Microbiol. Biotechnol.*, 53, 108-114
- Molly, K., Woestyne, M. V., Verstraete, W. (1993) Development of a 5-step multi-chamber reactor as a simulation of the human intestinal microbial ecosystem. *Appl. Microbiol. Biotechnol.*, 39, 254-258
- Moreno, F. J. (2007) Gastrointestinal digestion of food allergens: Effect on their allergenicity. *Biomedicine & Pharmacotherapy*, 61, 50-60
- Norris, D.A., Puri, N, Sinko, P.J. (1998) The effect of physical barriers and properties on the oral absorption of particulates. *Advanced Drug Delivery Reviews*, 34, 135-154
- Ogata, H., Aoyagi, N., Kaniwa, N., Ejima, A., Suzuki, K., Ishioka, T., Morishita, M., Ohta, K., Takagishi, Y., Doi, Y., Ogura, T. (1984) Development and evaluation of new peroral test agent GA-test for assessment of gastric acidity. *J. Pharmacobiodyn.*, 7, 656-664
- Oomen, A. G., Sips, A. J. A. M., Groten, J. P., Sijm, D.T. H. M., Tolls, J. (2000). Mobilization of PCBs and Lindane from soil during *in vitro* digestion and their distribution among bile salt micelles and proteins of human digestive fluid and the soil. *Environ. Sci. Technol.*, 34, 297-303
- Oomen, A. G., Rompelberg, C. J. M., Bruil, M. A., Dobbe, C. J. G., Pereboom, D. P. K. H., Sips, A. J. A. M. (2003). Development of an *in vitro* digestion mode for estimating the bioaccessibility of soil contaminants. *Arch. Environ. Contam. Toxicol.*, 44, 281-287

- Paramithiotis, S., Melissari, I., Drosinos, E.H. (2006) *In vitro* assessment of properties associated with the survival through the gastro-intestinal tract of staphylococci isolated from traditional sausage fermentation. *Food Microbiology*, 23, 663-671
- Perales, S., Barbera, R., Lagarda, M. J., Farre, R. (2007) Availability of iron from milk-based formulas and fruit juices containing milk and cereals estimated by *in vitro* methods (solubility, dialysability) and uptake and transport by Caco-2 cells. *Food Chemistry*, 102, 1296-1303
- Pond, K. R., Ellis, W. C. (1988) Compartment models for estimating attributes of digesta flow in cattle. *Brit. J. Nutri.*, 60, 571-595
- Porubcan, L., Serna, C., White, J., Hem, S. (1978). Mechanism of adsorption of clindamycin and tetracyclin by montmorillonite. *J. Pharm. Sci.*, 67, 1081-1087
- Possemiers, S., Verthé, K., Uyttendaele, S., Verstraete, W. (2004) PCR-DGGE –based quantification of stability of the microbial community in a simulator of the human intestinal microbial ecosystem. *FEMS Microbiology Ecology* 49, 495-507
- Possemiers, S., Camp, J.V., Bolca, S., Verstraete, W. (2005) Characterization of the bactericidal effect of dietary sphingosine and its activity under intestinal conditions. *International Journal of Food Microbiology* 105, 59-70
- Prinz, J. F., Lucas, P. W. (1997) An optimization model for mastication and swallowing in mammals. *Proc. R. Soc. Lond.*, 264, 1715-1721
- Prinz, J. F., Janssen, A. M., De Wijk, R. A. (2007) *In vitro* simulation of the oral processing of semi-solid foods. *Food Hydrocolloids*, 21, 397-401
- Rodriguez, R., Basta, N. T., Casteel, S. W., Pace, I. W. (1999) An *in vitro* gastrointestinal method to estimate bioavailable arsenic in contaminated soils and solid media. *Environ. Sci. Technol.*, 33, 642-649
- Ruby, M. V., Davis, A., Kempton, J. H., Drexler, J. W., Bergstrom, P. D. (1992) Lead bioavailability: dissolution kinetics under simulated gastric conditions. *Environ. Sci. Technol.*, 26 (6), 1242-1248
- Ruby, M. V., Davis, A., Schoof, R., Eberle, S., Sellstone, C. M. (1996) Estimation of lead and arsenic bioavailability using a physiologically based extraction test. *Environ. Sci. Technol.*, 30, 422-430
- Ruby, M. V., Schoof, R., Brattin, W., Goldade, M., Post, G., Harnois, M., Mosby, D. E., Casteel, S. W., Berti, W., Carpenter, M., Edwards, D., Cragin, D., Chappe, W. (1999) Advances in evaluating the oral bioavailability of inorganics in soil for use in human health risk assessment. *Environ. Sci. Technol.*, 33 (21), 3697-3705
- Salles, C., Tarrega, A., Mielle, P., Maratray, J., Gorria, P., Liaboeuf, J., Liodenot, J. J. (2007) Development of a chewing simulator for food breakdown and the analysis of *in vitro* flavour compound release in a mouth environment. *Journal of Food Engineering*, 82, 189-198
- Sanz, T., Luyten, H. (2006a) Release, partitioning and stability of isoflavones from enriched custards during mouth, stomach and intestine *in vitro* simulations. *Food Hydrocolloids*, 20, 892-900
- Sanz, T., Luyten, H. (2006b) Effect of thickening agent in the *in vitro* mouth, stomach and intestine release of tyrosol from enriched custards. *Food Hydrocolloids*, 20, 703-711
- Sanz, T., Luyten, H. (2007) *In vitro* evaluation of genistein bioaccessibility from enriched custards. *Food Hydrocolloids*, 21, 203-211
- Saura-Calixto, F., Serrano, J., Goni, I. (2007) Intake and bioaccessibility of total polyphenols in a whole diet. *Food Chemistry*, 101, 492-501
- Savage, G. P., Catherwood, D. J. (2007) Determination of oxalates in Japanese taro corms using an *in vitro* digestion assay. *Food Chemistry*, 105 (1), 383-388
- Savalle, B., Miranda, G., Pelissier, J. P. (1989) *In vitro* simulation of gastric digestion of milk proteins. *J. Agric. Food Chem.*, 37, 1336-1340
- Savoie, L. 1994. Digestion and absorption of food: Usefulness and limitations of *in vitro* models. *Can. J. Physiol. Pharmacol.*, 72, 407-414
- Schroder, J. L., Basta, N. T., Si, J., Casteel, S. W., Evans, T., Payton, M. (2003) *In Vitro* Gastrointestinal Method To Estimate Relative Bioavailable Cadmium in Contaminated Soil. *Environ. Sci. Technol.*, 37 (7), 1365-1370
- Schroder, J. L., Basta, N. T., Casteel, S. W., Evans, T. J., Payton, M. E., Si, J. (2004) Validation of the *in vitro* gastrointestinal (IVG) method to estimate relative bioavailable lead in contaminated soils. *J. Environ. Quality*, 33 (2), 513-521

- Sek, L., Porter, C. J. H., Charman, W. N. (2001) Characterization and quantification of medium chain and long chain triglycerides and their in vitro digestion products, by HPTLC coupled with in situ densitometric analysis. *J. Pharma. Biomed. Anal.*, 25, 651-661
- Shiowatana, J., Kitthikhun, W., Sottimai, U., Promchan, J., Kunajiraporn, K. (2006) Dynamic continuous-flow dialysis method to simulate intestinal digestion for in vitro estimation of mineral bioavailability of food. *Talanta*, 68, 549-557
- Smeets-Peeters, M. J. E., Minekus, M., Havenaar, R., Schaafsma, G., Verstegen, M. W. A. (1999) Description of a dynamic gastrointestinal in vitro model of the dog and evaluation of the different transit times for protein and Ca. *Alternatives to Laboratory Animals (ATLA)*, 27, 935-949
- Smeets-Peeters, M.J.E. (2000). Feeding FIDO: Development, validation and application of a dynamic in vitro model of the gastrointestinal tract of the dog. PhD Thesis Wageningen University. Universal Press, Veenendaal, The Netherlands
- Souliman, S., Blanquet, S., Beyssac, E., Cardot, J.M. (2006) A level A in vitro/in vivo correlation in fasted and fed states using different methods: Applied to solid immediate release oral dosage form. *European Journal of Pharmaceutical Sciences*, 27, 72-79
- Spratt, P., Nicolella, C., Pyle, D.L. (2005) An engineering model of the human colon. *Trans IChemE, Part C, Food and Bioproducts Processing*, 83 (C2), 147-157
- Stops, F., Fell, J.T., Collett, J.H., Martini, L.G., Sharma, H.L., Smith, A-M. (2006) The use of citric acid to prolong the in vivo gastro-retention of a floating dosage form in the fasted state. *International Journal of Pharmaceutics* 308, 8-13
- Sugawara, M., Kadomura, S., He, X., Takekuma, Y., Kohri, N., Miyazaki, K. (2005). The use of an in vitro dissolution and absorption system to evaluate oral absorption of two weak bases in pH-independent controlled-release formulations. *Euro. J. Pharm. Sci.*, 26, 1-8
- Tang, G., Yip, H-K., Cutress T. W., Samaranyake, L. P. (2003) Artificial mouth models systems and their contribution to caries research: a review. *Journal of Dentistry*, 31, 161-171
- Takagi, K., Teshima, R., Okunuki, H., Sawada, J. (2003) Comparative study of in vitro digestibility of food proteins and effect of preheating on the digestion. *Biol. Pharm. Bull.*, 26 (7), 969-973
- Terpstra, M. E. J., Janssen, A. M., Prinz, J. F., De Wijk, R. A., Weenen, H., Van der Linden, E. (2005) Modeling of thickness for semisolid foods. *J. Texture Studies*, 36, 213-233
- Trombetta, D., Mondello, M. R., Cimino, F., Cristani, M., Pergolizzi, S., Saija, A. (2005) Toxic effect of nickel in an in vitro model of human oral epithelium. *Toxicology Letters*, 159, 219-225
- Tuleu, C., Andrieux, C., Boy, P., Chaumeil, J.C. (1999) Gastrointestinal transit of pellets in rats: effect of size and density. *International Journal of Pharmaceutics*, 180, 123-131
- Van de Wiele, T. R., Peru, K. M., Verstraete, W., Siciliano, S. D., Headley, J. V. (2004a) Lipid chromatography-mass spectrometry analysis of hydroxylated polycyclic aromatic hydrocarbons, formed in a simulator of the human gastrointestinal tract. *J. Chromatography B*, 806, 245-253
- Van de Wiele, T. R., Boon, N., Possemiers, S., Jacobs, H., Verstraete, W. (2004b) Prebiotic effects of chicory inulin in the simulator of the human intestinal microbial system. *FEMS Microbiology Ecology*, 51, 143-153
- Van Ruth, S. M. and Roozen, J. P. (2000) Influence of mastication and saliva on aroma release in a model mouth system. *Food Chemistry*, 71, 339-345
- Vasiluk, L., Pinto, L. J., Tsang, W. S., Gobas, F. A. P. C., Eickhoff, C., Moore, M. M. (2007) The uptake and metabolism of benzo[a]pyrene from a sample food substrate in an in vitro model of digestion. *Food and Chemical Toxicology*, 46 (2), 610-618
- Vassilopoulou, E., Rigby, N., Moreno, F. J., Zuidmeer, L., Akkerdaas, J., Tassios, I., Papadopoulos, N. G., Saxoni-Papageorgiou, P., Van Ree, R., Mills, C. (2006) Effect of in vitro gastric and duodenal digestion on the allergenicity of grape lipid transfer protein. *J. Allergy Clin. Immunol.*, 118 (2), 473-480
- Vatier, J., Célice-Pingaud, C., Farinotti, R. (1998a) A computerized artificial stomach model to assess sodium alginate-induced pH gradient. *International Journal of Pharmaceutics*, 163, 225-229
- Vatier J., Lionmet, F., Vitre, M. T., Mignon, M. (1988b) A model of an artificial stomach for assessing the characteristics of an antacid. *Aliment. Pharmacol. Therap.*, 2, 461-470
- Versantvoort, C.H.M., Oomen, A.G., de Kamp, E.V., Rompelberg, C.J.M., Sips, A.J.A.M. (2005) Applicability of an in vitro digestion model in assessing the bioaccessibility of mycotoxins from food. *Food and Chemical Toxicology*, 43, 31-40

Wilfart, A., Jaguelin-Peyraud, Y., Simmins, H., Noblet, J., van Milgen, J., Montagne, L. (2008) Kinetics of enzymatic digestion of feeds as estimated by a stepwise in vitro method. *Animal Feed Science and Technology*, 141, 171-183

Chapter 3

Modeling of the *In vitro* Physicochemical Upper Gastrointestinal System (IPUGS) and the Modified *In vitro* Stomach Stir Tank (MISST)

In this chapter, a brief introduction of the key features which should be accounted for when making a physicochemical *in vitro* digestion model is discussed. Selection criteria of the test food materials are also described and a short review of starch hydrolysis and carbohydrates in the test foods is given. Materials and methods used in developing the *In vitro* Physicochemical Upper Gastrointestinal System (IPUGS) and the Modified *In vitro* Stomach Stir Tank (MISST) are discussed in details. The building materials and used by other *in vitro* digestion models in the literature and the MISST are compared and evaluated with that of the IPUGS. The IPUGS is composed of three parts to mimic the upper GIT – mouth, esophagus and stomach. These organs are linked to each other with each section having a manual sphincter control. A series of linked steps in mimicking motility and delivery of secretions to each part of the IPUGS, as well as the realistic composition of the GI secretions used are also described. Preliminary experimental results obtained from the IPUGS and the MISST are discussed.

3.1. Introduction to simulation of the human gastrointestinal functions

The human gastrointestinal tract (GIT) consists of mouth, esophagus, stomach, small intestine and large intestine that are controlled by a coordination of neural and hormonal signals (Burks *et al*, 1985) to maximize digestion and absorption of the ingested compounds. Each GI organ can be considered as a separate compartment with specific digestive function(s) of physiological relevance which should be accounted in simulating the characteristics of the GIT. Such simulations lead to building of a physicochemical model, or so called *in vitro* digestion model, with the intention of studying the fate of various ingested compounds such as nutrients, pharmaceuticals, toxic compounds from soil and children's toys, functional foods, microbials and genetically modified foods.

Table 3-1. Selective criteria to be considered when making a physicochemical model.

Selective Criteria	Possible Variations	IPUGS
Number of the organs to be simulated	Single/Multiple	Multiple
Nature of the organ conditions to be simulated	Static/Dynamic	Static/Dynamic
Anatomical and geometrical aspects	Consider/Ignore	Considered
Nature of the Building materials	Flexible/Rigid	Flexible
Sequential use of digestive enzymes	Yes/No	Yes
Sequential control of pH	Yes/No	Yes
Physiological residence time	Yes/No	Yes
Anaerobic environment	Yes/No	Yes
Control of temperature	Yes/No	Yes
Appropriate composition of GI secretions	Complex/Simplified	Complex
Sources of the digestive GI enzymes	Human/Other	Fungal/Porcine
Feed-back control of the GI secretion rates	Yes/No	Yes
Delivery of the GI secretions simulated	Pouring/Other	Other*
Simulation of peristaltic motility	Yes/No	Yes
Feed-back control of the GI motility	Yes/No	Yes
Absorption of metabolites and water	Yes/No	N/A
Presence of the mucosal lining	Yes/No	Yes
Immune system	Yes/No	No
Appropriate preparation of the test food	Yes/No	Yes
Appropriate ingestion rate of the test food	Yes/No	Yes
Inoculation of native bacteria in the GI	Yes/No	No
Adsorption of ingested bacteria to the GI walls	Yes/No	N/A (Yes)
Reproducibility of data	High/Low	High
Automation/robustness	Yes/No	Partially
Testing of various substances	Yes/No	Possible

Other*: please refer to the section 3.2.2 and Figure 3-2.

The model can be of a single reactor simulating the conditions, either static or dynamic, of one particular organ or multiple reactors sequentially simulating the conditions of more than one GI organ. The use of a physicochemical model is able to assist or may even replace *in vivo* trials with humans and animals, therefore saving time, costs and labor as

well as ethical constraints and restrictions. Often the use of such model is able to produce a large amount of results with higher reproducibility in a much shorter period compared to that of the *in vivo* trials as there are near to none or controllable, batch to batch variations. However, when designing of such model, a definitive aim of the study and the test material must be decided to initiate modeling. For instance, fabrication of a stomach reactor for the study of pharmaceuticals would be significantly different when compared to examining of a probiotic strain for microecological studies because for the drug compounds, absorption and dissolution are the key requirements in simulating the conditions of the stomach, whereas for the probiotics, the targeted area of concern is large intestine, thus the stomach compartment may remain simple to simulate the acidic conditions only. Once the aim of the study and the test material are decided, detailed selective criteria (Table 3-1) should be considered. *In vitro* Physicochemical Upper Gastrointestinal System (IPUGS) has been developed to examine the behavior of nutrients in the upper GIT of humans. Table 3-1 shows a guideline of key features in making a physicochemical model, showing some of the key features of the newly developed IPUGS.

Not all the features listed on the Table 3-1 were included in developing the IPUGS. This may introduce a limitation in the level of simulation; however, compared to other existing *in vitro* digestion models, the IPUGS do contain more specific features such as GI motility, feed-back control as well as delivery of the GI secretions, in order to simulate the human conditions in advance.

3.1.1. Selection criteria of the test meal – Baby Foods vs Rice

The main aim of the physicochemical model, IPUGS, is to study the behavior of nutrients *in vitro* thus it can be used as a screening tool in nutrition studies as well as screening of the behavior of the nutrients in the stomach (for instance rice starch hydrolysis). Selecting of a test meal is of importance when it comes to analyses and validation of such physicochemical model.

The test materials used by clinical studies in studying the disorders of the GIT are of every day balanced meals, containing both solid and liquid parts. For example, rice pudding (25g) with raspberry jam (34g) and orange juice (100ml) (Vincent *et al*, 1995), one-egg omelet with bread (50g) and orange juice (200ml) (Calabuig *et al*, 1989), a standardized breakfast consisting of orange juice (200ml), coffee (1 cup), 2 rolls filled

with sausage (total calorie content of 2500kj) (Allescher *et al*, 1998), chicken soup (100g) with non-fat dried milk (20g) and whole milk (50g), constituting 299kcal and total volume made to 250ml (Thompson *et al*,1982), ground sirloin steak (5 ounces) with two pieces of toast and water (360ml) (Fordtran and Walsh, 1973). In some cases, a pre-set standard meal has been used. The composition courtesy of GlaxoSmithKline standard breakfast states that the meal must be composed of 2 slices of toasted white bread with butter, 2 eggs fried in butter, 2 slices of bacon, 2 ounces of hash browned potatoes, 8ounces of whole milk which constitutes 967kCal (Klein *et al*, 2004). FDA Office of Generic Drugs states that the composition of standard breakfast meal should be composed of 1 English muffin with butter, 1 fried egg, 1 slice of cheese, 1 slice Canadian bacon, 1 serving of hash browned potatoes, 6 ounces of orange juice, 8ounces of whole milk, which add to 648kCal in total (Klein *et al*, 2004). Such balanced meals are often radio-labelled with Tc99m in feeding patients for scintigraphy studies (Vincent *et al*, 1995).

Table 3-2. A summary of the composition (per serving of 220g) of the HEINZ Little Kids 1-3 years baby foods used. (The source of information given on the tables was from the back of the package of the test meals).

Creamy Tuna with Veges	Vegetables 23% (carrots, sweet corn (5%),pumpkin onion, red capsicum (2.5%), spinach (1%)), Full cream milk, Rice, Tuna 8%, Maize Starch, Cream (0.5%), Romano cheese, unsalted butter, natural onion flavor, spice extract, spices and salt
Macaroni & Meatballs	Vegetables 67% (Tomatoes (46%), Carrots (8%), Potatoes (8%), Onion), Macaroni (Wheat, traces of milk and egg) 18%, Meatballs 14% (Beef, onion, wheat flour, wheat gluten, salt, vegetable oil, wheat starch, mineral salt (451), natural flour), Maize Thickener (1422), Potato Starch, Herb Extracts, Spice, Natural color (paprika extract)

However the test materials used by other *in vitro* digestion studies, often one food of a kind have been used with or without extraction of a particular nutrient of interest and in non-solid (either semi-liquid or liquid) form such as yoghurts (Marteau *et al*, 1997), irradiated kefir (Mainville *et al*, 2005), blended homogenized meal (Rao and Prabhavathi, 1978; Garrett *et al*, 1999), liquid formulae meal (Hurrell *et al*, 1988), low concentration (0.08w/v%) blue dextran solution (Minekus *et al*, 1995), dextrose meal (Schwizer *et al*, 1994; Fraser *et al*, 1994) and a mixture of amino acid solution (Schiller *et al*, 1982),

barley porridge (Haraldsson *et al*, 2005), peanut meal slurry (Kopper *et al*, 2006), finely ground wheat in water (Avantaggiato *et al*, 2003), homogenized fried meat (beef or chicken) (Krul *et al*, 2000). Although these may not optimally reflect the composition of the meals usually administered in everyday life (Klein *et al*, 2004), heterogenicity among different batches of samples can be minimized.

Recently, media simulating the fasting and fed conditions in the stomach (FASSIF and FESSIF) have been proposed by Galia *et al* (1998 and 1999) and used by Ingels *et al* (2002) and Souliman *et al* (2006) although these do not represent the real food impact but yet there is no solid standardized meal set to evaluate the impact of food on absorption and release of drugs (Souliman *et al*, 2006). As discussed by Klein *et al* (2004), the secretion of the gastric juice in response to the ingested test meal and the contribution of the solid components in the meal have often been ignored, resulting in a fast decrease in the pH of the fed stomach over time.

Table 3-3. A table of the nutritional information of the HEINZ Little Kids 1-3 years baby foods (per serving of 220g) used. (The source of information given on the tables was from the back of the package of the test meals).

Components	Creamy Tuna with Veges	Macaroni & Meatballs
Energy	450kj	725kj
Protein	7.5g	8.6g
Fat, Total	2.2g	6.4g
Saturated	1.3g	2.2g
Trans	0g	
Polyunsaturated	0.2g	
Omega-3	0.07g	
EPA	5.3mg	
DHA	27.5mg	
Monounsaturated	0.7g	
Carbohydrate	16.7g	19.1g
sugars	3.1g	4.4g
Dietary Fiber	3.3g	2.0g
Sodium	22mg	230mg
Potassium	175mg	255mg
Iron		20mg

In order to determine the preference between a balanced meal and one kind of food for clearer outcomes in analyses, baby foods (HEINZ Little Kids Baby Food, 220g in can – Product of Australia; Table 3-2 and 3-3) and rice (Sun Rice Japanese style Sushi Rice- Product of Australia; Table 3-4) were chosen as the test meal. Baby foods are the most commonly found balanced meal without any effort in considering the nutritional balance. Although adults do not sincerely eat the baby foods sold in supermarkets, these baby foods are essentially the smaller portion of a normal adult’s meal chopped into finer pieces. Baby foods are readily available (no need to cook or plan separate preparation methods), relatively cheap and nutritional information is supplied. It would seem that no complex mouth compartment would be required in terms of grinding and mastication with the use of the baby foods. Previously, baby foods have been used by Kapsoketalou *et al* (2005) and Garrett *et al* (1999) in studying the bioavailability of iron and carotenoids in meals, respectively.

Table 3-4. Nutritional information of the Sun Rice® Japanese style Sushi Rice (serving size of 100g). (The source of information given on the tables was from the back of the package of the test meals).

Components	Quantity
Energy	1460kJ 349Cal
Protein	5.9g
gluten	0mg
Fat, total	Less than 1g
saturated	Less than 1g
trans	Less than 1g
polyunsaturated	Less than 1g
monounsaturated	Less than 1g
Cholesterol	0mg
Carbohydrate, total	78.5g
sugars	Less than 1g
Dietary Fiber, total	Less than 1g
Sodium	Less than 5mg
Potassium	70mg

White short-grain rice was also chosen as a test meal as its macronutrient constituent is relatively simple, up to 78.5wt% of total carbohydrates (SunRice® Sushi Style – nutrition information, Table 3-4), compared with other balanced meal, therefore requiring analysis of carbohydrates mainly. The Sun Rice® Japanese style Sushi Rice is short grain rice (Koshihikari and Opus) with relatively low content of amylose (av. 19 wt%) and high amylopectin content, thus very sticky. It is almost spherical in shape and as the dimension of the rice grain (5.5 ± 0.4 mm in length x 3.0 ± 0.1 mm wide and 1.9 ± 0.1 mm thick as average of 20 cooked rice grains) is considered small, it can be swallowed easily if large clumps of the sticky rice can be separated, a complex mouth compartment is not essentially in demand. Studies of starch (including rice starch) underscored no significant differences between the *in vitro* enzymatic hydrolysis and *in vivo* digestion of starch (Williamson *et al*, 1992; Franco *et al*, 1992; Björck *et al*, 1994; Kim *et al*, 2004). Rice is a staple food of a kind in many countries (Frazier, 1997) with intensive research related to the postprandial glucose and insulin responses, diabetes, coronary heart disease, cancer and ageing are being conducted worldwide (Frazier *et al*, 1997; Kim *et al*, 2004). In general, the amount of amylose content determines the rate and extent of retrogradation of the rice starch, where high content of amylose result in less stickiness when cooked (Kurasawa *et al*, 1972; Arisaka and Yoshii, 1999; Raina *et al*, 2007). By using both baby foods and cooked rice, a comparison can be made whether a balanced meal is necessary in the validation process of the IPUGS. Since both meals have highly solid content, a cup (250ml) of drinking water (tap water) was used to ease the ingestion process.

3.1.2. Introduction to Dietary Carbohydrates and Starch Hydrolysis

Dietary carbohydrates can be classified into three groups – sugars, short chain carbohydrates and starch. Sugars often refer to monosaccharides (e.g. glucose and fructose) and disaccharides (e.g. maltose and sucrose) (Frazier *et al*, 1997). Short chain carbohydrates including oligosaccharides are of interest as they may be fermented in the large bowel and associate with probiotic strains (Frazier *et al*, 1997). Starch can be subdivided into rapidly digestible starch where studies linked to diabetes, coronary heart disease and ageing process are of demand and slow digestible starch, which are nutritionally the most desirable form of starch (Frazier *et al*, 1997).

Starch is the dominant carbohydrate constituent of rice which is a semi-crystalline granular substance (prior to cooking) consisting of amylose and amylopectin (Bertoft,

2007). Amylose is a linear macromolecule built up of α -(1-4)-linked D-glucopyranosyl units (Bertoft and Koch, 2000) which has a molecular weight of up to 10^6 Daltons (Frazier *et al*, 1997) and form simple hydrated micelles in the form of the twisted helical coil with hydrophobic core (Briedis *et al*, 1980). Amylopectin is a highly branched polysaccharide constructed from hundreds of short α -(1-4)-glucan chains, which are interlinked by α -(1-6) linkages (Frazier *et al*, 1997; Bertoft and Koch, 2000) which has a molecular weight of up to 4×10^8 Daltons (Frazier *et al*, 1997). These amylopectin chains are sub-classified into A, B and C chain referring to non-branched, branched at the C-6 position (s), and chain with a reducing residue, respectively. The ratio of the A to B chains provides useful information for characterization of the mode of branching of the amylopectin, in which the ratio for short grain white rice typically is about 0.38 usually (Frazier *et al*, 1997). In rice starch, single clusters consist of approximately 10-23 chains, each with a length of 6-36 glucosyl residues (Bertoft and Koch, 2000).

Starch can be degraded by acidic or enzymatic reactions. Hot acids hydrolyse the glycosidic bonds, producing maltodextrins first, and subsequently a mixture of glucose, maltose and malto-oligosaccharides (Whilstler *et al*, 1972). α -amylase (alpha-1, 4 glucan-4-glucanohydrolase, EC 3.2.1.1) from saliva and pancreas are involved in the hydrolysis of α -(1-4) bonds, producing maltose and maltodextrins (Frazier *et al*, 1997). This enzyme is able to bypass α -1,6 branching points but does not cleave them. In contrast to hydrolysis of amylose, which is randomly transformed into maltose, hydrolysis of amylopectin is non-random and produce maltose, maltotriose and branched α -limit dextrin composed of all the initial α -1,6 bonds and the adjacent α -1,4 linkages (Whilstler *et al*, 1972; Frazier *et al*, 1997). However extrinsic factors such as the degree of chewing, concentration of amylase in the mouth and the pancreas and transit time through the stomach and small intestine may affect the rate of starch hydrolysis (Frazier *et al*, 1997).

3.2. Building Materials and Methods used in development of the IPUGS

Existing *in vitro* digestion models comprised of glass materials in the form of glass vessels (Vatier *et al*, 1992; Molly *et al*, 1993; Minekus *et al*, 1995; Macfarlane *et al*, 1998; Castela-papin *et al*, 1999), glass beakers (Mainville *et al*, 2005; Sugawara *et al*, 2005), glass test tubes (Oomen *et al*, 2003), conical flask (Rao and Prabhavathi, 1978) have been widely used in various studies such as microecology, pharmaceuticals and other bioavailability. Alternatively, screw-cap vials (Alexandropoulou *et al*, 2006;

Kapsokefalou *et al*, 2005) and plastic centrifuge tubes (Lock and Bender, 1980; Turnbull *et al*, 2005) have also been used in some bioavailability and nutritional studies. The disadvantage of using glass and plastic building materials is that they are non flexible and non elastic like the human stomach wall. Also non-stretchable nature of the glass and plastic materials limit the expansion of the human stomach in accommodating a relatively fast ingestion rate, which has to be compensated by using of a large volume of reactor. Sometimes, unwanted adsorption of grease and other trace components on the wall of the glass reactor takes place if the force and the volume of mixing (motility) is not enough, thereby causing a great bias in analyzing results. The newly developed IPUGS is composed of three sequential compartments simulating the conditions of the mouth, esophagus and stomach of the humans. It is made of non-glass material to simulate the flexible, elastic and stretchable nature of the human GIT conditions as closely as possible.

3.2.1. Development of the Mouth Compartment in the IPUGS

The first compartment simulates the food ingestion in mouth, which is composed of a denture set with manually controlled mastication and continuous secretion of artificial saliva of $37\pm 0.5^{\circ}\text{C}$ which is transferred via a peristaltic pump at rate of $7.0\text{ml}\cdot\text{min}^{-1}$ (Edgar 1990; Humphrey and Williamson, 2001). White short grain rice (Sun Rice Japanese style Sushi Rice) was cooked in a conventional rice cooker with 1:1 volumetric ratio of rice grains to water. 100g of the cooked rice or a can of HEINZ baby food (220g) was transferred to the mouth reactor with 250ml of drinking water to be used as the feed material. As the cooked rice and the baby food used were relatively small in size which can be swallowed without much of mastication, it can be regarded as simpler foods for testing. 5min of gentle manual mastication was applied with the denture set with $20\text{chewing}\cdot\text{min}^{-1}$ to remove large clusters of food materials into smaller pieces to aid the swallowing process. The feed material was spoon fed to the next compartment, esophagus at a rate of $8.5\text{ml}\cdot 30\text{s}^{-1}$ (equivalent to $\frac{1}{2}$ table spoon (tbsp) $\cdot 30\text{s}^{-1}$). The pH of the artificial saliva was 7.02 ± 0.05 , the pH of the cooked rice with distilled water mixture was 5.40 ± 0.05 , pH range of the HEINZ baby foods with distilled water mixture was 7.15-7.58. (7.30 ± 0.15 for Creamy Tuna with Veges and 7.43 ± 0.15 for Macaroni & Meatballs). The pH of the bolus composed of the cooked rice, distilled water and artificial saliva was 5.85 ± 0.05 . The pH range of the bolus composed of the HEINZ baby foods with distilled water and artificial saliva was 7.2-7.63. The pH of the gastric secretion was 1.03 ± 0.01 . The pH of the mucosal secretions in the esophagus compartment was 6.8 ± 0.05 .

3.2.2. Development of Esophagus and Stomach Compartments in the IPUGS

The last two compartments simulating the conditions of the esophagus and the stomach were built with platinum cure silicon rubber (Figure 3-1A) composed of 75-85wt% polyorganosiloxanes, 20-25wt% of amorphous silica and 0.1wt% of platinum-siloxane for part A and 65-70 wt% of polyorganosiloxanes and 20-25wt% of amorphous silica for part B. 1:1 ratio of the parts A and B were mixed and coated to the plastic anatomy model of the stomach which resembles the average human stomach size at unfed state (20cm x 15cm x 8cm, Kararli, 1995; Pade *et al*, 1995) as well as its geometry of J-shaped curve. The coatings were repeated until the thickness of the stomach wall reached 0.50 ± 0.01 cm in average. Each coating took overnight (up to 8hrs) to cure completely in room temperature. The platinum cure silicon rubber is translucent in color thus by adding of food coloring agents to the feed mixture may help clearer view of the reactions in the inner stomach compartment. It offers negligible shrinkage and able to stretch and rebound to its original size and shape without distortion, able to withstand repetitive motion which seemed to be a perfect match for the continuous contractions of the stomach. It is relatively soft compared with other polymers which assist for easier manipulation of the gastric motility, water insoluble, heat resistant, non-sticky with rubber-like properties and has tensile strength of 475psi and the specific gravity of 1.07 ($H_2O = 1$, at $4^{\circ}C$) (http://tb.smodev.com/tb/uploads/Dragon_Skin_TB.pdf). Non-sticking property is a very important key to the building material as it would be very undesirable to operate and may cause a huge bias in results if the test materials (such as food or drugs) stick to the walls of the stomach and interfere with the patterns of the motility and sampling.



Figure 3-1. (A) One half of the stomach mold made with the platinum cure silicon rubber (left). (B) Initial stomach mold made with Equinox™ (right)

Previously, another material made of silicone rubber putty, nominally Equinox™ (Figure 3-1B) has been used. It is light purple in color and exhibits nearly the same property as the platinum cure silicon rubber except that it is less elastic, require more force for applying the same motility (more stiff in texture) and cures very fast, allowing molding time of less than 5mins, causing a technical difficulty. Thus it was decided to use platinum cure silicon rubber instead.

For the esophagus, paper roll of 1.5cm diameter and 20cm in length was made, and coatings of the silicon rubber were repeatedly made until the wall thickness reached 0.30 ± 0.01 cm in average (Al-Zaben and Chandrasekar, 2005). The paper roll and the plastic anatomic model were removed after coatings.

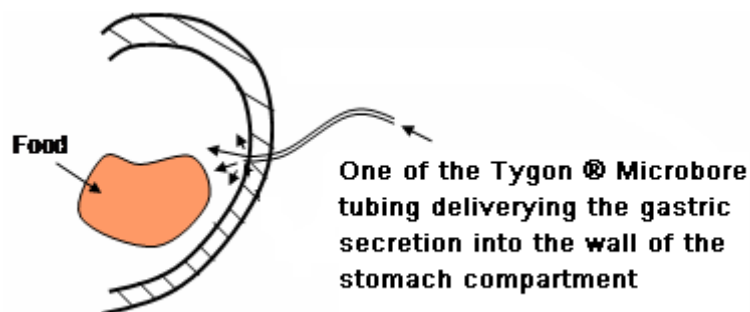


Figure 3-2. An illustration of one of the Tygon® Microbore secretion tubings inserted into the wall of the stomach compartment. 200 of these tubings were implanted with even distribution to deliver the artificial gastric secretions.

In order to deliver the gastric secretions to the wall of the stomach, a large number of Tygon® Microbore tubings ($n=200$) with inner diameter of 0.25mm were implanted, with the tips of these tubings pierced into the stomach wall to create a gradual dampening of the wall (Figure 3-2), secreting $3.5\text{ml}\cdot\text{min}^{-1}$ (Mainville *et al*, 2005) throughout the 3hr digestion period. These tubings are designed for precision injection and dispensing in laboratory applications with flexible and bendable resin. The tubings have a very smooth inner bore surface which reduces the risk of particulate build-up during sensitive fluid transfer and minimal extractable helps to assure fluid purity. Also, these tubings are transparent, thus the gastric secretions passing into the stomach wall can be seen clearly.

A tubing linkage set (Figure 3-3) was made by cutting the Tygon® Microbore tubing to 20cm long and joining the tips of 100 of them to fit into one larger-diameter (inner diameter of 1.5cm) transparent silicone tubing which was subsequently connected to the

smallest possible peristaltic tubing (inner diameter of 0.80mm). Because the larger peristaltic tubing was unable to meet the low flow rate of each secretion to be pumped into the stomach, the tubing linkage set was made. The lowest possible flow rate that could be achieved with the small peristaltic tubing was $0.5\text{ml}\cdot\text{min}^{-1}$. Two of these linked tubing sets (Figure 3-3) were made to pump mucus and gastric juice into the stomach compartment. After completion of each tubing linkage, water was run through with a peristaltic pump to examine the distribution of water pumping out of the micro-bore tubings and confirmed near to even distribution of the water droplets with nearly the same volume of the collected water droplets (Table 3-5).

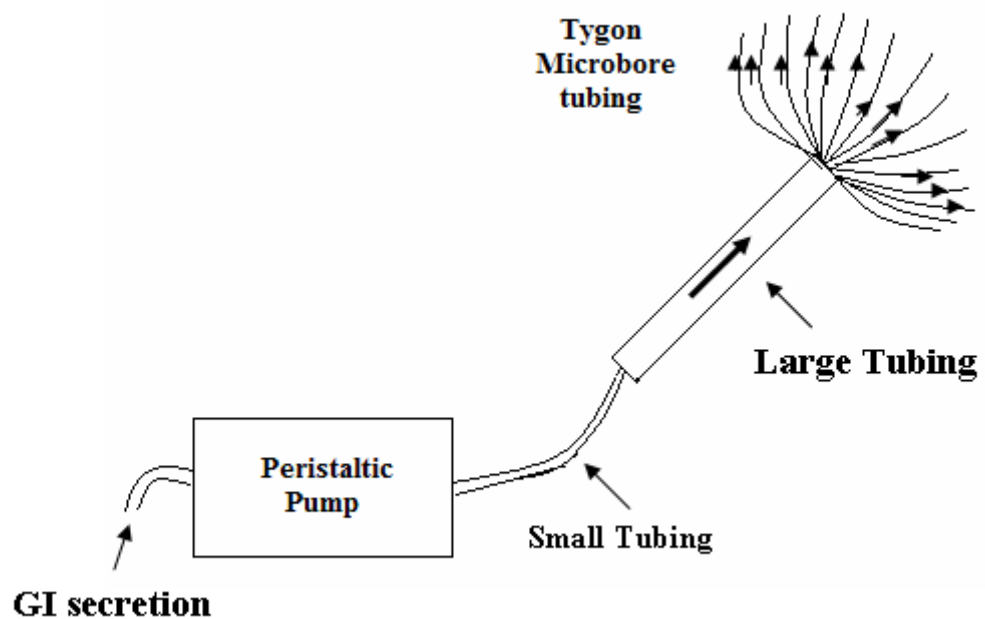


Figure 3-3. A schematic diagram of the tubing linkage set

For mucosal secretions in the esophagus compartment, slightly larger diameter of tubing was used. Micro-Line™ tubing (Thermoplastic Scientifics, Inc.) made of cross-linked ethyl vinyl acetate. These tubings are translucent, flexible and elastic with inner diameter of 0.51mm. One ends of these implanted tubings in both esophagus and the stomach were planted into the wall of each compartment to create gradual dampening effect from the wall to simulate the opening and closing of the pores in the gastric wall for secretion delivery. The other ends were gathered and squashed into a larger diameter silicone peristaltic tubings (inner diameter of 1.5cm), which are subsequently connected to the smallest possible peristaltic tubing (inner diameter of 0.80mm). Though the flow rate of the peristaltic pumps can be controlled, changing the peristaltic tubing size also helped to control the flow rate more accurately. For validation of motility experiments, only one

peristaltic pump (Autoclude® Peristaltic Pump - 54505) was used to deliver the artificial gastric juice to the stomach compartment.

The esophagus and the stomach compartments were placed in an anaerobic chamber with continuous nitrogen gas flow ($1.0\text{L}\cdot\text{hr}^{-1}$) and the temperature inside the chamber was maintained at $37\pm 1^\circ\text{C}$ with a hot plate placed inside the chamber. The esophagus and the stomach compartments were manually pressed with my hands to mimic the peristaltic waves. For the esophagus, coordinated contractions and relaxations of the peristaltic propulsions were simulated to push the ingested feed material (bolus) towards the stomach with the rate of 5 contractions per 30s. The wall of the esophageal compartment was squeezed both horizontally and vertically by gripping the esophagus using both hands, one on top of each other and in between a thumb and an index finger, squeezed gently to push down the bolus (Figure 3-4).

Table 3-5. A table of results showing an average value of 10 runs of the volume of the collected distilled water (ml) from the tip of the Tygon Microbore tubings through the tubing linkage set for 10min.

Secretion Rate ($\text{ml}\cdot\text{min}^{-1}$)	Volume of the Collected Water for 10min per Tubing (ml)									
	1	2	3	4	5	6	7	8	9	10
1	10.3 ± 0.5	10.0 ± 0.5	9.7 ± 0.5	9.6 ± 0.5	10.0 ± 0.5	10.4 ± 0.5	10.5 ± 0.5	10.2 ± 0.5	9.5 ± 0.5	9.8 ± 0.5
2	19.5 ± 0.5	20.0 ± 0.5	20.2 ± 0.5	20.5 ± 0.5	19.8 ± 0.5	20.0 ± 0.5	20.0 ± 0.5	20.0 ± 0.5	20.5 ± 0.5	20.0 ± 0.5
3	30.0 ± 0.5	29.9 ± 0.5	30.2 ± 0.5	30.4 ± 0.5	30.5 ± 0.5	29.5 ± 0.5	29.8 ± 0.5	29.7 ± 0.5	30.0 ± 0.5	30.1 ± 0.5
4	40.5 ± 0.5	40.5 ± 0.5	40.3 ± 0.5	39.5 ± 0.5	39.7 ± 0.5	39.5 ± 0.5	40.0 ± 0.5	40.0 ± 0.5	39.8 ± 0.5	40.4 ± 0.5

Note: margin of error of $\pm 0.5\text{ml}$ per reading comes from the error of the volumetric flask used.

The upper esophageal sphincter (UES) controlled the entrance of the feed mixture and the lower esophageal sphincter (LES) controlled the exit of the feed mixture into the stomach compartment. Each cycle of esophageal peristalsis lasted up to 6s (Pehlivanov *et al*, 2002).

Apart from mucosal secretions, there are neither digestive secretions nor absorption take place in the esophagus (Tortora and Grabowski, 2000) thus these features were excluded.

Hand squeezed actions to simulate the peristaltic waves of the human stomach was used in the stomach compartment as well. The first peristaltic wave was initiated from squeezing the proximal part of the stomach compartment (the fundus and upper body) and moved subsequently towards the lower antrum/pylorus area. This was to generate a pressure gradient from the body of the stomach to the pylorus, resulting an opening of the pyloric sphincter and emptying of fractions of the stored bolus towards the pylorus and mix with the gastric secretions, which resembles the action of a contractile grinder, crushing the small chunks of the bolus as described in the literature (Akin 1998; Luiking *et al*, 1998; Nguyen *et al*, 1999; Tortora and Grabowski, 2000) (Figure 3-5).

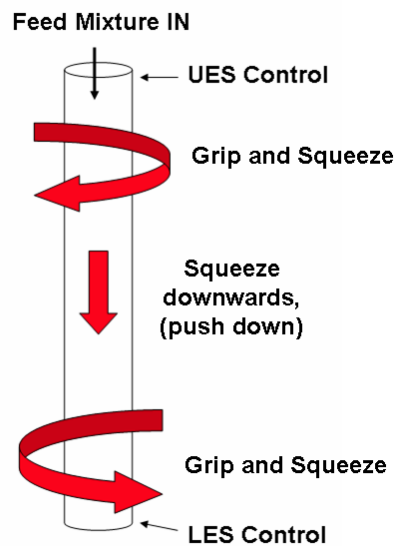


Figure 3-4. Diagram showing the motility of the esophageal compartment of the IPUGS. Red arrows indicate the direction of squeezing. UES refers to the upper esophageal sphincter and LES represents the lower esophageal sphincter.

The second peristaltic wave with closed cardiac and pyloric sphincters was initiated from the distal stomach (lower body and the antrum), squeezing the wall of the stomach towards the proximal direction (toward the fundus) (Figure 3-6). Sequential contractions of the antrum crushed the small chunks of the bolus against the closed pyloric sphincter with a large fraction of the remaining bolus squeezed back toward the proximal part for further digestion (Tortora and Grabowski, 2000; De Zwart *et al*, 2002), causing distention of the stomach compartment to accommodate more space for the incoming food which was facilitated by the elastic and stretchy nature of the building material (platinum cure silicon rubber). The overall gastric motility in the proximal stomach compartment

remained relatively constant, but for the distal part, stronger contractions with higher depth and amplitudes (Schwizer *et al*, 1994) were used. A schematic diagram of the IPUGS is provided in Figure 3-7.

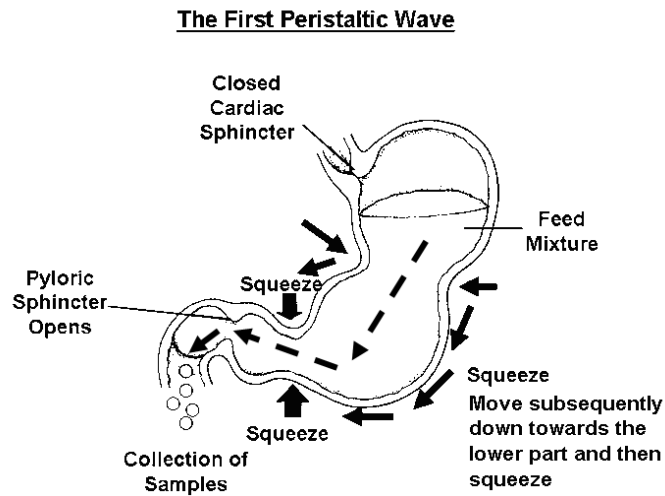


Figure 3-5. A diagram of the first peristaltic wave applied to the stomach compartment of the IPUGS. Black arrows drawn on the outside of the stomach indicate the directions of the squeezing action. Squeezing initiated from the body of the stomach and moved subsequently towards the lower antrum/pylorus area, followed by a strong squeezing in the lower antrum/pylorus area to open the pyloric sphincter and release the chyme. Dotted black arrows inside the stomach indicate the expected flow of the chyme inside the stomach compartment.

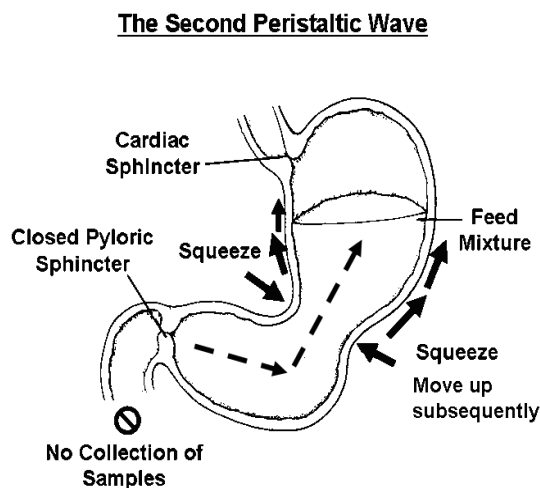


Figure 3-6. A diagram of the second peristaltic wave applied to the stomach compartment of the IPUGS. Black arrows drawn on the outside of the stomach indicate the directions of the squeezing action and red arrows indicate the expected flow of the chyme inside the stomach compartment. Black dotted arrows inside the stomach indicate the direction of the chyme movement.

The compositions of the artificial saliva and the gastric juice were kept as simple as possible to avoid any complications from salts in analyzing data. Thus α -amylase, pepsin, gastric lipase and hydrochloric acid, which are the main substances that are able to enzymatically digest carbohydrates, proteins and lipids, were used. 2g of fungal (*Aspergillus oryzae*) α -amylase (Grindamy1™ A5000, 5000U/g, Danisco 071314) was mixed with 200ml of deionized (MilliQ) water to be used as the artificial saliva and 0.15M HCl (Ajax, AF602394) with 1100kU/L of pepsin from porcine stomach mucosa (1:10000, Sigma-Aldrich P-7000, E.C.3.4.23.1) and 500kU/L of lipase from porcine pancreas (type II, Sigma-Aldrich L3126, E.C.3.1.1.3) were mixed to be used as the artificial gastric juice. Both of these secretions were warmed up to $37\pm 1^\circ\text{C}$. Hormonal control of altering the secretion rates and mucosal lining were excluded for this chapter as to compare the IPUGS to the MISST in simpler ways. However the results including the hormonal control and mucosal lining can be found in the chapters 6 and 7. The digestion period of 3hrs was set as the serving portion was relatively small and meals typically take 2-4hrs to be emptied into the small intestine (Suzuki, 1987; Mossi *et al*, 1994).

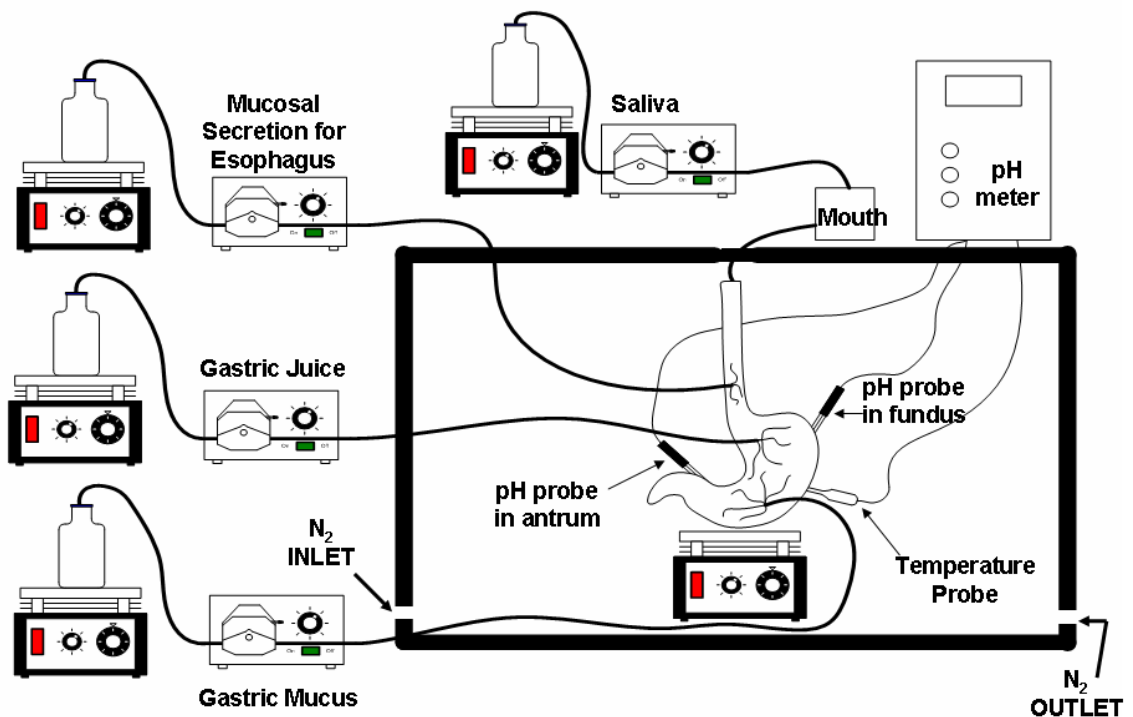


Figure 3-7. A schematic diagram of the IPUGS.

At time 0, 5ml of the homogenized pre-digested feed mixture was sampled to check for the consistency for each batch of the feed mixture preparation. From 10min to 30min, 20ml of samples were collected every 10min from the pylorus to simulate the gastric

emptying. From 30min to 180min where the gastric emptying was to be more active, 6.8ml of the chyme mixture was pumped out of the MISST per minute (Marciani *et al*, 2001; Mainville *et al*, 2005). The experiments via the IPUGS were conducted in triplicate runs.

3.2.3. Building Materials and Methods used in Modified *In vitro* Stomach Stir Tank (MISST)

To compare the IPUGS with other *in vitro* digestion models with the use of a magnetic stirrer and a glass vessel, a Modified *In vitro* Stomach Stir Tank (MISST) was made (Figure 3-8). A homogenizer (Wise Mix Homogenizer, Daihan Scientific HG-15D) was used with the speed of 400rpm for 10min to breakdown the test food material into a very fine particles (< 500 μ m in diameter) producing a smooth blend of the drinking water (liquid) and baby foods or cooked rice (solid). In the literatures, some *in vitro* digestion models have used such homogenization as an alternative for having a mouth reactor (Frazier *et al*, 1997) because the blended mixture allows for easier and more continuous pattern of pumping the feed mixture via peristaltic pumps as well as minimizing heterogeneity in the feeding mixture. Also, it inhibits any potential blockage in the peristaltic pump tubings to operate in a more controlled manner.

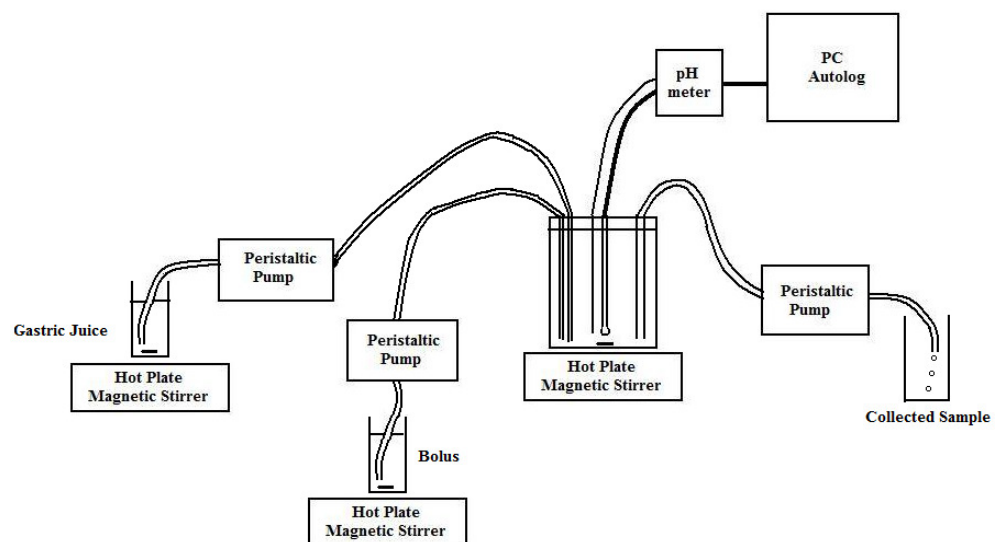


Figure 3-8. A schematic diagram of the MISST.

The stomach reactors used in the SHIME (Molly *et al*, 1993; De Boever *et al*, 2000), TIM (Minekus *et al*, 1995), and in the dynamic *in vitro* human upper GIT model system were transformed to make a ‘modified *in vitro* stomach stir tank (MISST)’. It was designed to

compare the results obtained from the IPUGS, paying attentions to the methods of motility and secretions in particular as well as to determine whether the IPUGS is a more advanced model or not.

A 1L glass beaker was used to represent the stomach. The open top was tightly sealed with a disc of styrofoam, with the thickness of $2.0\pm 0.1\text{cm}$, to mimic the anaerobic condition of the human GIT as well as to use it as an insulator to minimize the escape of heat. The pH and temperature probes were placed in the MISST as well as 3 peristaltic pump tubings for the delivery of the food and the gastric secretion to the MISST and withdrawing of the chyme from the MISST as to simulate the fill-and-draw mechanism used by Molly *et al* (1993). The styrofoam disc was pierced to tightly fit the probes and the tubings to the stomach reactor; therefore, the reactor was completely inhibited from interacting with the air and/or oxygen throughout the experiment. The pH and the temperature probes were placed in the middle of the stomach reactor. Tygon peristaltic tubings which deliver the food mixture and the gastric secretion were placed perpendicular to the pH and the temperature probes. The tubing for collecting of the chyme mixture was placed on the opposite side to the tubings of the food and the gastric secretion delivery. Thus the stomach reactor was anatomically coordinated. i.e. esophagus for the food delivery, fundus of the stomach for the gastric secretion and pylorus for the chyme collection. The MISST was heated to and maintained at $37\pm 1^\circ\text{C}$ on top of a hot plate magnetic stirrer, and it was constantly stirred at 150rpm with a magnetic stir bar (4cm x 0.5cm diameter) (Molly *et al*, 1993; Mainville *et al*, 2005). In order to simulate the cephalic phase of the stomach, the reactor was filled with 17.5ml of the gastric secretion prior to addition of the food (Mainville *et al*, 2005). 3.5ml of the gastric secretion was delivered per minute to the stomach reactor via peristaltic pump to simulate the gastric phase (Mainville *et al*, 2005). At time 0, 5ml of the homogenized pre-digested feed mixture was sampled to check for the consistency for each batch of the feed mixture preparation. All other times, 6.4ml of the chyme mixture was pumped out of the MISST per minute (Mainville *et al*, 2005; Marciani *et al*, 2001). The experiments via the MISST were conducted in triplicate runs.

3.2.4. Recording of pH and temperature

The measure of the pH profile is one of the simplest analyses which directly indicate the conditions of the stomach and it is of extreme importance as it is able to detect even

minor changes of the gastric conditions. For the IPUGS, two pH probes and one temperature probe were pierced into the wall of the stomach compartment in the IPUGS to record the pH in the fundus (probe 1) and the antrum (probe 2). The temperature probe was placed in the middle of the body of the stomach to measure the changes with respect to time. For the MISST, a pH probe and a temperature probe were placed in the middle of the stomach reactor. A pH meter from Hanna Instrument (HI 4212) was used with auto-logging mode of 30s for 3hr.

3.2.5. Observation of samples with a light microscope

A drop of 200 μ l of the collected sample was pipetted onto a glass slide and covered with a cover slip. Observations were made with magnification of 4 via a Motic light microscope (B1 series) and pictures were taken using a MotiCam 352 which was connected to a computer. A digital camera (8MP) was also used for taking pictures of the samples for the IPUGS as the rice grains were too large to be fitted to microscope scale.

3.3 Results and Discussions

3.3.1. Recording of the pH and temperature

The pH profiles obtained from the MISST and the IPUGS with the use of two different feeding materials, baby foods and white short grain rice, are shown in figures 3-8 and 3-9. Small changes in the pH profile were shown to affect dosage form performance, drug dissolution and absorption in normal human subjects (Dressman *et al*, 1990). Thus recording of the pH profile can be used as a brief evaluation tool in comparing the properties of the IPUGS and the MISST with the physiological data at a preliminary stage. As shown in Figure 8, the pH profiles of the MISST between the baby foods and the rice significantly differed from each other in both trends and values. Baby foods contained at least one kind of meat (either tuna or beef), with higher content of proteins and lipids compared to that of the rice (Tables 3-3 and 3-4). Thus a higher buffering capacity was expected, showing a very sharp increase of up to pH 4.32 from pH 1.03 in 13.5min. Although the initial pH value of both food kinds were the same, pH 1.03, referring to the pH of the artificial gastric secretion used, the change in pH profile especially during the

ingestion period, of up to 30min, differed largely. For the baby foods, the rapidly increased pH was maintained by the buffering capacity of the baby foods up to 15min, then decrease in pH had started. The MISST was unable to withhold the buffering capacity of the baby foods longer even during the ingestion period. However with rice in the MISST, the pH steadily increased until 29min, which was near to the end of the ingestion period. Relatively fast dropping of pH was seen with the baby foods in the MISST, especially between 25 to 60min. The rate of decrease in pH slowed from 60 to 120min. However from 120 to 130min, a slight elevation of the pH was seen. With the rice in the MISST, a gradual decrease from 30min (end of the ingestion period) to the end of the 3hr digestion period was seen, with the end pH value of nearly 1. Though the end pH value of the baby foods was higher, around 1.38, the major difference in the pH profile was seen in between the ingestion period, caused by the buffering capacity and during the first hr of digestion (up to 60min mark). In the TNO's gastroIntestinal Model-1 (TIM-1) the computer-controlled gastric pH was preset at pH 4.5, 4.2, 2.1 and 1.7 at 5, 20, 60 and 90min respectively (Minekus *et al*, 1995; De Boever *et al*, 2000; Blanquet *et al*, 2003).

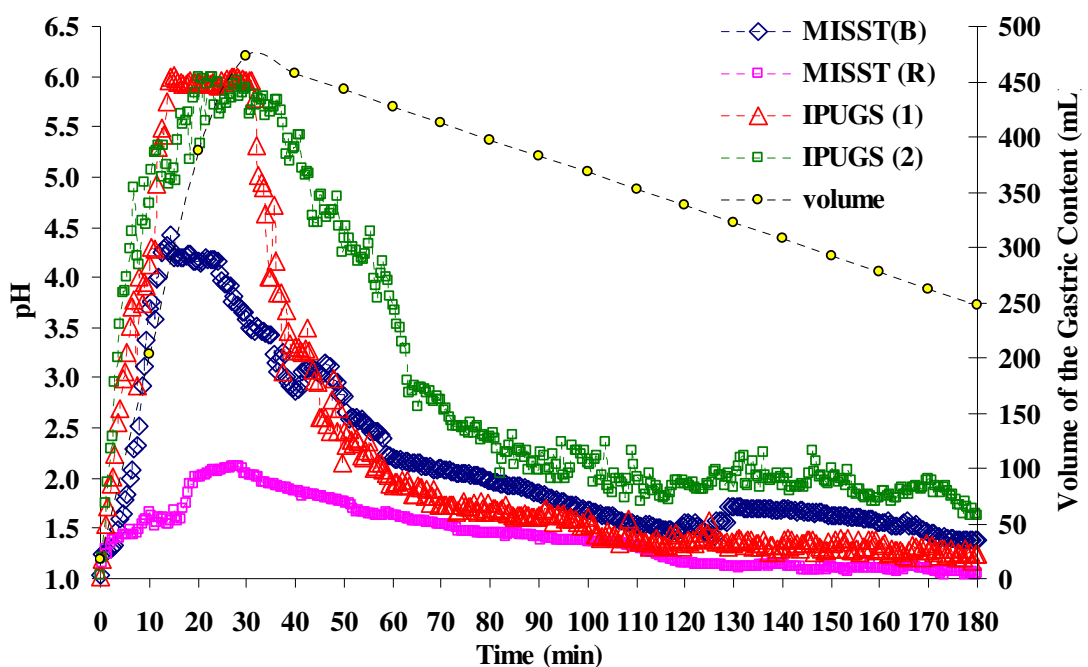


Figure 3-9. The pH profile of the MISST with baby foods (MISST (B)) and rice (MISST (R)) and the IPUGS with baby foods, pH probes 1 and 2. The volume of the gastric content (mL) is shown separately on the axis of right hand side.

The preset pH values were collected and averaged from clinical studies of normal human subjects with feeding of milk. The overall trend in the pH profile of the MISST with baby

foods was very similar to the preset pH values of the TIM-1. However as the milk contain higher protein content compared to rice, therefore offering smaller buffering capacity, the pH profile of the rice in the MISST was significantly lower in values. Overall, the MISST well-demonstrated the representative pH curve used by other *in vitro* digestion models.

Comparison of the IPUGS and the MISST results with the baby foods showed a very large difference in both trends and values of the pH. The maximal pH values obtained from the IPUGS, both pH probes 1 and 2 referring to the the fundus and the antrum, respectively, are much higher than that of the MISST. During the ingestion period, rapid increases in both pH probes of the IPUGS were seen, with the maximum pH of about 6.0 ± 0.1 . The overall trend and the maximum pH value were very similar to the gastric pH profile obtained from healthy normal subjects when fed with 458kcalories of a balanced meal (Hörter and Dressman, 2001). However 3-4hr after the meal intake, Hörter and Dressman (2001) found reestablishment of the fasting pH, which was around 1.3. This value also matches well with the pH probe 1 in the fundus area where majority of the acidic gastric secretions was delivered.

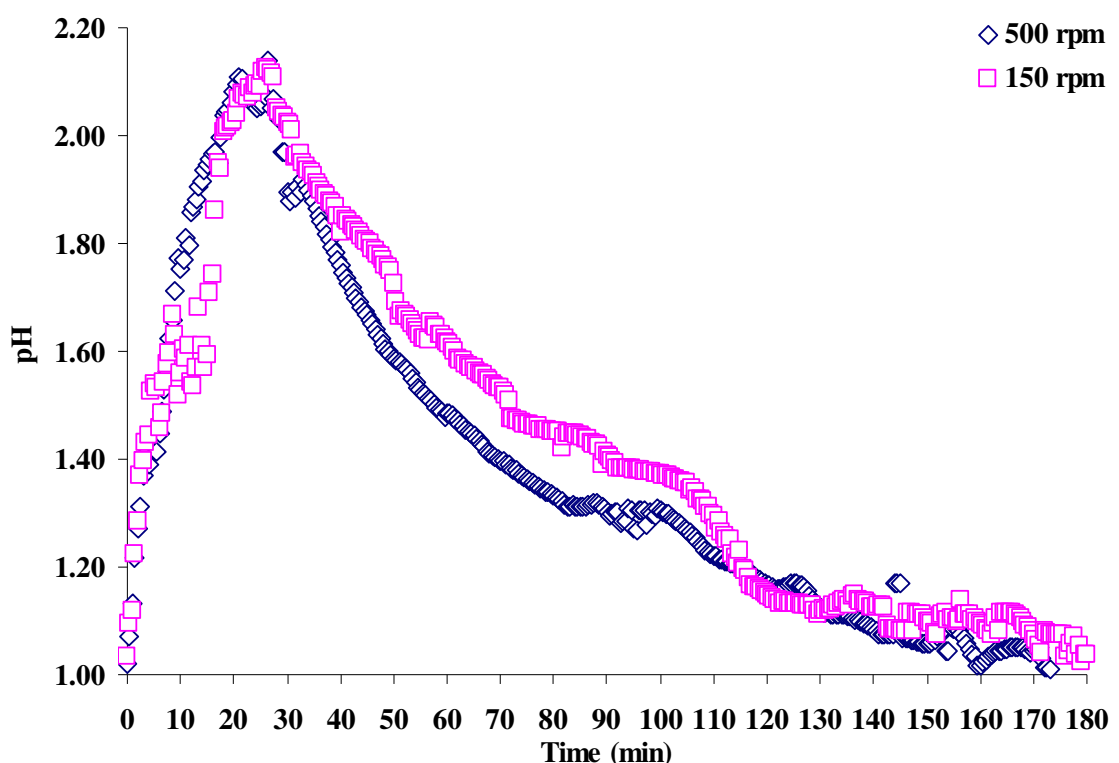


Figure 3-10. pH profile of testing rice feed mixture into the MISST with different stirring speed of 150rpm and 500rpm.

For the antrum (pH probe 2) which serves as a storage reservoir showed longer buffering effect of the ingested meal compared to the fundus (pH probe 1). Even after the ingestion period, the buffering effect slowed down the rate of decrease in pH in the fundus area. The pH of the MISST showed a very fast increase in pH especially up to 10min, then up to 30min there was not a significant change. From 15min mark, the pH started to drop relatively slowly compared to that of the IPUGS. During the first hr of digestion, the pH change was the most variable compared to that of the second and the third hr. At 180min mark, it can be seen that in the fundus (pH probe 1), the pH was about 1.24, which is very similar to the fasting gastric pH (1.3) of the normal human subjects (Hörter and Dressman, 2001). However in the antrum (pH probe 2), a slightly higher pH of about 1.63 was seen as the delivery of the acidic gastric secretion was minimized.

The pH profile of the MISST obtained by using the rice as the ingested feed material illustrated somewhat smaller variations than expected in the use of different stirring speeds of 150rpm and 500rpm (Figure 3-10). 150rpm is the most commonly used speed (Molly *et al*, 1993; Mainville *et al*, 2005) which seemed a bit slow in order to achieve a good mixing of the feed mixture with the secretions.

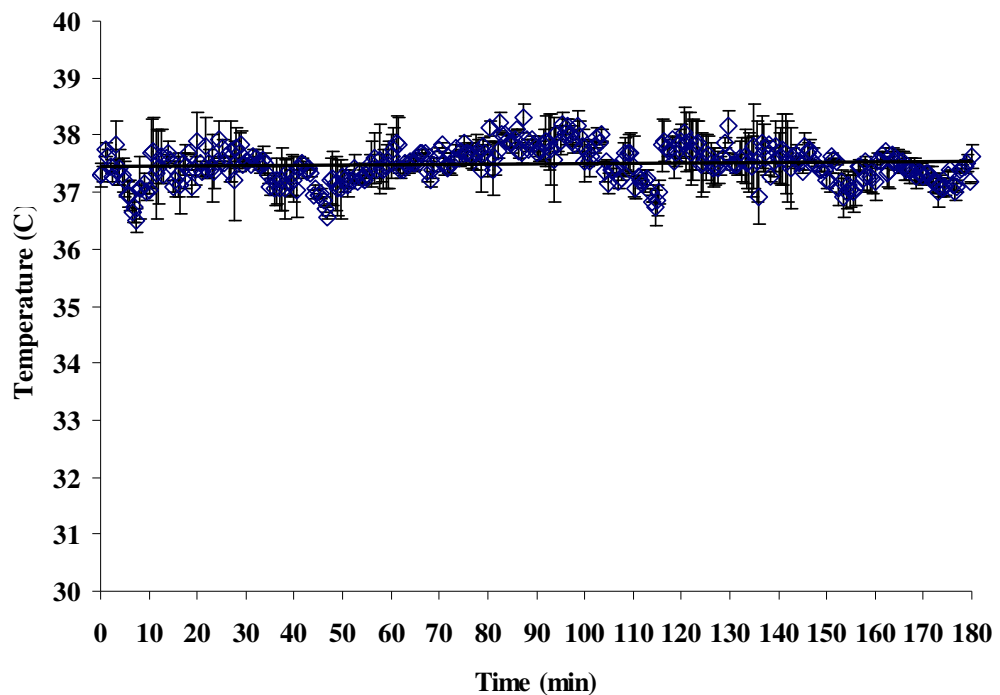


Figure 3-11. A plot of temperature profile showing the average temperatures of the MISST and the IPUGS.

Because the feed mixture was blended well by homogenization to break the particles into very small size (up to 500 μ m), this would have helped in avoiding gravitation of large

chunks of the feed material to the bottom of the stomach reactor in the MISST. Initially the pH values of the two different stirring speeds were nearly the same, 1.03 (150rpm) and 1.02 (500rpm). However with the ingestion of the feed material (rice with water), the change of pH with 150rpm up to 10min was not as fast as that of the 500rpm. Up to 30min, 500rpm showed a faster increase and more even rate of increase in pH, denoting a better mixed condition. However once the maximal pH was reached, 500rpm showed a faster reduction in the pH up to 115min mark. It would seem that the gastric emptying of the well mixed (500rpm) condition led to premature pumping of partially-digested or undigested rice particles out of the MISST, hence a faster drop of pH. From 115min to 180min, the difference between the two stirring speeds did not show a significant difference from one another. As shown in Figure 3-11, the temperature inside the stomach compartment of the MISST and the IPUGS was relatively constant, $37\pm 1^{\circ}\text{C}$ throughout the experiments.

3.3.2. Observation of samples with a light microscope

Observation of the obtained chyme samples of 10min interval was made by a light microscope and a digital camera as shown in Figure 3-12 to Figure 3-16. Initially, the cooked rice grains were mixed with water (refer to Figure 3-12a) and then homogenized to slurry-like rice mixture (Figure 3-12b). When this was observed by the light microscope, random distribution of large clusters of rice particles of various sizes were seen (Figure 3-12c). This was before salivary amylase as added. As shown by Figure 3-12d, a single cooked rice grain was off the scale to be fitted under the microscope.

At time 30min, the samples obtained from the IPUGS (Figure 3-13a) were purely liquid with slightly opaque white in color. No visible rice particles were observable with bare eyes. The samples obtained from the MISST contained rice particles that were visible with bare eyes. The samples from the MISST was observed under the light microscope, and compared to that of the time 0, the size of the clusters of rice particles has generally been reduced to smaller size. Up to 30min, the action of the salivary amylase was expected to be active due to the buffering capacity of the ingested meal. However by 60min, the clusters of the rice particles have significantly reduced in size as illustrated by Figure 3-14b. This would be due to digestion as well as due to the dilution by the gastric acid secretion (Castela-Papin *et al*, 1999), and gastric emptying.

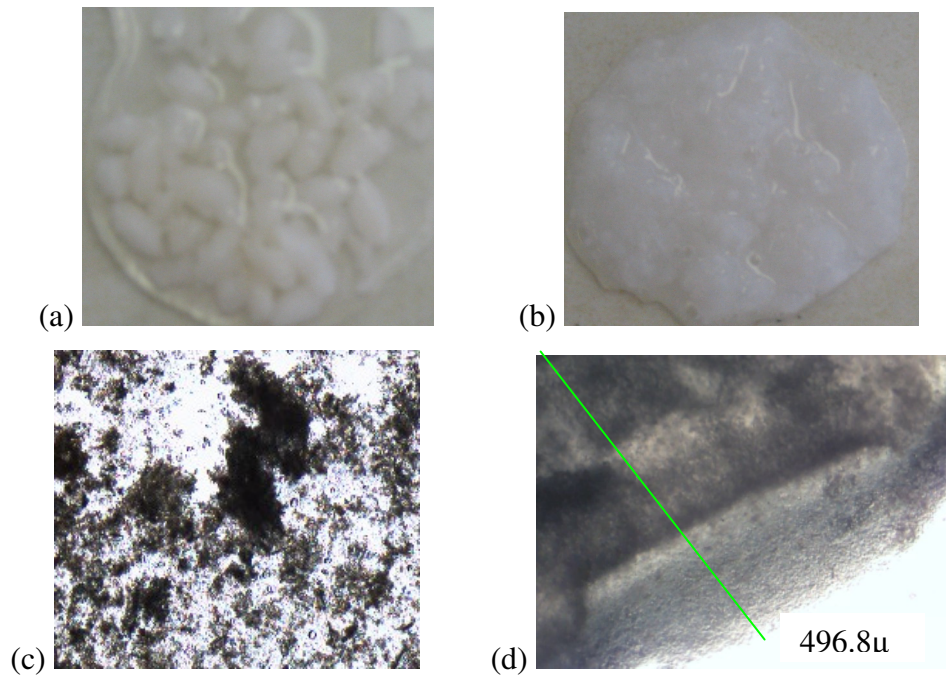


Figure 3-12. Images of the samples taken from the MISST and the IPUGS by the digital camera (a and b) and light microscope (c and d) at time 0. (a) refers to the IPUGS and (b) refers to the MISST.

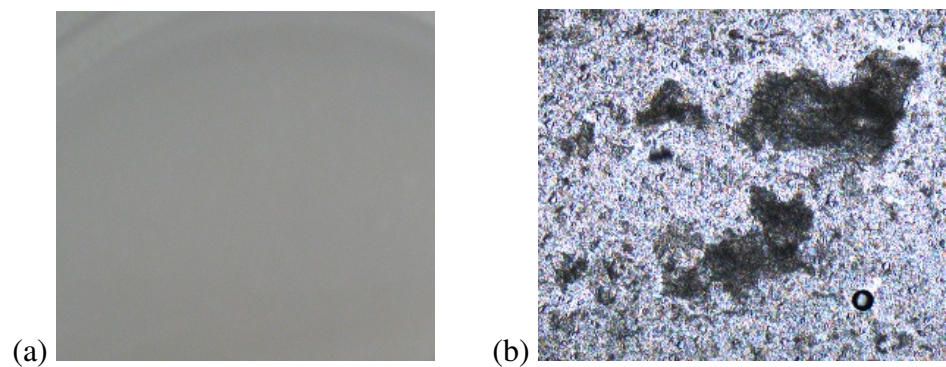


Figure 3-13. Images of the samples taken from the MISST and the IPUGS by the digital camera (a) and light microscope (b) at time 30min.

At 90min, which can be refer to the half time of the gastric emptying, the density of the rice particles in the MISST samples (Figure 3-15b) was much lower compared to that of the 60min (Figure 3-14b). However with the samples produced by the IPUGS, no visible rice particles were detected by bare eyes.

By the end of the 3hr digestion period, the volume of the content was small for both of the models, $250 \pm 3\text{ml}$, with small particles of rice grains remaining in the IPUGS and the

MISST as illustrated in Figures 3-16a and 3-16b, respectively. Compared to the images of the samples at different times, the size of the rice particles have significantly reduced and no clusters of particles were observable in the samples of the MISST. This seemed to be due to digestion by the gastric secretion, dilution by the gastric secretion, gastric emptying as well as premature escape of the undigested rice particles during the experiments. However with the IPUGS (Figure 3-16a), small sized (up to $0.20\pm 0.05\text{cm}$) rice particles remained near the pylorus of the stomach compartment of the IPUGS. Provided that Migrating Motor Complex (Chapter 1) in the humans is to be applied in the IPUGS, the remaining food particles can be expected to be pushed down to the duodenum.

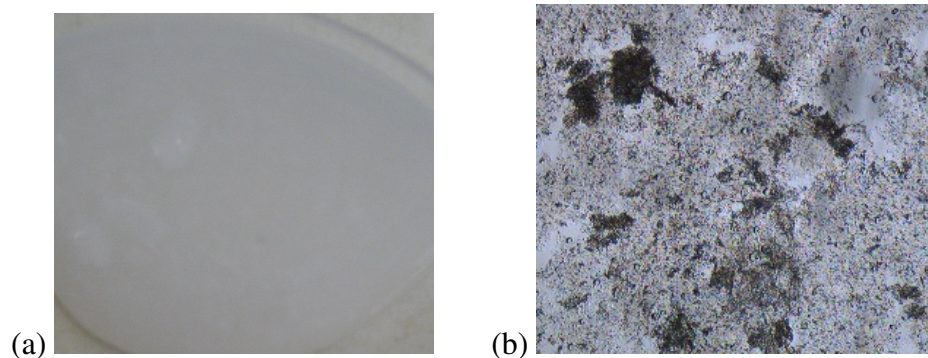


Figure 3-14. Images of the samples taken from the MISST and the IPUGS by the digital camera (a) and light microscope (b) at time 60min. (a) refers to the IPUGS and (b) refers to the MISST.

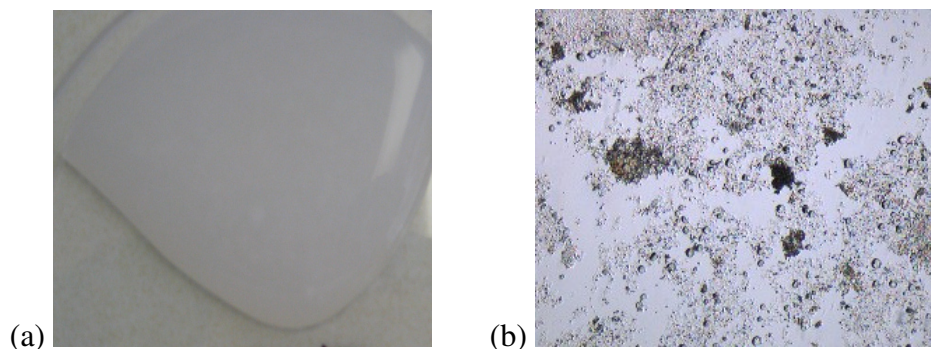


Figure 3-15. Images of the samples taken from the MISST and the IPUGS by the digital camera (a) and light microscope (b) at time 90min. (a) refers to the IPUGS and (b) refers to the MISST.

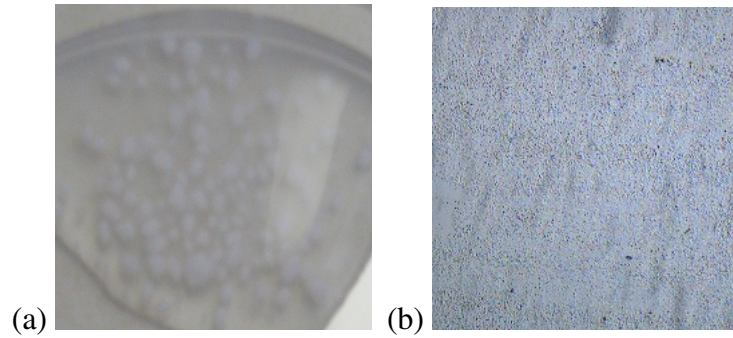


Figure 3-16. Images of the samples taken from the MISST and the IPUGS by the digital camera (a) and light microscope (b) at time 180min. (a) refers to the IPUGS and (b) refers to the MISST.

3.4. Concluding remarks and future works

The IPUGS was designed to simulate the conditions of the upper GI organs of the normal human subjects as closely as possible. Compared to the MISST which represents a typical *in vitro* digestion system in the literature, the IPUGS has achieved some improvements as shown on Table 3-6. Without the use of glass building materials or mechanical motility, more comprehensive secretion compositions were delivered to simulate the gradual dampening of the esophageal and the gastric wall rather than pouring or pipetting (to be discussed in details in Chapter 6). With the presence of mucosal lining, further studies with pharmaceutical products can possibly be conducted in the future.

Table 3-6. Key points of improvements required for *in vitro* digestion systems

Features	MISST	IPUGS
Use of glass building materials	√	X
Use of magnetic stirring or mechanical motility	√	X
Comprehensive composition of the GI secretions	X	√
Appropriate rate of delivering the GI secretions	√	√
Appropriate method of delivering the GI secretions	X	√
Feed-back control of delivering the GI secretions	X	√
Absorption of metabolites and water	X	X
Mucosal lining	X	√
Control over the pH for each compartment	X Possible	√

Anaerobic environment	√	√
Control over the transit time	√	√
Buffering capacity of the food	Low	√
Appropriate ingestion method of the food	X	√
Appropriate method of preparation of the test food	X	√
Appropriate ingestion rate of the food	√	√
Anatomy and Geometry of the human GIT considered	X	√
Strict temperature control	√	√
Inoculation of native bacteria in the mouth and the stomach	X	X
Use of peristaltic motility	√	√
Presence of a separate mouth reactor	X	√
Use of different motility pattern for fed and unfed state	X	X Applicable
Pre-filling of the reactors with secretions	√	X
Replacement of human enzymes with plant/animal/bacterial sources	√	√
Immune system	X	X
Control over the pH with respect to time	√	√
Ability to select for bacterial strains of interest	Possible	Possible
Adsorption ability of bacteria to the wall of the reactor	X	√
Reproducibility of data	√	√
Testing of trace amounts of materials (e.g. bioavailability of nutrients (including minerals and vitamins), toxic materials, allergens, pharmaceutical products)	√	√
Automatic/robustness	√	X
Premature gastric emptying	√	X

With the use of baby foods and white short grain rice, a brief comparison between the uses of test food materials has been conducted. The baby foods showed higher buffering capacity during the ingestion period and throughout the 3hr digestion period compared to that of the rice. Despite a more realistic composition of a balanced meal, it has been decided to use rice for further validation of the IPUGS (chapters 4 and 6) as well as for the study of GI disorders (chapters 5 and 7). Although the baby food composition, in terms of nutritional balance, contains more appropriate test meal when compared to the test meals used by clinical studies, analyses of food breakdown could cause a great

complication as carbohydrates, proteins and lipids need to be separated, extracted, and tested with various different methods. Such long analyses may require instant freezing of the collected samples to inhibit further breakdown by either chemically with HCl in the artificial gastric juice or enzymatically by salivary amylase, pepsin and lipases. Freezing and thawing process may further complicate the analyses further and the properties of the collected sample may change. Rice remains as staple food for many Asian countries, and recently research relating to postprandial glucose levels (plasma glucose), diabetes, coronary heart disease and ageing process are being actively conducted, thus it would seem that the study of rice behavior in the IPUGS would be simpler and may assist *in vivo* rice search in the future.

Comparison of the results obtained from the IPUGS with the MISST when the baby foods were used as the test meal showed that the IPUGS showed much higher buffering capacity of the ingested meal with prolonged higher range of pH throughout the experiments which was more similar to that obtained from the normal human subjects in the literature (Hörter and Dressman, 2001). It would seem that the curvature of the stomach compartment in the IPUGS allowed holding of undigested or partially digested food materials to be deposited for further digestion, thereby higher range of pH profile was seen for longer period. Measurement of pH would be the most simple validation process though only allows a limited scope analyses among the IPUGS, the MISST and the physiological data from the literature. However this can be used as a benchmark for further validation process which will be discussed in the forthcoming chapters (Chapters 4 to 8).

3.5. References

http://tb.smodev.com/tb/uploads/Dragon_Skin_TB.pdf

Akin, A. (1998) Non-invasive detection of spike activity of the stomach from cutaneous EGG. PhD Thesis Drexel University, Philadelphia

Alexandropoulou, I., Komaitis, M., Kapsokefalou, M. (2006) Effects of iron ascorbate, meat and casein on the antioxidant capacity of green tea under conditions of *in vitro* digestion. Food Chemistry, 94, 359-365

Allerscher, H. D., Abraham-Fuchs, K., Dunkel, R. E., Classen, M. (1998) Biomagnetic 3-Dimensional spatial and temporal characterization of electrical activity of human stomach. Digestive diseases and sciences, 43 (4), 683-693

Al-Zaben, A., Chandrasekar, V. (2005). Effect of esophagus status and catheter configuration on multiple intraluminal impedance measurements. Physiol. Meas., 26, 229-238

Arisaka, M., Yoshii, Y. (1999) Properties of high amylose starch paste. Applied Glycosciences, 41 (1), 1-7

- Avantaggiato, G., Havenaar, R., Visconti, A. (2003) Assessing the zearalenone-binding activity of adsorbent materials during passage through a dynamic in vitro gastrointestinal model. *Food and Chemical Toxicology*, 41, 1283-1290
- Bertoft, E and Koch, C. (2000) Composition of chains in waxy-rice starch and its structural units. *Carbohydrate Polymers*, 41 (2), 121-132
- Bertoft, E. (2007) Composition of building blocks in clusters from potato amylopectin. *Carbohydr. Polym.*, 70 (1), 123-136
- Björck, I., Granfeldt, Y., Liljeberg, H., Tovar, J., Asp, N. G. (1994) Food properties affecting the digestion and absorption of carbohydrates. *Am. J. Clin. Nutr.*, 59 (Suppl.), 699S-705S
- Blanquet, S., Meunier, J.P., Minekus, M., Marol-Bonnin, S., Alric, M. (2003) Recombinant *Saccharomyces cerevisiae* expressing P450 in artificial digestive systems: a model for biotransformation in the human digestive environment. *Applied and Environmental Microbiology*, 69(5), 2884-2892
- Briedis, D., Moutrie, M. F. M., Balmer, R. T. (1980). A study of the shear viscosity of human whole saliva. *Rheol. Acta.*, 19, 365-374
- Burks, T. F., Galligan, J. J., Porreca, F., Barber, W. D. (1985) Regulation of gastric emptying. *Federation Proc.*, 44, 2897-2901
- Calabuig, R., Navarro, S., Carrió, I., Artigas, V., Monés, J., La Calle, J.P. (1989) Gastric emptying and bezoars. *The American Journal of Surgery* 157, 287-290
- Castela-Papin, N., Cai, S., Vatier, J., Keller, F., Souleau, C.H., Farinotti, R. (1999) Drug interactions with diosmectite: a study using the artificial stomach-duodenum model. *International Journal of Pharmaceutics*, 182, 111-119
- De Boever, P., Deplancke, B., Verstraete, W. (2000) Fermentation by gut microbiota cultured in a simulator of the human intestinal microbial ecosystem is improved by supplementing a soy germ powder. *The Journal of Nutrition*, 130 (10), 2599-2606
- De Zwart, I. M., Mearadji, B., Lamb, H. J., Eilers, P. H. C., Masclee, A. A. M., De Roos, A., Kunz, P. (2002). Gastric motility: comparison of assessment with real-time MR imaging or barostat measurement - initial experience. *Radiology*, 224, 592-597
- Dressman, J. B., Berardi, R. R., Dermentzoglou, L. C., Russel, T. L., Schmaltz, S. P., Barnett, J. L., Jarvenpaa, K. M. (1990). Upper gastrointestinal (GI) pH in young, healthy men and women. *Pharmaceutical Research*, 7 (7), 756-761
- Edgar, W. M. (1990). Saliva and dental health. *British Dental Journal*, 169 (3-4), 96-98
- Fordtran, J. S., Walsh, J. H. (1973) Gastric acid secretion rate and buffer content of the stomach after eating. Results in normal subjects and in patients with duodenal ulcer. *J. Clin. Investigations*, 52, 645-657
- Franco, C. M. L., Preto, S. J. R., Ciacco, C. F. (1992) Factors that affect the enzymatic degradation of natural starch granules: effect of the size of the granules. *Starch*, 44, 422-426
- Fraser, R., Schwizer, W., Borovicka, J., Asal, K., Fried, M. (1994). Gastric motility measurement by MRI. *Digestive Diseases and Sciences*, 39 (12), 20S-23S
- Frazier, P. J., Richmond, P., Donald, A. M. (1997). *Starch: Structure and Functionality*. The Royal Society of Chemistry.
- Galia, E., Nicolaidis, E., Horter, D., Lobenberg, R., Reppas, C., Dressman, J. B. (1998) Evaluation of various dissolution media for predicting in vivo performance of class I and II drugs. *Pharm. Res.*, 15, 698-705
- Galia, E., Horton, J., Dressman, J. B. (1999) Albendazole generics - a comparative in vivo study. *Pharm. Res.*, 16, 1871-1875
- Garrett, D.A., Failla, M.L., Sarama, R.J. (1999) Development of an in vitro digestion method to assess carotenoid bioavailability from meals. *J. Agric. Food Chem.*, 47, 4301-4309
- Haraldsson, A-K., Rimsten, L., Alminger, M., Andersson, R., Aman, P., Sandberg, A-S. (2005). Digestion of barley malt porridges in a gastrointestinal model: Iron dialysability, iron uptake by Caco-2 cells and degradation of β -glucan. *J. Cereal Sci.*, 42, 243-254
- Hörter, D., Dressman, J.B. (2001) Influence of physicochemical properties on dissolution of drugs in the gastrointestinal tract. *Advanced Drug Delivery Reviews*, 46, 75-87
- Humphrey, S. P., Williamson, R. (2001). A review of saliva: Normal composition, flow and function. *The Journal of Prosthetic Dentistry*, 85 (2), 162-169
- Hurrell, R. F., Lynch, S. R., Trinidad, T. P., Dassenko, S. A., Cook, J. D. (1988) Iron absorption in humans: bovine serum albumin compared with beef muscle and egg white. *Am. J. Clin. Nutr.*, 47, 102-107

- Ingels, F., Deferme, S., Destexhe, E., Oth, M., Van den Mooter, G., Augustijns, P. (2002). Simulated intestinal fluid as transport medium in the Caco-2 cell culture model. *Int. J. Pharm.*, 232, 183-192
- Kapsokefalou, M., Alexandropoulou, I., Komaitis, M., Politis, I. (2005) In vitro evaluation of rion solubility and dialyzability of various iron fortificants and of iron-fortified milk products targeted for infants and toddlers. *Int. J. Food Sci. Nutr.*, 56 (4), 293-302
- Kararli, T. T. (1995). Review article: Comparison of the gastrointestinal anatomy, physiology and biochemistry of humans and commonly used laboratory animals. *Pharmaceutics & Drug Disposition*, 16, 351-380
- Kim, J. C., Kim, J. I., Kong, B. W., Kang, M. J., Kim, M. J., Cha, I. J. (2004) Influence of the physical form of processed rice products on the enzymatic hydrolysis of rice starch in vitro and on the postprandial glucose and insulin response in patients with Type 2 Diabetes Mellitus. *Biosci. Biotechnol. Biochem.*, 68 (9), 1831-1836
- Klein, S., Butler, J., Hempenstall, J. M., Reppas, C., Dressman, J. B. (2004) Media to simulate the postprandial stomach I. Matching the physicochemical characteristics of standard breakfasts. *J. Pharma. Pharmacol.*, 56, 605-610
- Kopper, R. A., West, C. M., Helm, R. M. (2006) Comparison of physiological and in vitro porcine gastric fluid digestion. *Int. Arch. Allergy Immunol.*, 141, 217-222
- Krul, C., Luiten-Schuite, A., Baan, R., Verhagen, H., Mohn, G., Feron, V., Havenaar, R. (2000) Research Section: Application of a dynamic in vitro gastrointestinal tract model to study the availability of food mutagens, using heterocyclic aromatic amines as model compounds. *Food and Chemical Toxicology* 38, 783-792
- Kurasawa, H., Kanauti, Y., Takei, K., Gawa, S., Okabe, T., Hoyakawa, T. (1972) Correlation analysis between eating quality, rheological property and amylose content of starch. *J. Agric. Biol. Chem.*, 36 (10), 1809-1813
- Lock, S., Bender, A. E. (1980) Measurement of chemically available iron in foods by incubation with human gastric juice in vitro. *Br. J. Nutr.*, 43, 413-420
- Luiking, Y. C., Peeters, T. L., Stolk, M. F., Nieuwenhuijs, V. B., Portincasa, P., Depoortere, I., van Berge Henegouwen, G. P., Akkermans, L. M. A. (1998). Motilin induces gall bladder emptying and antral contractions in the fasted state in humans. *Gut*, 42, 830-835
- Macfarlane, G.T., Macfarlane, S., Gibson, G.R. (1998) Validation of a three-stage compound continuous culture system for investigating the effect of retention time on the ecology and metabolism of bacteria in the human colon. *Microb. Ecol.*, 35, 180-187
- Mainville, I., Arcand, Y., Farnworth, E.R. (2005) A dynamic model that simulates the human upper gastrointestinal tract for the study of probiotics. *International Journal of Food Microbiology*, 99, 287-296
- Marciani, L., Gouwland, P. A., Spiller, R. C., Manoj, P., Moore, R. J., Young, P., Fillery-Travis, A. J. (2001) Effect of meal viscosity and nutrients on satiety, intragastric dilution and emptying assessed by MRI. *Am. J. Physiol. Gastrointest. Liver Physiol.*, 280, G1227-1233
- Marteau, P., Minekus, M., Havenaar, R., Huis in't Veld, J.H.J. (1997) Survival of Lactic Acid Bacteria in a dynamic model of the stomach and small intestine: validation and the effects of bile. *J.Dairy Science*, 80, 1031-1037
- Minekus, M., Marteau, P., Havenaar, R., Huis in't Veld, J. H. J. (1995). A multicompartmental dynamic computer-controlled model simulating the stomach and small intestine. *Alternatives to Laboratory Animals*, 23, 197-209
- Molly, K., Woestyne, M. V., Verstraete, W. (1993) Development of a 5-step multi-chamber reactor as a simulation of the human intestinal microbial ecosystem. *Appl. Microbiol. Biotechnol.*, 39, 254-258
- Mossi, S., Meyer-Wyss, B., Beglinger, C., Schwizer, W., Fried, M., Ajami, A., Brignoli, R. (1994). Gastric emptying of liquid meals measured noninvasively in humans with [13C] acetate breath test. *Digestive Diseases and Sciences*, 39(12), 107S-109S
- Nguyen, H. N., Silny, J., Matern, S. (1999). Multiple intraluminal electrical impedancometry for recording of upper gastrointestinal motility: current results and further implications. *Am. J. Gastroenterology*, 94 (2), 306-317
- Oomen, A. G., Rompelberg, C. J. M., Bruil, M. A., Dobbe, C. J. G., Pereboom, D. P. K. H., Sips, A. J. A. M. (2003). Development of an *in vitro* digestion mode for estimating the bioaccessibility of soil contaminants. *Arch. Environ. Contam. Toxicol.*, 44, 281-287

Pade, V., Aluri, J., Manning, L., Stavchansky, S. (1995) Bioavailability of pseudoephedrine from controlled release formulations in the presence of guaifenesin in human volunteers. *Biopharmaceutics & Drug Disposition*, 16, 381-391

Pehlivanov, N., Liu, J., Kassab, G. S., Beaumont, C., Mital, R. K. (2002). Relationship between esophageal muscle thickness and intraluminal pressure in patients with esophageal spasm. *Am. J. Physiol. Gastrointest. Liver Physiol.*, 282, 1016-1023

Raina, C. S., Singh, S., Bawa, A. S., Saxena, D. C. (2007) A comparative study of Indian rice starches using different modification model solutions. *LWT*, 40, 885-892

Rao, B. S., Prabhavathi, T. (1978) An in vitro method for predicting the bioavailability of iron from foods. *Am. J. Clin. Nutr.*, 31, 169-175

Schiller, L. R., Walsh, J. H., Feldman, M. (1982) Effect of atropine on gastrin release stimulated by an amino acid meal in humans. *Gastroenterology*, 83, 267-272

Schwizer, W., Frazer, R., Borovicka, J., Crelier, G., Boesiger, P., Fried, M. (1994). Measurement of gastric emptying and gastric motility by magnetic resonance imaging (MRI). *Digestive Diseases and Sciences*, 39 (12), 101S-103S

Souliman, S., Blanquet, S., Beyssac, E., Cardot, J.M. (2006) A level A in vitro/in vivo correlation in fasted and fed states using different methods: Applied to solid immediate release oral dosage form. *European Journal of Pharmaceutical Sciences*, 27, 72-79

Sugawara, M., Kadomura, S., He, X., Takekuma, Y., Kohri, N., Miyazaki, K. (2005). The use of an in vitro dissolution and absorption system to evaluate oral absorption of two weak bases in pH-independent controlled-release formulations. *Euro. J. Pharm. Sci.*, 26, 1-8

Suzuki, S. (1987) Experimental studies on the presumption of the time after food intake from stomach contents. *Forensic Science International*, 35, 83-117

Thompson, D. G., Richelson, E., Malagelada, J. R. (1982) Perturbation of gastric emptying and duodenal motility through the central nervous system. *Gastroenterology*, 83, 1200-1206

Tortora, G. J., Grabowski, S. R. (2000) Principles of anatomy and physiology. 9th Edition. John Wiley and Sons, Inc., Chapter 24, The Digestive System. pp.818-870

Turnbull, C. M., Baxter, A. L., Johnson, S. K. (2005) Water-binding capacity and viscosity of Australian sweet lupin kernel fibre under in vitro conditions simulating the human upper gastrointestinal tract. *International Journal of Food Sciences and Nutrition*, 56 (2), 87-94

Vatier, J. L., Gao, Z., Fu-Cheng, X-M., Vitre, M-T., Levy, D., Cohen, G., Mignon, M. (1992). Evidence for the interaction between antacid and gastric mucosa using an artificial stomach model including gastric mucosa. *J. Pharmacology and Experimental Therapeutics*, 263 (3), 1206-1211

Vincent R., Roberts, A. Frier, M., Perkins, A. C., McDonald, I. A., Spiller, R. C. (1995). Effect of bran particle size on gastric emptying and small bowel transit in humans: a scintigraphic study. *Gut*, 37, 216-219

Whistler, R. L., Wolfrom, M. L., BeMiller, J. N., Shafizadeh, F., Shaw, D., Manners, D. J., Sturgeon, R. J. (1972) *Methods in Carbohydrate Chemistry*. Published by Wiley-IEEE

Williamson, G., Belshaw, N. J., Sief, D. J., Noel, T. R., Rings, S. G., Cairns, P., Morris, V. J., Clark, S. A., Parker, M. L. (1992) Hydrolysis of A and B type crystalline polymorphs of starch by α -amylase, β -amylase and glucoamylase. *Carbohydr. Polym.*, 18, 179-187

Chapter 4

Validation of the Motility used in the *In vitro* Physicochemical Upper Gastrointestinal System (IPUGS)

In this chapter, a detailed review of the gastric motility in the humans and methods of gastric motility applied by previous models in the literature are discussed and compared with the results obtained from the IPUGS and the MISST.

4.1. Introduction

The pattern of the gastric motility in humans is controlled by a very complex set of neural and hormonal signals to maximize digestion and absorption by receptive relaxation of the proximal stomach and antral grinding to perform its dual function of storage and controlled release of the chyme to the duodenum (Marciani *et al*, 2001; Bitar, 2003; Lee *et al*, 2004). Electrical activity of the stomach is composed of the slow wave activity of 3 cycles per min, which is responsible for the timing of the contractions, and electrical response activity which is responsible for triggering the peristaltic contractions (Chen, 1998; Akin and Sun, 2002). *In vitro* digestion models in the literature have attempted to simulate the slow wave activity of the stomach in numerous approaches and these can be classified into six groups which seemed to be dependent fundamentally on the intention of study (Figure 4-1).

One of the most commonly used procedures in the studies of microecology and pharmaceuticals is to use a magnetic stirrer (Savoie, 1994) to mix the gastric contents in the stomach reactor. The use of a magnetic stirrer is relatively cheap, easy to operate and is readily available in laboratories as a common apparatus for mixing solid-liquid and/or liquid-liquid materials. However the degree of mixing could be affected by the use of a large volume, highly viscous materials such as mucus, size of the magnetic stir bar and the ratio of solid to liquid in the reactor, which may cause sinking of solid particles due to gravity if the speed is not fast enough. Also, the mixing via magnetic stirring cannot reproduce the fluid mechanics and the shear forces encountered at the walls of human GIT (Spratt *et al*, 2005). Miller and Wolin (1981) used a hot plate magnetic stirrer in their

in vitro semi-continuous culture system to study the microbial community in the human large intestine to mix the culture medium and the feed. Similarly, Molly *et al* (1993), Alander *et al* (1999), De Boever *et al* (2000 and 2001) incorporated a magnetic stirrer to their model, 'Simulator of the Human Intestinal Microbial Ecosystem (SHIME)', with the stirring speed of 150rpm for the stomach reactor. Furthermore, magnetic stirring has been used by the three-stage compound continuous culture system (Macfarlane *et al*, 1998a and 1998b), computerized artificial stomach model (Vatier *et al*, 1998) to assess sodium alginate induced pH gradient, dynamic model of simulating the human upper gastrointestinal tract (Mainville *et al*, 2005; Lo *et al*, 2006) with the stirring speed of 200rpm, oral absorption and dissolution model (Sugawara *et al*, 2005) to examine pH-independent controlled-release formulations, *in vitro* digestion method by Kulkarni *et al* (2007) to evaluate bioaccessibility of wheatgrass elements and biolysis model by Fatouros *et al* (2007) with agitation of 100rpm for lipid-based drug delivery. However in former models, a low stirring speed of 60rpm has been used by Fordtran and Walsh (1973) and Suzuki (1987) as relatively small volume (up to 50ml) was to be mixed. Often these models are glass-jacketed where water is circulated outside the stomach reactor to maintain 37°C (e.g. dynamic model of simulating the human upper gastrointestinal tract by Mainville *et al*, 2005). If not, hot plate magnetic stirrer is used where the temperature is maintained by a thermostat (e.g. SHIME by Molly *et al*, 1993).

Shaking water bath has been extensively used for various studies of bioavailability in association with nutrients. It is also a relatively cheap and standard laboratory apparatus which is easy to operate, readily available and commonly used for mixing solutions for long hours. One key feature of using the shaking water bath is that temperature maintenance can easily be achieved. However, the shaking water bath only allows mixing in horizontal directions which does not guarantee a thorough mixing if used for short time with small volumes and small sized reactors such as test tubes. The rates of shaking water bath ranged between 55 and 120 oscillations.min⁻¹. *In vitro* digestion/Caco-2 cell culture model by Laurent *et al* (2007) which was designed to explore bioavailability of flavonoids, used 55oscillations.min⁻¹ to simulate the mastication in mouth as well as the gastric motility. Bhagavan *et al* (2007) used 90oscillations.min⁻¹ to simulate gastric motility to assess coenzyme Q10 absorption, Garrett *et al* (1999) and Beysseriat *et al* (2006) and used 95oscillations.min⁻¹ to examine bioavailability of carotenoid and dietary fiber, respectively. The fastest rate used was 120oscillations.min⁻¹ used by Turnbull *et al* (2005) and Perales *et al* (2007) to examine the water binding capacity and viscosity of sweet lupin kernel fiber and iron availability from milk-based formulas and fruit juices,

respectively. The study of bioavailability of iron (Rao and Prabhavathi, 1978; Miller *et al*, 1981; Hurrell *et al*, 1988; Kapsokafalou and Miller, 1991; Frazier *et al*, 1997; Kapsokafalou *et al*, 2005; Argyri *et al*, 2006; Kapsokafalou *et al*, 2007), anti-oxidants (Alexandropoulou *et al*, 2006) and polyphenols (Bermúdez-Soto *et al*, 2007) also used vigorous shaking at unspecified rates.

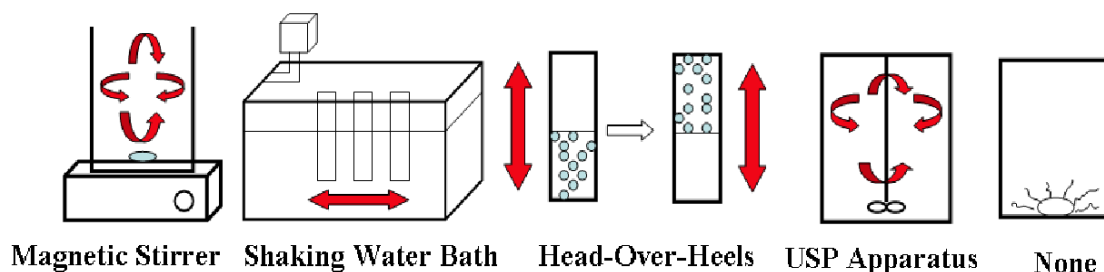


Figure 4-1. A diagram showing the apparatus used by other *in vitro* digestion models. Red arrows indicate the possible directions of the mixing patterns.

Test tube inversion, so called head-over-heels method, is a widely used method in bioaccessibility studies coupled with toxicology. Typically, such studies require trace amounts of the test materials which can be better mixed with vertical movements. Simoneau *et al* (2001) observed more reproducible results in inspecting phthalate mobilization from toys compared with the horizontal shaking method. Oomen *et al* (2002), Oomen *et al* (2003) and Brandon *et al* (2006) used this method with the rotation speed of 55rpm to simulate motility in the compartments of mouth, stomach and small intestine.

Studies of absorption and dissolution of pharmaceuticals often use the United States Pharmacopoeia (USP) apparatus. As the study of pharmaceuticals frequently involves small amount of the test material, uncertainties contributed by the use of various mixing methods may cause difficulties in analyses which can be minimized by using a pre-determined method by the USP. Chavanpatil *et al* (2005) used the USP dissolution apparatus I with the rotation speed of 100rpm to study sustained release of ofloxacin. Galia *et al* (1999) used the USP apparatus 2 (paddle method) to investigate the absorption of albendazole formulation, employing a rotational speed of 100rpm. Souliman *et al* (2006) also used the USP apparatus 2 (paddle method) with rotation speed of 60rpm to study the impact of food intake on acetaminophen release. From their study, more than 95% of acetaminophen tablets was dissolved in less than 10min at pH 5.8, and showed no changes at pH 1.3 (Souliman *et al*, 2006).

Some of the pharmaceutical studies excluded gastric motility thereby simulating static conditions to study dissolution and disintegration of encapsulated/coated drug particles (Blanquet *et al*, 2004; Vasiluk *et al*, 2007) and drug interactions with other components (Castela-Papin *et al*, 1999), with the intention of quality control for batch-to-batch reproducibility rather than simulating dynamic conditions of the GIT. The European and US Pharmacopoeia demanded that the fate of a new drug compound after oral administration to be studied in simple static *in vitro* systems as dissolution is a key parameter in pharmaceutical dosage forms (Blanquet *et al*, 2004). Although these *in vitro* systems are conducted with *in vivo* studies, such systems are not effective in providing the risks concerned with the specific conditions of the GI disorders, control of dosage in formulations, interactions and influence on bioavailability caused by the presence of food and other drugs (Blanquet *et al*, 2004). Without any forms of gastric motility, the diffusion of drugs may be inhibited as the drug molecules are unable to move in all directions and thus constrained to surrounding available sites (Dokoumetzidis *et al*, 2004). In such under-stirred cases, the rate constant of drug movement was found to be non-proportional to the diffusion coefficient of drug molecules, thus disobeying the Fick's laws of diffusion (Dokoumetzidis *et al*, 2004).

Other than the above mentioned methods, computer-controlled flexible walls in the artificial dynamic GI system (TIM-1) by Minekus *et al* (1995) which simulates the peristaltic movements of 3contractions.min⁻¹ in the stomach reactor seemed to be the closest possible alternative to such simulation. Squeezing of the flexible walls is attained by varying the water pressure in between the flexible wall and the outermost wall of the stomach reactor, forcing the chyme to circulate through the loop-shaped TIM-1 (Minekus *et al*, 1999). Ruby *et al* (1996) used somewhat different and aggressive approach in mixing the gastric contents for their Physiologically Based Extraction Test (PBET) for estimation of lead and arsenic bioavailability. Without the use of mechanical stirring, heated (37°C) argon gas of 1.0L.min⁻¹ was passed from the bottom of the stomach reactor through a 70µm frit in which the control of mixing rate is accomplished by adjusting the flow rate of the argon gas. Despite many different approaches to simulate the human gastric motility in perfect mechanical ways, Dokoumetzidis *et al* (2004) argued that the assumptions of homogeneity and well-stirred mixing are contrary to the anatomical and physiological complexity of the humans.

In order to validate and compare the motility patterns used in the *In vitro* Physicochemical Upper Gastrointestinal System (IPUGS), short grain white rice (Sun

Rice Japanese style Sushi Rice, Koshihikari and Opus type) was chosen as a test material as the constituent of the macronutrients is relatively simple (up to 78.5wt% of total carbohydrates) compared to other balanced test meals composed of a mixture of carbohydrates, proteins and fats, thus analyses of carbohydrates would be of the main concern and complications emerging from having to analyze all the nutrients as well as intra and inter-actions of nutrients can be avoided. Studies of starch (including rice starch) underscored no significant differences between the *in vitro* enzymatic hydrolysis and *in vivo* digestion of starch (Williamson *et al*, 1992; Franco *et al*, 1992; Björck *et al*, 1994; Kim *et al*, 2004). Yet, rice is one of the most abundant staple food worldwide (Frazier *et al*, 1997), where intensive research related to the postprandial glucose and insulin responses, diabetes, coronary heart disease, cancer and ageing are being conducted (Frazier *et al*, 1997; Kim *et al*, 2004). Thus the use of IPUGS can be further applied to such studies. The aim of the chapter is to validate the motility patterns used in the IPUGS with available data collected from healthy normal human subjects in the literature. Applied gastric motility methods by other *in vitro* digestion models are compared with that of the IPUGS to evaluate whether the current method is an improvement to the use of magnetic stirring.

4.2. Materials and Methods

4.2.1. The new *In vitro* Physicochemical Upper Gastrointestinal System (IPUGS)

The IPUGS consists of three consecutive compartments simulating the conditions of the upper GI organs in humans. The first compartment simulates the food ingestion in mouth, which is composed of a denture set with manually controlled mastication and continuous secretion of artificial saliva of $37\pm 0.5^{\circ}\text{C}$ which is transferred via a peristaltic pump at rate of $7.0\text{ml}\cdot\text{min}^{-1}$ (Edgar 1990; Humphrey and Williamson, 2001). White short grain rice (Sun Rice Japanese style Sushi Rice) was cooked in a conventional rice cooker with 1:1 volumetric ratio of rice grains to water. 100g of the cooked rice was transferred to the mouth reactor with 250ml of drinking water to be used as the feed material. As the cooked rice is relatively small in size which can be swallowed without much of mastication, it can be regarded as simpler foods for testing. 5mins of gentle manual mastication was applied with the denture set with $20\text{chewing}\cdot\text{min}^{-1}$ to remove large

clusters of rice into smaller pieces to aid the swallowing process. The feed material was spoon fed to the next compartment, esophagus at a rate of $8.5\text{ml}\cdot 30\text{s}^{-1}$ (equivalent to $\frac{1}{2}$ tbsp. 30s^{-1}).

The last two compartments simulating the conditions of the esophagus and the stomach were built with platinum cure silicon rubber composed of 75-85wt% polyorganosiloxanes, 20-25wt% of amorphous silica and 0.1wt% of platinum-siloxane for part A and 65-70 wt% of polyorganosiloxanes and 20-25wt% of amorphous silica for part B. 1:1 ratio of the parts A and B were mixed and coated to the plastic anatomy model of the stomach which resembles the average human stomach size at unfed state (20cm x 15cm x 8cm, Kararli, 1995; Pade *et al*, 1995) as well as its geometry of J-shaped curve. The coatings were repeated until the thickness of the stomach wall reached $0.50\pm 0.01\text{cm}$ in average. The material is translucent in color thus by adding of food coloring agents to the feed mixture may help clearer view of the reactions in the inner stomach compartment. It offers negligible shrinkage and able to stretch and rebound to its original size and shape without distortion. For the esophagus, paper roll of 1.5cm diameter and 20cm in length was made, and coatings of the silicon rubber were repeatedly made until the wall thickness reached $0.30\pm 0.01\text{cm}$ in average (Al-Zaben and Chandrasekar, 2005). The paper roll and the plastic anatomic model were removed after coatings. In order to deliver the gastric secretions to the wall of the stomach, a large number of Tygon ® Microbore tubings (n=200) with inner diameter of 0.25mm were implanted, with the tips of these tubings pierced into the stomach wall to create a gradual dampening of the wall (Figure 4-2), secreting $3.5\text{ml}\cdot \text{min}^{-1}$ (Mainville *et al*, 2005) throughout the 3hr digestion period. These tubings are designed for precision injection and dispensing in laboratory applications with flexible and bendable resin. The tubings have a very smooth inner bore surface which reduces the risk of particulate build-up during sensitive fluid transfer and minimal extractable helps to assure fluid purity. Also, these tubings are transparent, thus the gastric secretions passing into the stomach wall can be seen clearly. For mucosal secretions in the esophagus compartment, slightly larger diameter of tubing was used. Micro-Line™ tubing (Thermoplastic Scientifics, Inc.) made of cross-linked ethyl vinyl acetate. These tubings are translucent, flexible and elastic with inner diameter of 0.51mm. One ends of these implanted tubings in both esophagus and the stomach were planted into the wall of each compartment to create gradual dampening effect from the wall to simulate the opening and closing of the pores in the gastric wall for secretion delivery. The other ends were gathered and squashed into a larger diameter Tygon peristaltic tubings (inner diameter of 1.5cm), which are subsequently connected to the smallest

possible peristaltic tubing (inner diameter of 0.80mm). Though the flow rate of the peristaltic pumps can be controlled, changing the peristaltic tubing size also helped to control the flow rate more accurately. For validation of motility experiments, only one peristaltic pump (Autoclude® Peristaltic Pump - 54505) was used to deliver the artificial gastric juice to the stomach compartment.

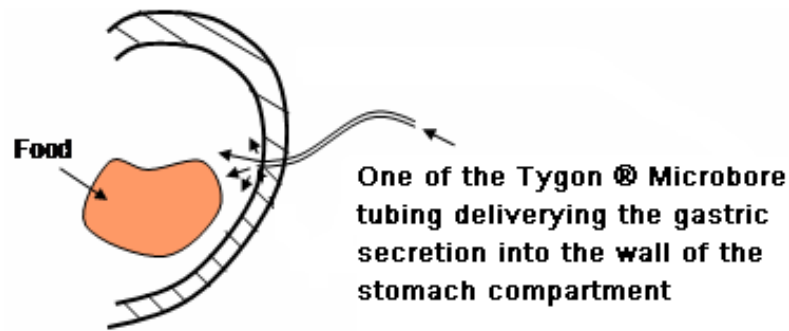


Figure 4-2. An illustration of one of the Tygon® Microbore secretion tubings inserted into the wall of the stomach compartment. 200 of these tubings were implanted with even distribution to deliver the artificial gastric secretions.

The esophagus and the stomach compartments were placed in an anaerobic chamber with continuous nitrogen gas flow ($1.0\text{L}\cdot\text{hr}^{-1}$) and the temperature inside the chamber was maintained at $37\pm 1^\circ\text{C}$ with a hot plate placed inside the chamber. The compositions of the artificial saliva and the gastric juice were kept as simple as possible to avoid any complications from salts in analyzing data. Thus α -amylase and hydrochloric acid, which are the main substances that are able to hydrolyze rice starch, were used. Other constituents were excluded for these experiments. 2g of fungal (*Aspergillus oryzae*) α -amylase (GrindamyI™ A5000, 5000U/g, Danisco 071314) was mixed with 200ml of deionized (MilliQ) water to be used as the artificial saliva and 0.15M HCl (Ajax, AF602394) was used as the artificial gastric juice, which were both warmed up to $37\pm 1^\circ\text{C}$. The α -amylase from *Aspergillus oryzae* (E.C.3.2.1.1) was one of the closet and cheap alternative to the human α -amylase (E.C.3.2.1.1). Hormonal control of altering the secretion rates was also excluded as to compare the IPUGS to other models in terms of motility only.

The esophagus and the stomach compartments were manually pressed with my hands to mimic the peristaltic waves. For the esophagus, coordinated contractions and relaxations of the peristaltic propulsions were simulated to push the ingested feed material (bolus) towards the stomach with the rate of 5 contractions per 30s. The wall of the esophageal

compartment was squeezed both horizontally and vertically by gripping the esophagus using both hands, one on top of each other and in between a thumb and an index finger, squeezed gently to push down the bolus (Figure 4-3).

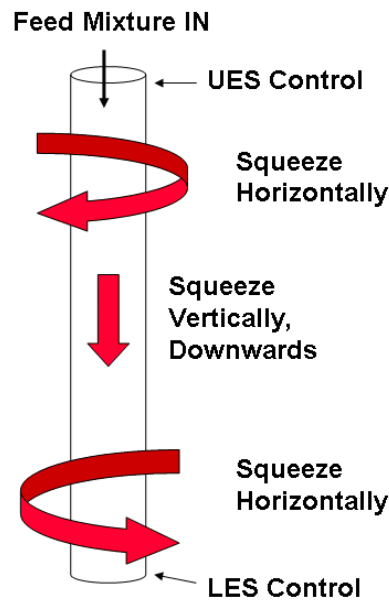


Figure 4-3. Diagram showing the motility of the esophageal compartment of the IPUGS. Red arrows indicate the direction of squeezing. UES refers to the upper esophageal sphincter and LES represents the lower esophageal sphincter.

The upper esophageal sphincter (UES) controlled the entrance of the feed mixture and the lower esophageal sphincter (LES) controlled the exit of the feed mixture into the stomach compartment. Each cycle of esophageal peristalsis lasted up to 6s (Pehlivanov *et al*, 2002). Apart from mucosal secretions, there are neither digestive secretions nor absorption take place in the esophagus (Tortora and Grabowski, 2000) thus these features were excluded.

Hand squeezed actions to simulate the peristaltic waves of the human stomach was used in the stomach compartment as well. The first peristaltic wave was initiated from squeezing the proximal part of the stomach compartment (the fundus and upper body). This was to generate a pressure gradient from the body of the stomach to the pylorus, resulting an opening of the pyloric sphincter and emptying of fractions of the stored bolus towards and mix with the gastric secretions, which resembles the action of a contractile grinder, crushing the small chunks of the bolus as described in the literature (Akin 1998; Luiking *et al*, 1998; Nguyen *et al*, 1999; Tortora and Grabowski, 2000) (Figure 4-4).

The First Peristaltic Wave

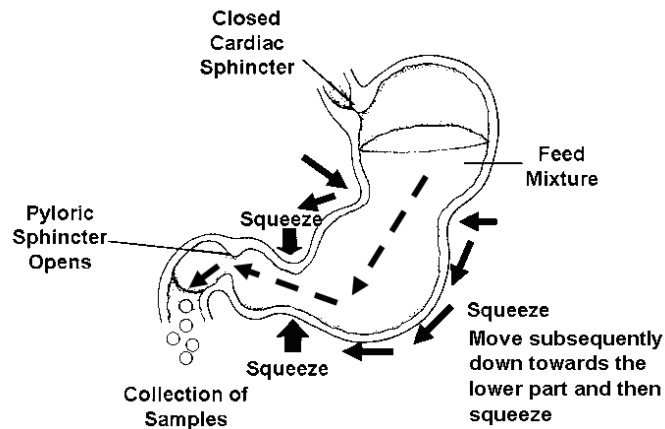


Figure 4-4. A diagram of the first peristaltic wave applied to the stomach compartment of the IPUGS. Black arrows drawn on the outside of the stomach indicate the directions of the squeezing action. Squeezing initiated from the body of the stomach and moved subsequently towards the lower antrum/pylorus area, followed by a strong squeezing in the lower antrum/pylorus area to open the pyloric sphincter and release the chyme. Dotted black arrows inside the stomach indicate the expected flow of the chyme inside the stomach compartment.

The Second Peristaltic Wave

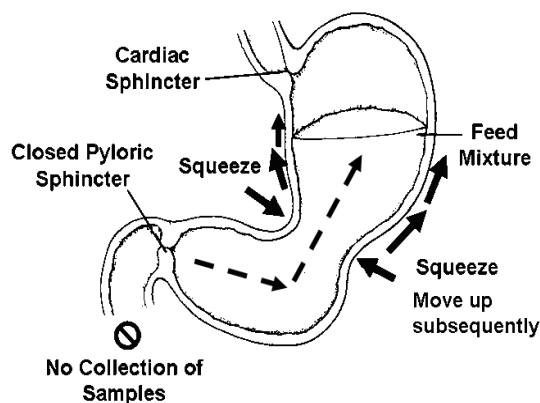


Figure 4-5. A diagram of the second peristaltic wave applied to the stomach compartment of the IPUGS. Black arrows drawn on the outside of the stomach indicate the directions of the squeezing action and red arrows indicate the expected flow of the chyme inside the stomach compartment. Black dotted arrows inside the stomach indicate the direction of the chyme movement.

The second peristaltic wave with closed cardiac and pyloric sphincters was initiated from the distal stomach (lower body and the antrum), squeezing the wall of the stomach towards the proximal direction (toward the fundus) (Figure 4-5). Sequential contractions of the antrum crushed the small chunks of the bolus against the closed pyloric sphincter with a large fraction of the remaining bolus squeezed back toward the proximal part for further digestion (Tortora and Grabowski, 2000; De Zwart *et al*, 2002), causing distention of the stomach compartment to accommodate more space for the incoming food which was facilitated by the elastic and stretchy nature of the building material (platinum cure silicon rubber). The overall gastric motility in the proximal stomach compartment remained relatively constant, but for the distal part, stronger contractions with higher depth and amplitudes (Schwizer *et al*, 1994) were used.

The digestion period of 3hrs was set as carbohydrates typically take 2-4hr to be emptied into the small intestine (Suzuki, 1987; Mossi *et al*, 1994). Initially, 5ml of the samples were taken from the mouth compartment to check the consistency of each batch. From 10min to 30min, 20ml of samples were collected every 10min from the pylorus.

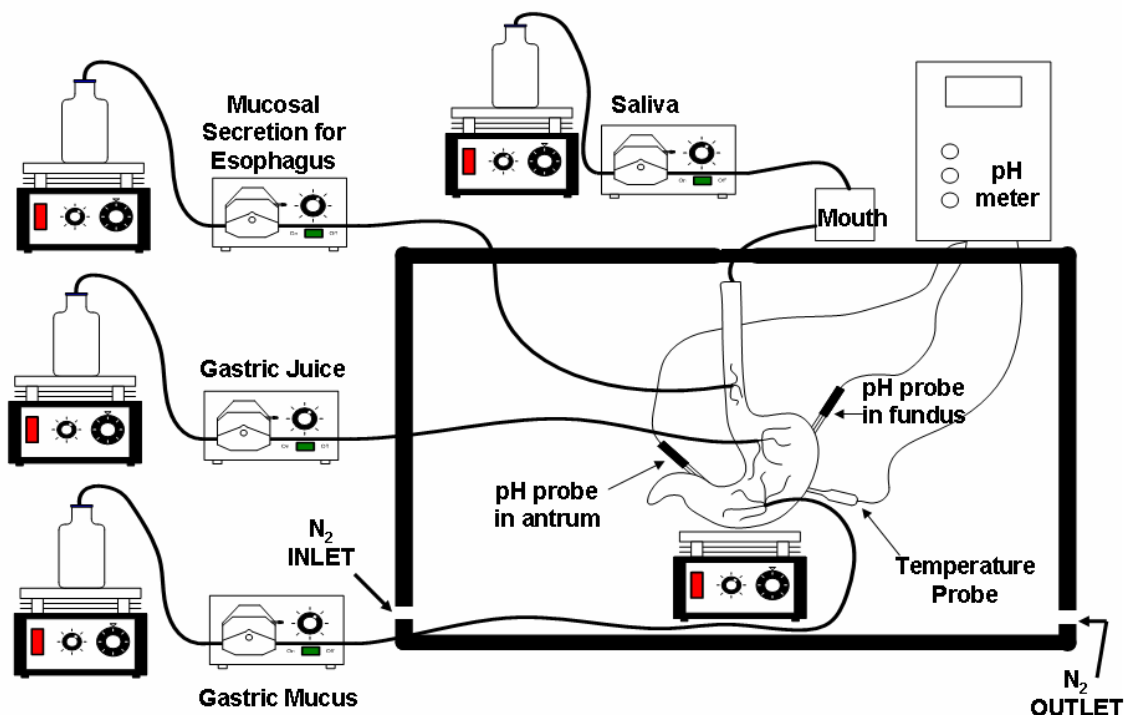


Figure 4-6. A schematic diagram of the IPUGS

From 30min to 180min where the gastric emptying was to be more active, 6.8ml of the chyme mixture was pumped out of the MISST per minute (Marciani *et al*, 2001; Mainville *et al*, 2005), collected and stored in sampling bottles with closed lids and

placed in an ice water bath (0-2°C) while the experiment was running. Then the samples were centrifuged at 3000rpm for 30mins (Klein *et al*, 2004) at 2°C. The supernatants were diluted accordingly for each of the analytical methods used. The experiments via the IPUGS were conducted triplicate. A schematic diagram of the IPUGS can be found in Figure 4-6.

4.2.2 Modified *In vitro* Stomach Stir Tank (MISST)

To compare the motility used in the IPUGS with other *in vitro* digestion models with the use of a magnetic stirrer, a Modified *In vitro* Stomach Stir Tank (MISST) was made (Figure 4-7). In order to investigate the effectiveness of the mouth compartment in the IPUGS, a homogenizer (Wise Mix Homogenizer, Daihan Scientific HG-15D) was used in the MISST. For a better comparison, the IPUGS with (IPUGS-1) and without (IPUGS-2) the use of a homogenizer was used. (i.e. IPUGS-1 used homogenization which was the exactly the same as the MISST thus the only difference between the MISST and the IPUGS-1 was the gastric motility, and IPUGS-2 used mastication as described in section 4.2.1). The homogenizer was used instead to breakdown the test food material into a very fine particles (< 500µm in diameter) and a smooth blend of the drinking water (liquid) and cooked rice (solid). The resultant feed mixture (food and water) was placed in a 1L beaker and homogenized at 400rpm for 10mins. In the literatures, some *in vitro* digestion models have used such homogenization as an alternative for having a mouth reactor (Frazier *et al*, 1997) because the blended mixture allows for easier and more continuous pattern of pumping the feed mixture via peristaltic pumps. Also, it inhibits any potential blockage in the peristaltic pump tubings to operate in a more controlled manner.

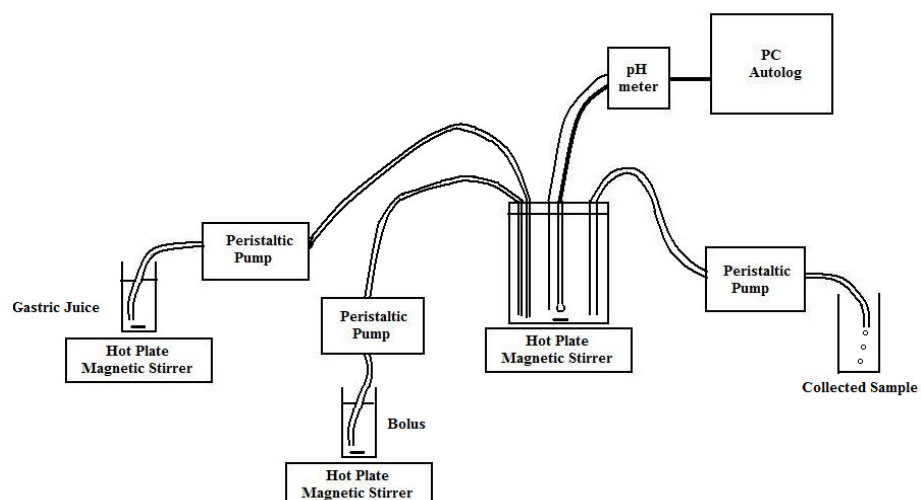


Figure 4-7. A schematic diagram of the MISST.

The stomach reactors used in the SHIME (Molly *et al*, 1993; De Boever *et al*, 2000), TIM (Minekus *et al*, 1995), and in the dynamic *in vitro* human upper GIT model system were transformed to make a 'modified *in vitro* stomach stir tank (MISST)' (Figure 4-7). It was designed to compare the results obtained from the IPUGS, paying attentions to the methods of motility and secretions in particular as well as to determine whether the IPUGS is a more advanced model or not.

A 1L glass beaker was used to represent the stomach. The open top was tightly sealed with a disc of Styrofoam, with the thickness of 2.0 ± 0.1 cm, to mimic the anaerobic condition of the human GIT. The pH and temperature probes were placed in the MISST as well as 3 peristaltic pump tubings for the delivery of the food and the gastric secretion to the MISST and withdrawing of the chyme from the MISST as to simulate the fill-and-draw mechanism used by Molly *et al* (1993). The styrofoam disc was pierced to tightly fit the probes and the tubings to the stomach reactor; therefore, the reactor was completely inhibited from interacting with the air and/or oxygen throughout the experiment. The pH and the temperature probes were placed in the middle of the stomach reactor. Tygon peristaltic tubings which deliver the food mixture and the gastric secretion were placed perpendicular to the pH and the temperature probes. The tubing for collecting of the chyme mixture was placed on the opposite side to the tubings of the food and the gastric secretion delivery. Thus the stomach reactor was anatomically coordinated. i.e. esophagus for the food delivery, fundus of the stomach for the gastric secretion and pylorus for the chyme collection. The MISST was heated to and maintained at $37\pm 1^\circ\text{C}$ on top of a hot plate magnetic stirrer, and it was constantly stirred at 150rpm with a magnetic stir bar (4cm x 0.5cm diameter) (Molly *et al*, 1993; Mainville *et al*, 2005). In order to simulate the cephalic phase of the stomach, the reactor was filled with 17.5ml of the gastric secretion prior to addition of the food (Mainville *et al*, 2005). 3.5ml of the gastric secretion was delivered per minute to the stomach reactor via peristaltic pump to simulate the gastric phase (Mainville *et al*, 2005). At time 0, 5ml of the homogenized pre-digested feed mixture was sampled to check for the consistency for each batch of the feed mixture preparation. All other times, 6.4ml of the chyme mixture was pumped out of the MISST per minute (Mainville *et al*, 2005; Marciani *et al*, 2001), collected and stored in sampling bottles and placed in an ice water bath ($2\pm 1^\circ\text{C}$) while the experiment was running. Then the samples were centrifuged at 3000rpm for 30mins (Klein *et al*, 2004) at 2°C . The supernatants were diluted accordingly for each of the analytical methods used. The experiments via the MISST were conducted quadruplicate.

4.2.3. Phenol-Sulfuric Acid Assay

Phenol-Sulfuric acid assay is one of the most widely used analytical methods in measuring neutral sugars in oligosaccharides, proteoglycans, glycoproteins and glycolipids. It is a simple, fast, reliable and sensitive method which has been developed by Dubois *et al* (1951) and (1956). Rao and Pattabiraman (1989) reported that phenol underwent sulfonation in situ and the phenol-sulfuric acid complex decreased the color intensity for many hexoses and pentoses. Similar results were seen by Masuko *et al* (2005) whom modified the original method by Dubois *et al* (1951) and (1956) by adding concentrated sulfuric acid to the sample followed by phenol. Instead of using microplate proposed by Masuko *et al* (2005), larger volumes were reconstituted following the ratio of sample to conc. sulfuric acid to phenol. The method was used to determine the concentration of total water soluble carbohydrates from the obtained samples.

3ml of concentrated sulfuric acid was added to 1ml of diluted (factor of 100) sample in a test tube followed by vigorous shaking at high speed in a vortex mixer. 600 μ L of 5% (w/v) phenol was pipetted into the mixed solution and placed in a water bath at 90°C for 10min. The prepared samples were vortexed at high speed for 30s and left at room temperature for 5mins cooling before reading the absorbance via the UV spectrophotometer (Agilent 8453, UV G1103A) at 490nm.

4.2.4. Somogyi-Nelson Method

Somogyi-Nelson method (Somogyi, 1926; Somogyi, 1937, Somogyi, 1945; Nelson, 1944; Wrolstad *et al*, 2005) is an extensively used highly accurate method for determining the amount of reducing sugars (e.g. maltose). Low alkalinity copper reagent and arsenomolybdate reagent were prepared as follows.

12g of sodium potassium tartate and 24g of anhydrous sodium carbonate with 250ml of distilled water were mixed. 4g of copper sulfate pentahydrate and 16g of sodium bicarbonate were added to 200ml of distilled water. 180g of anhydrous sodium sulfate in 500ml of boiling distilled water was separately prepared. Three mixtures were combined and diluted to 1L to make the low alkalinity copper reagent. The arsenomolybdate reagent was made by mixing 25g ammonium molybdate to 450ml of distilled water. 21ml of

concentrated sulfuric acid and 25ml of distilled water containing 3g of disodium hydrogen arsenate heptahydrate were added to the ammonium molybdate solution with stirring. The mixture was continuously stirred for 24hrs at 37°C and kept in brown glass stopped bottle until use.

1ml of the diluted (factor of 100) sample and 1ml of the low alkalinity copper reagent were placed in a test tube and vigorously mixed by a vortex mixer at a high speed for 30s. The test tube was placed in a boiling water bath (100°C) for 10mins, and cooled at room temperature for 5mins. 1ml of the arsenomolybdate reagent was then added and the mixture was vortexed at a high speed for 30s. Absorbance at 500nm was read via the UV spectrophotometer (Agilent 8453, UV G1103A). Blanks for the absorbance were prepared by replacing the sample with 1ml distilled water.

Blue color of the low alkalinity copper reagent and green color of the arsenomolybdate reagent gave a greenish blue color in all the samples. The samples which contained less maltose showed a light green solution, but as the concentration of maltose increased, the color of the sample became darker and bluish. As the arseno reagent is extremely toxic and may cause cancer, particular cares were taken to avoid inhalation and contacts at all times.

4.2.5. High Performance Liquid Chromatography (HPLC)

High Performance Liquid Chromatography (HPLC) is able to provide both qualitative and quantitative analyses with a small amount of diluted sample of carbohydrates including malto-oligomers (Jodál *et al*, 1984). As HPLC requires a prestigious level of accuracy, it was used to ensure the compatibility of results from the phenol-sulfuric acid assay and the Somogyi-Nelson method, as well as to screen for any unexpected components (e.g. glucose) in the collected samples.

A carbohydrate ES column (Prevail™ Carbohydrate ES Column-W 150x4.6mm, 5 μm (Alltech Part No. 35102)) was used to specifically analyze maltose, maltotriose and other undigested starch in the samples. A mixture of degassed (Elite™ Degassing System) acetonitrile (Merck, HPLC grade) and deionized water was used as mobile phase and was pumped into the column via a quaternary gradient pump (Alltech, 726) at 1.0ml.min. Isocratic gradient was used for a better separation of carbohydrates – initially 65% to 35%

of acetonitrile to water and then from 15min onwards, 50% to 50%, respectively. Collected samples were diluted (x40) with deionized water, followed by syringe filtration with nylon membranes and automatically injected (Alltech Autosampler 570) into the column with 30min of analysis time per sample. Evaporative Light Scattering Detector (ELSD) and EZStart software were used to detect and record the findings. The heating column temperature of 50°C with Nitrogen (5.0) gas flow rate of 1.5L.min⁻¹ was used and the gain on the ELSD was set at 2.

4.2.6. Recording of pH

The measure of the pH profile is one of the simplest analyses which directly indicate the conditions of the stomach and it is of extreme importance as it is able to detect even minor changes of the gastric conditions. For the IPUGS, two pH probes and one temperature probe were pierced into the wall of the stomach compartment in the IPUGS to record the pH in the fundus (probe 1) and the antrum (probe 2). The temperature probe was placed in the middle of the body of the stomach to measure the changes with respect to time. For the MISST, a pH probe and a temperature probe were placed in the middle of the stomach reactor. A pH meter from Hanna Instrument (HI 4212) was used with auto-logging mode of 30s for 3hr.

4.3. Results and Discussions

4.3.1. Phenol-Sulfuric Acid Assay

The Phenol-Sulfuric Acid Assay provided information on the concentration and the mass of total water soluble carbohydrates present in the stomach compartment of the MISST and the IPUGS with respect to time. As shown in the Figure 4-8 and 4-9. The concentration of total carbohydrates (g.L⁻¹) varied significantly between the two models, MISST and IPUGS, over the 3hr digestion period. The concentration of total carbohydrates indicates the available amount of rice carbohydrates, including both of amylopectin and amylose, in the stomach compartment at given times, which denotes the rate of gastric emptying and how effectively the motility and the secretions were

controlled throughout the experiments, thus a very useful in analyzing the effectiveness of the models.

As it has been proposed by Elashoff *et al* (1982) that for uniformity, time 0 was defined as the point at which the meal ingestion began. Therefore the collected samples at time 0min can be referred to as the bolus which was about to be swallowed as the samples were taken before they were ingested into the esophagus. Initially, the values of the total carbohydrates concentration in the MISST and the IPUGS 1 were relatively similar to each other, $106\pm 3\text{g.L}^{-1}$ and $112\pm 1\text{g.L}^{-1}$, respectively. This indicates that a good control of preparing the feed mixture was maintained throughout the experiments, as the procedures for preparing the feed mixture were the same for the MISST and the IPUGS-1. A calibration error from the weight balance when weighing hot cooked rice as well as slight variations occurred from homogenization process seemed to have caused a small difference in the initial starch concentrations. However the the total carbohydrates concentration in the IPUGS-2 samples showed the lowest value, $96\pm 3\text{g.L}^{-1}$, among the three models.

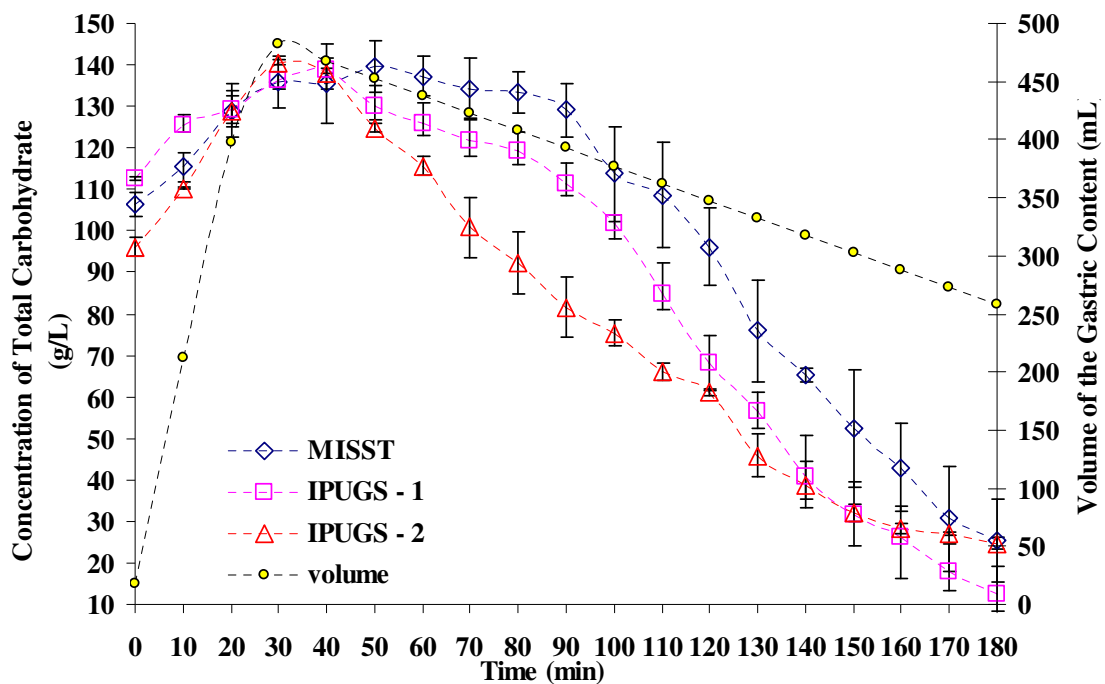


Figure 4-8. A graph showing the concentration of total water soluble carbohydrates (g.L^{-1}) during the 3hr digestion time (min). The results obtained from the MISST are marked in blue, the IPUGS-1 in pink and the IPUGS-2 in red. The volume of the gastric content (mL) is shown with the axis on the right hand side.

It should be noted that different types of feeding materials were used to compare the mastication of the mouth - the IPUGS-2 has a mouth part to simulate mastication,

continuous saliva secretion and swallowing action to simulate the human conditions as closely as possible whereas for the MISST and the IPUGS-1, saliva was poured into the homogenized cooked rice in water and allowed 5min of pre-digestion in the mouth part. The pre-digestion of homogenized test meal, which was almost like a thick starch paste, has been very commonly used in many nutritional studies (Frazier *et al*, 1997). As the food particles became significantly smaller (up to 500 μ m in length) compared to non-homogenized cooked rice grains (5.5 \pm 0.4mm in length, 1.9 \pm 0.1mm in thickness and 3.0 \pm 0.1mm in width; average values of 25 rice grains), a faster the total water soluble carbohydrates extraction from the rice grains, the total carbohydrates dissolution in water and overall carbohydrates digestion were expected as it would have a higher chance to interact with salivary amylase.

It was speculated that the strong mechanical homogenization may have induced a breakdown of amylopectin to amylose, which would have fasten the overall rate of starch hydrolysis, releasing reducing sugar molecules of maltose. Although the difference in concentrations of the the total carbohydrates in the three models varied noticeably, when the masses of the total carbohydrates present in the samples were calculated, there was near to none difference during the ingestion period between the MISST (1.87 \pm 0.05g) and the IPUGS-1 (1.97 \pm 0.05g), and slightly lower mass of the total carbohydrates was found (1.68 \pm 0.05g) for the IPUGS-2 (Figure 4-9). This seemed to be due to small volume (5ml) of the samples withdrawn from the model. As the main purpose of the study was to determine and compare different gastric motility patterns used in the IPUGS and the MISST, it was decided to take only a small amount of sample that was enough to prepare for the analyses. By analyzing the initial starch content, the presence of the mouth part in the model can be evaluated compared to the traditional nutritional study preparation of homogenization/grinding. Also these results can be referred as the reference/control point for further analyses.

As the ingestion had initiated, the feed mixture was delivered through the esophagus then deposited predominantly in the proximal stomach with progressive distribution into the distal stomach as the gastric emptying progressed. This was also seen by Lee *et al* (2004) in the human stomach. During the ingestion period of up to 30min, there was not a significant difference in both the concentration and the mass of total carbohydrates among the three models. They all showed a very sharp and constant increase in the concentration and the mass of total carbohydrates, along with the increase in the volume of the gastric content. All of the models reached maximal gastric volume of 473 \pm 3ml, maximal starch

concentrations of $135\pm 3\text{g}\cdot\text{L}^{-1}$ (MISST), $136\pm 2\text{g}\cdot\text{L}^{-1}$ (IPUGS-1), $140\pm 1\text{g}\cdot\text{L}^{-1}$ (IPUGS-2) and maximal total carbohydrates masses of $64\pm 3\text{g}$ (MISST), $64\pm 4\text{g}$ (IPUGS-1), $67\pm 2\text{g}$ (IPUGS-2) at 30min, which was the end time of the ingestion period. Physiologically under the normal condition (without any disorders) in the humans, there is not much of the chyme passing from the stomach to the duodenum during the ingestion period and if there is, it would only be liquids (e.g. water). The samples obtained from the MISST showed a gradient between the solid rice particles and liquid part when stored vertically in the ice water bath for 3hrs, whereas the samples obtained from both of the IPUGS-1 and 2 contained no visible solid materials in the samples collected during the ingestion period. It is assumed that the greater curvature of the stomach in the IPUGS allowed the solid particles to be deposited and remained in the stomach compartment for further digestion. All the samples were opaque white in color but not viscous as there was no mucosal secretions.

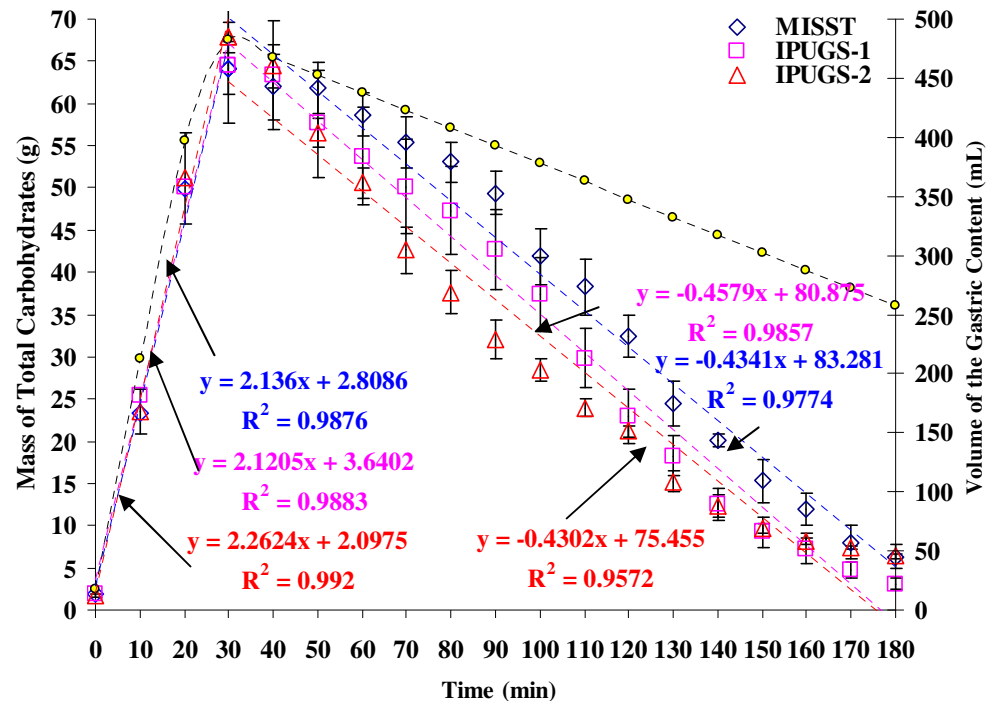


Figure 4-9. A graph showing the mass of total water soluble carbohydrates (g) during the 3hr digestion period (min). The results obtained from the MISST are marked in blue, the IPUGS-1 in pink and the IPUGS-2 in red. The volume of the gastric content (mL) is shown with the axis on the right hand side.

Figure 4-9 shows the mass of total carbohydrates (g) with respect to time (min) during the ingestion period. All the models showed a linear relationship ($R^2 \geq 0.9876$), where the slope of the graph differed slightly from one another. The IPUGS-2 showed rate of $2.2624\text{g}\cdot\text{min}^{-1}$, which was the fast among the three models, showing a fast sharp increase

of the total carbohydrates mass during the ingestion period. The MISST and the IPUGS-1 showed gradients of $2.136\text{g}\cdot\text{min}^{-1}$ and $2.1205\text{g}\cdot\text{min}^{-1}$, which were almost undistinguishable.

As soon as the meal ingestion ceased, the volume of the gastric content as well as the concentration and the mass of total carbohydrates started to decrease and the gastric emptying period had initiated. It should be noted that the total carbohydrates concentration ($\text{g}\cdot\text{L}^{-1}$) measured refers to the concentration of total carbohydrates present in the collected sample which is typically of 50ml, which is the size of the sampling bottle. The remainder of the collected samples, approximately 14ml, was discarded. It is an arbitrary phenomenon that the stated numerical values of the total carbohydrates concentration exceeded the total mass of rice added (100g). In order to avoid confusion, the change in the volume of the gastric content for MISST and IPUGS 1 and 2 was made exactly the same; a graph showing the change in the gastric content volume with respect to time is shown on each graph. From 20 to 40min, the total carbohydrates concentrations of the three models were almost indistinguishable. Although the gastric secretions were delivered to the stomach constantly, the chyme samples, which were of greater volumes than the volume of the gastric secretion, were also withdrawn at the same time. Thus the volume of the gastric content has decreased over time, and therefore the concentration and the mass of starch in the stomach also decreased over time.

Though from about 42min mark, the trend of decrease in the concentration and the mass of total carbohydrates diverted from one another. Even though the rate of gastric secretions, the composition of the gastric secretion, the rate and the volume of sample withdrawal from each model were kept the same, the pattern and the amount (both the concentration and the mass) of total carbohydrates declined in different manners. From 50min till the end of the digestion period, the MISST showed the highest concentration and the mass of total carbohydrates at all times, meaning the gastric emptying was the slowest. The result was contradictory to the fact that premature gastric emptying of solid rice particles were contained in the samples obtained during the ingestion period. Nevertheless the finely homogenized rice particles could be regarded as almost evenly dispersed in the gastric secretion even at low stirring speed of 150rpm. The stirring speed of 500rpm has been used to investigate any possibilities of uneven mixing and gravitational effect of rice particles in the stomach reactor of the MISST, however, the values of the total carbohydrates concentration as well as other measurements taken, such

as the concentrations and the masses of maltose and maltotriose and pH, were very similar to each other (results shown in Chapter 3).

However with the IPUGS-1, a similar trend in the rate of gastric emptying was observed to that of the MISST, but it showed the fastest reduction in the starch concentration and the starch mass, especially between 90min and 130min. This is due to the small sized particles used in the IPUGS-1 compared to that of the IPUGS-2 as the particle size of the feed mixture is proportional to the evacuation time in the gastric emptying process. Miller *et al* (1920a and 1920b) observed that rice pudding which has a smooth texture and considerably smaller sized particles to that of the rice grains, was emptied to the duodenum in 2hr, where 100g of boiled rice took 2.5hr to 3hr. Similar results were seen by Najib *et al* (1988) who demonstrated that the ratio of mean residence time (s) of particles to mean residence time of fluid (s) was raised sharply when the diameter of the food increased from 15 μ m to 63 μ m. Another important factor is that the building material of the IPUGS (platinum cure silicon rubber) is very elastic and able to stretch many times as its original size. Thus the surface area of the IPUGS is much larger than that of the MISST, enabling a faster digestion process. Therefore the gastric emptying of the rice starch in the IPUGS-1 was the fastest among the three models.

Unlike the ingestion period, the trend of decrease in the mass of the total carbohydrates was different to the decrease in the volume of the gastric content over time as shown in Figures 4-8 and 4-9. For IPUGS-2, the overall rate of gastric emptying was the fastest among the three models. At the 90min mark, which can be considered as the half time of the overall digestion period, the difference in the gastric total carbohydrates concentrations and the masses among the three models was the largest – 129 \pm 3g.L⁻¹ and 82 \pm 4g.L⁻¹, 50 \pm 3g and 32 \pm 2g for the MISST and the IPUGS-2 respectively. From the 120min to the 160min mark, the mass of the total carbohydrates in the IPUGS 1 and 2 was almost indistinguishable. It was suspected that due to the curvature of the stomach compartment in the IPUGS, which allowed the undigested solid rice particles to be deposited in the stomach compartment for further digestion, the rate of decrease in the starch concentration slowed down toward the end of the experiments. The rate of decrease in the concentration and the mass of total carbohydrates in the MISST was very constant from the 50mins till the end of the experiment and almost linear especially from 120min to the end of the experiment. The MISST not only represents a combined model from the literature review but it also denotes a perfect mixing condition. As rice is a carbohydrate rich source of food, the gastric emptying is relatively faster than other foods, especially

those which are rich in proteins and fats. Thus by allowing the digestion period of up to 3hr the gastric content, including the feed mixture and the secreted gastric juice, were mostly emptied at the end of each experiments. From 130min to 180min, the rates of gastric emptying for the MISST and the IPUGS-2 were very similar to one another. Although the rice grains fed to the IPUGS-2 were considerably large compared to that of the homogenized feed mixture for the MISST and the IPUGS-1, very small amount of solid rice particles which were significantly reduced in size (up to 0.5mm in length and diameter) and almost perfectly spherical in shape, were found at the end of the experiments. As shown in the Figure 18, the mass of the total carbohydrates (g) over time, indicating the gastric emptying, showed linear relationship ($R^2 \geq 0.9572$). This has been observed by others who studied gastric emptying by scintigraphy with radio-labeled solid foods, showing linear relationship with R^2 of 0.95 (Schwartz *et al*, 1982; McCallum *et al*, 1980; McCallum *et al*, 1981; Ruby *et al*, 1996). In Figure 4-9, the period between 40 and 180min was considered as the time of major gastric emptying of solid materials because during the ingestion period of up to 30min, the gastric emptying was minimized and only small volume of the samples was extracted, thus it was excluded from the graph. IPUGS-1 showed the fastest gastric rate with the rate of $-0.4579\text{g}\cdot\text{min}^{-1}$, as it was expected with having the small sized particles as the feed mixture as well as having a larger surface area compared to that of the MISST, $-0.4341\text{g}\cdot\text{min}^{-1}$. The MISST showed the slowest gastric emptying rate, and the IPUGS-2 showed the medium rate of $-0.4302\text{g}\cdot\text{min}^{-1}$.

The nutritional information on Table 3-4 (refer to 3.1.2. pg. 64) shows that the total amount of carbohydrates in 100g of the rice (Sun Rice Japanese style Sushi Rice) is 78.5g, which matches well with the maximal mass of the total carbohydrates on Figure 4-9, approximately 78.5g. The time taken to empty half of the stomach compartment was approximately 90min, 110min and 115min in the IPUGS-2, IPUGS-1 and MISST, respectively. It must be noted that the first 30min of the experiment was the ingestion period where near to none of gastric emptying took place. Thus when comparing the experimental data to the clinical or physiological data in the literature, 30min should be subtracted from the general time line, and by doing so, the experimental results confirmed the results from Marciani *et al* (2001) who used high viscosity nutrient meal consisting of 37% lipid and 63% carbohydrates, and the time taken to empty the stomach in humans was $76 \pm 6\text{min}$. They also tested low viscosity nutrient meal (similar to the case of rice) and the time taken to empty half of the stomach was $67 \pm 9\text{min}$.

The volume of food increases with each successive meal during the day and ranges between 0 and 1.0L, with 1.5L being the maximal capacity of the stomach (Joseph *et al*, 2003). Bouras *et al* (2002) measured the gastric volumes in 73 healthy volunteers using SPECT (single photon emission computed tomography) imaging. In the fasted state, average volume of the stomach was 213ml, with males 215ml and females 211ml. However after a meal (postprandial condition), the volume increased to 698ml – 744ml for males and 675ml for females, where postprandial minus fasting showed 483ml (521ml for males and 464ml for females), resulting the ratio of postprandial to fasting volume to 3.4. The meal fed to the subjects was not specified but it is assumed that just like other clinical studies, it would contain a balanced meal rather than just a bowl of rice and a cup of water. When compared to Figures 4-8 and 4-9, where the fasting volume of 250 ± 3 ml was seen at 180min, the change of gastric volume, and hence the gastric emptying rate, was quite relevant to that of the actual human conditions. Despite that the amount of the test material fed to the MISST and IPUGS was small compared to that of the standard meals used in clinical studies, it showed peak volume of 472 ± 3 ml. Under fasting conditions, mean gastric volume with the barostat was $225\text{ml}\pm 51$ and with MRI was $331\text{ml}\pm 56$ (De Zwart *et al*, 2002).

4.3.2. Somogyi-Nelson Method

The Somogyi-Nelson method was used to analyze the concentration and the mass of maltose ($\text{g}\cdot\text{L}^{-1}$) in the stomach compartment which varied considerably from 35 to $5\text{g}\cdot\text{L}^{-1}$ and 0 to 16g, respectively, throughout the experiment as illustrated by Figures 4-10 and 4-11. Maltose is a reducing sugar which is a byproduct released during the conversion of amylopectin to amylose and/or amylose converted to a shorter chain of carbohydrate in the process of starch hydrolysis (Frazier *et al*, 1997). Hence observing the trend of the concentration and the mass of maltose in the collected chyme sample over the 3hr digestion period facilitates the evaluation of whether the results obtained from the IPUGS are compatible to that of the human conditions. Another reason of the study is to investigate the effect of different motility applied and whether there is a significant difference in the digestion of rice between the manually pressed motility patterns in the IPUGS and constant and stable motility via magnetic stirring in the MISST.

Initially, the concentration of maltose in the MISST and the IPUGS-1 were detected at high level, about $35\pm 1\text{g}\cdot\text{L}^{-1}$ and $34\pm 1\text{g}\cdot\text{L}^{-1}$, respectively. It should be noted that 5min of

pre-digestion period in the MISST and the IPUGS-1 facilitated the starch hydrolysis process to release maltose in a faster rate compared to that of the IPUGS-2. Also having a finely grinded feed material induced more of starch to amylase interactions compared to the use of non-grinded rice grains. Thus by comparing the concentration of maltose for the three models showed an enormous variation of having a proper mouth model and replacing the mouth model by homogenizer. As discussed earlier, the volume of the sample withdrawn was considerably low (5ml) to allow minimal variation in the overall volume of the gastric content. Therefore when a comparison of the mass of maltose is compared, the difference was not as huge as it was of the concentrations – $0.61\pm 0.02\text{g}$ and $35\pm 1\text{g.L}^{-1}$ (MISST), $0.60\pm 0.05\text{g}$ and $34\pm 1\text{g.L}^{-1}$ (IPUGS-1) and $0.026\pm 0.001\text{g}$ and $1.47\pm 0.02\text{g.L}^{-1}$ (IPUGS-2). This was due to the availability of larger amounts of water soluble total carbohydrates for salivary amylase digestion in the MISST and the IPUGS-1 as shown in the Figures 4-8 and 4-9. For the IPUGS-2, the maltose mass detected was almost similar to the blank (distilled water) when analyzed by the UV-photospectrometer and the HPLC.

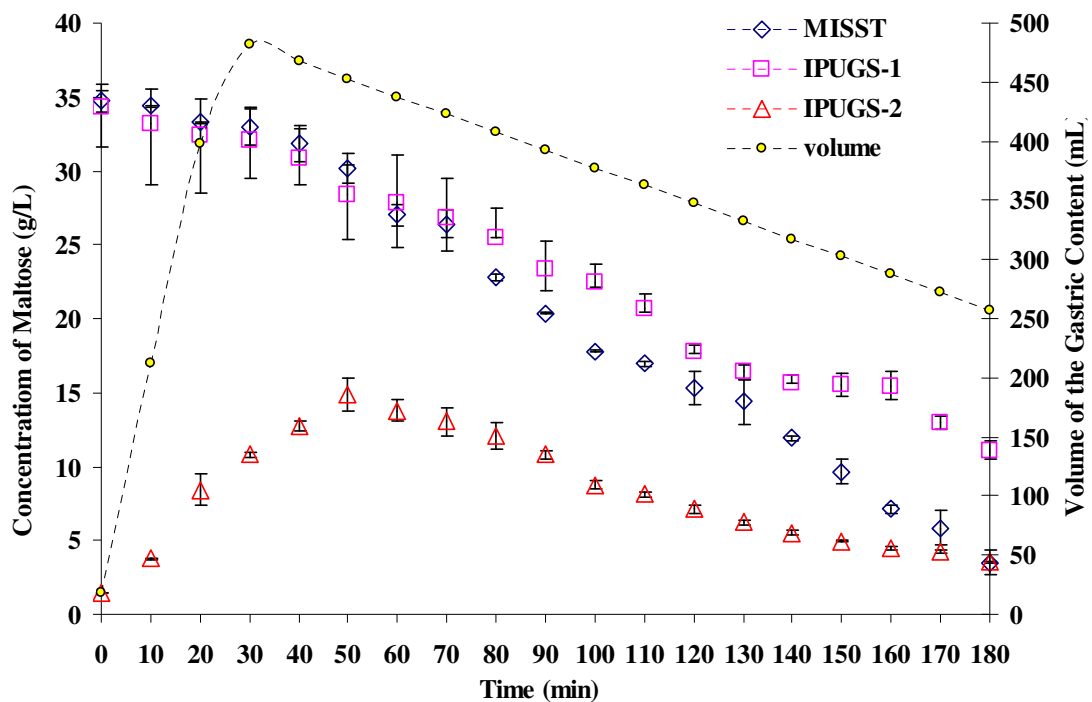


Figure 4-10. A graph showing the concentration of maltose (g.L^{-1}) during the 3hr digestion time (min). The results obtained from the MISST are marked in blue, the IPUGS-1 in pink and the IPUGS-2 in red. The volume of the gastric content (mL) is shown with the axis on the right hand side.

The MISST and the IPUGS-1 which had finely homogenized particles as feeding material, showed much faster loading rate of maltose. It can be concluded that the fine grinding of

the cooked rice grains by the homogenizer enhanced a faster rice starch hydrolysis, producing the reducing sugar, maltose, faster than compared to non-homogenized fed materials. The values of the mass of the maltose in MISST and IPUGS-1 were very similar to each other throughout the experiments, especially during the feeding period, up to 30min. By end of 30min, when the mass of the available starch in the stomach reactor was the highest, the highest mass of maltose was seen for both MISST and IPUGS-1. However from 40min to the end of the experiments, IPUGS-1 showed higher values of mass of maltose concentration when compared to that of the MISST. This can be due to having a geometrical resemblance to the human stomach, where the curvatures of the stomach played a key role.

During the ingestion period, the concentrations of maltose molecules in both the MISST and the IPUGS-1 have slightly decreased. Up to 30min mark, the changes in overall maltose concentration were very small for the MISST and the IPUGS – $35\pm 1\text{g.L}^{-1}$ to $33\pm 1\text{g.L}^{-1}$ and $34\pm 1\text{g.L}^{-1}$ to $32\pm 2\text{g.L}^{-1}$, respectively. The pattern of the increase in the mass of maltose was very similar to that of the volume of the gastric content. However for the IPUGS-2, completely different pattern was shown.

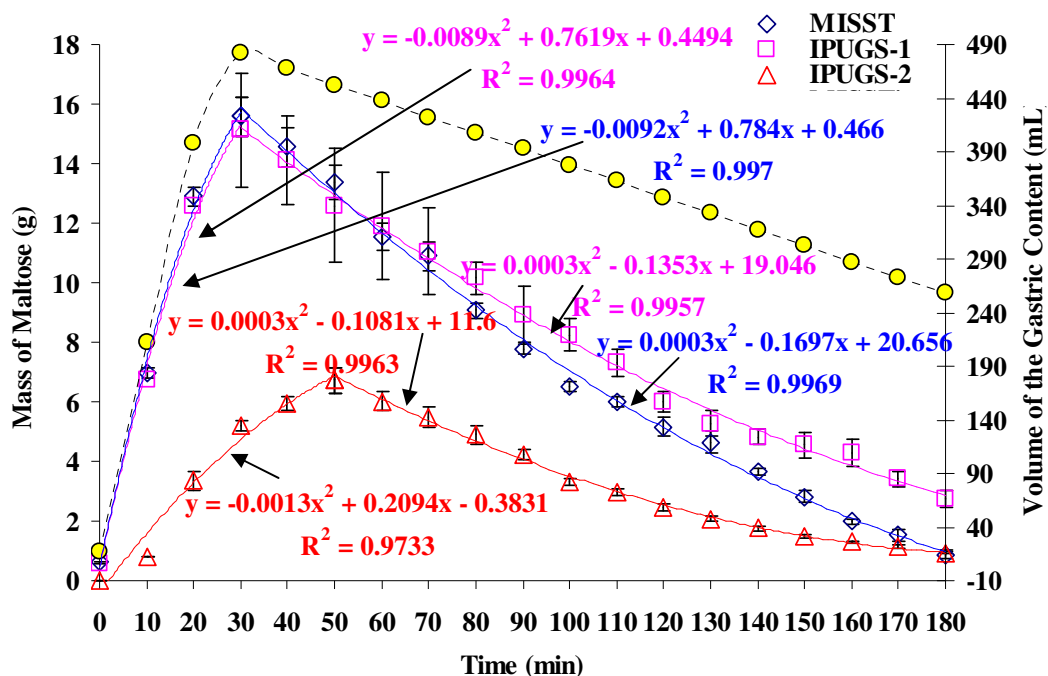


Figure 4-11. A graph showing the mass of maltose (g) during the 3hr digestion time (min). The results obtained from the MISST are marked in blue, the IPUGS-1 in pink and the IPUGS-2 in red. The volume of the gastric content (mL) is shown with the axis on the right hand side.

There was an increase in maltose concentration from $1.47 \pm 0.02 \text{ g.L}^{-1}$ to $10.8 \pm 0.2 \text{ g.L}^{-1}$ during the ingestion period. This was due to increasing availability of water soluble total carbohydrates in the stomach that is susceptible to either enzymatic (salivary amylase) or acidic (gastric juice) hydrolysis. When the masses of maltose in the MISST and the IPUGS-1 were compared, a very rapid increase has been noticed. Irrespective of how high the concentrations were, the volume of the gastric content for all the models was relatively small; $482.5 \pm 3 \text{ ml}$. Although in terms of concentrations, the fluctuations of the maltose between the MISST and the IPUGS-2 seemed very high, when the actual mass of maltose present in the stomach was calculated by multiplying the gastric content volume (mL) and the concentration (g.L^{-1}), the difference was rather smaller than expected. At 30min mark where both the volume of the gastric content as well as the amount (both concentration and mass) of total carbohydrates (Figures 4-8 and 4-9) were the highest, the maltose mass reached its maximal point in the MISST and the IPUGS-1. Especially up to 30min, the values of the maltose mass and the rate of maltose change in the stomach compartments of both of these models were almost indistinguishable (Figure 4-11).

However for the IPUGS-2, the maximal mass and the concentration of maltose were detected at 50min mark. It would seem that the greater curvature of the stomach in the IPUGS held back the undigested starch for further digestion as the hydrolysis of maltose carried on at high rate even after the gastric emptying initiated. The trend of concentration and mass of maltose from 30min to 70min in the MISST and the IPUGS-1 demonstrated a faster rate of decrease in maltose with respect to time, and both models showed very similar values to one another. However from 80min to the end of the experiment, IPUGS-1 showed highest concentration and the mass of maltose at all times. It can be speculated that due to the greater curvature of the stomach of the IPUGS, undigested starch molecules were deposited for further hydrolysis, and allowed liquid portion of the gastric content to be passed to the pylorus. In the MISST, the collected samples contained very fine rice particles and the proportion of the solid to liquid of the collected samples was somewhat greater than that compared to the samples from both the IPUGS 1 and 2. The rate of decrease in maltose concentration and mass for the IPUGS-1 were very slow and gradual over time, whereas for the MISST, a faster rate of reduction in maltose mass was evident especially between 60min and 120min. Along with constantly decreasing starch and the gastric volume, it would seem that the amount of maltose decreased together.

In order to exhibit the rice starch hydrolysis during the gastric emptying period in more details, the mass of the maltose was derivatized with respect to time (min), shown in

Figure 4-12. A very clear difference between the IPUGS and the MISST was shown. The MISST showed the fastest rate of maltose mass over time (0.008) compared to that of the IPUGS 1 and 2 (0.006 for both). For the IPUGS-2, changes in both the mass and the concentration of maltose were very constant throughout the experiment, and the rate of decrease was greater between 60 to 120min than 120min to 180min. Some literatures argued that as the rice is rich in carbohydrates and carbohydrate portion of the ingested meal is always the fastest to be processed to the next part (duodenum), the transit time of rice can be as short as 2hr. Some literatures also argued that in some cases, where meat is ingested with the rice (as in most cases of meal consumption, a balanced meal was fed for clinical studies and gastric scintigraphy), the overall digestion took up to 4hrs. In order to fully exhibit the effect of all the rice being properly digested, the digestion time of 3hrs was chosen.

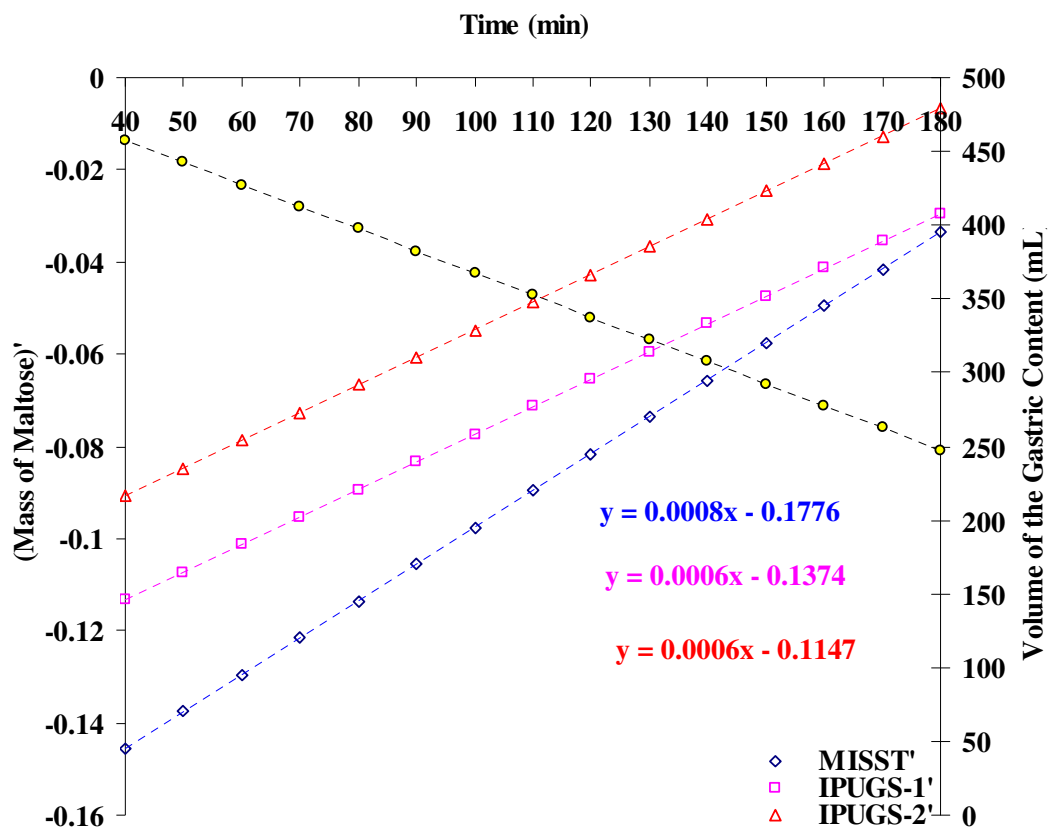


Figure 4-12. A graph showing the derivatised maltose mass over time. The results obtained from the MISST are marked in blue, the IPUGS-1 in pink and the IPUGS-2 in red. The volume of the gastric content (mL) is shown with the axis on the right hand side.

However with the control of secretion and the rate of gastric emptying used for such study, 200 to 250ml of the fluid remained in the stomach even after the 3hr digestion period. This is due to the absence of feed back control, where the rate of gastric secretion was once set at 3.5ml, which is more representative of the secretion rates at stimulated state,

and kept at the same rate till the end of the experiments. This was why the samples collected toward the end of the experiment were very dilute (Castela-Papin *et al*, 1999).

The rate of decrease in maltose mass was the fastest in the MISST in between 120min and 180min. Even though the rate is slower compared to that of the period between 60min and 120min, it did not differ much for the MISST. As the conditions and controls of the MISST were more of an ideal situation, where everything was set at constant and mechanical, the results are reasonable. IPUGS-1 also showed a very much of similar trend with the MISST and also the values were very constantly decreased over time. However with the IPUGS-2, very small amount of reduction in the maltose mass was shown in between 120min and 180min – $2.47\pm 0.12\text{g}$ to $0.92\pm 0.03\text{g}$. At 180min, the mass of maltose in the MISST was even lower than that of the IPUGS-2 – $0.87\pm 0.14\text{g}$. At 180min, the concentration of maltose in the MISST and the IPUGS-2 were very similar to each other, $3.51\pm 0.43\text{g}\cdot\text{L}^{-1}$ and $3.56\pm 0.05\text{g}\cdot\text{L}^{-1}$, respectively. The IPUGS-1 showed the highest concentration and the highest mass of maltose of $11.09\pm 0.62\text{g}\cdot\text{L}^{-1}$ and $2.74\pm 0.29\text{g}$, respectively.

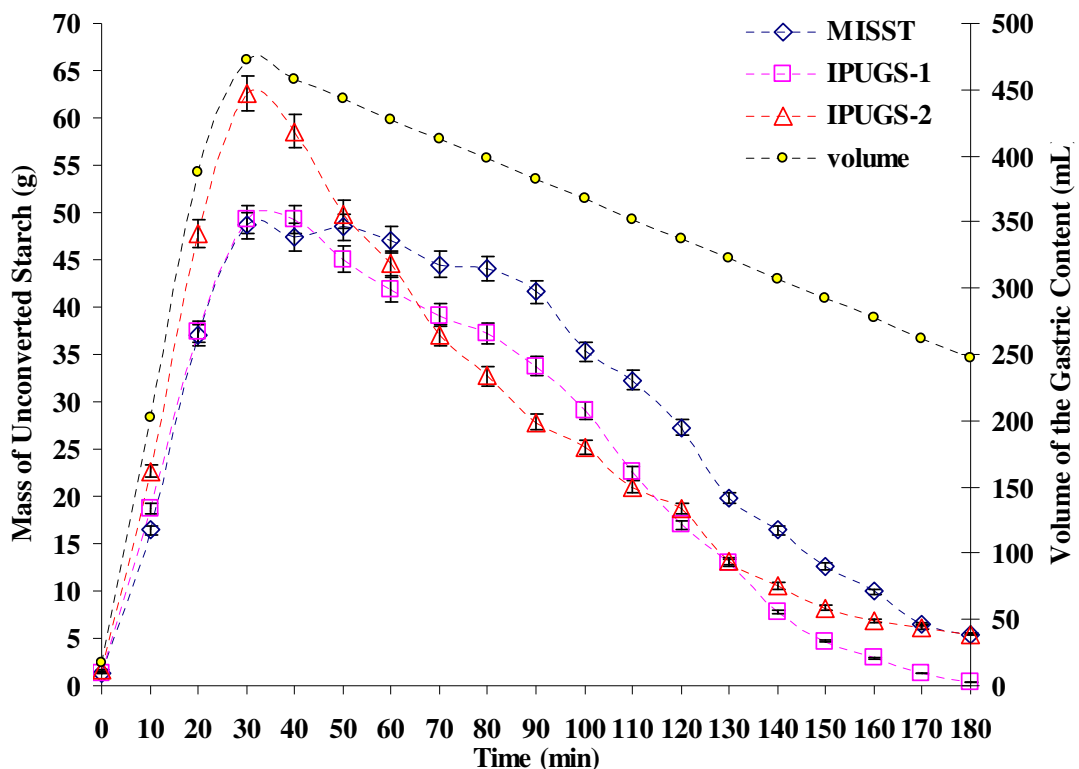


Figure 4-13. A graph showing the mass of unconverted starch (g). The results obtained from the MISST are marked in blue, the IPUGS-1 in pink and the IPUGS-2 in red. The volume of the gastric content (mL) is shown with the axis on the right hand side.

Figure 4-13 shows the mass of unconverted starch (long chain carbohydrates) in the stomach compartment during the 3hr digestion period. The trend of change in the mass of the unconverted starch was slightly different to that of the change in the mass of the total carbohydrates (Figure 4-9). The masses of the unconverted starch were indistinguishable between the MISST and the IPUGS-1 during the ingestion period. The IPUGS-2 showed higher maximum value, $62.6 \pm 1.5\text{g}$. The rate of decrease in the unconverted starch of the IPUGS-2 was much faster compared to the MISST and the IPUGS-2. From 45min mark, the mass of the unconverted starch for the MISST and the IPUGS-1 started to diverge, with the values of the MISST showing higher range compared to that of the IPUGS-1. This denotes that the motility used in the IPUGS was more effective in the starch hydrolysis compared to the mechanical stirring used in the MISST. From 53min mark, the mass of the unconverted starch of the MISST exceeded that of the IPUGS-2. Despite of the mechanical breakdown of the rice meal in the MISST, it showed the highest range of the unconverted starch mass, implying the least efficient motility method among the three models.

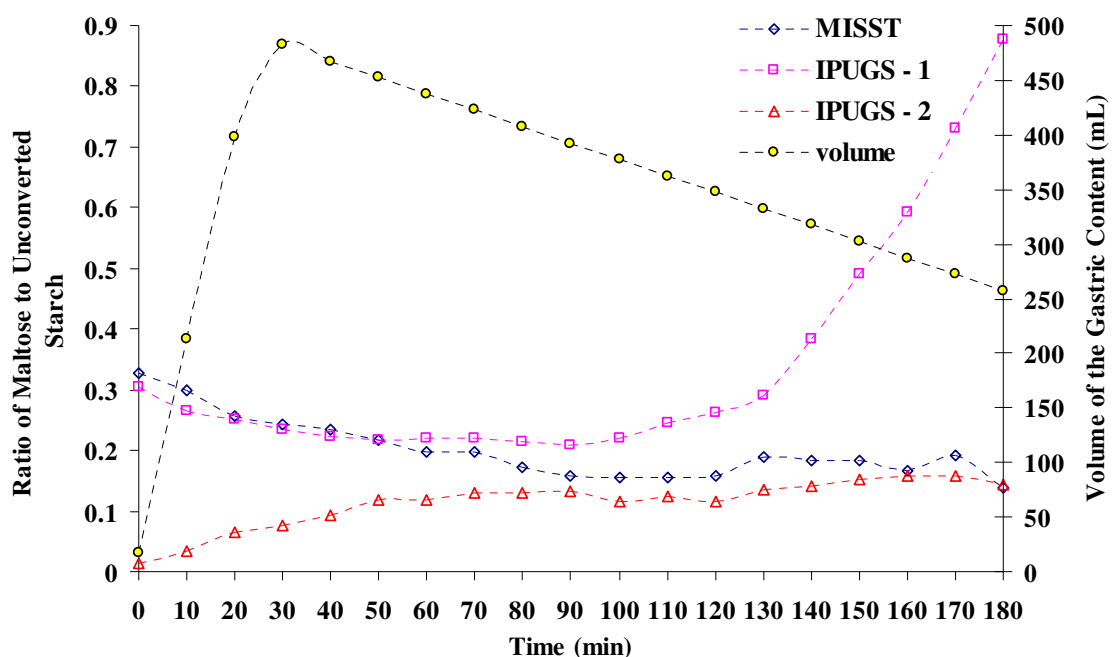


Figure 4-14. A graph showing the ratio of the mass of the maltose to the mass of the unconverted starch during the 3hr digestion time (min). The results obtained from the MISST are marked in blue, the IPUGS-1 in pink and the IPUGS-2 in red. The volume of the gastric content (mL) is shown with the axis on the right hand side. Note that Undigested starch = Total Water Soluble Carbohydrates – Maltose – Maltotriose.

The ratio of maltose to unconverted starch is an important indication to how much of amylopectin and amylose were hydrolyzed to release the reducing sugar, maltose. A

distinctively different pattern of the ratio of maltose to unconverted starch is shown in the Figure 4-14. As the mass and the concentration of maltose in the IPUGS-2 were nearly zero, the initial ratio of maltose to unconverted starch was very different to the ratios of the MISST and the IPUGS-1 where finely homogenized feed materials showed higher content of maltose due to mechanical breakdown via homogenization and higher susceptibility to salivary amylase digestion. Up to 60min, the ratio of maltose to starch increased in the IPUGS-2, however for the MISST and IPUGS-1 which showed nearly the same values up to 50min mark, diminished slightly from 0.33 and 0.30 to 0.22 and 0.21 respectively. The ratio of the MISST constantly decreased up to 120min to a level similar to that of the IPUGS-2, and from 120min to 180min the ratios of both the MISST and the IPUGS-2 were similar to one another, showing very small fluctuations and an overall increase. However for the IPUGS-1, from 110min to 180min, the ratio of maltose to unconverted starch increased almost exponentially. This indicates that provided the same feed materials and the same secretion conditions were supplied, the IPUGS was more efficient in digestion of starch (amylopectin and amylose) to maltose which benefited from a larger surface area for interaction of the bolus particles and the gastric secretion, more realistic gastric motility to aid the digestion process and the geometrical resemblance to the human stomach, holding the undigested particles back in the stomach until it is ready to be passed to the next level of the GI system.

4.3.3. HPLC

Using the HPLC, an overall screening of the collected samples was made to clarify the presence of maltose and to identify the possible byproducts of the rice starch hydrolysis. As a result, maltose and maltotriose were detected. The starch hydrolysis in the normal human subjects usually do not result in glucose, as the partially unconverted starch as well as maltose are further digested by pancreatic α -amylase in the small intestines.

In general, the mass of maltose (g) analyzed from the HPLC showed slightly lower values (Figure 4-15) compared to that of the UV-spectrophotometer. This seemed to be caused by the waiting period of the samples collected from the models until the analysis. Although the samples were kept in an ice water bath, and diluted accordingly to a factor of 40, some samples had to wait over 10hr until the analysis began. However the standing time at room temperature for the UV-spectrophotometric measurements was much shorter when compared to that of the HPLC. Also after dilutions, the samples were

chemically treated with arseno and somogyi reagents, where there were no treatments for the HPLC samples. Even with the use of the shortest column to examine the sample in the HPLC, it took 15-30min, as the HPLC column requires cleaning time to avoid any blockage and accumulation of carbohydrate molecules which may cause interference amongst the samples for analyses.

Maltotriose concentration was detected by the HPLC. In order to avoid any arbitrary confusions, the obtained values of the concentration (g.L^{-1}) were converted to the mass of maltotriose present (g) by multiplying the gastric content volume (Figure 4-16) to the concentration. For the MISST, the mass of maltotriose was the highest at 40min, reaching approximately 12g, which was the highest among the three models. The IPUGS-1 reached its maximal value of about 9.5g at 30min. Both of the MISST and the IPUGS-1 showed a sharp increase during the ingestion period. However with the IPUGS-2, the exponential increase of the mass of maltotriose was seen between 0min to 20min. At 30min mark, it reached its maximal value of about 3.5g, which was much smaller compared to that of the other two models. Despite its smallest maximal mass of maltotriose, nearly no change in the mass was seen throughout the 3hr digestion period in the IPUGS-2, resulting indistinguishable difference in the final mass of the maltotriose compared with the other two models.

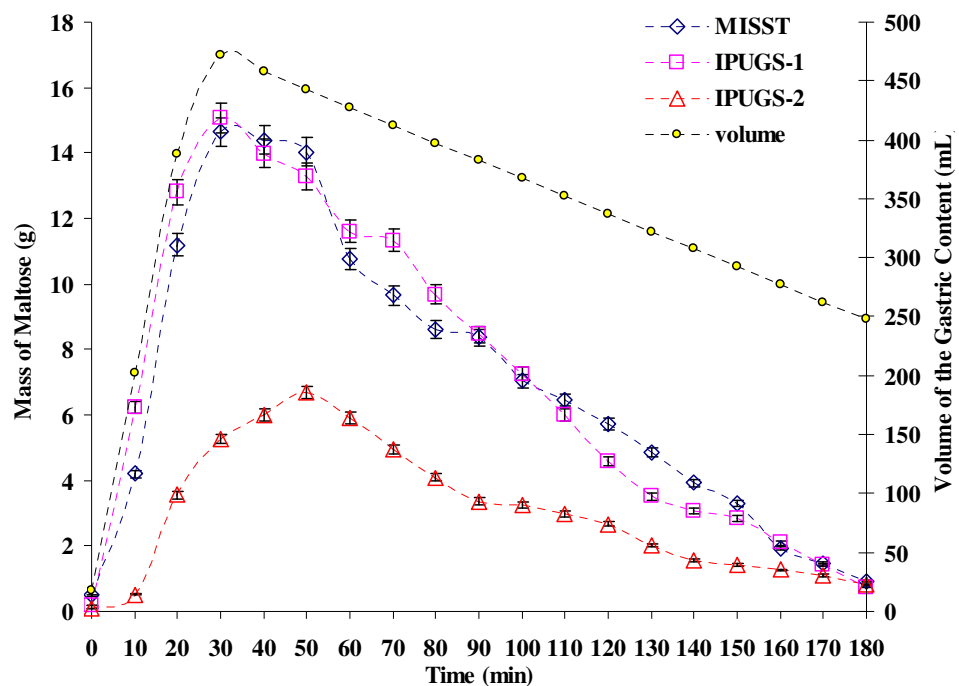


Figure 4-15. A graph showing the mass of maltose over time which was measured by the HPLC. The results obtained from the MISST are marked in blue, the IPUGS-1 in pink

and the IPUGS-2 in red. The volume of the gastric content (mL) is shown with the axis on the right hand side.

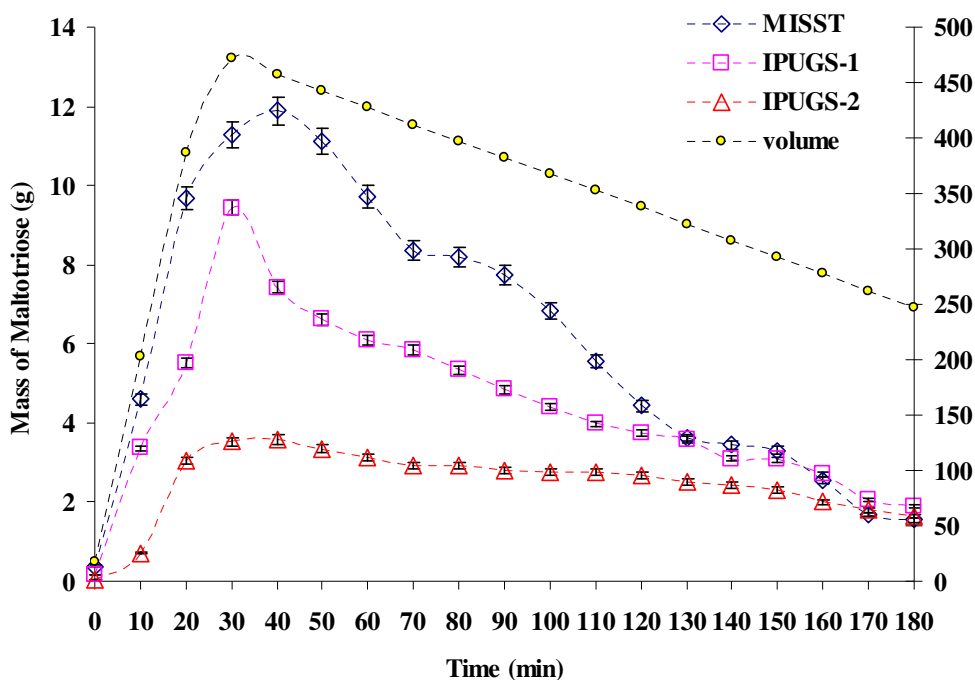


Figure 4-16. A graph showing the mass of maltotriose over time which was measured by the HPLC. The results obtained from the MISST are marked in blue, the IPUGS-1 in pink and the IPUGS-2 in red. The volume of the gastric content (mL) is shown with the axis on the right hand side.

4.3.4. Recording of the pH

The pH profile is one of the widely used tools to indicate the feasibility of an *in vitro* testing method, especially for clinical studies such as the interaction of drug and the gastric secretions, disintegration of coating materials and capsules, and possible interference of more than one type of drug taken at the same time (Dressman *et al*, 1990; Horter and Dressman, 2001). The pH profile is able to emphasize the overall control of motility as well as secretions applied, and in conjunction with results from the Phenol-Sulfuric acid assay, the Somogyi-Nelson method and the HPLC, a better understanding of the effect of motility can be perceived. Two probes were used for measuring the pH of the IPUGS 1 and 2. Probe 1 (Figure 4-17) refers to the pH probe which was implanted at the wall of the fundus, where the majority of the acidic gastric secretions take place, and probe 2 (Figure 4-18) was implanted on the wall of the antrum, where acidic chyme awaits to be passed out of the stomach.

The three models showed distinctively different patterns of pH change over time. Initially, the pHs of the three models were of a similar value of 1.03 ± 0.01 . This value refers to the pH of the 0.15M HCl which was used as a simplified gastric juice for these experiments.

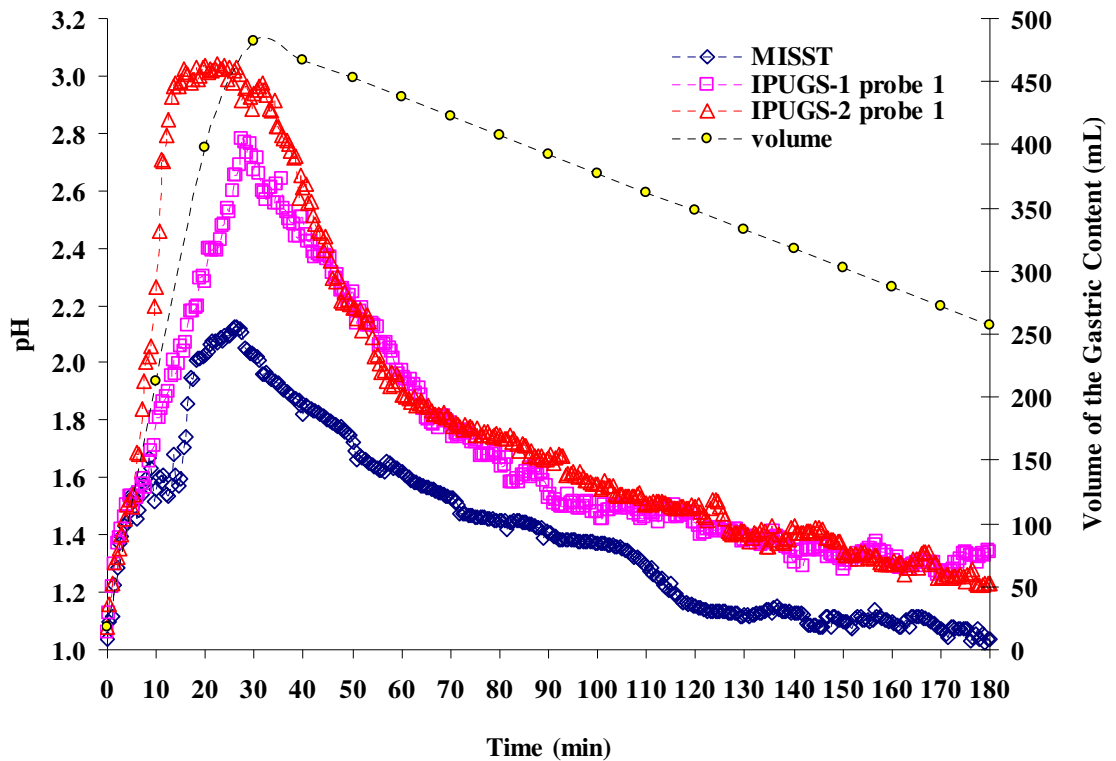


Figure 4-17. The pH profile of the pH probe 1 (fundus) over 3hr digestion period. The results obtained from the MISST are marked in blue, the IPUGS-1 in pink and the IPUGS-2 in red. The volume of the gastric content (mL) is shown with the axis on the right hand side.

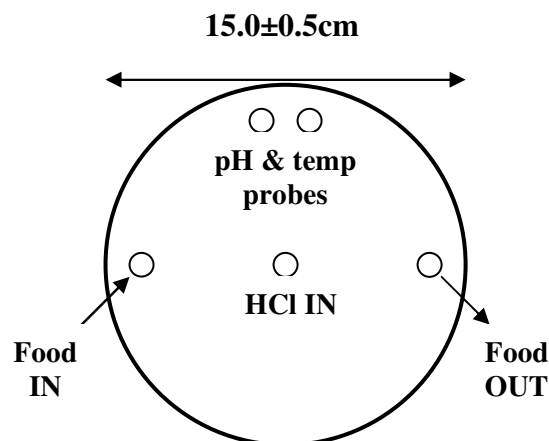


Figure 4-18. A diagram showing the arrangement of peristaltic tubings and probes used in the MISST.

Unlike the IPUGS 1 and 2, the MISST did not show a rapid increase in pH for the first 10min. Instead it showed a very slow change of increase in about 0.2 over the first 10min. This could be due to the position of the pH probe placed in the MISST. The pH probe was placed right in the middle of the stomach reactor to measure an average change of pH within the stomach reactor. In the beginning it seemed like a good approach to measure pH however the tip of the pH probe was made of glass, and continuous stirring by a magnetic stir bar eventually broke the probe. Thus it was decided to move the pH and the temperature probes to the north (Fig. 4-18).

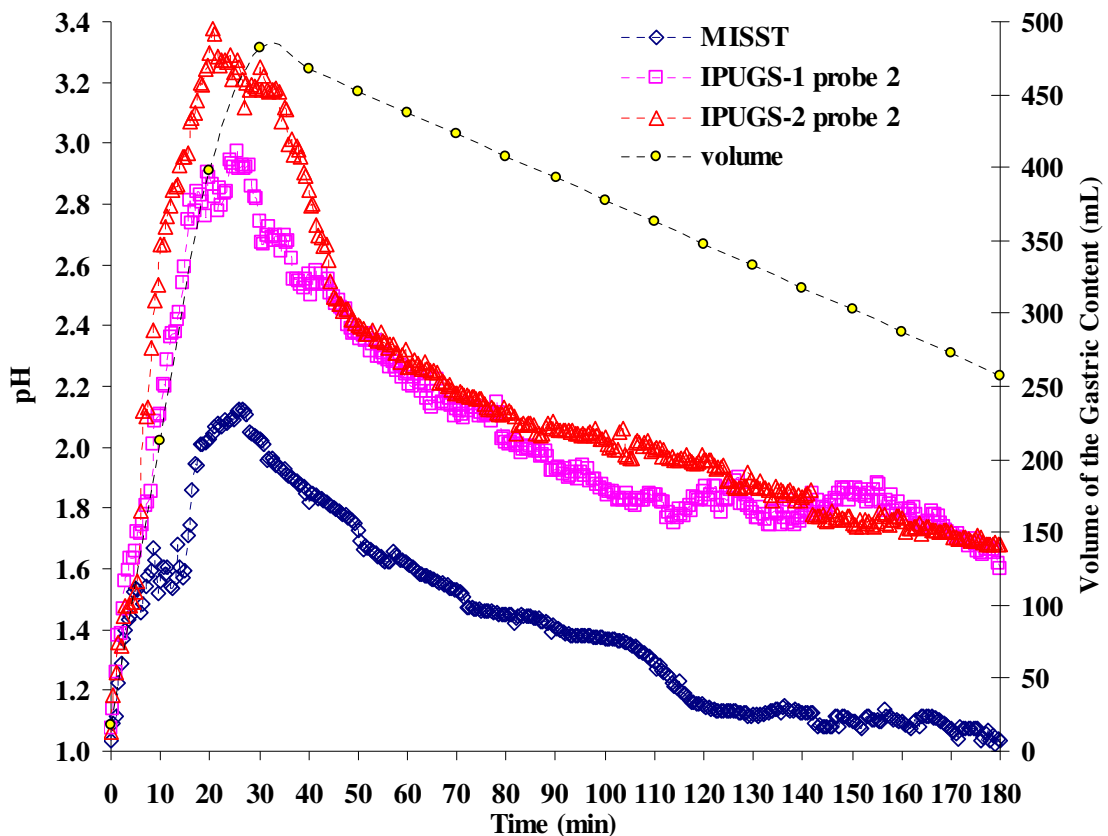


Figure 4-19. The pH profile of the pH probe 2 (antrum) over 3hr digestion period. The results obtained from the MISST are marked in blue, the IPUGS-1 in pink and the IPUGS-2 in red. The volume of the gastric content (mL) is shown with the axis on the right hand side.

Although the applied magnetic stirring of 150rpm in the MISST provided a reasonably good mixing to combine the secretions with the feed mixture, some of the rice particles sunk to the bottom of the reactor due to gravity. This was evident especially when the volume of the gastric content reached its maximum at 30min. It would seem that a reasonably good mixing has been achieved by the use of a magnetic stirrer because when the speed of stirring was increased to 500rpm, the overall pH profile was very similar to

that of the 150rpm used in the MISST. Nevertheless it has been widely used by many studies, for example SHIME, although the test materials used by others were either milk based or yoghurts which did not contain solid particles. The entry of the gastric secretion (hydrochloric acid) which had pH of 1.03 ± 0.01 was closer to the position of the pH probe in the MISST compared to that of the entry of the feed material. This appeared to have affected the rate of increase in the pH initially in the MISST. However after the first 10min, a rapid increase in the pH has been shown, up to 2.13 ± 0.02 which was very similar to the pH of the stomach reactor in the SHIME, pH of 2.0 to 2.5 (De Boever *et al*, 2000). Compared to the pH values of the IPUGS-1 and 2, the maximum pH is considerably low, reinforcing that a poor buffering capacity. In the TIM-1, the computer-controlled gastric pH was preset at pH 4.5, 4.2, 2.1 and 1.7 at 5, 20, 60 and 90min respectively (Blanquet *et al*, 2003) where more buffering capacity was shown by the use of milk (higher protein content).

Completely different trends in the pH profiles were seen in the IPUGS 1 and 2. The IPUGS-1 showed almost linear increase in the pH during the ingestion period and reached its maximum of pH 2.76 ± 0.09 at 25min in the probe 1 which is straight after the meal ingestion ceased. However for the IPUGS-2, the increase in the gastric pH was almost exponential and reached the pH of 3.02 ± 0.07 in the probe 1 at 10min. From 10mins to 30min, a very small fluctuation of the pH values, between 2.97 and 3.03, was observed. It would seem that the greater curvature of the IPUGS was able to hold the non-digested rice grains from slipping through the pylorus and due to this geometrical enhancement of the model, the buffering capacity of the ingested meal has prolonged a bit longer compared to the other two models.

As soon as the ingestion of the meal was ceased, at 25min, the pH of both of the IPUGS began to drop rapidly. From 45min to the end of the experiment, the values of the pH in both of the IPUGS were very similar to each other, showing a gradual decrease in the pH over time. The rate of decrease in pH in the IPUGS-1 and 2 and the MISST were similar to one another from 60min to 180min, although the values of the pH in the MISST were significantly lower than that of the IPUGS-1 and 2.

The decrease in pH over time was relatively constant up to 100min. However from 110mins, slower decrease in pH over time was shown. It was astonishing to find that the final pH value of the MISST was lower than the initial pH of the gastric juice (HCl). The overall trend of the pH change in the IPUGS-1 and 2 was somewhat similar to that of the

MISST. For the IPUGS-1, a sharp increase of pH was shown during the ingestion period, up to 25min. It demonstrates the buffering capacity of the bolus well, however when compared to the pH profile of the IPUGS-2, the rate of increase in pH was much slower. An increase in pH for the IPUGS-2 urged in the first 10min due to the ingestion of the bolus, as well as the secretion of mucus. The highest pH of the IPUGS-2 in probe 1 was 3.04 ± 0.04 whereas for the IPUGS-1, it was 2.83 ± 0.06 . As rice is rich in starch but deficient in proteins and fats, the buffering capacity is relatively low compared to other types of foods containing meat. Along with mucosal secretion from the gastric wall and continuous motility of 3cycles/min performed, the mucus covered around the bolus, enhancing a buffering effect. Thus a prolonged buffering effect was noticeably shown over the ingestion period. As soon as the ingestion period has ceased, the pH of both IPUGS-1 and 2 had started to drop. At 45min, the pH value of the IPUGS-1 and 2 meet, and since then the rate of pH change until the end of the 3hr digestion period was very similar to one another.

A very high buffering effect of the ingested foods was shown by Dressman *et al* (1990), with the use of 1000kCal meal (pH of 5.72) consisting of hamburger, bread, hash brown potatoes, ketchup and mayonnaise, showing the pH increase of up to 6. Malagelada *et al* (1976) used a standard meal of ground steak, bread, butter, vanilla ice cream with chocolate syrup and water (total 458kcal) and the buffering capacity of the ingested meal showed up to pH 5. After 3hr of digestion in the MISST and the IPUGS-1 and 2, the pH of the fasting state (approximately 1.3) was reestablished which matches with the data in humans (Hörter and Dressman, 2001).

The pH profiles of the MISST and the probe 2 implanted in the wall of the antrum of the IPUGS-1 and 2 are shown in Figure 4-19. The trend in change of pH over time was very similar to that of what was found in the fundus of the stomach by the probe 1. As the antrum is where mucosal secretion is largely taking place and the partially digested bolus is stored momentarily, slightly elevated level of pH was expected over the 3hr digestion period compared to that of the probe 1 in the fundus. Only one pH probe was used for the MISST as the space was limited. The maximal pH value of 3.37 ± 0.07 was detected at 20 ± 1 min for the IPUGS 2 and for the IPUGS-1, the maximum pH of 2.98 ± 0.12 at 25 ± 1 min was detected. The shape of the pH profile was found to be different to some extent when compared to the probe 1. The buffering capacity of the antrum prolonged as the partially digested acidic chyme was passing down to the pylorus. It should be noted that the pH of the artificial gastric juice used was lower (more acidic) than the chyme.

Usually the antrum is the area where very small amount of the gastric juice is secreted compared to the mucosal secretions. Although mucosal secretions were excluded for these experiments, the pH of the antrum still showed higher pH range than that of the fundus. In the fundus area, the buffering capacity did not last long, and already started to decrease even before the meal ingestion period stopped. From 40min to the end of the experiment, the pH values found in the probe 2 of the IPUGS 1 and 2 were very similar to one another, except a period between 80min and 120min where a sudden drop of pH was found in the IPUGS-1. Overall compared to the results obtained from the probe 1, the pH values at 180min were much higher in the antrum area of the IPUGS 1 and 2, 1.60 ± 0.06 and 1.68 ± 0.04 respectively. Since the acidic gastric juice is secreted from the walls of the fundus, the pH in the probe 1 must be lower than that of the probe 2, where processed, less acidic chyme are present in the antrum.

4.4. Concluding Remarks and Future Works

The IPUGS was designed to simulate the motility associated with the upper GI organs of the normal human subjects as closely as possible. The test results had demonstrated that the IPUGS performed with different patterns of rice starch hydrolysis when compared to that of the MISST. The MISST represents the traditional *in vitro* digestion model with the use of a homogenizer (mouth) and a magnetically stirred glass beaker (stomach). By comparing the concentration and the mass of rice starch in the stomach part of the MISST, IPUGS-1 and 2, the difference may not be seen all that obvious. However when the concentration and the mass of maltose and maltotriose, which are the byproducts of the rice starch hydrolysis caused by α -amylase and HCl from the gastric juice, were compared, there was an obvious difference between the two models. Comparison of the ratio of the mass of the maltose to the mass of the unconverted rice starch confirmed a clear difference between the MISST and the IPUGS once more. The pH profiles among the three models also differed significantly especially during the ingestion period where the buffering capacity of the ingested rice was not shown very well with the MISST. By comparing the data from many physiological and clinical sources in the literature, it would seem that the hand squeeze method used in the IPUGS can be considered as very appropriate to generate more reliable data to simulate the motility of the human upper GI organs compared to the traditional mechanical device utilizing a homogenizer and a magnetic stirrer. In the future, the IPUGS should be automated to ease labor. Also computer-controlled and computer-recorded data by possibly designing a new soft ware

or equations would be desirable to implicate a better understanding of the upper GI motility. Overall, the IPUGS can be used as a useful tool in predicting and screening for a new nutritional or pharmaceutical product as it demonstrated a close resemblance to the clinical and the physiological data of the normal human subjects in the literatures in many ways. Furthermore, conditions of the motility disorders can be simulated with the IPUGS (described in Chapter 5) to further validate the IPUGS with the data from various patients.

4.5. References

- Akin, A. (1998) Non-invasive detection of spike activity of the stomach from cutaneous EGG. PhD Thesis Drexel University, Philadelphia
- Akin, A., Sun, H. H. (2002). Non-invasive gastric motility monitor: fast electrogastrogram (fEGG). *Physiol. Meas.*, 23, 505-519
- Alander, M., De Smet, I., Nollet, L., Verstraete, W., Von Wright, A., Mattila-Sandholm, T. (1999) The effect of probiotic strains on the microbiota of the simulator of the human intestinal microbial ecosystem (SHIME). *International Journal of Food Microbiology*, 46, 71-79
- Alexandropoulou, I., Komaitis, M., Kapsokefalou, M. (2006) Effects of iron ascorbate, meat and casein on the antioxidant capacity of green tea under conditions of in vitro digestion. *Food Chemistry*, 94, 359-365
- Al-Zaben, A., Chandrasekar, V. (2005). Effect of esophagus status and catheter configuration on multiple intraluminal impedance measurements. *Physiol. Meas.*, 26, 229-238
- Argyri, K., Komaitis, M., Kapsokefalou, M. (2006) Iron decreases the antioxidant capacity of red wine under conditions of in vitro digestion. *Food Chemistry*, 96, 281-289
- Bermúdez-Soto, M. J., Tomas-Barberan, F. A., Carcia-Conesa, M. T. (2007) Stability of polyphenols in chokeberry (*aronia melanocarpa*) subjected to in vitro gastric and pancreatic digestion. *Food Chemistry*, 102, 865-874
- Beysseriat, M., Decker, E. A., McClements, D. J. (2006) Preliminary study of the influence of dietary fiber on the properties of oil-in-water emulsions passing through an in vitro human digestion model. *Food Hydrocolloids*, 20, 800-809
- Bhagavan, H. N., Chopra, R. K., Craft, N. E., Chitchumroonchokchai, C., Failla, M. L. (2007) Assessment of coenzyme Q10 absorption using an in vitro digestion caco-2 cell model. *Int. J. Pharma.*, 333, 112-117
- Bitar, K. N. (2003) Function of gastrointestinal smooth muscle: from signaling to contractile proteins. *Am. J. Med.*, 115 (3A), 15S-23S
- Björck, I., Granfeldt, Y., Liljeberg, H., Tovar, J., Asp, N. G. (1994) Food properties affecting the digestion and absorption of carbohydrates. *Am. J. Clin. Nutr.*, 59 (Suppl.), 699S-705S
- Blanquet, S., Meunier, J.P., Minekus, M., Marol-Bonnin, S., Alric, M. (2003) Recombinant *Saccharomyces cerevisiae* expressing P450 in artificial digestive systems: a model for biodegradation in the human digestive environment. *Applied and Environmental Microbiology*, 69(5), 2884-2892
- Blanquet, S., Zeijdner, E., Beyssac, E., Meunier, J. P., Denis, S., Havenaar, R., Alric, M. (2004) A dynamic artificial gastrointestinal system for studying the behavior of orally administered drug dosage forms under various physiological conditions. *Pharma. Res.*, 21 (4), 585-591
- Bouras, E. P., Delgado-Aros, S., Camilleri, M., Castillo, E. J., Burton, D. D., Thomforde, G. M., Chial, H. J. (2002). SPECT imaging of the stomach: comparison with barostat, and effects of sex, age, body mass index and fundoplication. *Gut*, 51, 781-786
- Brandon, E. A., Oomen, A. G., Rompelberg, C. J. M., Versantvoort, C. H. M., Van Engelen, J. G. M., Sips, A. J. A. M. (2006) Consumer product in vitro digestion model: bioaccessibility of contaminants and its application in risk assessment. *Regulatory Toxicology and Pharmacology*, 44, 161-171

- Castela-Papin, N., Cai, S., Vatieer, J., Keller, F., Souleau, C.H., Farinotti, R. (1999) Drug interactions with diosmectite: a study using the artificial stomach-duodenum model. *International Journal of Pharmaceutics*, 182, 111-119
- Chavanpatil, M., Jain, P., Chaudhari, S., Shear, R., Vavia, P. (2005) Development of sustained release gastroretentive drug delivery system for ofloxacin: *in vitro* and *in vivo* evaluation. *International Journal of Pharmaceutics*, 304, 178-184
- Chen, J. D. Z. (1998). Non-invasive measurement of gastric myoelectrical activity and its analysis and applications. *Proceedings of the 20th Annual International Conference of the IEE Engineering in Medicine and Biology Society*, 20 (6), 2802-2807
- De Boever, P., Deplancke, B., Verstraete, W. (2000) Fermentation by gut microbiota cultured in a simulator of the human intestinal microbial ecosystem is improved by supplementing a soy germ powder. *The Journal of Nutrition*, 130 (10), 2599-2606
- De Boever, P., Wouters, R., Vermeirssen, V., Boon, N., Verstraete, W. (2001) Development of a six-stage culture system for simulating the gastrointestinal microbiota of weaned infants. *Microbial Ecology in Health and Disease*, 13, 111-123
- De Zwart, I. M., Mearadji, B., Lamb, H. J., Eilers, P. H. C., Masclee, A. A. M., De Roos, A., Kunz, P. (2002). Gastric motility: comparison of assessment with real-time MR imaging or barostat measurement - initial experience. *Radiology*, 224, 592-597
- Dokoumetzidis, A., Karalis, V., Iliadis, A., Macheras, P. (2004) The heterogeneous course of drug transit through the body. *Trends in Pharmacological Sciences*, 25 (3), 140-146
- Dressman, J. B., Berardi, R. R., Dermentzoglou, L. C., Russel, T. L., Schmaltz, S. P., Barnett, J. L., Jarvenpaa, K. M. (1990). Upper gastrointestinal (GI) pH in young, healthy men and women. *Pharmaceutical Research*, 7 (7), 756-761
- Dubois, M., Gilles, K., Hamilton, J. K., Rebers, P. A., Smith, F. (1951). A colorimetric method for the determination of sugars. *Nature*, 168, 167
- Dubois, M., Gilles, K., Hamilton, J. K., Rebers, P. A., Smith, F. (1956). Colorimetric method for the determination of sugars and related substances, *Anal. Chem.*, 28, 350-356
- Edgar, W. M. (1990). Saliva and dental health. *British Dental Journal*, 169 (3-4), 96-98
- Elashoff, J. D., Reedy, T. J., Meyer, J. H. (1982). Analysis of gastric emptying data. *Gastroenterology*, 83, 1306-1312
- Fatouros, D. G., Bergenstahl, B., Mullertz, A. (2007). Morphological observations on a lipid-based drug delivery system during *in vitro* digestion. *European J. Pharm. Sci.*, 31, 85-94
- Fordtran, J. S., Walsh, J. H. (1973) Gastric acid secretion rate and buffer content of the stomach after eating. Results in normal subjects and in patients with duodenal ulcer. *J. Clin. Investigations*, 52, 645-657
- Franco, C. M. L., Preto, S. J. R., Ciacco, C. F. (1992) Factors that affect the enzymatic degradation of natural starch granules: effect of the size of the granules. *Starch*, 44, 422-426
- Frazier, P. J., Richmond, P., Donald, A. M. (1997). *Starch: Structure and Functionality*. The Royal Society of Chemistry.
- Galia, E., Horton, J., Dressman, J. B. (1999) Albendazole generics - a comparative *in vivo* study. *Pharm. Res.*, 16, 1871-1875
- Garrett, D.A., Failla, M.L., Sarama, R.J. (1999) Development of an *in vitro* digestion method to assess carotenoid bioavailability from meals. *J. Agric. Food Chem.*, 47, 4301-4309
- Hörter, D., Dressman, J.B. (2001) Influence of physicochemical properties on dissolution of drugs in the gastrointestinal tract. *Advanced Drug Delivery Reviews*, 46, 75-87
- Humphrey, S. P., Williamson, R. (2001). A review of saliva: Normal composition, flow and function. *The Journal of Prosthetic Dentistry*, 85 (2), 162-169
- Hurrell, R. F., Lynch, S. R., Trinidad, T. P., Dassenko, S. A., Cook, J. D. (1988) Iron absorption in humans: bovine serum albumin compared with beef muscle and egg white. *Am. J. Clin. Nutr.*, 47, 102-107
- Jodál, I., Kandra, L., Harangi, J., Nanasi, P., Debrecen, Szejtli, J. (1984) Hydrolysis of cyclodextrin by *Aspergillus oryzae* α -amylase. *Starch*, 36 (4), 140-143
- Joseph, I. M. P., Zavros, Y., Merchant, J. L., Kirschner, D. (2003) A model for integrative study of human gastric acid secretion. *J. Appl. Physiol.*, 94, 1602-1618
- Kapsokefalou, M., Alexandropoulou, I., Komaitis, M., Politis, I. (2005) *In vitro* evaluation of iron solubility and dialyzability of various iron fortificants and of iron-fortified milk products targeted for infants and toddlers. *Int. J. Food Sci. Nutr.*, 56 (4), 293-302

- Kapsokefalou, M., Kakouris, V., Makris, K., Galiotou-Panayotou, M., Komaitis, M. (2007) Oxidative activity and dialyzability of some iron compounds under conditions of a simulated gastrointestinal digestion in the presence of phytate. *Food Chemistry*, 101-419-427
- Kapsokefalou, M., Miller, D. D. (1991) Effects of meat and selected food components on the valence of nonheme iron during in vitro digestion. *J. Food Sci.*, 56 (2), 352-358
- Kararli, T. T. (1995). Review article: Comparison of the gastrointestinal anatomy, physiology and biochemistry of humans and commonly used laboratory animals. *Pharmaceutics & Drug Disposition*, 16, 351-380
- Kim, J. C., Kim, J. I., Kong, B. W., Kang, M. J., Kim, M. J., Cha, I. J. (2004) Influence of the physical form of processed rice products on the enzymatic hydrolysis of rice starch in vitro and on the postprandial glucose and insulin response in patients with Type 2 Diabetes Mellitus. *Biosci. Biotechnol. Biochem.*, 68 (9), 1831-1836
- Klein, S., Butler, J., Hempenstall, J. M., Reppas, C., Dressman, J. B. (2004) Media to simulate the postprandial stomach I. Matching the physicochemical characteristics of standard breakfasts. *J. Pharma. Pharmacol.*, 56, 605-610
- Kulkarni, S. D., Acharya, R., Rajurkar, N. S., Reddy, A. V. R. (2007) Evaluation of bioaccessibility of some essential elements from wheatgrass (*Triticum aestivum* L.) by in vitro digestion method. *Food Chemistry*, 103, 681-688
- Laurent, C., Besancon, P., Caporiccio, B. (2007) Flavonoids from a grape seed extract interact with digestive secretions and intestinal cells as assessed in an in vitro digestion/Caco-2 cell culture model. *Food Chemistry*, 100, 1704-1712
- Lee, K-J., Vos, R., Janssens, J., Tack, J. (2004). Differences in the sensorimotor response to distension between the proximal and distal stomach in humans. *Gut*, 53, 938-943
- Lo, W. M. Y., Farnworth, E. R., Li-Chan, E. C. Y. (2006) Angiotensin I - converting enzyme inhibitory activity of soy protein digests in a dynamic model system simulating the upper gastrointestinal tract. *J. Food Sci.*, 71 (3), S231-S237
- Luiking, Y. C., Peeters, T. L., Stolk, M. F., Nieuwenhuijs, V. B., Portincasa, P., Depoortere, I., van Berge Henegouwen, G. P., Akkermans, L. M. A. (1998). Motilin induces gall bladder emptying and antral contractions in the fasted state in humans. *Gut*, 42, 830-835
- Macfarlane, G.T., Macfarlane, S., Gibson, G.R. (1998a) Validation of a three-stage compound continuous culture system for investigating the effect of retention time on the ecology and metabolism of bacteria in the human colon. *Microb. Ecol.*, 35, 180-187
- Macfarlane, S., Quigley, M.E., Hopkins, M.J., Newton, D.F., Macfarlane, G.T. (1998b) Polysaccharide degradation by human intestinal bacteria during growth under multi-substrate limiting conditions in a three-stage continuous culture system. *FEMS Microbiology Ecology*, 26, 231-243
- Mainville, I., Arcand, Y., Farnworth, E.R. (2005) A dynamic model that simulates the human upper gastrointestinal tract for the study of probiotics. *International Journal of Food Microbiology*, 99, 287-296
- Malagelada, J. R., Longstreth, G. F., Summerskill, W. H. J., Go, V. L. W. (1976) Measurement of gastric functions during digestion of ordinary solid meals in man. *Gastroenterology*, 70, 203-210
- Marciani, L., Gouwland, P. A., Spiller, R. C., Manoj, P., Moore, R. J., Young, P., Fillery-Travis, A. J. (2001) Effect of meal viscosity and nutrients on satiety, intragastric dilution and emptying assessed by MRI. *Am. J. Physiol. Gastrointest. Liver Physiol.*, 280, G1227-1233
- Masuko, T., Minami, A., Iwasaki, N., Majima, T., Nishimura, S-I., Lee, Y. C. (2005) Carbohydrate analysis by a phenol-sulfuric acid method in microplate format. *Analytical Biochemistry*, 339, 69-72
- McCallum, R. W., Saladino, T., Lange, R. (1980) Comparison of gastric emptying rates of intracellular and surface labeled chicken liver in normal subjects. *J. Nuc. Med.*, 21, P67
- McCallum, R. W., Berkowitz, D. M., Lerner, E. (1981) Gastric emptying in patients with gastroesophageal reflux. *Gastroenterology*, 80, 281-291
- Miller, T.L., Wolin, M.J. (1981) Fermentation by the human large intestine microbial community in an in vitro semi continuous culture system. *Applied and Environmental Microbiology*, 42 (3), 400-407
- Miller, R. J., Fowler, H. L., Bergeim, O., Rehfuss, M. E., Hawk, P. B. (1920) The gastric response to foods. XII. The response of the human stomach to pies, cakes and puddings. *Am. J. Physiol.*, 52 (2), 248-275

- Miller, R. J., Fowler, H. L., Bergeim, O., Rehfuss, M. E., Hawk, P. B. (1920) The gastric response to foods. VII. The response of the normal human stomach to vegetables prepared in different ways. *Am. J. Physiol.*, 51 (2), 332-365
- Miller, D. D., Schrickler, B. R., Rasmussen, R. R., Van Campen, D. (1981). An *in vitro* method for the estimation of iron from meals. *Am. J. Clin. Nutr.*, 34, 2248-2256
- Minekus, M., Marteau, P., Havenaar, R., Huis in't Veld, J. H. J. (1995). A multicompartmental dynamic computer-controlled model simulating the stomach and small intestine. *Alternatives to Laboratory Animals*, 23, 197-209
- Minekus, M., Smeets-Peeters, M., Bernalier, A., Marol-Bonnin, S., Havenaar, R., Marteau, P., Alric, M., Fonty, G., Huis in't Veld, J.H.J. (1999) A computer-controlled system to simulate conditions of the large intestine with peristaltic mixing, water absorption and absorption of fermentation products. *Appl. Microbiol. Biotechnol.*, 53, 108-114
- Molly, K., Woestyne, M. V., Verstraete, W. (1993) Development of a 5-step multi-chamber reactor as a simulation of the human intestinal microbial ecosystem. *Appl. Microbiol. Biotechnol.*, 39, 254-258
- Mossi, S., Meyer-Wyss, B., Beglinger, C., Schwizer, W., Fried, M., Ajami, A., Brignoli, R. (1994). Gastric emptying of liquid meals measured noninvasively in humans with [13C] acetate breath test. *Digestive Diseases and Sciences*, 39(12), 107S-109S
- Najib, N., Mansour, A. R., Amidon, G. L. (1988). Gastrointestinal tract times: an *in vitro* study of parameters controlling the mean relative residence times of particles in a laminar fluid flowing in a horizontal tube. *The Chemical Engineering Journal*, 37, B39-B46
- Nelson, N. (1944) A photometric adaption of the Somogyi method for the determination of glucose. *J. Biol. Chem.*, 153, 375-380
- Nguyen, H. N., Silny, J., Matern, S. (1999). Multiple intraluminal electrical impedancometry for recording of upper gastrointestinal motility: current results and further implications. *Am. J. Gastroenterology*, 94 (2), 306-317
- Oomen, A. G., Hack, A., Minekus, M., Zeijdner, E., Cornelis, C., Choeters, G., Verstraete, W., Van de Wiele, T., Wragg, J., Rempelberg, C. J. M., Sips, A. J. A. M., Van Wijnen, J. H. (2002) Comparison of five *in vitro* digestion models to study the bioaccessibility of soil contaminants. *Environ. Sci. Technol.*, 36, 3326-3334
- Oomen, A. G., Rempelberg, C. J. M., Bruil, M. A., Dobbe, C. J. G., Pereboom, D. P. K. H., Sips, A. J. A. M. (2003). Development of an *in vitro* digestion mode for estimating the bioaccessibility of soil contaminants. *Arch. Environ. Contam. Toxicol.*, 44, 281-287
- Pade, V., Aluri, J., Manning, L., Stavchansky, S. (1995) Bioavailability of pseudoephedrine from controlled release formulations in the presence of guaifenesin in human volunteers. *Biopharmaceutics & Drug Disposition*, 16, 381-391
- Pehlivanov, N., Liu, J., Kassab, G. S., Beaumont, C., Mital, R. K. (2002). Relationship between esophageal muscle thickness and intraluminal pressure in patients with esophageal spasm. *Am. J. Physiol. Gastrointest. Liver Physiol.*, 282, 1016-1023
- Perales, S., Barbera, R., Lagarda, M. J., Farre, R. (2007) Availability of iron from milk-based formulas and fruit juices containing milk and cereals estimated by *in vitro* methods (solubility, dialysability) and uptake and transport by caco-2 cells. *Food Chemistry*, 102, 1296-1303
- Rao, B. S., Prabhavathi, T. (1978) An *in vitro* method for predicting the bioavailability of iron from foods. *Am. J. Clin. Nutr.*, 31, 169-175
- Rao, P., Pattabiraman, T. N. (1989). Reevaluation of the phenol-sulfuric acid reaction for the estimation of hexoses and pentoses. *Anal. Biochem.*, 181, 18-22
- Ruby, M. V., Davis, A., Schoof, R., Eberle, S., Sellstone, C. M. (1996) Estimation of lead and arsenic bioavailability using a physiologically based extraction test. *Environ. Sci. Technol.*, 30, 422-430
- Savoie, L. 1994. Digestion and absorption of food: Usefulness and limitations of *in vitro* models. *Can. J. Physiol. Pharmacol.* 72: 407-414
- Schwartz, S. E., Levine, R. A., Singh, A., Scheidecker, J. R., Track, N. S. (1982). Sustained pectin ingestion delays gastric emptying. *Gastroenterology*, 83 (4), 812-817
- Schwizer, W., Frazer, R., Borovicka, J., Crelier, G., Boesiger, P., Fried, M. (1994). Measurement of gastric emptying and gastric motility by magnetic resonance imaging (MRI). *Digestive Diseases and Sciences*, 39 (12), 101S-103S
- Simoneau, C., Geiss, H., Roncari, A., Zocchi, P., Hannaert, P. (2001) Validation of methodologies for the release of di-isononylphthalate (DINP) in saliva stimulant from toys.

European Commission, DG Joint Research Centre, Food Products Unit, Institute for Health and Consumer Protection, Ispra, Italy.

Somogyi, M. (1926) Notes on sugars determination. *J. Biol. Chem.*, 79, 599-613

Somogyi, M. (1937) A reagent for the copper iodometric determination of very small amounts of sugar. *J. Biol. Chem.*, 117, 771-776

Somogyi, M. (1945) A new reagent for the determination of sugars. *J. Biol. Chem.*, 160, 61- 68

Souliman, S., Blanquet, S., Beyssac, E., Cardot, J.M. (2006) A level A in vitro/in vivo correlation in fasted and fed states using different methods: Applied to solid immediate release oral dosage form. *European Journal of Pharmaceutical Sciences*, 27, 72-79

Spratt, P., Nicoletta, C., Pyle, D.L. (2005) An engineering model of the human colon. *Trans IChemE, Part C, Food and Bioproducts Processing*, 83 (C2), 147-157

Sugawara, M., Kadomura, S., He, X., Takekuma, Y., Kohri, N., Miyazaki, K. (2005). The use of an in vitro dissolution and absorption system to evaluate oral absorption of two weak bases in pH-independent controlled-release formulations. *Euro. J. Pharm. Sci.*, 26, 1-8

Suzuki, S. (1987) Experimental studies on the presumption of the time after food intake from stomach contents. *Forensic Science International*, 35, 83-117

Tortora, G. J., Grabowski, S. R. (2000) *Principles of anatomy and physiology*. 9th Edition. John Wiley and Sons, Inc., Chapter 24, The Digestive System. pp.818-870

Turnbull, C. M., Baxter, A. L., Johnson, S. K. (2005) Water-binding capacity and viscosity of Australian sweet lupin kernel fibre under in vitro conditions simulating the human upper gastrointestinal tract. *International Journal of Food Sciences and Nutrition*, 56 (2), 87-94

Vasiluk, L., Pinto, L. J., Tsang, W. S., Gobas, F. A. P. C., Eickhoff, C., Moore, M. M. (2008) The uptake and metabolism of benzo[a]pyrene from a sample food substrate in an in vitro model of digestion. *Food and Chemical Toxicology*, 46 (2), 610-618

Vatier, J., Célice-Pingaud, C., Farinotti, R. (1998) A computerized artificial stomach model to assess sodium alginate-induced pH gradient. *International Journal of Pharmaceutics*, 163, 225-229

Williamson, G., Belshaw, N. J., Sief, D. J., Noel, T. R., Rings, S. G., Cairns, P., Morris, V. J., Clark, S. A., Parker, M. L. (1992) Hydrolysis of A and B type crystalline polymorphs of starch by α -amylase, β -amylase and glucoamylase. *Carbohydr. Polym.*, 18, 179-187

Wrolstad, R. E., Acree, T. E., Decker, E. A., Penner, M. H., Reid, D. S., Schwartz, S. J., Schoemaker, C. F., Smith, D. M., Sporns, P. (2005) *Handbook of food analytical chemistry*. Water, proteins, enzymes, lipids and carbohydrates. Hoboken, N. J. Wiley.

Chapter 5

Clinical Application of the IPUGS to Study Motility Disorders

In this chapter, a short review of the common disorders associated with dysfunction of the gastric motility is provided. Using the IPUGS in the present study, the conditions of such disorders were simulated and compared with the physiological data obtained from the literature.

5.1. Introduction

Gastric motility and gastric emptying are coordinated with extrinsic modulation by the central nervous system to control the receptive relaxation of the fundus for the increase of the gastric volume to accommodate the ingested foods without a rise in the gastric pressure, grinding contractions of the antrum and relaxation of the pyloric sphincter to allow the exit of the chyme (gastric emptying) into the small intestine (Kelly, 1974; Barker *et al*, 1979; Schwizer *et al*, 2003). The rate and the pattern of gastric emptying are largely dependent on the gastric motility where impaired gastric emptying, both prolonged and premature, may cause disorders such as delayed gastric emptying (gastroparesis) and rapid gastric emptying (dumping syndrome) though the importance of the gastric dysrhythmias has not yet been clearly defined (Parkman *et al*, 2004; Maurer, 2006).

Gastroparesis is a chronic gastrointestinal disorder caused by delayed gastric emptying (increased retention time) of the solid portion of the ingested foods, in which the vagus nerve controlling the muscles of the stomach and the intestines are impaired, resulting mechanical obstructions in the pylorus (Jalilian *et al*, 2006; Karamanolis and Tack, 2006; Maurer and Parkman, 2006). Thus the normal gastric contractions of 3cycle.min⁻¹ of the distal (antrum and pylorus) part of the stomach become disorganized, diminishing or disrupting the timing, the strength and frequency of antral contractions in transferring the bolus and the chyme (Akin and Sun, 2002; Parkman *et al*, 2004). In some patients, increased tonic and phasic activity of the pylorus (pylospasm), irregular bursts of small intestinal contractions and reductions in the postprandial antral contractions, which can be correlated with impaired gastric emptying of solids, have been evident (Parkman *et al*,

2004). The common symptoms of the gastroparesis include bloating, early satiety, heartburn, nausea, vomiting of undigested food, upper abdominal discomfort, distention of the stomach (increase in intragastric pressure and volume), weight loss due to poor absorption of nutrients or low calorie intake, high and low blood glucose levels, lack of appetite, gastroesophageal reflux, spasms in the stomach area (Notivol *et al*, 1995; Harrison *et al*, 2004; Grundy *et al*, 2006).

Gastroparesis can be a complication of diabetes mellitus (Harrison *et al*, 2004) which is caused by the prolonged retention of food in the fundus as well as the decreased strength of antral contractions occurring at a higher frequency thus gastric emptying becomes unpredictable and therefore the increase in blood glucose level becomes random (Maurer and Parkman, 2006). Diabetic patients have high blood glucose which may damage the vagus nerve thus disrupting the control of the gastric motility. In general, prolonged retention of foods in the stomach may cause bacterial overgrowth from the fermentation of foods, and in some cases the food may harden into solid masses, forming bezoars which may cause blockage of the pylorus. Other than diabetes mellitus, gastroparesis can be induced by impaired rhythm of the gastric motility due to gastric electrical stimulation (gastric pacing) (Wang and Chen, 2000), drug-induced delays which affect the pharmacokinetics of the administered drugs (Harrison *et al*, 2004) and post-surgical symptoms. Yet is unknown which part of the stomach is responsible for generation of early satiety related to impair gastric accommodation of the ingested meal (Lee *et al*, 2004). For treatment of the gastroparesis, small and frequent servings of homogenized solid meals with low fat content but rich in carbohydrates (e.g. rice) are recommended (Karamanolis and Tack, 2006).

Dumping syndrome refers to rapid gastric emptying, in which the upper end of the small intestine is filled excessively in a short period with undigested or partially digested foods from the stomach (Pulvertaft, 1953; Madsen and Rasmussen, 1964; Engelholm *et al*, 1966) irrespective of the physiological transit time in the gastrointestinal tract (GIT). Thus fluids and electrolytes of high osmolarities are passed into the small intestine rapidly with loss of intravascular volume, excessive release of vasoactive peptides and insulin resulting in elevated blood sugar level, causing early hyperglycemia (high blood sugar, glucose level $>166\text{mg}\cdot\text{dl}^{-1}$) and/or delayed hypoglycaemia (low blood sugar, glucose $<50\text{mg}\cdot\text{dl}^{-1}$) (Buchwald, 1968; Borovoy *et al*, 1998; Karamanolis and Tack, 2006). Dumping syndrome can be caused by gastric surgeries such as surgical vagotomies, damaged vagal nerve and surgeries with drainage procedures including pyloroplasty,

antrectomy or gastric resections (Karamanolis and Tack, 2006), occurring in 5-10% of the patients (Vecht *et al*, 1998).

The dumping syndrome can be divided into early and late dumping though many people have both types (Vecht *et al*, 1998). Early dumping begins either during or 5-30min after a meal with each attack lasting from 20-60min (Buchwald, 1968). Symptoms of nausea, vomiting, diarrhoea, light-headedness, increased pulse rate, flushing, sweating and postural hypotension were seen when hyperosmotic diet was ingested (Creaghe *et al*, 1977; Caulfield *et al*, 1986). These symptoms are expected to be caused by an absolute or relative reduction in plasma volume, a peripheral vasodilation, and increased flow in the superior mesenteric artery (Vecht *et al*, 1998). Late dumping is less common compared to the early dumping. It takes place in 90-240min after a meal (Karamanolis and Tack, 2006) which typically results from reactive hypoglycaemia (Vecht *et al*, 1998), causing adrenergic discharge which may be due to the release of gut glucagon (Creaghe *et al*, 1977). Nausea, vomiting, diarrhoea and abdominal discomfort are common symptoms of the late dumping (Creaghe *et al*, 1977). Ingestion of a meal rich in carbohydrates and liquids are generally not tolerated well with patients, although under fasting conditions, such patients are free of symptoms (Karamanolis and Tack, 2006). Patients with the dumping syndrome are more susceptible to diabetes, gastroesophageal reflux disease (GERD) and Zollinger-Ellison syndrome which causes severe peptic ulcers.

In vitro Physicochemical Upper Gastrointestinal System (IPUGS) has been, in the current study, used to mimic the conditions of such impaired motility, gastroparesis and dumping syndrome, by varying the rates of motility cycle applied and the gastric emptying, in order to distinguish feasibility of the IPUGS to be used as a clinical tool. As a test material, white short grain rice (Sun Rice Japanese style Sushi Rice, Koshihikari and Opus type) was used as the constituent of the macronutrients is relatively simple (up to 78.5wt% of total carbohydrates) compared to other balanced test meals composed of a mixture of carbohydrates, proteins and fats, thus analyses of carbohydrates would be of the main concern and complications emerging from having to analyze all the nutrients as well as intra and inter-actions of nutrients can be avoided. The test material must have solid portion as the motility disorders have been shown to be associated with solids rather than liquids in meals (Camilleri *et al*, 1998; Chen, 1998; Maurer and Parkman, 2006; Karamanolis and Tack, 2006). Studies of starch (including rice starch) have underscored no significant differences between the *in vitro* enzymatic hydrolysis and *in vivo* digestion of starch (Williamson *et al*, 1992; Franco *et al*, 1992; Björck *et al*, 1994; Kim *et al*, 2004).

Yet, rice is one of the most abundant staple food worldwide (Frazier *et al*, 1997), where intensive research related to the postprandial glucose and insulin responses, diabetes, coronary heart disease, cancer and ageing are being conducted (Frazier *et al*, 1997; Kim *et al*, 2004). By comparing the results obtained from the IPUGS with the available data collected from patients with motility disorders in the literature, evaluation of the IPUGS as a clinical tool to be used with or without *in vivo* studies can be determined.

5.2 Materials and Methods

5.2.1. The new *In vitro* Physicochemical Upper Gastrointestinal System (IPUGS)

The IPUGS consists of three consecutive compartments simulating the conditions of the upper GI organs in humans. The first compartment simulates the food ingestion in mouth, which is composed of a denture set with manually controlled mastication and continuous secretion of artificial saliva of $37\pm 0.5^{\circ}\text{C}$ which is transferred via a peristaltic pump at rate of $7.0\text{ml}\cdot\text{min}^{-1}$ (Edgar 1990; Humphrey and Williamson, 2001). White short grain rice (Sun Rice Japanese style Sushi Rice) was cooked in a conventional rice cooker with 1:1 volumetric ratio of rice grains to water. 100g of the cooked rice was transferred to the mouth reactor with 250ml of drinking water to be used as the feed material. As the cooked rice is relatively small in size which can be swallowed without much of mastication, it can be regarded as simpler foods for testing. 5mins of gentle manual mastication was applied with the denture set with $20\text{chewings}\cdot\text{min}^{-1}$ to remove large clusters of rice into smaller pieces to aid the swallowing process. The feed material was spoon fed to the next compartment, esophagus at a rate of $8.5\text{ml}\cdot 30\text{s}^{-1}$ (equivalent to $\frac{1}{2}$ Tablespoon (tbsp) $\cdot 30\text{s}^{-1}$).

The next two compartments simulating the conditions of the esophagus and the stomach were built with platinum cure silicon rubber composed of 75-85wt% polyorganosiloxanes, 20-25wt% of amorphous silica and 0.1wt% of platinum-siloxane for part A and 65-70 wt% of polyorganosiloxanes and 20-25wt% of amorphous silica for part B. 1:1 ratio of the parts A and B were mixed and coated to the plastic anatomy model of the stomach which resembles the average human stomach size at unfed state (20cm x 15cm x 8cm, Kararli, 1995; Pade *et al*, 1995) as well as its geometry of J-shaped curve. The coatings

were repeated until the thickness of the stomach wall reached $0.50\pm 0.01\text{cm}$ in average. The material is translucent in color thus by adding of food coloring agents to the feed mixture may help clearer view of the reactions in the inner stomach compartment. It offers negligible shrinkage and able to stretch and rebound to its original size and shape without distortion. For the esophagus, paper roll of 1.5cm diameter and 20cm in length was made, and coatings of the silicon rubber were repeatedly made until the wall thickness reached $0.30\pm 0.01\text{cm}$ in average (Al-Zaben and Chandrasekar, 2005). The paper roll and the plastic anatomic model were removed after coatings. In order to deliver the gastric secretions to the wall of the stomach, a large number of Tygon® Microbore tubings (n=200) with inner diameter of 0.25mm were implanted, with the tips of these tubings pierced into the stomach wall to create a gradual dampening of the wall (Figure 5-1), secreting $3.5\text{ml}\cdot\text{min}^{-1}$ (Mainville *et al*, 2005) throughout the 3hr digestion period. These tubings are designed for precision injection and dispensing in laboratory applications with flexible and bendable resin. The tubings have a very smooth inner bore surface which reduces the risk of particulate build-up during sensitive fluid transfer and minimal extractable helps to assure fluid purity. Also, these tubings are transparent, thus the gastric secretions passing into the stomach wall can be seen clearly. For mucosal secretions in the esophagus compartment, slightly larger diameter of tubing was used. Micro-Line™ tubing (Thermoplastic Scientifics, Inc.) made of cross-linked ethyl vinyl acetate. These tubings are translucent, flexible and elastic with inner diameter of 0.51mm.

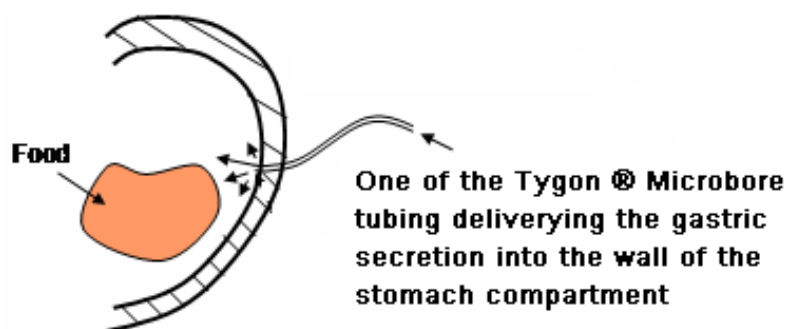


Figure 5-1. An illustration of one of the Tygon® Microbore secretion tubings inserted into the wall of the stomach compartment. 200 of these tubings were implanted with even distribution to deliver the artificial gastric secretions.

One ends of these implanted tubings in both esophagus and the stomach were planted into the wall of each compartment to create gradual dampening effect from the wall to simulate the opening and closing of the pores in the gastric wall for secretion delivery.

The other ends were gathered and squashed into a larger diameter Tygon peristaltic tubings (inner diameter of 1.5cm), which are subsequently connected to the smallest possible peristaltic tubing (inner diameter of 0.80mm). Though the flow rate of the peristaltic pumps can be controlled, changing the peristaltic tubing size also helped to control the flow rate more accurately. For validation of motility experiments, only one peristaltic pump (Autoclude® Peristaltic Pump - 54505) was used to deliver the artificial gastric juice to the stomach compartment.

The esophagus and the stomach compartments were placed in an anaerobic chamber with continuous nitrogen gas flow ($1.0\text{L}\cdot\text{hr}^{-1}$) and the temperature inside the chamber was maintained at $37\pm 1^\circ\text{C}$ with a hot plate placed inside the chamber. The compositions of the artificial saliva and the gastric juice were kept as simple as possible to avoid any complications from salts in analyzing data. Thus α -amylase and hydrochloric acid, which are the main substances that are able to hydrolyze rice starch, were used. Other constituents were excluded for these experiments. 2g of fungal (*Aspergillus oryzae*) α -amylase (GrindamyI™ A5000, 5000U/g, Danisco 071314) was mixed with 200ml of deionized (MilliQ) water to be used as the artificial saliva and 0.15M HCl (Ajax, AF602394) was used as the artificial gastric juice, which were both warmed up to $37\pm 1^\circ\text{C}$. The α -amylase from *Aspergillus oryzae* (E.C.3.2.1.1) was one of the closet and cheap alternative to the human α -amylase (E.C.3.2.1.1). Hormonal control of altering the secretion rates was also excluded as to compare the IPUGS to other models in terms of motility only.

The esophagus and the stomach compartments were manually pressed with my hands to mimic the peristaltic waves. For the esophagus, coordinated contractions and relaxations of the peristaltic propulsions were simulated to push the ingested feed material (bolus) towards the stomach with the rate of 5 contractions per 30s. The wall of the esophageal compartment was squeezed both horizontally and vertically by gripping the esophagus using both hands, one on top of each other and in between a thumb and an index finger, squeezed gently to push down the bolus (Figure 5-2).

The upper esophageal sphincter (UES) controlled the entrance of the feed mixture and the lower esophageal sphincter (LES) controlled the exit of the feed mixture into the stomach compartment. Each cycle of esophageal peristalsis lasted up to 6s (Pehlivanov *et al*, 2002). Apart from mucosal secretions, there are neither digestive secretions nor absorption take place in the esophagus (Tortora and Grabowski, 2000) thus these features were excluded.

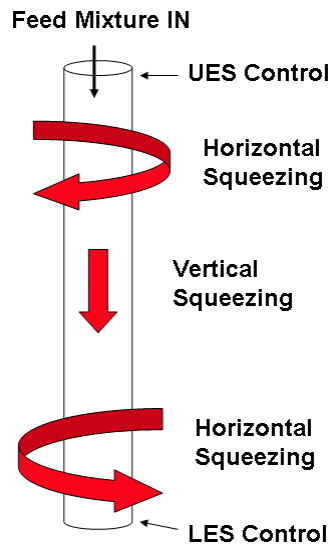


Figure 5-2. Diagram showing the motility of the esophageal compartment of the IPUGS. Red arrows indicate the direction of squeezing. UES refers to the upper esophageal sphincter and LES represents the lower esophageal sphincter.

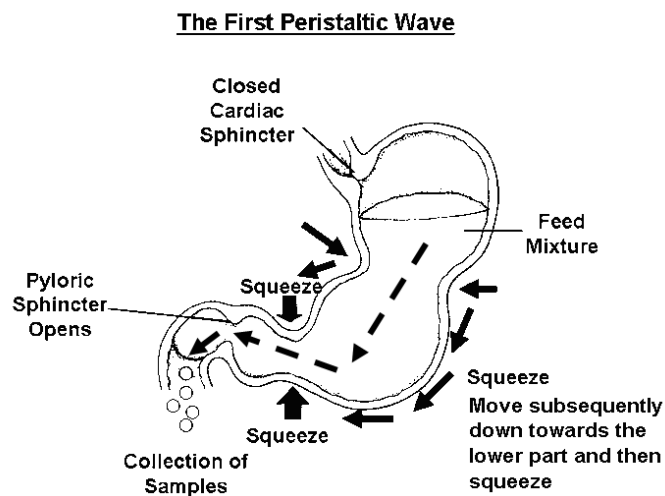


Figure 5-3. A diagram of the first peristaltic wave applied to the stomach compartment of the IPUGS. Black arrows drawn on the outside of the stomach indicate the directions of the squeezing action. Squeezing initiated from the body of the stomach and moved subsequently towards the lower antrum/pylorus area, followed by a strong squeezing in the lower antrum/pylorus area to open the pyloric sphincter and release the chyme. Dotted black arrows inside the stomach indicate the expected flow of the chyme inside the stomach compartment.

Hand squeezed actions to simulate the peristaltic waves of the human stomach was used in the stomach compartment as well. The first peristaltic wave was initiated from

squeezing the proximal part of the stomach compartment (the fundus and upper body) and moved subsequently towards the lower antrum/pylorus area. This was to generate a pressure gradient from the body of the stomach to the pylorus, resulting an opening of the pyloric sphincter and emptying of fractions of the stored bolus towards the pylorus and mix with the gastric secretions, which resembles the action of a contractile grinder, crushing the small chunks of the bolus as described in the literature (Akin 1998; Luiking *et al*, 1998; Nguyen *et al*, 1999; Tortora and Grabowski, 2000) (Figure 5-3).

The second peristaltic wave with closed cardiac and pyloric sphincters was initiated from the distal stomach (lower body and the antrum), squeezing the wall of the stomach towards the proximal direction (toward the fundus) (Figure 5-4).

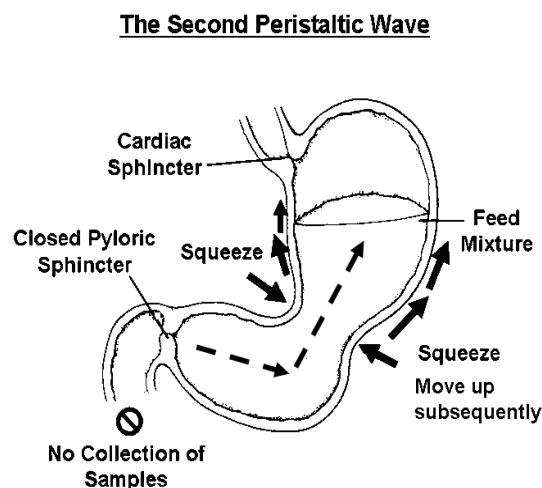


Figure 5-4. A diagram of the second peristaltic wave applied to the stomach compartment of the IPUGS. Black arrows drawn on the outside of the stomach indicate the directions of the squeezing action and red arrows indicate the expected flow of the chyme inside the stomach compartment. Black dotted arrows inside the stomach indicate the direction of the chyme movement.

Sequential contractions of the antrum crushed the small chunks of the bolus against the closed pyloric sphincter with a large fraction of the remaining bolus squeezed back toward the proximal part for further digestion (Kelly, 1974; Barker *et al*, 1979; Tortora and Grabowski, 2000; De Zwart *et al*, 2002), causing distention of the stomach compartment to accommodate more space for the incoming food which was facilitated by the elastic and stretchy nature of the building material (platinum cure silicon rubber). The overall gastric motility in the proximal stomach compartment remained relatively

constant, but for the distal part, stronger contractions with higher depth and amplitudes (Schwizer *et al*, 1994), were used. The first and the second peristaltic waves constitute one wave cycle of the gastric motility. To simulate the normal condition at fed state, $3\text{cycle}\cdot\text{min}^{-1}$ with average duration of wave cycle of $21.5\pm 3.8\text{s}$ (Allescher *et al*, 1998) was used. To simulate the motility conditions of gastric dumping with tachygastric, $5\text{cycle}\cdot\text{min}^{-1}$ was used with $11.4\pm 0.3\text{s}$ of average wave cycle duration as stated by Allescher *et al* (1998). The maximum and the minimum amplitudes of the wave cycle for the normal subjects were $3.33\pm 1.1\text{pT}$ and $-3.06\pm 1.02\text{pT}$, and $12.5\pm 2.3\text{pT}$ and $-14.5\pm 2.2\text{pT}$ for tachygastric when the electrical activity of the human stomach was measured by biomagnetic measurement with superconducting quantum interference devices (SQUIDS) (Allescher *et al*, 1998). Thus with tachygastric attacks in the dumping syndrome condition, the amplitude of the magnetic signal was five times higher than the average amplitude of the normal subjects therefore stronger and faster contractions were applied to simulate the dumping syndrome. $1\text{cycle}\cdot\text{min}^{-1}$ for gastroparesis with bradygastric was used with similar force of contractions compared to that of the normal conditions (Parkman *et al*, 2004).

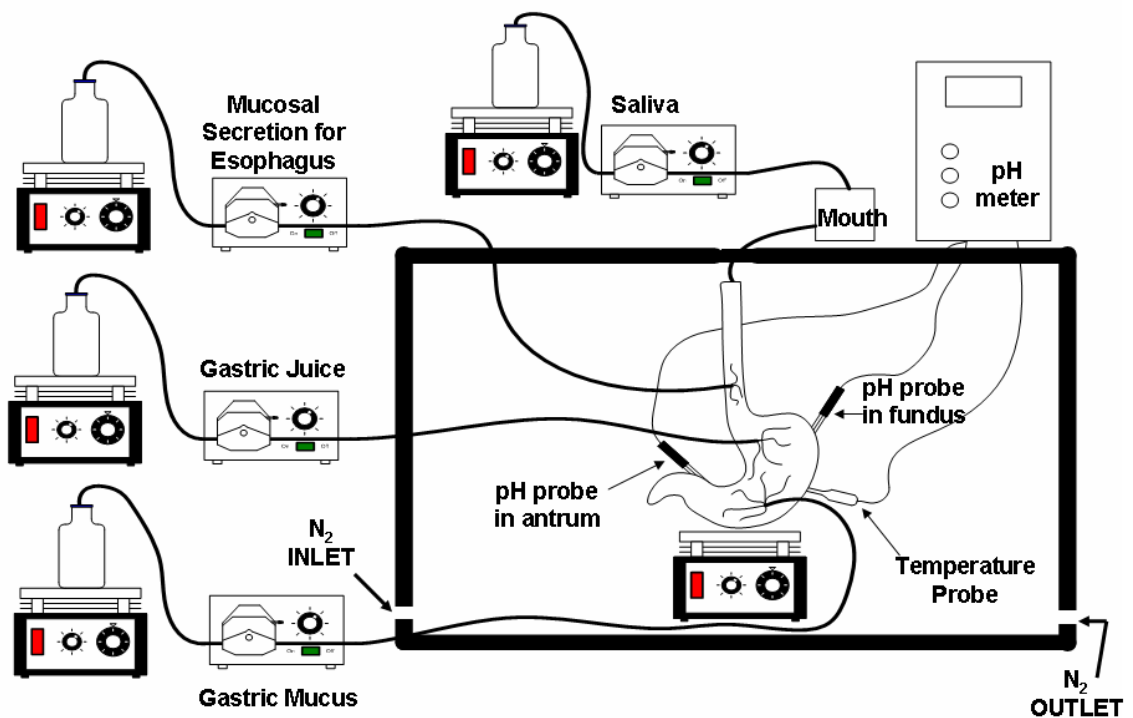


Figure 5-5. A schematic diagram of the IPUGS

The digestion period of 3hrs was set as carbohydrates typically take 2-4hrs to be emptied into the small intestine (Suzuki, 1987; Mossi *et al*, 1994). Initially, 5ml of the samples were taken from the mouth compartment to check the consistency of each batch. From

10min to 30min, 20ml of samples were collected every 10min from the pylorus. From 30min to 180min where the gastric emptying was to be more active, 6.8ml of the chyme mixture was pumped out of the MISST per minute (Marciani *et al*, 2001; Mainville *et al*, 2005), collected and stored in sampling bottles with closed lids and placed in an ice water bath (0-2°C) while the experiment was running. Then the samples were centrifuged at 3000rpm for 30min (Klein *et al*, 2004) at 2°C. The supernatants were diluted accordingly for each of the analytical methods used. The experiments via the IPUGS were conducted triplicate. A schematic diagram of the IPUGS can be found in the Figure 5-5.

5.2.2. Phenol-Sulfuric Acid Assay

Phenol-Sulfuric acid assay is one of the most widely used analytical methods in measuring neutral sugars in oligosaccharides, proteoglycans, glycoproteins and glycolipids. It is a simple, fast, reliable and sensitive method which has been developed by Dubois *et al* (1951) and (1956). Rao and Pattabiraman (1989) reported that phenol underwent sulfonation in situ and the phenol-sulfuric acid complex decreased the color intensity for many hexoses and pentoses. Similar results were seen by Masuko *et al* (2005) whom modified the original method by Dubois *et al* (1951) and (1956) by adding concentrated sulfuric acid to the sample followed by phenol. Instead of using microplate proposed by Masuko *et al* (2005), larger volumes were reconstituted following the ratio of sample to conc. sulfuric acid to phenol. The method was used to determine the concentration of total water soluble carbohydrates from the obtained samples.

3ml of concentrated sulfuric acid was added to 1ml of diluted (factor of 100) sample in a test tube followed by vigorous shaking at high speed in a vortex mixer. 600µL of 5% (w/v) phenol was pipetted into the mixed solution and placed in a water bath at 90°C for 10min. The prepared samples were vortexed at high speed for 30s and left at room temperature for 5mins cooling before reading the absorbance via the UV spectrophotometer (Agilent 8453, UV G1103A) at 490nm.

5.2.3. Somogyi-Nelson Method

Somogyi-Nelson method (Somogyi, 1926; Somogyi, 1937, Somogyi, 1945; Nelson, 1944; Wrolstad *et al*, 2005) is an extensively used highly accurate method for determining the amount of reducing sugars (e.g. maltose). Low alkalinity copper reagent and arsenomolybdate reagent were prepared as follows.

12g of sodium potassium tartate and 24g of anhydrous sodium carbonate with 250ml of distilled water were mixed. 4g of copper sulfate pentahydrate and 16g of sodium bicarbonate were added to 200ml of distilled water. 180g of anhydrous sodium sulfate in 500ml of boiling distilled water was separately prepared. Three mixtures were combined and diluted to 1L to make the low alkalinity copper reagent. The arsenomolybdate reagent was made by mixing 25g ammonium molybdate to 450ml of distilled water. 21ml of concentrated sulfuric acid and 25ml of distilled water containing 3g of disodium hydrogen arsenate heptahydrate were added to the ammonium molybdate solution with stirring. The mixture was continuously stirred for 24hrs at 37°C and kept in brown glass stopped bottle until use.

1ml of the diluted (factor of 100) sample and 1ml of the low alkalinity copper reagent were placed in a test tube and vigorously mixed by a vortex mixer at a high speed for 30s. The test tube was placed in a boiling water bath (100°C) for 10mins, and cooled at room temperature for 5mins. 1ml of the arsenomolybdate reagent was then added and the mixture was vortexed at a high speed for 30s. Absorbance at 500nm was read via the UV spectrophotometer (Agilent 8453, UV G1103A). Blanks for the absorbance were prepared by replacing the sample with 1ml distilled water.

Blue color of the low alkalinity copper reagent and green color of the arsenomolybdate reagent gave a greenish blue color in all the samples. The samples which contained less maltose showed a light green solution, but as the concentration of maltose increased, the color of the sample became darker and bluish. As the arseno reagent is extremely toxic and may cause cancer, particular cares were taken to avoid inhalation and contacts at all times.

5.2.4. High Performance Liquid Chromatography (HPLC)

High Performance Liquid Chromatography (HPLC) is able to provide both qualitative and quantitative analyses with a small amount of diluted sample of oligosaccharides (Zhao *et al*, 1997) and other carbohydrates. As HPLC requires a prestigious level of accuracy, it was used to ensure the compatibility of results from the phenol-sulfuric acid assay and the Somogyi-Nelson method, as well as to screen for any unexpected components (e.g. glucose) in the collected samples.

A carbohydrate ES column (Prevail™ Carbohydrate ES Column-W 150x4.6mm, 5 μm (Alltech Part No. 35102)) was used to specifically analyze maltose, maltotriose and other undigested starch in the samples. A mixture of degassed (Elite™ Degassing System) acetonitrile (Merck, HPLC grade) and deionized water was used as mobile phase and was pumped into the column via a quaternary gradient pump (Alltech, 726) at 1.0ml.min. Isocratic gradient was used for a better separation of carbohydrates – initially 65% to 35% of acetonitrile to water and then from 15mins onwards, 50% to 50%, respectively. Collected samples were diluted (x40) with deionized water, followed by syringe filtration with nylon membranes and automatically injected (Alltech Autosampler 570) into the column with 30min of analysis time per sample. Evaporative Light Scattering Detector (ELSD) and EZStart software were used to detect and record the findings. The heating column temperature of 50°C with Nitrogen (5.0) gas flow rate of 1.5L.min⁻¹ was used and the gain on the ELSD was set at 2.

5.2.5. Recording of pH

The measure of the pH profile is one of the simplest analyses which directly indicates the conditions of the stomach and it is of extreme importance as it is able to detect even minor changes of the gastric conditions. For the IPUGS, two pH probes and one temperature probe were pierced into the wall of the stomach compartment in the IPUGS to record the pH in the fundus (probe 1) and the antrum (probe 2). The temperature probe was placed in the middle of the body of the stomach to measure the changes with respect to time. For the MISST, a pH probe and a temperature probe were placed in the middle of the stomach reactor. A pH meter from Hanna Instrument (HI 4212) was used with auto-logging mode of 30s for 3hr.

5.3 Results and Discussion

5.3.1 Phenol-Sulfuric Acid Assay

As shown in the Figure 5-6, the concentration of total water soluble carbohydrates varied noticeably depending on the rate of the applied gastric motility as well as the gastric emptying rate over the 3hr digestion period. The concentration and the mass of total water soluble carbohydrates over time (Figures 5-6 and 5-7) indicate the available amount of rice carbohydrates (mainly starch initially) in the stomach compartment of the IPUGS at given times, which signifies the rate of ingestion as well as the rate of gastric emptying. By examining the amount (both concentration and mass) of the total carbohydrates as well as the amount of maltose and maltotriose (Figures 5-8, 5-9, 5-14 and 5-15) in the stomach compartment, the amount of undigested (unconverted) rice starch (Figure 5-10) can be determined (i.e. Undigested starch = Total carbohydrates – Maltose – Maltotriose). The ratio of maltose to unconverted starch (Figure 5-11) can then be calculated to observe the effect of varying the rate of the gastric motility applied to the pattern of the rice starch hydrolysis, which can be used as a screening tool to simulate the conditions of the patients as well as used with clinical *in vivo* studies for assistance. The effectiveness of the motility control, including the sensitivity of each motility cycle in terms of strength and frequency, throughout the experiments can also be evaluated and by using the normal motility of 3 cycles.min⁻¹ as a control, comparison to the conditions of the disorders can be made.

As it has been proposed by Elashoff *et al* (1982) that for uniformity, time 0 was defined as the point at which the meal ingestion began. Therefore the collected samples at time 0min can be referred to as the bolus from the mouth compartment which was about to be swallowed. These samples were taken before they were ingested into the esophagus. Initially, the values of the total carbohydrate concentration for the three cases were very similar to each other, with average values of 89.0±2.3g.L⁻¹ and 1.56±0.06g for simulation of gastroparesis (slow motility), 91.0±1.9g.L⁻¹ and 1.59±0.06g for dumping syndrome (fast motility), and 96.0±2.1g.L⁻¹ and 1.68±0.06g for the normal motility condition. This indicates that a good control of preparing the feed mixture was maintained throughout the experiments, as the procedures for preparing the feed mixture and the rate of mastication applied in the mouth compartment were the same.

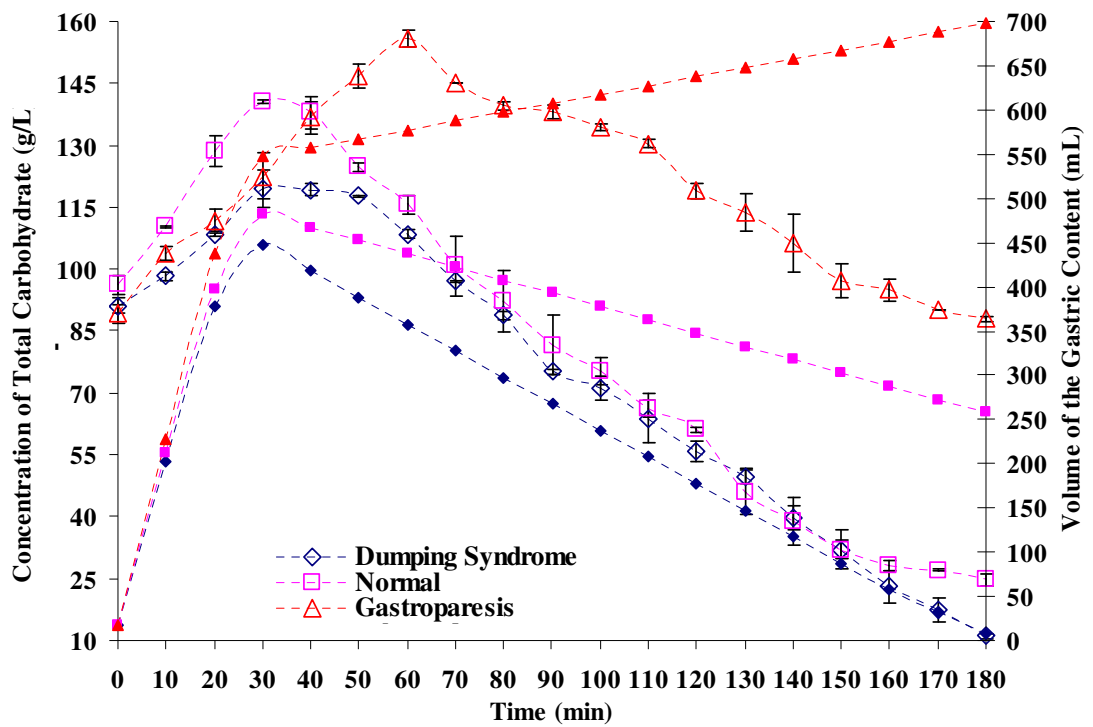


Figure 5-6. A graph showing the concentration of total water soluble carbohydrates ($\text{g}\cdot\text{L}^{-1}$) during the 3hr digestion time (min). The results obtained from the dumping syndrome are marked with empty dots in blue, the normal state in pink and the gastroparesis in red. The volumes of the gastric content (mL) for different motility conditions are shown with filled dots with accordance of color for each condition.

Calibration errors from the weight balance when weighing hot cooked rice may have occurred, which seemed to have caused a small difference in the initial starch concentrations. Although the difference in concentrations of the total carbohydrates and unconverted starch in the three cases varied noticeably, when the masses of total carbohydrates and the unconverted starch present in the samples were calculated, there was near to none difference between the three cases (Figures 5-6, 5-7 and 5-10). This was due to the small gastric volume (17.5ml) and small volume (5ml) of the samples collected from the model. As the main purpose of the study was to determine and compare different rate of gastric motility cycles used to simulate the conditions of the motility disorders, initial starch content can only be used as a reference(control) for the latter data, thus it was decided to only collect the amount (volume) required to conduct analyses. As the initial carbohydrate constituent of rice was mainly starch, the values of the mass of unconverted starch and the values of the mass of the total water soluble carbohydrates were almost the same.

Gastric emptying time refers to when a very small amount of the meal remained among the gastric rugae (Whitehouse and Temple, 1977). Whitehouse and Temple (1977) reported that the total gastric emptying time for normal healthy subjects took 192 ± 12 min when a balanced meal constituted of carbohydrates, proteins and fats, were fed. For the patients with severe and persistent post-operational dumping, the total gastric emptying time took 172 ± 27 min, and only 112 ± 39 min was taken for severe and persistent post operational dumping patients with diarrhoea (Whitehouse and Temple, 1977). However, Duthie and McKellar (1960), Stemmer *et al* (1969), Sigstad (1971) and Whitehouse and Temple (1977) found no statistically significant difference between the gastric emptying of clinical dumpers and non-dumpers. As shown in the Figure 5-16, the rates of gastric emptying were varied to alter the total gastric emptying times. Although 180min of digestion was allowed for three conditions, rapid gastric emptying ($6.5\text{ml}\cdot\text{min}^{-1}$), normal emptying ($5.0\text{ml}\cdot\text{min}^{-1}$) and slow gastric emptying ($2.5\text{ml}\cdot\text{min}^{-1}$) were applied to simulate a variable total gastric emptying times.

As the ingestion had initiated, the feed mixture was delivered through the esophagus and deposited predominantly in the proximal stomach with progressive distribution into the distal stomach as the gastric emptying progressed. This was also seen by Lee *et al* (2004) in the human stomach. Under the normal physiological motility conditions, with $3\text{cycle}\cdot\text{min}^{-1}$, the total carbohydrates and unconverted starch concentration showed a sharp linear increase during the ingestion period and reached its peak point by the end of the ingestion period, about 30mins. With dumping syndrome where 5 cycles of gastric motility $\cdot\text{min}^{-1}$ were applied, the total carbohydrates and the unconverted starch concentrations also reached its maximum value at 30min mark. However in terms of the value, the simulated dumping syndrome showed the lowest available total carbohydrates and the unconverted starch concentrations and masses throughout the 3hr digestion period. This was due to fast gastric emptying induced by nearly doubled rate of the gastric motility, where not enough time was allowed for the feed material to be deposited in the stomach compartment for digestion – i.e. premature emptying. The simulated conditions of the gastroparesis, with 1 cycle of gastric motility $\cdot\text{min}^{-1}$, showed a steady increase in both total carbohydrates and unconverted starch masses and concentrations during the ingestion period, which resembles the trends shown by the normal and the dumping syndrome cases. The conditions of the normal and the dumping syndrome reached their maximal total carbohydrates points of $140.65\pm 0.52\text{g}\cdot\text{L}^{-1}$ and $67.86\pm 1.83\text{g}$ and $119.63\pm 4.54\text{g}\cdot\text{L}^{-1}$ and $53.53\pm 2.40\text{g}$, respectively, at the end of its ingestion period which was between 25 and 30min. Despite that the ingestion time for all three conditions was

kept the same, it took 60min for the gastroparesis condition to reach its peak value of $155.81 \pm 2.21 \text{g.L}^{-1}$ and $89.98 \pm 2.92 \text{g}$. The increase in the mass of the total carbohydrates seen in the normal and the dumping syndrome conditions were fitted with linear function ($R^2 \geq 0.9911$), with the loading rates of 2.26g.min^{-1} and 1.77g.min^{-1} , respectively. For the gastroparesis condition, the loading rate of the mass of total carbohydrates was fitted better with a square function ($R^2 = 0.9966$).

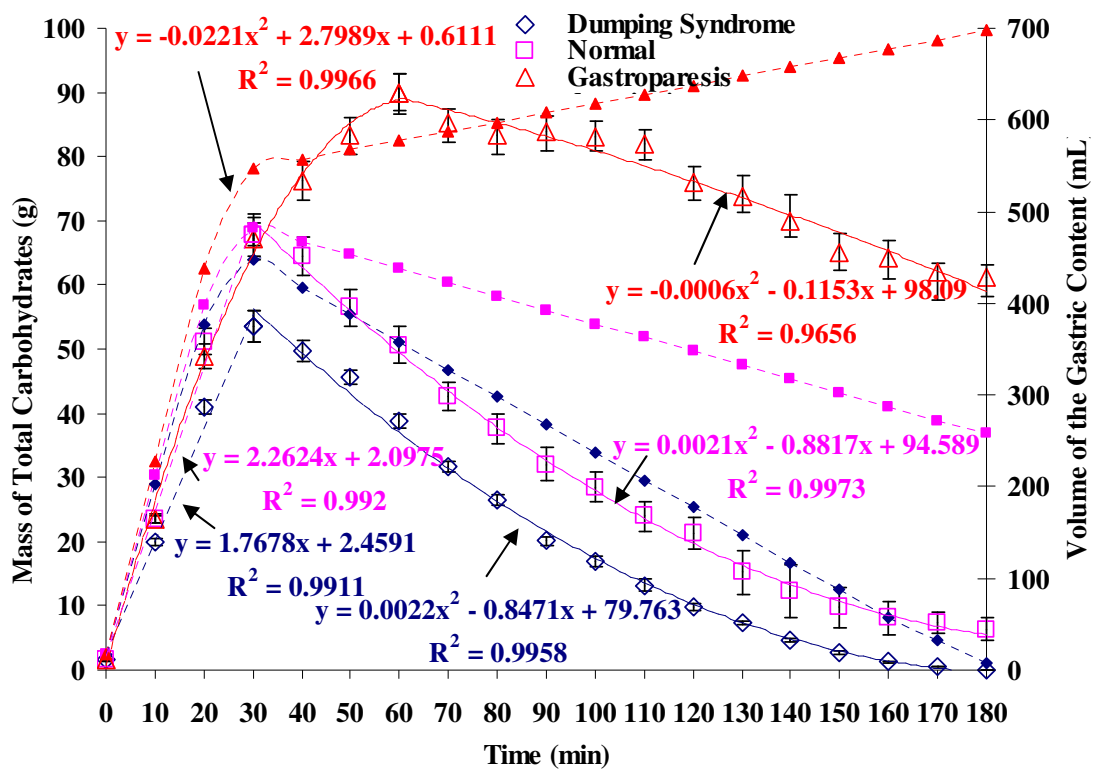


Figure 5-7. A graph showing the mass of total water soluble carbohydrates (g) during the 3hr digestion time (min). The results obtained from the dumping syndrome are marked with empty dots in blue, the normal state in pink and the gastroparesis in red. The volumes of the gastric content (mL) for different motility conditions are shown with filled dots with accordance of color for each condition.

During the ingestion period, the increasing trends of both the concentration and the mass of total carbohydrates resemble that of the increase in the volume of the gastric content. However during the period of gastric emptying, 30min to 180min, the rate of decrease is non-linear which is in disagreement with the linearly decreasing volume of the gastric content with respect to time. As soon as the meal ingestion ceased, the volume of the gastric content as well as the concentration and the mass of total carbohydrates and unconverted starch started to decrease and the gastric emptying period had initiated. It is an arbitrary phenomenon that the stated numerical values of the total carbohydrates

concentration exceeded the total mass of rice added (100g). Although the gastric secretions ($3.5\text{mL}\cdot\text{min}^{-1}$) were delivered to the stomach constantly, the chyme samples, which were of greater volumes than the volume of the gastric secretion, were also withdrawn at the same time. Thus the volume of the gastric content has decreased over time, and therefore the concentration and the mass of total carbohydrates and unconverted starch in the stomach also decreased over time. However for the gastroparesis condition, the amount of sample withdrawn was less than that of the gastric secretions in 10min basis, thus the volume of the gastric content increased over time, which was accommodated by the expansion of the elastic nature of the building material used in the IPUGS.

For the gastric emptying pattern of the normal and the dumping syndrome conditions, a square function fitted well ($R^2 \geq 0.9963$) for both conditions, with slightly higher values of the total mass of carbohydrates for the normal condition at all times. For the gastroparesis condition in which the gastric emptying time was initiated from 60min, the overall decrease in the mass of the total carbohydrates was much lower compared to the other two conditions, and fitted with a cubic function ($R^2=0.9741$). Similar trends were seen with the mass of the unconverted starch with respect to time, as starch is the main constituent of the rice where limited hydrolysis via salivary amylase and HCl took place.

Especially with the dumping syndrome application, the decrease in the starch concentration was almost constant, indicating a well controlled gastric emptying even at a faster speed. At 90min mark which is considered to be the time at which half of the gastric contents are expected to be emptied under the normal conditions, the concentration and the mass of total carbohydrates for the gastroparesis ($138.1 \pm 1.5\text{g}\cdot\text{L}^{-1}$ and $83.9 \pm 2.6\text{g}$) was nearly 1.5 times higher when compared to the normal ($92.3 \pm 3.5\text{g}\cdot\text{L}^{-1}$ and $37.6 \pm 2.5\text{g}$) and nearly doubled when compared to the dumping syndrome ($75.2 \pm 0.5\text{g}\cdot\text{L}^{-1}$ and $20.1 \pm 0.3\text{g}$). This has corresponded well with the findings of Lien *et al* (1998), who showed intragastric retention at 90min of $88 \pm 23\%$ in the gastroparesis group of patients. Considering high content of carbohydrates in the rice, the gastric emptying has been expected to be faster than compared with that when using a balanced meal (refer to Chapter 3). With the use of a balanced meal, Lien *et al* (1998) also reported that 50% emptying time in the normal emptying group was $113 \pm 11\text{min}$ and in the gastroparesis group, it took $296 \pm 256\text{min}$ which would be likely if the experimental digestion period was extended. The large difference between the gastroparesis condition versus the normal and the dumping syndrome was continuously observed until the end of the experiments.

The largest difference was seen at 180min, where the dumping syndrome had near to zero gastric content in the stomach. A slightly lowered total carbohydrates concentration value was obtained compared to the initial concentration value for the gastroparesis application. Even after 3hr digestion period, large chunks of undigested rice particles remained in the stomach for the gastroparesis application. Physiologically under the normal condition (without any disorders) in the humans, there is not much of the chyme passing from the stomach to the duodenum during the ingestion period and if there is, it would only be liquids (e.g. water). It is assumed that the greater curvature of the stomach in the IPUGS allowed the solid particles to be deposited and remained in the stomach compartment for further digestion. All the samples were opaque white in color but not viscous as there was no mucosal secretions. The concentrations and the masses of both total carbohydrates and unconverted starch of the gastroparesis condition showed a distinctively different pattern throughout the experiments. The rates of decrease in the amounts (both concentrations and masses) were also the slowest, indicating slower gastric emptying. However with the normal and the dumping syndrome states, the total carbohydrates and unconverted starch concentrations showed similar trends with similar values throughout the experiments. Thus the amounts of total carbohydrates and unconverted starch in the stomach compartment were correlated with the speed of motility; the faster the motility, the faster the gastric emptying, thus the lesser amount of total carbohydrates and unconverted starch remaining in the stomach compartment.

5.3.2. Somogyi-Nelson Method

The Somogyi-Nelson method was used to analyze the concentration (g.L^{-1}) and the mass of maltose (g) in the stomach compartment which varied considerably from 0.5 to 19g.L^{-1} and 0 to 11g, respectively, throughout the experiment as illustrated by the Figures 5-8 and 5-9. Maltose is a reducing sugar which is a byproduct released during the conversion of amylopectin to amylose and/or amylose converted to a shorter chain of carbohydrate in the process of starch hydrolysis (Frazier *et al*, 1997). Hence observing the trend of the concentration and the mass of maltose in the collected chyme samples over the 3hr digestion period facilitates the evaluation of whether the application of different rates of motility in the IPUGS was able to detect a significant difference in the digestion of rice between the normal and the impaired motility patterns seen in dumping syndrome and gastroparesis.

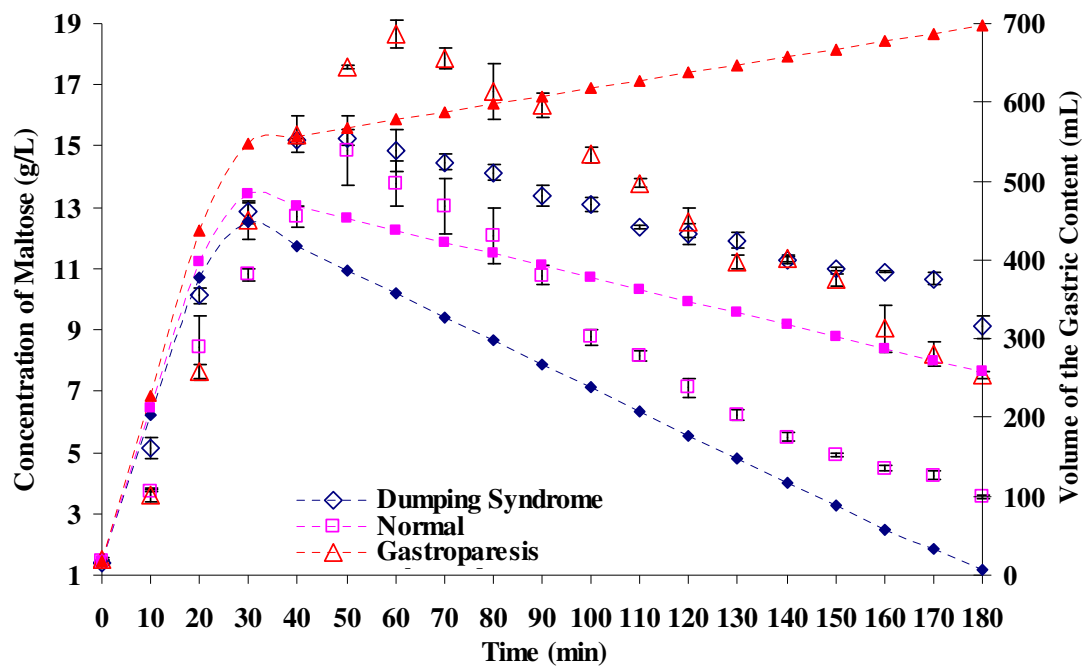


Figure 5-8. A graph showing the concentration of maltose (g.L^{-1}) during the 3hr digestion time (min). The results obtained from the dumping syndrome are marked with empty dots in blue, the normal state in pink and the gastroparesis in red. The volumes of the gastric content (mL) for different motility conditions are shown with filled dots with accordance of color for each condition.

Initially, the concentrations of maltose in the normal, gastroparesis (slow) and dumping syndrome (fast) were very low and showed almost the same values, of $1.47 \pm 0.02 \text{g.L}^{-1}$, $1.50 \pm 0.05 \text{g.L}^{-1}$ and $1.41 \pm 0.04 \text{g.L}^{-1}$, respectively. The initial mass of maltose was of $0.027 \pm 0.002 \text{g}$ for all the conditions. As discussed earlier, the volume of the sample withdrawn was considerably low (5ml) to allow minimal variation in the overall volume of the gastric content. Therefore when the mass of maltose was compared, the difference was not as large as it was of the concentrations. Along with the rapid increase of total carbohydrates as seen in the Figures 5-6 and 5-7, the amounts of maltose also increased rapidly up to 40, 50 and 60min for the dumping syndrome, normal and gastroparesis conditions. The faster the rate of the applied gastric motility, the faster the hydrolysis of the rice starch, thus the rate of maltose production was faster. The values of the mass of maltose in the normal and the dumping syndrome conditions were very similar to each other throughout the experiments, especially during the feeding period, up to 30min. Even after the ingestion has ceased, the mass of maltose in all the simulated conditions kept on increasing. However once it reached its maximal point of $6.3 \pm 0.2 \text{g}$ (dumping syndrome), $6.7 \pm 0.4 \text{g}$ (normal) and $10.8 \pm 0.4 \text{g}$ (gastroparesis), the mass of maltose has started to decrease in an approximately linear fashion for the gastroparesis ($R^2=0.9852$). For the

normal and the dumping syndrome conditions, a parabolic function was fitted better. It would seem that if longer digestion period was allowed, the final mass of maltose would also have reached near zero, like the other conditions.

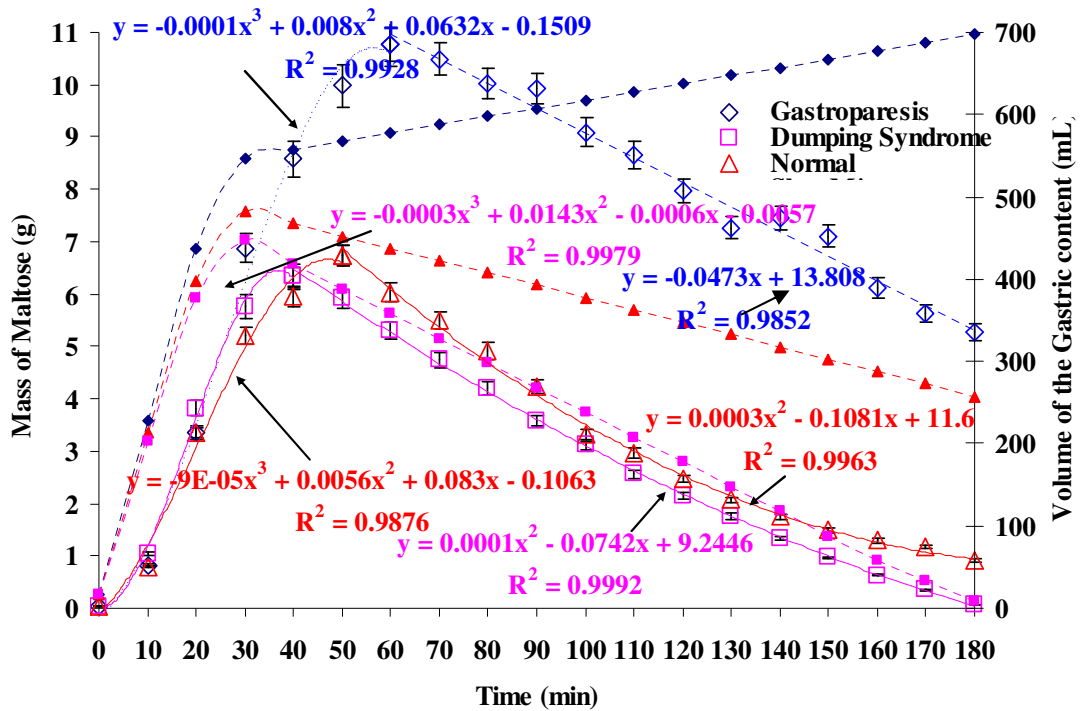


Figure 5-9. A graph showing the mass of maltose (g) during the 3hr digestion time (min). The results obtained from the gastroparesis condition are marked with empty dots in blue, the dumping syndrome in pink and the normal motility in red. The volumes of the gastric content (mL) for different motility conditions are shown with filled dots with accordance of color for each condition.

However as mentioned in Lien *et al* (1998), the total gastric emptying time would take much longer for the gastroparesis condition, thus the digestion period would have to be extended to at least 5hrs. However, the rate of decrease in the mass of maltose seemed to be very similar to one another, about $0.0473\text{g}\cdot\text{min}^{-1}$ as shown by the equation of the gastroparesis in the Figure 5-9.

The trend of increase in maltose concentration was very similar to that of the maltose mass especially for the first 60min of the experiment. A sharp increase in maltose concentration was seen when the total water soluble carbohydrates and the mass of the unconverted starch in the stomach compartment kept increasing. The difference in the concentrations of maltose among the three conditions was not so well shown by the concentration because the change of the volume of the gastric content was ignored. Thus it was decided to use the mass of maltose in comparing data as it was calculated with respect to the different rates of the motility cycles and different amounts of gastric

emptying for a clearer view. However with the control of secretion and the rate of gastric emptying used for such study, 200 to 250ml of the fluid remained in the stomach compartment even after the 3hr digestion period under the normal condition. However under the gastroparesis condition, about 700ml of the gastric content remained. This was due to the absence of feed back control, where the rate of gastric secretion was once set at $3.5\text{ml}\cdot\text{min}^{-1}$, which is more representative of the secretion rates at stimulated state, and kept at the same rate till the end of the experiments. This was why the samples collected toward the end of the experiment were very dilute. However with the dumping syndrome, only 5 to 7.5ml of the gastric content remained, causing difficulty in sampling towards the end of the experiments (Figure 5-10).

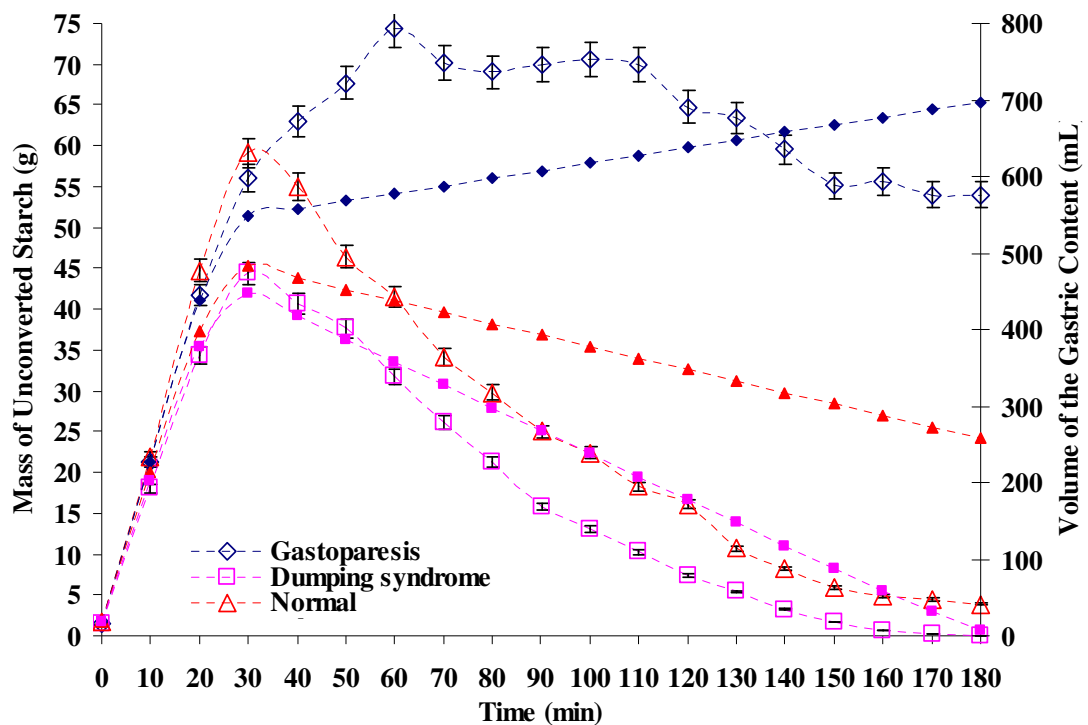


Figure 5-10. A graph showing the mass of the unconverted starch (g) during the 3hr digestion time (min). The results obtained from the gastroparesis are marked with empty dots in blue, the dumping syndrome in pink and the normal in red. The volumes of the gastric content (mL) for different motility conditions are shown with filled dots with accordance of color and shape for each condition. Note that Undigested starch = Total Water Soluble Carbohydrates – Maltose – Maltotriose.

The change of unconverted starch (Figure 5-10) was very similar to that of the total carbohydrates (Figure 5-7), which in turn was very similar to the volum of the gastric content (mL) over time. Although the differences in the amounts of the total carbohydrates, unconverted starch and maltose have been shown clearly, a better understanding of the rice starch hydrolysis was attained when the ratio of maltose to

unconverted starch, in terms of mass, was plotted (Figure 5-11). The ratio of maltose to starch is an important indication to how much of amylopectin and amylose were hydrolyzed to release the reducing sugar (maltose). The ratio of maltose to unconverted starch was increased very slowly over time for all the conditions up to 80min mark. However from 90min, the values of the ratio started to diverge. At 160min, the normal condition reached the maximum ratio of 0.2665, and for the gastroparesis condition, the maximum ratio of 0.1497 was reached at 70min. Since then the ratio for the gastroparesis condition started to decrease slowly, reaching the final value of 0.0974. This would seem to be caused by the slow rate of motility and overloaded gastric content by slowing the rate of emptying. As the limited amounts of secretions were available to compensate for excessive amount of the food, the interaction of the secretions and the undigested foods seemed to have diminished.

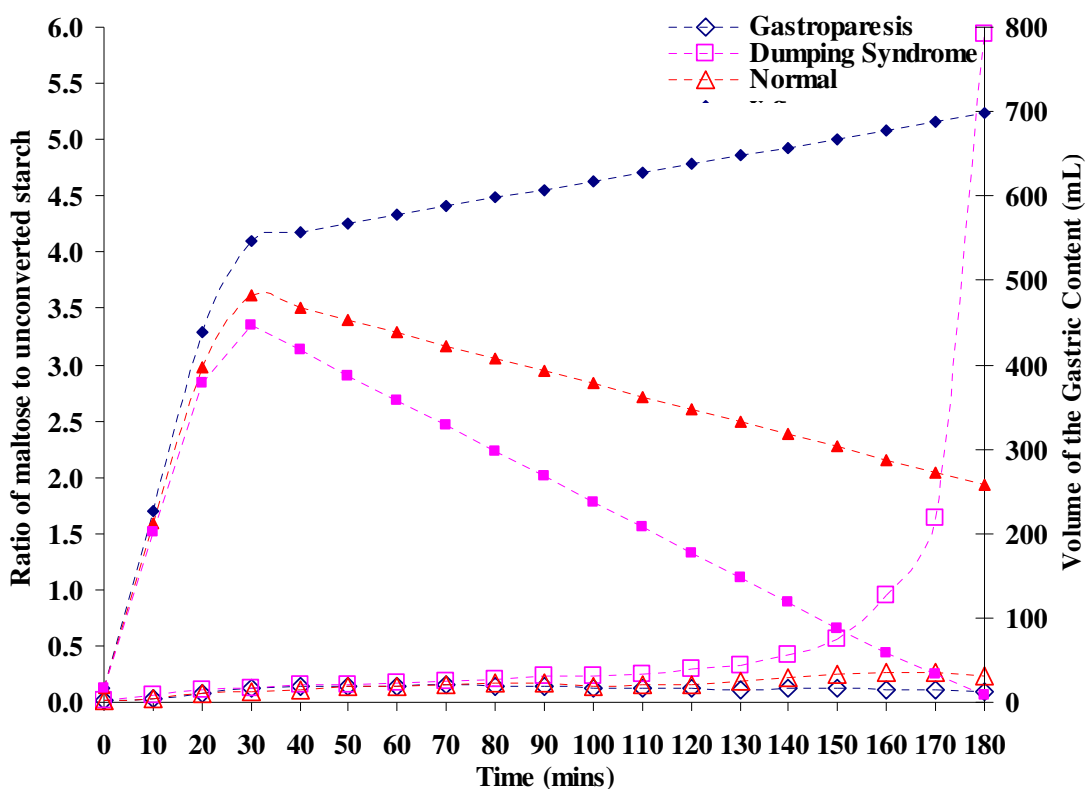


Figure 5-11. A graph showing the ratio of the mass of the maltose (g) to the mass of the unconverted starch (g) during the 3hr digestion time (min). The results obtained from the gastroparesis are marked with empty dots in blue, the dumping syndrome in pink and the normal in red. The volumes of the gastric content (mL) for different motility conditions are shown with filled dots with accordance of color and shape for each condition.

However for the dumping syndrome, along with rapid gastric emptying and faster rate of applied motility, the newly delivered gastric secretions have higher chance of reacting with the ingested food materials. Also by rapidly removing the undigested or partially

digested materials out of the stomach compartment, the amount of the gastric secretion gradually exceeds the amount of the undigested foods in the stomach. Thus the increase in the ratio was almost exponential, from 80min mark, reaching the maximum ratio of 5.9327 at 180min. This confirms the early hyperglycemia which would be seen due to the premature rapid gastric emptying of the undigested starch which will be broken down by pancreatic amylase to excessively generate glucose and delayed hypoglycemia which would be accomplished by lack of carbohydrates toward the end of the 3hr digestion period, as seen by the patients of the dumping syndrome (Buchwald, 1968; Borovoy *et al*, 1998; Karamanolis and Tack, 2006). The results indicate that provided the same feed materials and the same secretion conditions were supplied, the effect of motility, both frequency and force, on starch hydrolysis can be perceived. Taking natural log (ln) of the ratio of the maltose to unconverted starch (Figure 5-12) showed that from 50min, the values among the three different motility conditions have started to diverge. The largest difference in ratio was seen at 180min, where the Dumping syndrome showed the highest ratio and the gastroparesis, the slowest. Thus it can be concluded that the ratio of the maltose to unconverted starch is proportional to the rate of motility applied.

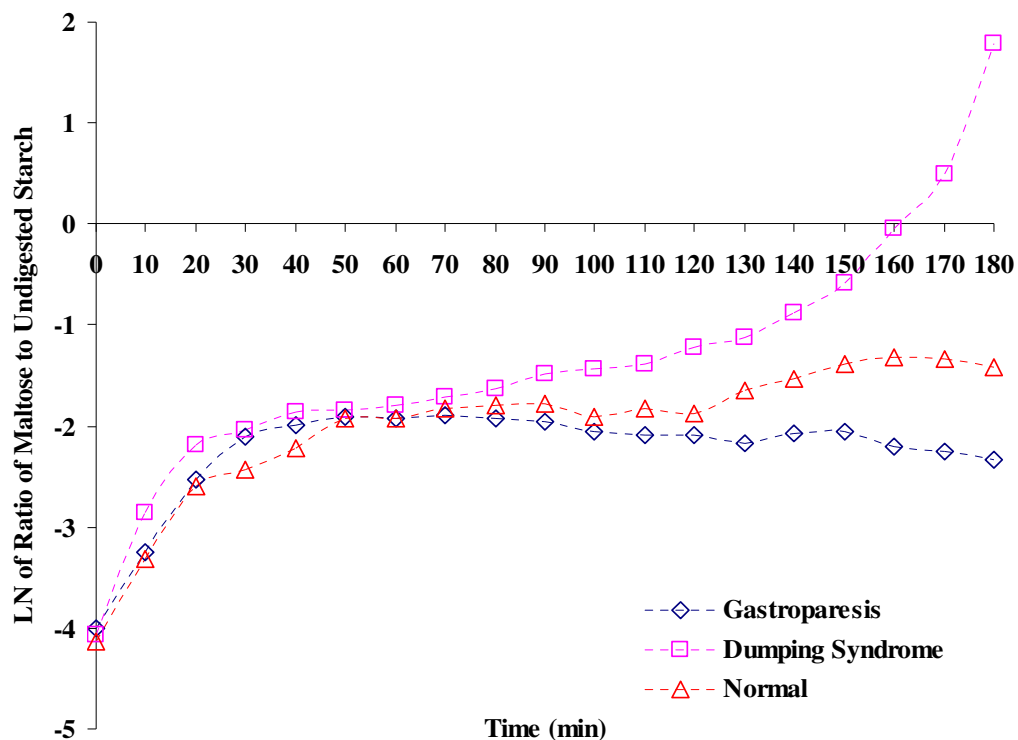


Figure 5-12. A graph showing the natural log (ln) of the ratio of the mass of the maltose (g) to the mass of the unconverted starch (g) during the 3hr digestion time (min). The results obtained from the gastroparesis are marked with empty dots in blue, the dumping syndrome in pink and the normal in red. The volumes of the gastric content (mL) for different motility conditions are shown with filled dots with accordance of color and shape for each condition.

5.3.3. HPLC

Using the HPLC, an overall screening of the collected samples was made to clarify the presence of maltose and to identify the possible byproducts of the rice starch hydrolysis. As a result, maltose and maltotriose were detected. The starch hydrolysis in the normal human subjects usually do not result in glucose, as the partially unconverted starch as well as maltose are further digested by pancreatic α -amylase in the small intestines.

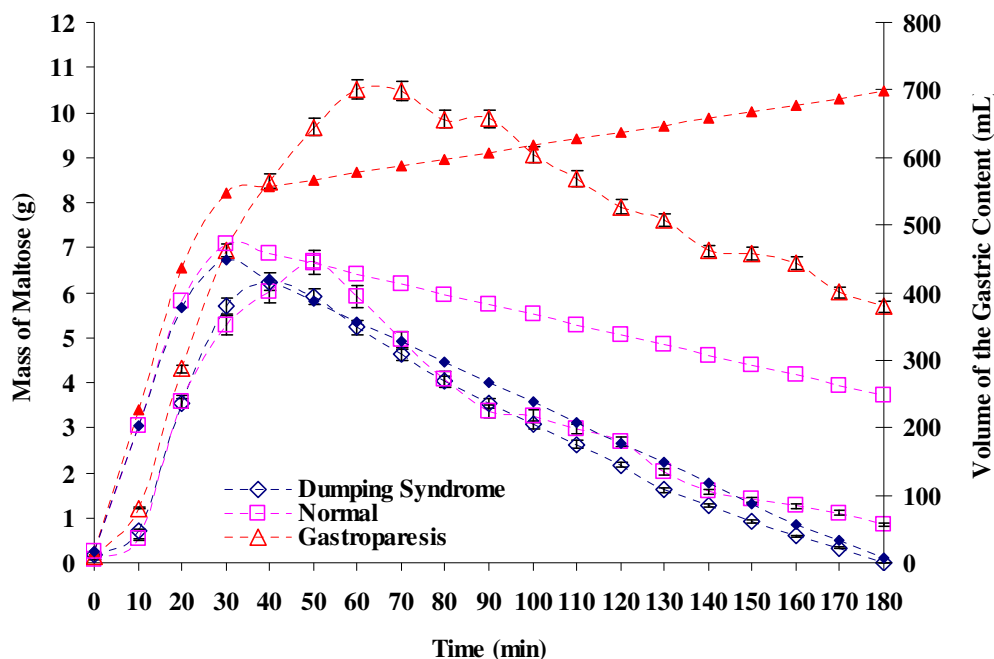


Figure 5-13. A graph showing the mass of maltose (g) measured by HPLC. The results obtained from the dumping syndrome are marked with empty dots in blue, the normal state in pink and the gastroparesis in red. The volumes of the gastric content (mL) for different motility conditions are shown with filled dots with accordance of color for each condition.

In general, the mass of maltose analyzed from the HPLC showed slightly lower values (Figure 5-13) compared to that of the UV-spectrophotometer. This seemed to be caused by the waiting period of the samples collected from the models until the analysis. Although the samples were kept in an ice water bath, and diluted accordingly to a factor of 40, some samples had to wait over 10hrs until the analysis began. However the standing time at room temperature for the UV-spectrophotometric measurements was much shorter when compared to that of the HPLC. Also after dilutions, the samples were chemically treated with arseno and somogyi reagents, where there were no treatments for

the HPLC samples. Even with the use of the shortest column to examine the sample in the HPLC, it took 15-30min, as the HPLC column requires cleaning time to avoid any blockage and accumulation of carbohydrate molecules which may cause interference amongst the samples for analyses. As many of the samples were kept in the auto-sampler at room temperature overnight, it might have caused a further digestion, most likely to be acidic hydrolysis, during the waiting period to be analyzed. In spite of this, the overall trend of the maltose mass was very similar to that found using the UV-spectrophotometer.

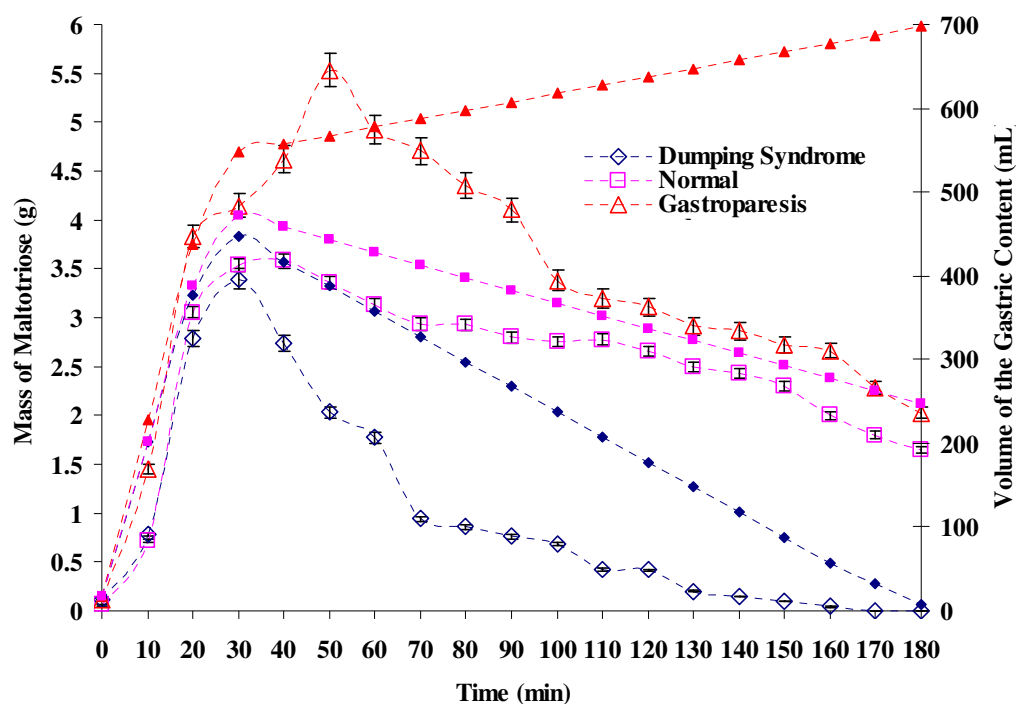


Figure 5-14. A graph showing the mass of maltotriose (g) measured by HPLC. The results obtained from the dumping syndrome are marked with empty dots in blue, the normal state in pink and the gastroparesis in red. The volumes of the gastric content (mL) for different motility conditions are shown with filled dots with accordance of color for each condition.

Maltotriose concentration was detected by the HPLC. In order to avoid any arbitrary confusions, the obtained values of the concentration ($\text{g}\cdot\text{L}^{-1}$) were converted to the mass of maltotriose present (g) by multiplying the gastric content volume (Figure 5-14) to the concentration. The highest mass of maltotriose among the three conditions all initially increased exponentially, to the maximal values of 3.58g at 40min for the normal condition, 5.53g at 50min for the gastroparesis and 3.40g at 30min for the dumping syndrome. The gastroparesis condition showed the highest mass of maltotriose compared to the other conditions, and the final mass of the maltotriose at 180min was also the highest, 2.03g,

conveying somewhat incomplete digestion. The final mass of the maltotriose was the lowest (0.003g) as the final volume of the gastric content was very small, 5-7.5ml which largely constituted of the newly delivered gastric secretion. For the normal condition, a very gradual decrease of the mass of the maltotriose mass was observed with the final value of 1.65g. Overall, the trend of the mass of maltotriose over time was very similar to that of the mass of maltose, where the lowest values were seen with the dumping syndrome condition throughout the experiments, followed by the normal and the gastroparesis conditions.

5.3.4. Recording of the pH

The pH profile is one of the widely used tools to indicate the feasibility of an *in vitro* testing method, especially for clinical studies such as the interaction of drug and the gastric secretions, disintegration of coating materials and capsules, and possible interference of more than one type of drug taken at the same time (Dressman *et al*, 1990; Hörter and Dressman, 1997; Hörter and Dressman, 2001). The pH profile is able to emphasize the overall control of motility as well as secretions applied, and in conjunction with results from the Phenol-Sulfuric acid assay, the Somogyi-Nelson method and the HPLC, a better understanding of the effect of different frequency of the motility can be perceived. Two probes were used for measuring the pH of the IPUGS. Probe 1 (Figure 5-15) refers to the pH probe which was implanted at the wall of the fundus, where the majority of the acidic gastric secretions took place, and probe 2 (Figure 5-16) was implanted on the wall of the antrum which acts as a temporal reservoir in storing of the ingested foods.

The pH profiles of the normal condition and the dumping syndrome were very similar to each other, especially during the ingestion period. However the pH profile of the gastroparesis condition was distinctively different to the other two conditions throughout the 3hr digestion period. Initially the pH values of the three conditions were nearly the same, about 1.03 ± 0.01 , which reflects the pH of the 0.15M HCl used as a simplified gastric juice for these experiments. A rapid increase in pH was shown in the normal and the dumping syndrome cases, where relatively faster rates of motility (3 and 5 cycles.min⁻¹, respectively) were applied compared to that of the gastroparesis. Thus the ingested feed mixture and the gastric secretion in the antrum (major acidic secretory site) would have been mixed more thoroughly compared to the gastroparesis, resulting in a more rapid

increase in the pH caused by the buffering capacity of the ingested feed mixture initially. However the increase of pH in the antrum of the gastroparesis condition was much slower. At 10min mark, the pH of the gastroparesis condition showed the lowest value of pH of 1.74 ± 0.14 , whereas for the normal and the dumping syndrome, similar values of 2.20 ± 0.02 and 2.01 ± 0.10 were found, respectively.

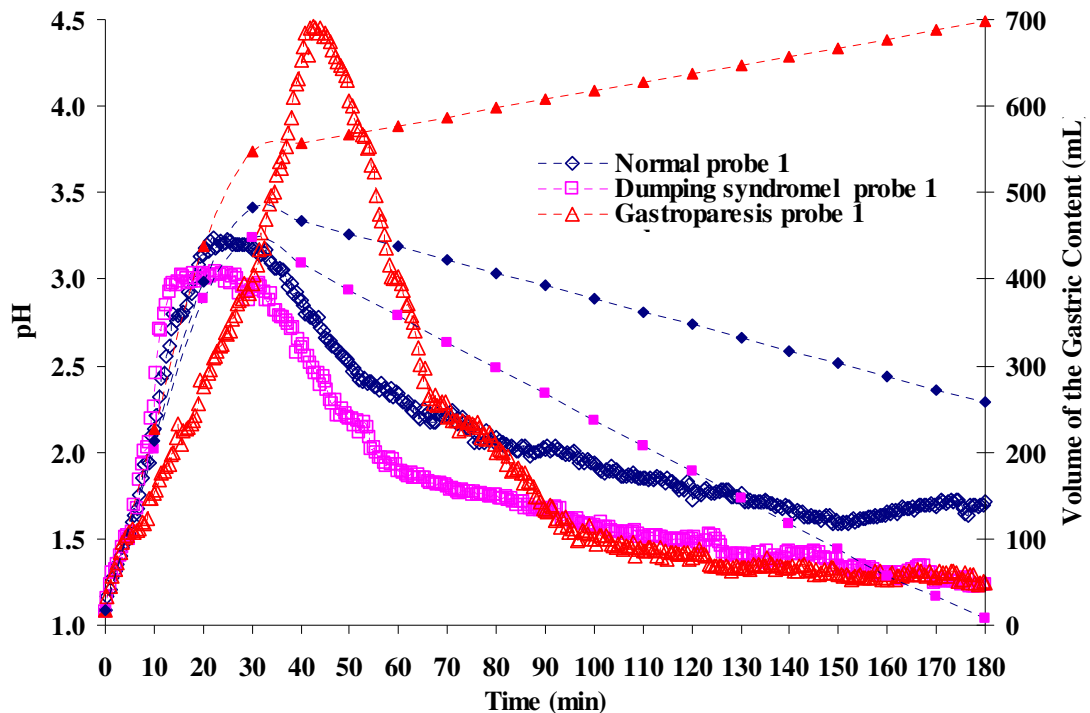


Figure 5-15. The pH profile of the pH probe 1 (fundus) over 3hr digestion period. The results obtained from the normal condition are marked in blue, the dumping syndrome in pink and the gastroparesis in red. The volumes of the gastric content (mL) for different motility conditions are shown with filled dots with accordance of color and shape for each condition.

The peak pH of 3.04 ± 0.06 in the fundus area was found at 23min with the dumping syndrome condition, showing the fastest establishment of well-mixed condition. For the normal condition, slightly more acidic pH was reached, 3.24 ± 0.06 at 24min mark. The gastroparesis condition took 43min, which was after the ingestion ceased. As the ingested feed material was building up in the fundus without being mixed well with the acidic gastric secretion, the pH in the fundus as well as in the antrum (Figure 5-16) have kept on increasing. In the fundus, the peak pH reached 4.46 ± 0.04 , which was the highest amongst the three conditions. From the collected samples of the gastroparesis condition during the ingestion period contained small portion of rice grain chunks, which were found deposited at the bottom of the sampling bottles due to gravity over time. However with the normal and the dumping syndrome conditions, the samples obtained during the

ingestion period as well as throughout the experiments were mostly water and opaque in color with very fine particles which seemed to have broken apart from the ingested rice grains by the gastric motility applied. It would seem that the greater curvature of the IPUGS was able to hold the non-digested rice grains from slipping through the pylorus even when simulating the conditions of the dumping syndrome. The buffering capacity of the ingested feed was therefore higher and lasted longer than expected when considering near to none containment of proteins and fats in the rice grains.

Even before the ingestion period has ceased, the pH of both the normal and the dumping syndrome conditions started to fall. Up to 20min mark, the pH profiles of the normal and the dumping syndrome conditions were almost indistinguishable, though it started to diverge since then. From 35min to 60min, the rate of decrease in pH was the most rapid in the dumping syndrome, owing to the fastest rate ($6.5\text{ml}\cdot\text{min}^{-1}$) of gastric emptying as well as the spatial and geometrical division of the fundus and the antrum. Due to the position of the pH probe 1, which was in the proximal area (fundus/body) of the stomach, the acidity of the gastric secretions played a role in keeping the pH low. Therefore a very rapid drop of the pH profile was seen with the gastroparesis condition, where poor mixing of the secretions and ingested feed as well as slow gastric emptying ($2.5\text{ml}\cdot\text{min}^{-1}$) was achieved. The pH profile measured by the probe 1 for the gastroparesis condition reflects the acidic gastric secretions over time. By 60min, the pH of the gastroparesis ($\text{pH } 2.31\pm 0.07$) was almost equivalent to that of the normal condition ($\text{pH } 2.21\pm 0.04$). Rapid decrease of the gastroparesis condition was constant, but at a slower rate from 60min to 90min. By 90min, which can be considered as the time taken for half of the gastric content to be emptied under normal condition, the pH in the antrum was the highest in the dumping syndrome condition, followed by the normal and the gastroparesis conditions. The volume of the gastric content under the gastroparesis condition was almost doubled ($605\pm 2\text{ml}$) the volume of the dumping syndrome ($267\pm 2\text{ml}$), though the difference in the pH was less than 1.0. From 90min to 180min, slow decrease of the pH was seen in all three conditions, with the dumping syndrome showing the highest pH range, followed by the normal condition and the lowest pH range by the gastroparesis condition.

The pH probe 2 measured the pH profile of the distal area (antrum) in the stomach compartment of the IPUGS, therefore showing a higher range of the pH over time when compared to the recordings of the pH probe 1. The normal and the dumping syndrome conditions showed similar trends in increase and decrease in pH over the ingestion period and the gastric emptying period, reaching their maximal pH of 3.37 ± 0.07 and 3.25 ± 0.04

at 20min, respectively, which were slightly elevated compared to that of the fundus (pH probe 1) as shown in the Figure 5-15.

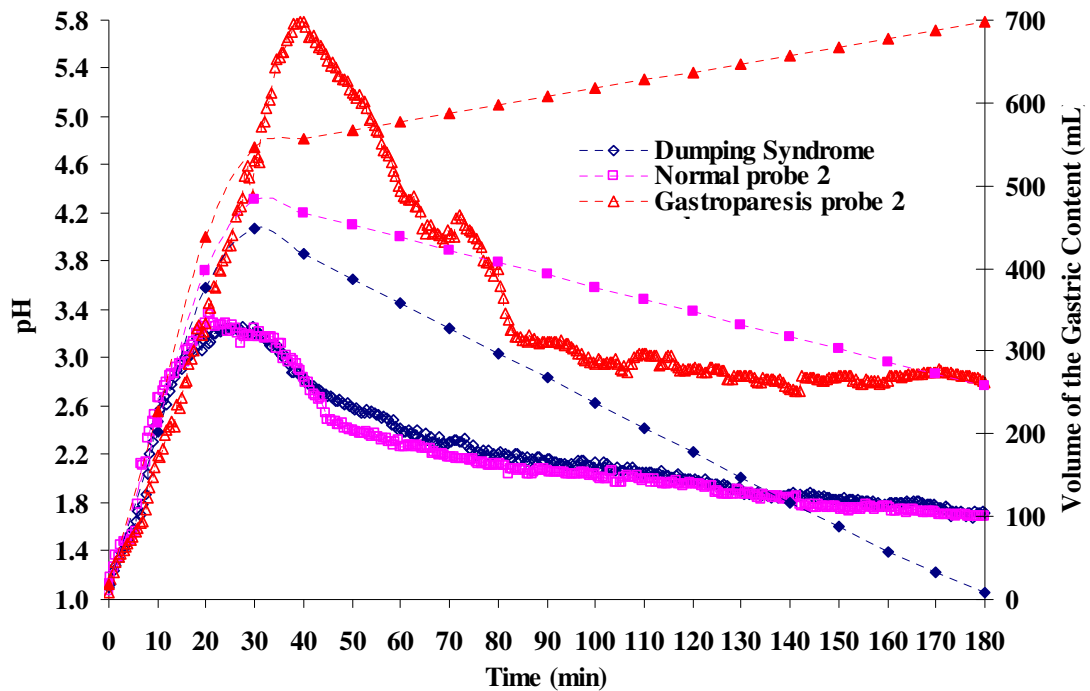


Figure 5-16. The pH profile of the pH probe 2 (antrum) over 3hr digestion period. The results obtained from the dumping syndrome are marked in blue, the normal in pink and the gastroparesis in red. The volumes of the gastric content (mL) for different motility conditions are shown with filled dots with accordance of color and shape for each condition.

Overall, similar trends of change in the pH over time were shown for both of the conditions when compared to the pH profile in the antrum in the Figure 12. However with the gastroparesis condition, even higher buffering effect was observed, with the maximal pH of 5.79 ± 0.03 at 40min. This is similar to the high buffering effect shown by Dressman *et al* (1990) and Malagelada *et al* (1976), although the ingested meal used in their studies contained a standard meal including proteins and fats. From 80min mark, the pH of the gastroparesis and the dumping syndrome were very similar to one another, with even higher pH level shown by the gastroparesis condition than the normal condition. This can be explained by the change of volume of the gastric content with respect to time. Fundus is the area which acts as a temporal reservoir for holding the ingested foods until it gets further digested. By 80min, more than half of the ingested feed material has been emptied for the dumping syndrome, hence there was not enough foods to overcome the acidic pH of the gastric secretions, therefore poor buffering effect was shown in the fundus.

However with the gastroparesis, the rate of chyme removal from the stomach compartment was set at $2.5\text{ml}\cdot\text{min}^{-1}$, therefore even after the ingestion period has stopped, the volume of the gastric content kept on increasing. i.e. $3.5\text{ml}\cdot\text{min}^{-1}$ of secretions delivered and $2.5\text{ml}\cdot\text{min}^{-1}$ of the gastric contents removed. As a result, higher buffering capacity was shown throughout the experiments for the gastroparesis condition. However after 3hr digestion period, similar pH values were found for the normal (1.68 ± 0.05) and the dumping syndrome (1.72 ± 0.04) conditions, though the end pH of the gastroparesis (2.80 ± 0.05) was much higher compared to the other two conditions due to the prolonged buffering effect of the ingested feed and delayed gastric emptying.

5.4. Concluding Remarks and Future Works

The rate of the gastric motility in the IPUGS was varied to study two common GI motility disorders, gastroparesis and dumping syndrome. Yet, the study of motility disorders have never been conducted via *in vitro* digestion models in the literature. Provided a detailed clinical data of such patients, parameters used in the IPUGS can be altered to simulate other uncommon conditions of GI disorders to understand and predict bolus movement within the GI lumen with peristaltic movements, as suggested by Nguyen *et al* (1999). With the use of slower and faster rates of the gastric motility, variations in the pattern and the values of the total water soluble carbohydrates, maltose, maltotriose and unconverted rice starch were perceived. Comparison of the ratio of the mass of the maltose to the mass of the unconverted rice starch confirmed a clearer difference between the dumping syndrome, the gastroparesis and the normal conditions once more. The pH profiles among the three conditions also differed noticeably, especially between the gastroparesis and the other conditions (both normal and the dumping syndrome).

By using the data from many physiological and clinical sources in the literature, the parameters such as the frequency and the force of motility, transit time and digestion period in the IPUGS can be altered to further study motility disorders of not only humans but in animals as well. Overall, the IPUGS was able to simulate the conditions of the gastric motility disorders as described in the literatures and resulted similar outcomes in many ways. The IPUGS can be of a useful tool in predicting of the bolus transit and can also be used as a clinical tool with or without *in vivo* studies. Furthermore, conditions of the disorders related to the gastric secretions can be simulated with the IPUGS (described in Chapter 7) to further validate the IPUGS with the data from various patients.

5.5. References

- Akin, A. (1998) Non-invasive detection of spike activity of the stomach from cutaneous EGG. PhD Thesis Drexel University, Philadelphia
- Akin, A., Sun, H. H. (2002). Non-invasive gastric motility monitor: fast electrogastrogram (fEGG). *Physiol. Meas.*, 23, 505-519
- Allerscher, H. D., Abraham-Fuchs, K., Dunkel, R. E., Classen, M. (1998) Biomagnetic 3-Dimensional spatial and temporal characterization of electrical activity of human stomach. *Digestive diseases and sciences*, 43 (4), 683-693
- Al-Zaben, A., Chandrasekar, V. (2005). Effect of esophagus status and catheter configuration on multiple intraluminal impedance measurements. *Physiol. Meas.*, 26, 229-238
- Barker, M. C., Cobden, I., Axon, A. T. (1979). Proximal stomach and antrum in stomach emptying. *Gut*, 20, 309-311
- Björck, I., Granfeldt, Y., Liljeberg, H., Tovar, J., Asp, N. G. (1994) Food properties affecting the digestion and absorption of carbohydrates. *Am. J. Clin. Nutr.*, 59 (Suppl.), 699S-705S
- Borovoy, J., Furuta, L., Nurko, S. (1998) Benefit of uncooked cornstarch in the management of children with dumping syndrome fed exclusively by gastrostomy. *Am. J. Gastroenterol.*, 93 (5), 814-818
- Buchwald, H. (1968) The dumping syndrome and its treatment. *Am. J. Surg.*, 116, 81-88
- Camilleri, M., Hasler, W. L., Parkman, H. P., Quigley, E. M. M., Soffer, E. (1998). Measurement of gastrointestinal motility in the GI laboratory. *Gastroenterology*, 115, 747-762
- Caulfield, M. E., Wyllie, R., Firor, H. V., Michener, W. (1986) Dumping syndrome in children. *J. Pediatrics*, 110 (2), 212-215
- Chen, J. D. Z. (1998). Non-invasive measurement of gastric myoelectrical activity and its analysis and applications. *Proceedings of the 20th Annual International Conference of the IEE Engineering in Medicine and Biology Society*, 20 (6), 2802-2807
- Creaghe, S. B., Saik, R. P., Pearl, J., Peskin, G. W. (1977) Noninvasive vascular assessment of dumping syndrome. *J. Surg. Res.*, 22, 328-332
- De Zwart, I. M., Mearadji, B., Lamb, H. J., Eilers, P. H. C., Masclee, A. A. M., De Roos, A., Kunz, P. (2002). Gastric motility: comparison of assessment with real-time MR imaging or barostat measurement - initial experience. *Radiology*, 224, 592-597
- Dressman, J. B., Berardi, R. R., Dermentzoglou, L. C., Russel, T. L., Schmaltz, S. P., Barnett, J. L., Jarvenpaa, K. M. (1990). Upper gastrointestinal (GI) pH in young, healthy men and women. *Pharmaceutical Research*, 7 (7), 756-761
- Dubois, M., Gilles, K., Hamilton, J. K., Rebers, P. A., Smith, F. (1951). A colorimetric method for the determination of sugars. *Nature*, 168, 167
- Dubois, M., Gilles, K., Hamilton, J. K., Rebers, P. A., Smith, F. (1956). Colorimetric method for the determination of sugars and related substances, *Anal. Chem.*, 28, 350-356
- Duthie, H. L., McKellar, N. J. (1960) Radiological appearances in the postgastrectomy syndrome. *British J. Radiology*, 33, 171-177
- Edgar, W. M. (1990). Saliva and dental health. *British Dental Journal*, 169 (3-4), 96-98
- Elashoff, J. D., Reedy, T. J., Meyer, J. H. (1982). Analysis of gastric emptying data. *Gastroenterology*, 83, 1306-1312
- Engelholm, L., Govzerts, J. P., Kiekens, R., Potvliege, R. (1966) Gastrointestinal transit with a test meal in gastric operations. *Medical Audiovision*, 5, 191-200
- Franco, C. M. L., Preto, S. J. R., Ciacco, C. F. (1992) Factors that affect the enzymatic degradation of natural starch granules: effect of the size of the granules. *Starch*, 44, 422-426
- Frazier, P. J., Richmond, P., Donald, A. M. (1997). *Starch: Structure and Functionality*. The Royal Society of Chemistry.
- Grundy, D., Al-Chaer, E.D., Aziz, Q., Collins, S.M., Ke, M., Taché, Y., Wood, J.D. (2006) Fundamentals of neurogastroenterology: Basic science. *Gastroenterology*, 130, 1391-1411
- Harrison, A. P., Erlwanger, K. H., Elbrond, V. S., Andersen, N. K., Unmack, M. A. (2004). Gastrointestinal tract models and techniques for use in safety pharmacology. *J. Pharma. Toxic. Methods.*, 49, 187-199
- Hörter, D., Dressman, J.B. (1997) Influence of physicochemical properties on dissolution of drugs in the gastrointestinal tract. *Advanced Drug Delivery Reviews* 25, 3-14
- Hörter, D., Dressman, J.B. (2001) Influence of physicochemical properties on dissolution of drugs in the gastrointestinal tract. *Advanced Drug Delivery Reviews* 46, 75-87

- Humphrey, S. P., Williamson, R. (2001). A review of saliva: Normal composition, flow and function. *The Journal of Prosthetic Dentistry*, 85 (2), 162-169
- Jalilian, E., Onen, D., Neshev, E., Mintchev, M. P. (2007). Implantable neural electrical stimulator for external control of gastrointestinal motility. *Medical Engineering & Physics*, 29 (2), 238-252
- Karamanolis, G., Tack, J. (2006) Nutrition and motility disorders. *Best Practice & Research Clinical Gastroenterology*, 20 (3), 485-505
- Kararli, T. T. (1995). Review article: Comparison of the gastrointestinal anatomy, physiology and biochemistry of humans and commonly used laboratory animals. *Pharmaceutics & Drug Disposition*, 16, 351-380
- Kelly, K. A. (1974) Gastric motility after gastric operations. *Surgery Annual.*, 6, 103-123
- Kim, J. C., Kim, J. I., Kong, B. W., Kang, M. J., Kim, M. J., Cha, I. J. (2004) Influence of the physical form of processed rice products on the enzymatic hydrolysis of rice starch in vitro and on the postprandial glucose and insulin response in patients with Type 2 Diabetes Mellitus. *Biosci. Biotechnol. Biochem.*, 68 (9), 1831-1836
- Klein, S., Butler, J., Hempenstall, J. M., Reppas, C., Dressman, J. B. (2004) Media to simulate the postprandial stomach I. Matching the physicochemical characteristics of standard breakfasts. *J. Pharma. Pharmacol.*, 56, 605-610
- Lee, K-J., Vos, R., Janssens, J., Tack, J. (2004a). Differences in the sensorimotor response to distension between the proximal and distal stomach in humans. *Gut*, 53, 938-943
- Lien, H. C., Chang, C. S., Chen, G. H., Kao, C. H., Tsai, S. C., Wang, S. J. (1998). Evaluation of gastric emptying by measurement of proportion of intra-abdominal radioactivity in stomach. *Gastroenterology*, 114 (4), Supplement 1, A790 AGA abstracts, G3251
- Luiking, Y. C., Peeters, T. L., Stolk, M. F., Nieuwenhuijs, V. B., Portincasa, P., Depoortere, I., van Berge Henegouwen, G. P., Akkermans, L. M. A. (1998). Motilin induces gall bladder emptying and antral contractions in the fasted state in humans. *Gut*, 42, 830-835
- Madsen, P., Rasmussen, T. (1964) Postgastroctomy roentgenography with a physiological contrast medium. *Acta. Radiologica (Diagnosis)*, 2, 153-160
- Mainville, I., Arcand, Y., Farnworth, E.R. (2005) A dynamic model that simulates the human upper gastrointestinal tract for the study of probiotics. *International Journal of Food Microbiology*, 99, 287-296
- Malagelada, J. R., Longstreth, G. F., Summerskill, W. H. J., Go, V. L. W. (1976) Measurement of gastric functions during digestion of ordinary solid meals in man. *Gastroenterology*, 70, 203-210
- Marciani, L., Gouwland, P. A., Spiller, R. C., Manoj, P., Moore, R. J., Young, P., Fillery-Travis, A. J. (2001) Effect of meal viscosity and nutrients on satiety, intragastric dilution and emptying assessed by MRI. *Am. J. Physiol. Gastrointest. Liver Physiol.*, 280, G1227-1233
- Masuko, T., Minami, A., Iwasaki, N., Majima, T., Nishimura, S-I., Lee, Y. C. (2005) Carbohydrate analysis by a phenol-sulfuric acid method in microplate format. *Analytical Biochemistry*, 339, 69-72
- Maurer, A. H., Parkman, H. P. (2006). Update on gastrointestinal scintigraphy. *Semin. Nucl. Med.*, 36, 110-118
- Mossi, S., Meyer-Wyss, B., Beglinger, C., Schwizer, W., Fried, M., Ajami, A., Brignoli, R. (1994). Gastric emptying of liquid meals measured noninvasively in humans with [¹³C] acetate breath test. *Digestive Diseases and Sciences*, 39(12), 107S-109S
- Nelson, N. (1944) A photometric adaption of the Somogyi method for the determination of glucose. *J. Biol. Chem.*, 153, 375-380
- Nguyen, H. N., Silny, J., Matern, S. (1999). Multiple intraluminal electrical impedancometry for recording of upper gastrointestinal motility: current results and further implications. *Am. J. Gastroenterology*, 94 (2), 306-317
- Notivol, R., Coffin, B., Azpiroz, F., Mearin, F., Serra, J., Malagelada, J-R. (1995). Gastric tone determines the sensitivity of the stomach to distention. *Gastroenterology*, 108, 330-336
- Pade, V., Aluri, J., Manning, L., Stavchansky, S. (1995) Bioavailability of pseudoephedrine from controlled release formulations in the presence of guaifenesin in human volunteers. *Biopharmaceutics & Drug Disposition*, 16, 381-391
- Parkman, H. P., Hasler, W. L., Fisher, R. S. (2004) American gastroenterological association technical review on the diagnosis and treatment of gastroparesis. *Gastroenterology*, 127, 1592-1622

- Pehlivanov, N., Liu, J., Kassab, G. S., Beaumont, C., Mital, R. K. (2002). Relationship between esophageal muscle thickness and intraluminal pressure in patients with esophageal spasm. *Am. J. Physiol. Gastrointest. Liver Physiol.*, 282, 1016-1023
- Pulvertaft, C. N. (1953) The postgastrectomy stomach remnant. *J. Faculty of Radiologists*, 5, 19-32
- Rao, P., Pattabiraman, T. N. (1989). Reevaluation of the phenol-sulfuric acid reaction for the estimation of hexoses and pentoses. *Anal. Biochem.*, 181, 18-22
- Schwizer, W., Fox, M., Steingöter, A. (2003) Non-invasive investigation of gastrointestinal functions with magnetic resonance imaging: towards an ideal investigation of gastrointestinal function. *Gut*, 52 (Suppl. IV), iv34-iv39
- Schwizer, W., Frazer, R., Borovicka, J., Crelier, G., Boesiger, P., Fried, M. (1994). Measurement of gastric emptying and gastric motility by magnetic resonance imaging (MRI). *Digestive Diseases and Sciences*, 39 (12), 101S-103S
- Sigstad, H. (1971) Postgasterctomy radiology with a physiologicla contrast medium. Comparison between dumpers and non-dumpers. *British J. Radiol.*, 44, 37-43
- Somogyi, M. (1926) Notes on sugars determination. *J. Biol. Chem.*, 79, 599-613
- Somogyi, M. (1937) A reagent for the copper iodometric determination of vary small amounts of sugar. *J. Biol. Chem.*, 117, 771-776
- Somogyi, M. (1945) A new reagent for the determination of sugars. *J. Biol. Chem.*, 160, 61- 68
- Stemmer, E. A., Jones, S. A., Pearson, S. C., Connolly, J. G. (1969) Antiperistaltic segments of jejunum in the treatment of the dumping syndrome. *Archives of Surgery*, 98, 396-405
- Suzuki, S. (1987) Experimental studies on the presumption of the time after food intake from stomach contents. *Forensic Science International*, 35, 83-117
- Tortora, G. J., Grabowski, S. R. (2000) Principles of anatomy and physiology. 9th Edition. John Wiley and Sons, Inc., Chapter 24, The Digestive System. pp.818-870
- Vecht, J., Van Oostayen, J. A., Lamers, C. B. H. W., Masclee, A. A. M. (1998) Measurement of superior mesenteric activity artery flow by means of doppler ultrasound in early dumping syndrome. *AM. J. Gastroenterol.*, 93 (12), 2380-2384
- Wang, Z. S., Chen, J. D. Z. (2000). Mathematical modeling of nonlinear coupling mechanisms of gastric slow wave propagation and its SIMULINK simulation for investigating gastric dysrhythmia and pacing. *Computer-Based Medical Systems, 2000. CBMS 2000. Proceedings. 13th IEEE Symposium.* 89-94
- Whitehouse, G. H., Temple, J. G. (1977) The evaluation of dumping and diarrhoea after gastric surgery using a physiological test meal. *Clin. Radiol.*, 28, 143-149
- Williamson, G., Belshaw, N. J., Sief, D. J., Noel, T. R., Rings, S. G., Cairns, P., Morris, V. J., Clark, S. A., Parker, M. L. (1992) Hydrolysis of A and B type crystalline polymorphs of starch by α -amylase, β -amylase and glucoamylase. *Carbohydr. Polym.*, 18, 179-187
- Wrolstad, R. E., Acree, T. E., Decker, E. A., Penner, M. H., Reid, D. S., Schwartz, S. J., Schoemaker, C. F., Smith, D. M., Sporns, P. (2005) Handbook of food analytical chemistry. Water, proteins, enzymes, lipids and carbohydrates. Hoboke, N. J. J. Wiley.
- Zhao, Y., Kent, S. B. H., Chait, B. T. (1997) Rapid, sensitive structure analysis of oligosaccharides. *Proc. Natl. Acad. Sci. USA*, 94, 1629-1633

Chapter 6

Validation of the Secretion used in the *In vitro* Physicochemical Upper Gastrointestinal System (IPUGS)

In this chapter, a comparative review of the gastrointestinal secretions, in terms of the compositions and the methods of delivering the secretions, in the humans, the *in vitro* physicochemical upper gastrointestinal system (IPUGS) and the existing *in vitro* digestion models in the literature is discussed.

6.1. Introduction

Gastrointestinal (GI) secretions are dynamic processes regulated via hormonal and/or neural signals to optimize the digestion of the ingested foods and to maintain the homeostasis of the GI pH within a strict range (Joseph *et al*, 2003). About 7L of the GI secretions are secreted through the mucosa of the upper gastrointestinal tract (GIT) on daily basis (DeSesso and Jacobson, 2001). The upper GI secretions can be divided into saliva, mucosal secretions in the esophagus and the stomach and gastric juice. 1-1.5L of saliva is produced by the salivary glands in the mouth to aid chewing and swallowing processes to facilitate the ingestion of foods (Schenkels *et al*, 1995). Saliva is composed of 99.5% of water and 0.5% solutes including ions, mucus, immunoglobulin A, salivary α -amylase and lingual lipases (Tortora and Grabowski, 2000). In the esophagus, mucus is secreted to facilitate the peristalsis of the ingested foods into the stomach. Majority of the gastric juice, including HCl, pepsin, intrinsic factor and gastric lipase, is secreted via the mucosa of the fundus in the stomach. Gastric mucus is secreted through the mucous surface cells and mucous neck cells in the stomach to protect the stomach lining from being digested by the acidic and digestive gastric juice (Tortora and Grabowski, 2000).

In vitro digestion models in the literature have attempted to simulate the secretion process with the use of peristaltic pump(s) for continuous secretions for complex and dynamic systems like SHIME (Molly *et al*, 1993) and TIM (Minekus *et al*, 1995) or auto-burette(s)/pipettes for non-continuous (one-off) secretions which have been widely used by bioavailability studies (Fatouros *et al*, 2007) and replaced the human digestive enzymes with bacterial, fungal or animal sources as they are economic and readily available. As the natural GI secretions of human source have numerous constituents

which are variable according to the time of day and the fed/fasting state, duplication has been expected to be impossible (Gal *et al*, 2001). Galia *et al* (1998 and 1999) developed a media to simulate the gastric secretion of the stomach under fasting conditions for the studies of bioavailability and pharmaceuticals. However, the constituents of the media was over-simplified, pre-made homogenized meals were used and no hormonal control of the secretion in response to the meal, resulting decrease in pH even in the fed stomach over time, thus unable to reflect the dynamic nature of the human stomach (Klein *et al*, 2004). Most of the *in vitro* digestion models used simplified gastric secretions composed of a brief ionic balance with digestive enzymes. Yet, mucosal secretions have never been used in the existing models, and addition of saliva into such models was found to be relatively uncommon. Commercially available human salivary amylase has been used (Turnbull *et al*, 2005; Laurent *et al*, 2007) to constitute the artificial saliva in bioavailability studies.

Simplified gastric juice composed of HCl and pepsin has been found to be the most commonly used gastric juice in the existing *in vitro* digestion models. Such composition has been used by bioavailability studies (Rao and Prabhavathi, 1978; Lock and Bender, 1980; Miller *et al*, 1981; Kapsokefalou *et al*, 2005; Alexandropoulou *et al*, 2006; Laurent *et al*, 2007). Pepsin from porcine stomach mucosa has been commonly used (Haraldsson *et al*, 2005; Turnbull *et al*, 2005; Laurent *et al*, 2007) to replace the human pepsin as is relatively cheap, easy to find, available in large quantity and have similar characteristics to the humans (Bhaskar *et al*, 1991 and 1992). Alternatively, pepsin from hog stomach mucosa has been used as well (Miller *et al*, 1981).

Along with HCl and pepsin, NaCl has been added by Longland *et al* (1977) and Suzuki (1987) for iso-osmolarity of the human gastric secretion. More comprehensive constituents of the gastric juice have been used by the studies using the TNO's gastrointestinal model (TIM). Electrolyte solution composed of NaCl, KCl, CaCl₂ and NaHCO₃ with pepsinogen and rhizopus lipase have been secreted into the stomach compartment of the TIM at 0.25ml.min⁻¹ and 0.10N HCl was pumped into the stomach compartment separately at 0.25ml.min⁻¹ continuously irrespective of the fed and the fasted states (Minekus *et al*, 1995; Havenaar and Minekus, 1996; Minekus *et al*, 1999; Marteau *et al*, 1997; Krul *et al*, 2000; Avantaggiato *et al*, 2003; Blanquet *et al*, 2004; Dominy *et al*, 2004; Haraldsson *et al*, 2005; Souliman *et al*, 2006).

Depending on the studies, digestive enzymes have been omitted in the artificial GI secretions. Lee and Heo (2000) and Zimmermann and Müller (2001) used simulated

gastric juice without pepsin, which is composed of HCl and NaCl only. This seemed appropriate as the test materials, *Bifidobacterium longum* immobilized in calcium alginate beads (Lee and Heo, 2000) and solid lipid nano-particles (Zimmermann and Müller, 2001) did not contain any proteins to be digested. However, pre-filling of the stomach compartment prior to the ingestion of the test materials has been used by the TIM as well as Castela-Papin *et al* (1999) and Mainville *et al* (2005) to simulate the cephalic phase of the acid secretion.

Despite many attempts to simulate the GI secretions for *in vitro* digestion models in the literature, only average compositions was able to be designed to standardize the procedure of the testing (Gal *et al*, 2001). However as these artificial secretions use purified enzymes which are more reproducible when compared to the use of live microbes, relatively small batch-to-batch variations are expected without a further need of enzyme preparation standardizations (Coles *et al*, 2005).

The extent of simulating the human GI conditions as closely as possible, in terms of the composition as well as the delivery of site-specific sequential use of the secretions, was studied using the *vitro* physicochemical upper GI system (IPUGS) to evaluate whether the IPUGS has made improvements to the existing *in vitro* digestion models in the literature. Short grain white rice (Sun Rice Japanese style Sushi Rice, Koshihikari and Opus type) was chosen as a test material as the constituent of the macronutrients is relatively simple (up to 78.5wt% of total carbohydrates) compared to other balanced test meals composed of a mixture of carbohydrates, proteins and fats, thus analyses of carbohydrates would be of the main concern and complications emerging from having to analyze all the nutrients as well as intra and inter-actions of nutrients can be avoided. Studies of starch (including rice starch) underscored no significant differences between the *in vitro* enzymatic hydrolysis and *in vivo* digestion of starch (Williamson *et al*, 1992; Franco *et al*, 1992; Björck *et al*, 1994; Kim *et al*, 2004). Yet, rice is one of the most abundant staple food worldwide (Frazier *et al*, 1997), where intensive research related to the postprandial glucose and insulin responses, diabetes, coronary heart disease, cancer and ageing are being conducted (Frazier *et al*, 1997; Kim *et al*, 2004). Thus the use of IPUGS can be further applied to such studies.

6.2 Materials and Methods

6.2.1. *In vitro* Physicochemical Upper Gastrointestinal System (IPUGS)

The IPUGS consists of three consecutive compartments simulating the conditions of the upper GI organs in humans. The first compartment simulates the food ingestion in mouth, which is composed of a denture set with manually controlled mastication and continuous secretion of artificial saliva of $37\pm 0.5^{\circ}\text{C}$ which is transferred via a peristaltic pump at rate of $7.0\text{ml}\cdot\text{min}^{-1}$ (Edgar 1990; Humphrey and Williamson, 2001). White short grain rice (Sun Rice Japanese style Sushi Rice) was cooked in a conventional rice cooker with 1:1 volumetric ratio of rice grains to water. 100g of the cooked rice was transferred to the mouth reactor with 250ml of drinking water to be used as the feed material. As the cooked rice is relatively small in size which can be swallowed without much of mastication, it can be regarded as simpler foods for testing. 5min of gentle manual mastication was applied with the denture set with $20\text{chewingings}\cdot\text{min}^{-1}$ to remove large clusters of rice into smaller pieces to aid the swallowing process. The feed material was spoon fed to the next compartment, esophagus at a rate of $8.5\text{ml}\cdot 30\text{s}^{-1}$ (equivalent to $\frac{1}{2}$ Tablespoon (tbsp) $\cdot 30\text{s}^{-1}$).

The next two compartments simulating the conditions of the esophagus and the stomach were built with platinum cure silicon rubber composed of 75-85wt% polyorganosiloxanes, 20-25wt% of amorphous silica and 0.1wt% of platinum-siloxane for part A and 65-70 wt% of polyorganosiloxanes and 20-25wt% of amorphous silica for part B. 1:1 ratio of the parts A and B were mixed and coated to the plastic anatomy model of the stomach which resembles the average human stomach size at unfed state (20cm x 15cm x 8cm, Kararli, 1995; Pade *et al*, 1995) as well as its geometry of J-shaped curve. The coatings were repeated until the thickness of the stomach wall reached $0.50\pm 0.01\text{cm}$ in average. The material is translucent in color thus by adding of food coloring agents to the feed mixture may help clearer view of the reactions in the inner stomach compartment. It offers negligible shrinkage and able to stretch and rebound to its original size and shape without distortion. For the esophagus, paper roll of 1.5cm diameter and 20cm in length was made, and coatings of the silicon rubber were repeatedly made until the wall thickness reached $0.30\pm 0.01\text{cm}$ in average (Al-Zaben and Chandrasekar, 2005). The paper roll and the plastic anatomic model were removed after coatings. In order to deliver the gastric secretions to the wall of the stomach, a large number of Tygon ® Microbore

tubings (n=200) with inner diameter of 0.25mm were implanted, with the tips of these tubings pierced into the stomach wall to create a gradual dampening of the wall (Figure 6-1), secreting $3.5\text{ml}\cdot\text{min}^{-1}$ (Mainville *et al*, 2005) throughout the 3hr digestion period. These tubings are designed for precision injection and dispensing in laboratory applications with flexible and bendable resin. The tubings have a very smooth inner bore surface which reduces the risk of particulate build-up during sensitive fluid transfer and minimal extractable helps to assure fluid purity. Also, these tubings are transparent, thus the gastric secretions passing into the stomach wall can be seen clearly. For mucosal secretions in the esophagus compartment, slightly larger diameter of tubing was used. Micro-Line™ tubing (Thermoplastic Scientifics, Inc.) made of cross-linked ethyl vinyl acetate. These tubings are translucent, flexible and elastic with inner diameter of 0.51mm.

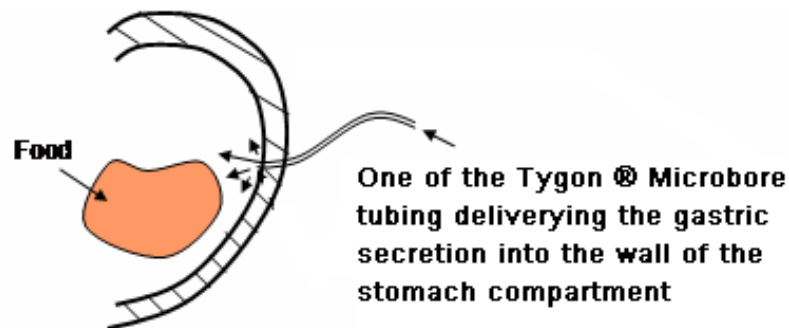


Figure 6-1. An illustration of one of the Tygon® Microbore secretion tubings inserted into the wall of the stomach compartment. 200 of these tubings were implanted with even distribution to deliver the artificial gastric secretions.

One ends of these implanted tubings in both esophagus and the stomach were planted into the wall of each compartment to create gradual dampening effect from the wall to simulate the opening and closing of the pores in the gastric wall for secretion delivery. The other ends were gathered and squashed into a larger diameter Tygon peristaltic tubings (inner diameter of 1.5cm), which are subsequently connected to the smallest possible peristaltic tubing (inner diameter of 0.80mm). Though the flow rate of the peristaltic pumps can be controlled, changing the peristaltic tubing size also helped to control the flow rate more accurately. For validation of motility experiments, only one peristaltic pump (Autoclude® Peristaltic Pump - 54505) was used to deliver the artificial gastric juice to the stomach compartment.

The esophagus and the stomach compartments were placed in an anaerobic chamber with continuous nitrogen gas flow ($1.0\text{L}\cdot\text{hr}^{-1}$) and the temperature inside the chamber was maintained at $37\pm 1^\circ\text{C}$ with a hot plate placed inside the chamber.

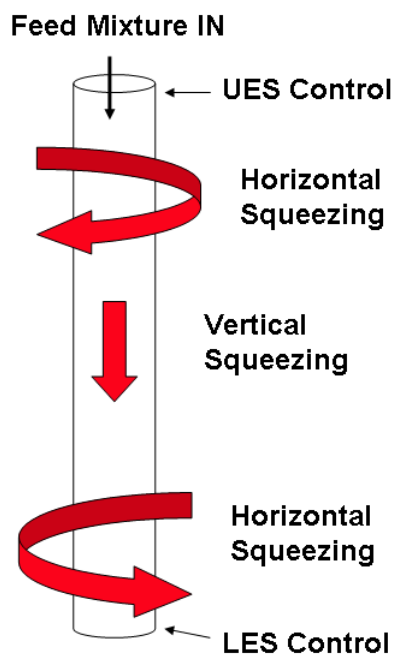


Figure 6-2. Diagram showing the motility of the esophageal compartment of the IPUGS. Red arrows indicate the direction of squeezing. UES refers to the upper esophageal sphincter and LES represents the lower esophageal sphincter.

For the experiments with simplified composition of the GI secretions, the constituents of the artificial saliva and the gastric juice were kept as simple as possible to avoid any complications from salts in analyzing data and to compare the effect of having more constituents, both ionic and enzymatic, to the digestive processes. Thus α -amylase and hydrochloric acid, which are the main substances that are able to hydrolyze rice starch, were used for the simplified secretions, and mucosal secretions were omitted as they do not have direct effect on digestion. 2g of fungal (*Aspergillus oryzae*) α -amylase (Grindamyl™ A5000, 5000U/g, Danisco 071314) was mixed with 200ml of deionized (MilliQ) water to be used as the artificial saliva and 0.15M HCl (Ajax, AF602394) was used as the artificial gastric juice, which were both warmed up to $37\pm 1^\circ\text{C}$. The α -amylase from *Aspergillus oryzae* (E.C.3.2.1.1) was one of the closest and cheap alternative to the human α -amylase (E.C.3.2.1.1). Hormonal control of altering the secretion rates was also excluded as to compare the IPUGS to other models in terms of motility only.

The esophagus and the stomach compartments were manually pressed with my hands to mimic the peristaltic waves. For the esophagus, coordinated contractions and relaxations of the peristaltic propulsions were simulated to push the ingested feed material (bolus) towards the stomach with the rate of 5 contractions per 30s. The wall of the esophageal compartment was squeezed both horizontally and vertically by gripping the esophagus using both hands, one on top of each other and in between a thumb and an index finger, squeezed gently to push down the bolus (Figure 6-2).

The upper esophageal sphincter (UES) controlled the entrance of the feed mixture and the lower esophageal sphincter (LES) controlled the exit of the feed mixture into the stomach compartment. Each cycle of esophageal peristalsis lasted up to 6s (Pehlivanov *et al*, 2002). Apart from mucosal secretions, there are neither digestive secretions nor absorption take place in the esophagus (Tortora and Grabowski, 2000) thus these features were excluded.

Hand squeezed actions to simulate the peristaltic waves of the human stomach was used in the stomach compartment as well. The first peristaltic wave was initiated from squeezing the proximal part of the stomach compartment (the fundus and upper body) and moved subsequently towards the lower antrum/pylorus area. This was to generate a pressure gradient from the body of the stomach to the pylorus, resulting an opening of the pyloric sphincter and emptying of fractions of the stored bolus towards the pylorus and mix with the gastric secretions, which resembles the action of a contractile grinder, crushing the small chunks of the bolus as described in the literature (Akin 1998; Luiking *et al*, 1998; Nguyen *et al*, 1999; Tortora and Grabowski, 2000) (Figure 6-3).

The second peristaltic wave with closed cardiac and pyloric sphincters was initiated from the distal stomach (lower body and the antrum), squeezing the wall of the stomach towards the proximal direction (toward the fundus) (Figure 6-4). Sequential contractions of the antrum crushed the small chunks of the bolus against the closed pyloric sphincter with a large fraction of the remaining bolus squeezed back toward the proximal part for further digestion (Kelly, 1974; Barker *et al*, 1979; Tortora and Grabowski, 2000; De Zwart *et al*, 2002), causing distention of the stomach compartment to accommodate more space for the incoming food which was facilitated by the elastic and stretchy nature of the building material (platinum cure silicon rubber).

The First Peristaltic Wave

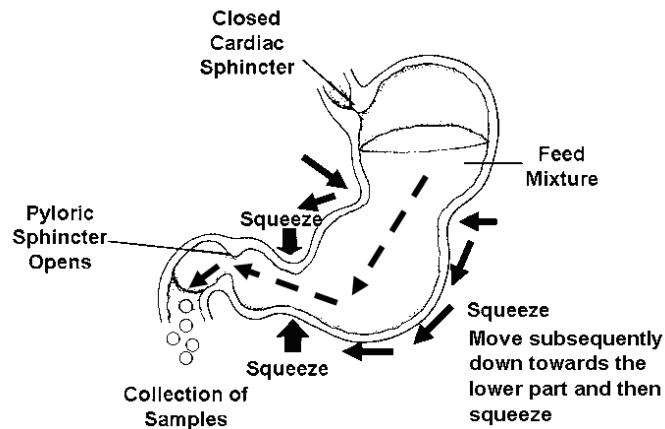


Figure 6-3. A diagram of the first peristaltic wave applied to the stomach compartment of the IPUGS. Black arrows drawn on the outside of the stomach indicate the directions of the squeezing action. Squeezing initiated from the body of the stomach and moved subsequently towards the lower antrum/pylorus area, followed by a strong squeezing in the lower antrum/pylorus area to open the pyloric sphincter and release the chyme. Dotted black arrows inside the stomach indicate the expected flow of the chyme inside the stomach compartment.

The Second Peristaltic Wave

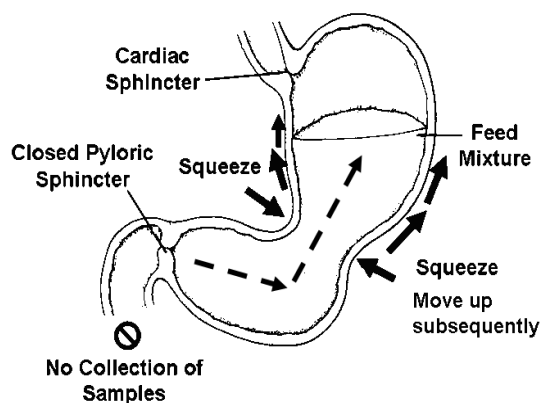


Figure 6-4. A diagram of the second peristaltic wave applied to the stomach compartment of the IPUGS. Black arrows drawn on the outside of the stomach indicate the directions of the squeezing action and red arrows indicate the expected flow of the chyme inside the stomach compartment. Black dotted arrows inside the stomach indicate the direction of the chyme movement.

The overall gastric motility in the proximal stomach compartment remained relatively constant, but for the distal part, stronger contractions with higher depth and amplitudes

(Schwizer *et al*, 1994), were used. The first and the second peristaltic waves constitute one wave cycle of the gastric motility. To simulate the normal condition at fed state, $3\text{cycle}\cdot\text{min}^{-1}$ with average duration of wave cycle of $21.5\pm 3.8\text{s}$ (Allescher *et al*, 1998) was used.

The digestion period of 3hrs was set as carbohydrates typically take 2-4hrs to be emptied into the small intestine (Suzuki, 1987; Mossi *et al*, 1994). Initially, 5ml of the samples were taken from the mouth compartment to check the consistency of each batch. From 10min to 30min, 20ml of samples were collected every 10min from the pylorus. From 30min to 180min where the gastric emptying was to be more active, 6.8ml of the chyme mixture was pumped out of the MISST per minute (Marciani *et al*, 2001; Mainville *et al*, 2005), collected and stored in sampling bottles with closed lids and placed in an ice water bath ($0-2^{\circ}\text{C}$) while the experiment was running. Then the samples were centrifuged at 3000rpm for 30min (Klein *et al*, 2004) at 2°C . The supernatants were diluted accordingly for each of the analytical methods used. The experiments via the IPUGS were conducted triplicate.

6.2.2. Comprehensive compositions of the GI secretions in the IPUGS

6.2.2.1. Saliva

Artificial saliva was made from the list of compositions stated by Shellis (1978) (Table 6-1) as it is the closest possible chemically defined synthetic saliva in the literature (Wong and Sessions, 2001), which contain numerous ions, amino acids, vitamins, growth factors and mucin of appropriate amounts in accordance to the humans. All the chemicals were purchased from Sigma-Aldrich with reagent plus® grade. Salivary α -amylase (46-60kDa), also known as diastase, glycogenase and ptyalin, catalyses the endohydrolysis of α -1,4-glycosidic linkage between glucose residues of oligosaccharides and polysaccharides such as starch, glycogen and dextrans (Schenkels *et al*, 1995; Tortora and Grabowski, 2000; PDB sum database*). For the salivary α -amylase, fungal source, *Aspergillus oryzae* (Grindamyl™ A5000, 5000U/g, Danisco 071314), has been used. It is much cheaper than the commercially available human α -amylase, falls in the same enzyme class of E.C.3.2.1.1, has the same function of catalysing the endohydrolysis reaction, and has similar gene ontology functional annotations to that of the humans. The gene ontology

functional annotations including biological process of carbohydrate metabolic process, and catalytic activities including cation binding, calcium ion binding and α -amylase activity for its biochemical function, matched well with that of the humans (PDB sum database). However extracellular space is missing in the α -amylase of *Aspergillus oryzae* compared to that of the humans, which is not of crucial importance to the digestive function of saliva.

Table 6-1. Composition of the Shellis synthetic saliva (Shellis, 1978).

Constituent	Concentration (mg.L ⁻¹)
Ammonium chloride	233
Calcium chloride, dehydrate	210
Magnesium chloride, hexahydrate	43
Potassium chloride	1162
Potassium di-hydrogen orthophosphate	354
Potassium thiocyanate	222
Sodium citrate	13
Sodium hydrogen carbonate	535
di-Sodium hydrogen orthophosphate	375
Glycoprotein	2500
Albumin	25
Urea	173
Uric acid	10.5
Creatinine	0.1
Choline	13
Mixture of amino acids *	41
Mixture of vitamins **	0.8
Alpha amylase	3 x 10 ⁵ Somogyi Units.L ⁻¹

* mixture of amino acids are shown in table 6-2.

** mixture of vitamins are shown in table 6-3.

The activity of bacterial α -amylases was much lower than human α -amylase due to a large difference in optimum temperature range (70°C) compared to the human conditions (37°C) (Van Ruth and Roozen, 2000) whereas α -amylases from *Aspergillus oryzae* showed similar level of the rate of cyclodextrins hydrolysis (Jodál *et al*, 1984) with

optimum range of pH between 5 and 7 (Carlsen *et al*, 1996) and optimum temperature range of 35 to 37 °C with inactivation temperature of 65 to 70 °C (Jodál *et al*, 1984; MSDS of Grindamyl™ A5000 from Danisco). Thus it was decided to replace the human α -amylase to α -amylase of *Aspergillus oryzae*. 2.00±0.02g of α -amylase powder was mixed with 200ml deionized distilled water with the electrolytes from the Shellis synthetic saliva.

Table 6-2. Composition of mixture of amino acids (Shellis, 1978).

Amino Acid Constituent	Concentration (mg.L ⁻¹)
Alanine	3.3
Arginine	1.9
Aspartic acid	1.6
Glutamic acid	3.9
Glycine	8.9
Histidine	1.0
Leucine	2.9
Iso-Leucine	2.9
Lysine	2.7
Methionine	0.03
Phenylalanine	2.9
Proline	0.2
Serine	2.1
Threonine	2.9
Tyrosine	2.1
Valine	1.8

In addition to the Shellis synthetic saliva with α -amylase (*Aspergillus oryzae*), lingual lipase has been added to simulate the hydrolysis of triglycerides in the ingested meals into fatty acids and monoglycerides (Tortora and Grabowski, 2000). Lipase, which is also known as triacylglycerol acylhydrolase and triacylglycerol lipase, from *Candida rugosa* (fungal source) with greater or equal to 700U/mg (Sigma-Aldrich, L1754) was used to replace the human lingual lipase in saliva as it showed relatively similar biochemistry with the same enzyme class of E.C.3.1.1.3 and similar optimum temperature of 37°C. Lingual lipases from humans and *Candida rugosa* both have the function of triglyceride hydrolysis and optimum pH range of 3.0-6.5 (Abrams *et al*, 1984) where more than 90%

of the ingested lipase has been shown to be inactivated in the acidic medium of the stomach (Abrams *et al*, 1984; Griffin *et al*, 1989). For lipases from *Candida rugosa*, 1 unit is able to hydrolyze 1.0 meq of fatty acid from triacetin in 1hr at 37°C (MSDS from Sigma-Aldrich). 0.10±0.02g of lipase from *Candida rugosa* was added to the artificial saliva mixture of 200ml and secreted at a rate of 7.0ml.min⁻¹.

Lysozyme belongs to the enzyme class E.C.3.2.1.17, with molecular weight of 14kDa, which provide anti-bacterial defence to the host (Fleming and Allison, 1922) for the innate immune system (Schenkels *et al*, 1995). As the primary aim of the IPUGS is to observe digestive processes rather than the study of toxins, immunity was not taken into account, thus lysozyme was not added to the artificial saliva used for the IPUGS.

Table 6-3. Composition of mixture of vitamins (Shellis, 1978).

Vitamin Constituent	Concentration (mg.L ⁻¹)
Thiamine	0.007
Riboflavin	0.05
Folic acid	0.0001
Nicotinic acid	0.03
Pyridoxine	0.6
Panthenic acid, Ca salt	0.08
Biotin	0.0008
Vitamin B12 (Cyanocobalamin)	0.003
Vitamin K (menaphthone)	0.015

In order to simulate the non-Newtonian shear-thinning characteristics of the natural human saliva, which is essential to provide lubrication and proper mixing of the ingested foods (Preetha and Banerjee, 2005), 2500mg.L⁻¹ of mucus (Sigma-Aldrich, M2378) which is classified as glycoproteins, have been added to the artificial saliva mixture (Table 6-1). Yet, no other *in vitro* digestion models have attempted to simulate the viscous nature of the human saliva although the viscosity is able to influence the diffusion rates of solutes and overall reaction rates which may have an effect in overall digestive processes (Gal *et al*, 2001). The artificial saliva mixture was made prior to each experiment and kept at 37°C until use as the temperature changes may influence the digestive processes in the mouth (Taylor and Linforth, 1996). However, the solutions of mixed amino acids (Table 6-2) and mixed vitamins (Table 6-3) from the Shellis synthetic

saliva (Shellis, 1978) were made concentrated (x1000) as numerous kinds of chemicals were required in trace amounts, and diluted accordingly per each experiment.

6.2.2.2. Mucosal secretions for the compartments of esophagus and stomach of the IPUGS

Mucus is a viscoelastic adherent secretion which forms a protective layer over the surface of the gastric epithelium with macromolecules such as immunoglobulin A, lysozyme and lactoferrin (Desai and Vadgama, 1991), to act as a diffusion barrier to nutrients and drugs (Desai and Vadgama, 1991; Atuma *et al*, 2001; Bansil and Turner, 2006) and restrict the penetration of large molecules (Norris *et al*, 1998; Holzapfel *et al*, 1998; Flemström, 1999), pepsin (Bhaskar *et al*, 1991) and gastric acid (Holm and Flemström, 1990; Bhaskar *et al*, 1992) via Donnan equilibrium (Bansil and Turner, 2006). The secretion of mucus is controlled by neural, hormonal and paracrine effects (Atuma *et al*, 2001) to replenish the continuously degraded mucus to maintain the homeostasis of the pH (Harding *et al*, 1983; Sarosiek and McCallum, 2000). The thickness of the gastric mucus falls in the range of 50 to 500µm (Norris *et al*, 1998; Atuma *et al*, 2001; Ho *et al*, 2004) which is largely dependent on the rate of secretions and the rate of proteolytic degradation by luminal acid, pepsin and shear stress during peristaltic waves and mechanical forces caused by the propagation of the bolus (Harding *et al*, 1983; Sarosiek and McCallum, 2000). HCO₃⁻ ions secreted by the gastric epithelium are trapped in the mucus gel lining to establish a pH gradient between the lumen (pH 1-2) and the apical cell surface (pH 6-7) (Hollander, 1954; Flemström, 1987; Cao *et al*, 1999). In humans, about 12-13 billions of gastric mucous cells exist (Haber *et al*, 1996).

The main constituents of the gastric mucus layer include up to 95wt% of water, 3-5wt% of mucin and up to 1wt% of inorganic salts, carbohydrate and lipids (Allen, 1989; Bansil and Turner, 2006). Mucin represents more than 80% of the organic components of the gastric mucus (Lichtenberger, 1995) which is the key constituent to determine the viscous and elastic properties of the mucus gel layer (Hollander, 1954; Bansil and Turner, 2006). Mucins are O-linked glycoprotein subunits (Strous and Dekker, 1992; Bansil *et al*, 1995) with up to 70%w/w carbohydrates (mainly oligosaccharides) confined to certain regions along the linear protein core (McAdam, 1993; Peppas and Huang, 2004) and have random coil conformations (Sheehan and Carstedt, 1989). Adhesion of the bacterial strains,

including probiotic strains, is an important step for microecological study as it promotes colonization of these bacteria inside the *in vitro* digestion model, enhance the transit tolerance to the acidic gastric pH and alter the availability of receptor sites for pathogenic microorganisms (Charteris *et al*, 1998; Holzapfel *et al*, 1998). The underlying mechanisms of the formation of the mucus gel layer by mucin macromolecules are still under investigation (Peppas and Huang, 2004).

However it is very difficult to obtain a reasonable quantity of mucins from the humans and the required level of purity is also under question (Harding *et al*, 1983). Thus, commercially available porcine gastric mucin powder (Sigma-Aldrich, M2378) was dispersed in phosphate buffer solution (pH 6.7) to make 30w/v% mucus solution by stirring at room temperature for 30min at 500rpm to be used as a replacement to the human mucus, which has been widely used by other *in vitro* studies due to its similar structures and functions (Allen *et al*, 1976; Bell *et al*, 1985; Hills, 1985). The mucosal secretions for the esophagus and the stomach compartments of the IPUGS were kept the same in terms of composition. The secretion was delivered to the walls of the esophagus at a rate of $1\text{ml}\cdot\text{min}^{-1}$ to barely cover the walls of the esophagus compartment to aid the movement of the bolus during the ingestion period of up to 30min. As soon as the ingestion period ceased, the mucosal secretion in the esophagus was stopped. For the esophagus, the mucus was secreted via the Micro-Line™ tubings (Chapter 3, 3.2.2) which were implanted throughout the wall of the esophagus in the IPUGS to aid the peristaltic movement of the bolus. For the gastric mucosal secretions, the secretion channels were implanted more on the antrum (60%) and fewer to the fundus (40%) of the IPUGS (Rees *et al*, 1982; Marieb, 1998; Tortora and Grabowski, 2000) to create a pH gradient across the surface of the mucus gel layer. The mucosal secretion was delivered to the walls of the stomach at a rate of $2\text{ml}\cdot\text{min}^{-1}$ to barely cover the walls of the stomach compartment to create a thin layer to simulate protection against the pepsin and the acidic gastric juice.

More ordered internal structure of the mucus gel layer with the use of higher concentrations of mucins (up to 60%w/v) which provide more intensive cross-linking, could have been obtained (Allen *et al*, 1976; Bell *et al*, 1985). However, considering of the high cost of the mucins, it was decided to use 30%w/v, which still falls in the compatible range to the human condition (20-60%w/v) (Allen *et al*, 1976; Bell *et al*, 1985), mimicking the non-Newtonian characteristics (Kočevár-Nared *et al*, 1997). Despite many attempts to simulate the rheological properties of the human natural mucus, the extent of the simulated viscoelastic properties was limited even with 60%w/v

concentration, due to the change in physicochemical properties such as non-specific entanglements of mucins or hydrophobic interactions, during the isolation and rehydration procedures (Bell *et al*, 1984; Tasman-Jones *et al*, 1989; Kočevár-Nared *et al*, 1997).

6.2.2.3. Gastric Secretion

As the partially digested foods (bolus) enter the stomach, the pH and volume of the stomach changes to stimulate the gastric acid secretion in G cells within the antrum to secrete gastrin, which is released into antral blood capillaries and diffuses into the corpus of the stomach to stimulate parietal cells to secrete gastric acid and to release histamine and neurotransmitters of the enteric nervous system (Tortora and Grabowski, 2000; DeSesso and Jacobson, 2001; Joseph *et al*, 2003). Approximately 1200 to 2000ml of gastric juice is secreted daily (Talwar and Srivastava, 2004). Under the normal stomach conditions, Joseph *et al* (2003) observed increases in neural and effector activities with food intake and such activities were also affected by either direct interaction of drugs with receptors in the stomach or by alteration of the gastric mucosa via the drugs (Spencer, 1982). The composition of the complex gastric juice used in the IPUGS is shown in Table 6-4, which contains KCl, HCl, NaCl, CaCl₂ and NaHCO₃ (Minekus *et al*, 1999) for ionic part and pepsin and gastric lipase for the enzyme part. The mean basal acid output in normal humans is 1.56mM of HCl (McArthur *et al*, 1982), thus instead of using 0.1N HCl as stated by Minekus *et al* (1995), 0.15N HCl was used. McArthur *et al* (1982) stated no significant correlation exists between gastric emptying time and acid out put, as well as between total acid output and original pH, osmolarity, calories and buffering capacity.

Many of the *in vitro* digestion models (Minekus *et al*, 1995; Krul *et al*, 2000; Avantaggiato *et al*, 2003; Dominy *et al*, 2004; Krul *et al*, 2004; Mainville *et al*, 2005) used pepsin from porcine gastric mucosa (Sigma-Aldrich, P7000) containing 800 to 2500U.mg⁻¹, as it is a relatively cheap and commercially available in large quantities which falls in the same enzyme category of E.C. 3.4.23.1 with that of the humans and cleaves C-terminal to the amino acid residues, Phe, Leu and Glu (MSDS, Sigma-Aldrich). It has optimal pH range of 2-4, which is compatible with the human gastric pH range.

Table 6-4. The composition of the gastric secretion used

Component	Concentration (g.L ⁻¹)
KCl	2.2
HCl	0.15N
Pepsin	500kU/L
Lipase	500kU/L
NaCl	5
CaCl ₂	0.22
NaHCO ₃	1.5

Human gastric lipase, also known as glycerol ester hydrolase and triacylglycerol lipase, (E.C 3.1.1.3) is the major enzyme secreted by the chief cells of the fundus of the stomach to initiate the digestion of dietary triacylglycerols (Lohse *et al*, 1997a; Armand *et al*, 1999; Wicker-Planquart *et al*, 1999). Human gastric lipase has a molecular mass of 50kDa and is a highly glycosylated molecule (10-15% of the protein mass) (Wicker-Planquart *et al*, 1999) with decrease in activity for pH below 2.0 and above 7.0 (Ville *et al*, 2002; Chahinian *et al*, 2006). In healthy normal subjects, 10-30% of the ingested triacylglycerols were lypolysed into fatty acids and a mixture of diacylglycerols and monoacylglycerols in the stomach (Hamosh *et al*, 1975; Armand *et al*, 1999; Mun *et al*, 2007). The gastric lipase of various sources including bacteria, fungi and mammals, all have serine esterases belonging to the α/β hydrolase superfamily, in which the nucleophilic serine, which is part of the Ser-His-Asp/Glu catalytic triad, was found to be located in the nucleophilic end (Chahinian *et al*, 2006; Roussel *et al*, 1999). The catalytic triad facilitates the hydrolysis of ester bonds in neutral lipids via nucleophilic attack (Lohse *et al*, 1997b). Lipase from porcine pancreas (Sigma-Aldrich, L3126) containing 100-400U.mg⁻¹ was used to replace the human gastric lipase. It belongs to the same enzyme commission of E.C.3.1.1.3, with the hydrolysing function of tri-, di- and monoglycerides (MSDS of Sigma-Aldrich) where 1 unit can hydrolyse 1.0 meq of fatty acid from triacetin in 1hr at 37°C. The optimal pH of the lipase from the porcine pancreas is 7.4, which is well outside the pH range of the stomach compartment of the IPUGS. However, this was the closest possible lipase that was commercially available at cheap price. As the test material was rice, where the content of fats is negligible, it was decided to use the lipase from the porcine pancreas. In terms of biochemical 3D structures, the lipase from the humans and porcine pancreas were similar to each other with the presence

of CATH 3.40.50.950 from the biochemistry database (www.biochem.ucl.ac.uk/bsm/enzymes/ec3/ec01/ec01/ec0003.html). Intrinsic factors contributing to the immune system of the stomach (Tortora and Grabowski, 2000) were not included in the artificial gastric secretion as the current study is focused on the digestive processes. The relative amounts of the human gastric lipase measured from the collected human gastric juice sample under basal (non-stimulated) conditions contained about 90 lipase units per ml (Wicker-Planquart *et al*, 1999). As the model is mainly focused on the stimulated condition, much higher concentration of 500kU.L⁻¹ was used, as stated by Minekus *et al* (1995). The combined solution containing the electrolytes with 150mM HCl, pepsin and lipase were mixed at 1000rpm at 37°C for 10min prior to experiments, and delivered at 3.5ml.min⁻¹ up to 90min, and 2ml.min⁻¹ from 90min to 180min.

6.2.3. Phenol-Sulfuric Acid Assay

Phenol-Sulfuric acid assay is one of the most widely used analytical methods in measuring neutral sugars in oligosaccharides, proteoglycans, glycoproteins and glycolipids. It is a simple, fast, reliable and sensitive method which has been developed by Dubois *et al* (1951) and (1956). Rao and Pattabiraman (1989) reported that phenol underwent sulfonation in situ and the phenol-sulfuric acid complex decreased the color intensity for many hexoses and pentoses. Similar results were seen by Masuko *et al* (2005) whom modified the original method by Dubois *et al* (1951) and (1956) by adding concentrated sulfuric acid to the sample followed by phenol. Instead of using microplate proposed by Masuko *et al* (2005), larger volumes were reconstituted following the ratio of sample to conc. sulfuric acid to phenol. The method was used to determine the concentration of total water soluble carbohydrates from the obtained samples.

3ml of concentrated sulfuric acid was added to 1ml of diluted (factor of 100) sample in a test tube followed by vigorous shaking at high speed in a vortex mixer. 600µL of 5% (w/v) phenol was pipetted into the mixed solution and placed in a water bath at 90°C for 10min. The prepared samples were vortexed at high speed for 30s and left at room temperature for 5mins cooling before reading the absorbance via the UV spectrophotometer (Agilent 8453, UV G1103A) at 490nm.

6.2.4. Somogyi-Nelson Method

Somogyi-Nelson method (Somogyi, 1926; Somogyi, 1937, Somogyi, 1945; Nelson, 1944; Wrolstad *et al*, 2005) is an extensively used highly accurate method for determining the amount of reducing sugars (e.g. maltose). Low alkalinity copper reagent and arsenomolybdate reagent were prepared as follows.

12g of sodium potassium tartate and 24g of anhydrous sodium carbonate with 250ml of distilled water were mixed. 4g of copper sulfate pentahydrate and 16g of sodium bicarbonate were added to 200ml of distilled water. 180g of anhydrous sodium sulfate in 500ml of boiling distilled water was separately prepared. Three mixtures were combined and diluted to 1L to make the low alkalinity copper reagent. The arsenomolybdate reagent was made by mixing 25g ammonium molybdate to 450ml of distilled water. 21ml of concentrated sulfuric acid and 25ml of distilled water containing 3g of disodium hydrogen arsenate heptahydrate were added to the ammonium molybdate solution with stirring. The mixture was continuously stirred for 24hrs at 37°C and kept in brown glass stopped bottle until use.

1ml of the diluted (factor of 100) sample and 1ml of the low alkalinity copper reagent were placed in a test tube and vigorously mixed by a vortex mixer at a high speed for 30s. The test tube was placed in a boiling water bath (100°C) for 10mins, and cooled at room temperature for 5mins. 1ml of the arsenomolybdate reagent was then added and the mixture was vortexed at a high speed for 30s. Absorbance at 500nm was read via the UV spectrophotometer (Agilent 8453, UV G1103A). Blanks for the absorbance were prepared by replacing the sample with 1ml distilled water.

Blue color of the low alkalinity copper reagent and green color of the arsenomolybdate reagent gave a greenish blue color in all the samples. The samples which contained less maltose showed a light green solution, but as the concentration of maltose increased, the color of the sample became darker and bluish. As the arseno reagent is extremely toxic and may cause cancer, particular cares were taken to avoid inhalation and contacts at all times.

6.2.5. High Performance Liquid Chromatography (HPLC)

High Performance Liquid Chromatography (HPLC) is able to provide both qualitative and quantitative analyses with a small amount of diluted sample. As HPLC requires a prestigious level of accuracy, it was used to ensure the compatibility of results from the phenol-sulfuric acid assay and the Somogyi-Nelson method, as well as to screen for any unexpected components (e.g. glucose) in the collected samples.

A carbohydrate ES column (Prevail™ Carbohydrate ES Column-W 150x4.6mm, 5 μm (Alltech Part No. 35102)) was used to specifically analyze maltose, maltotriose and other undigested starch in the samples. A mixture of degassed (Elite™ Degassing System) acetonitrile (Merck, HPLC grade) and deionized water was used as mobile phase and was pumped into the column via a quaternary gradient pump (Alltech, 726) at 1.0ml.min. Isocratic gradient was used for a better separation of carbohydrates – initially 65% to 35% of acetonitrile to water and then from 15mins onwards, 50% to 50%, respectively. Collected samples were diluted (x40) with deionized water, followed by syringe filtration with nylon membranes and automatically injected (Alltech Autosampler 570) into the column with 30min of analysis time per sample. Evaporative Light Scattering Detector (ELSD) and EZStart software were used to detect and record the findings. The heating column temperature of 50°C with Nitrogen (5.0) gas flow rate of 1.5L.min⁻¹ was used and the gain on the ELSD was set at 2.

6.2.6. Recording of pH

The measure of the pH profile is one of the simplest analyses which directly indicates the conditions of the stomach and it is of extreme importance as it is able to detect even minor changes of the gastric conditions. For the IPUGS, two pH probes and one temperature probe were pierced into the wall of the stomach compartment in the IPUGS to record the pH in the fundus (probe 1) and the antrum (probe 2). The temperature probe was placed in the middle of the body of the stomach to measure the changes with respect to time. For the MISST, a pH probe and a temperature probe were placed in the middle of the stomach reactor. A pH meter from Hanna Instrument (HI 4212) was used with auto-logging mode of 30s for 3hr.

6.3. Results and Discussions

6.3.1 Phenol-Sulfuric Acid Assay

The concentrations (g.L^{-1}) of the total water soluble carbohydrates detected by the Phenol-Sulfuric Acid Assay for the MISST (refer to section 4.2.2 for materials and methods) and the IPUGS with the simplified compositions and the IPUGS with complex compositions are illustrated on the Figure 6-5. The simplified compositions refer to the use of GI secretions with α -amylase in deionized water as artificial saliva and 0.15N HCl as artificial gastric juice. The complex secretions refer to the use of the closest possible constituents to the human GI secretions, considering the ionic balance, mucosal secretion and additional digestive enzymes such as lingual lipase, pepsin and gastric lipase. Although the concentrations and the rates of the GI secretions of various constituents may vary in accordance to the stimulated and non-stimulated state (Gal *et al*, 2001) where the hormonal feedback mechanism plays a key role in controlling the rate of secretions, it was decided to run experiments at the stimulated state only for the MISST and the IPUGS with simplified secretion compositions, as this is the state of active digestion. However for the IPUGS with complex secretion compositions, feed-back control of adjusting the gastric secretion rate from 3.5ml.min^{-1} to 2ml.min^{-1} and the mucosal secretion rate from 2ml.min^{-1} to 1ml.min^{-1} , from the 90min mark which is half time of the 3hr digestion period. This was to simulate the conditions of the upper GI of the humans as closely as possible, and to compare the impact of the feed-back control on the digestion of the rice meal provided. The concentrations (Figure 6-5) and the mass (Figure 6-6) of the total water soluble carbohydrates over time indicate the available amount of rice carbohydrates (mainly starch initially) in the stomach compartment of the MISST and the IPUGS at given times, which signifies the rate of ingestion as well as the rate of gastric emptying. By examining the amount (both concentration and mass) of the total carbohydrates as well as the amount of maltose and maltotriose (Figures 6-7, 6-8, 6-11 and 6-12) in the stomach compartment, the amount of undigested (unconverted) rice starch (Figure 6-9) can be determined (i.e. Undigested starch = Total carbohydrates – Maltose – Maltotriose). The ratio of maltose to unconverted starch (Figure 10) can then be calculated to observe the effect of varying the compositions and the rates of the secretions to the pattern of the rice starch hydrolysis, thus a valid conclusion can be drawn on the extent of GI secretions to the overall *in vitro* digestion process. As it has been proposed by Elashoff *et al* (1982) that for uniformity, time 0 was defined as the point at which the meal ingestion began.

Therefore the collected samples at time 0min can be referred to as the bolus which were about to be swallowed into the IPUGS as the samples were taken before they were ingested into the esophagus.

The changes in the concentrations and the masses of the total water soluble carbohydrates, which include the undigested rice starch as well as hydrolysed short chain carbohydrates such as maltose, were evident for both simplified and complex compositions of the IPUGS as well as in the MISST throughout the 3hr digestion period. Initially at time 0, the values of the total carbohydrate concentration for the three conditions were similar to each other, with average values of $106.4 \pm 2.96 \text{ g.L}^{-1}$ and $1.86 \pm 0.07 \text{ g}$ for the MISST, $96.2 \pm 2.13 \text{ g.L}^{-1}$ and $1.68 \pm 0.06 \text{ g}$ for the IPUGS with simplified secretions, and $93.8 \pm 1.15 \text{ g.L}^{-1}$ and $1.64 \pm 0.05 \text{ g}$ for the IPUGS with complex secretions.

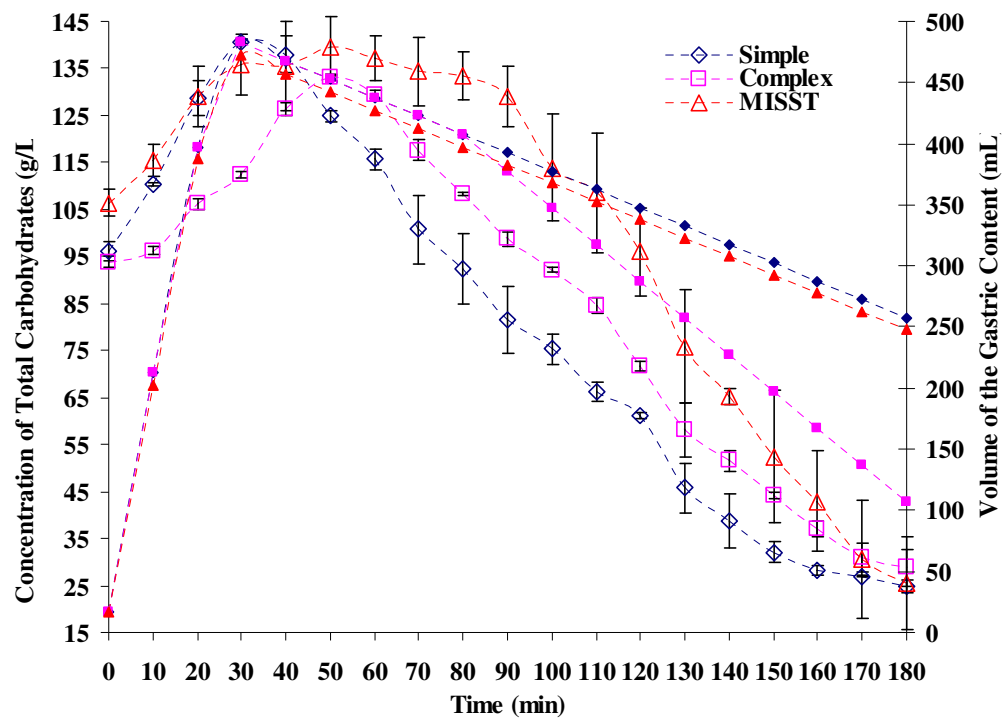


Figure 6-5. A graph showing the concentration of total carbohydrates (g.L^{-1}) during the 3hr digestion time (min). The results obtained from the use of the simplified gastrointestinal (GI) secretions are marked with empty dots in blue, the complex GI compositions in pink and the the simplified GI secretions of the MISST in red. The volumes of the gastric content (mL) for different secretion conditions are shown with filled dots with accordance of color and shape for each condition.

The values of the IPUGS were especially close to each other, indicating a good consistency in the feed mixture preparation throughout the experiments, as the procedures

for preparing the feed mixture and the rate of mastication applied in the mouth compartment were the same for the IPUGS experiments. For the MISST, finely homogenized rice meal (up to 500µm in diameter) was used, which had significantly smaller particle size compared to that of the non-homogenized rice grains (1.5±0.2cm) used in the IPUGS, therefore the small rice particles in the MISST accelerated the rate of carbohydrates extraction from the ingested meal, resulting faster dissolution and overall starch digestion were expected as it would have a higher chance to interact with salivary amylase. It can be speculated that the strong mechanical homogenization may have induced a breakdown of amylopectin to amylose, which would have fasten the overall rate of the rice starch hydrolysis, releasing reducing sugar molecules of maltose.

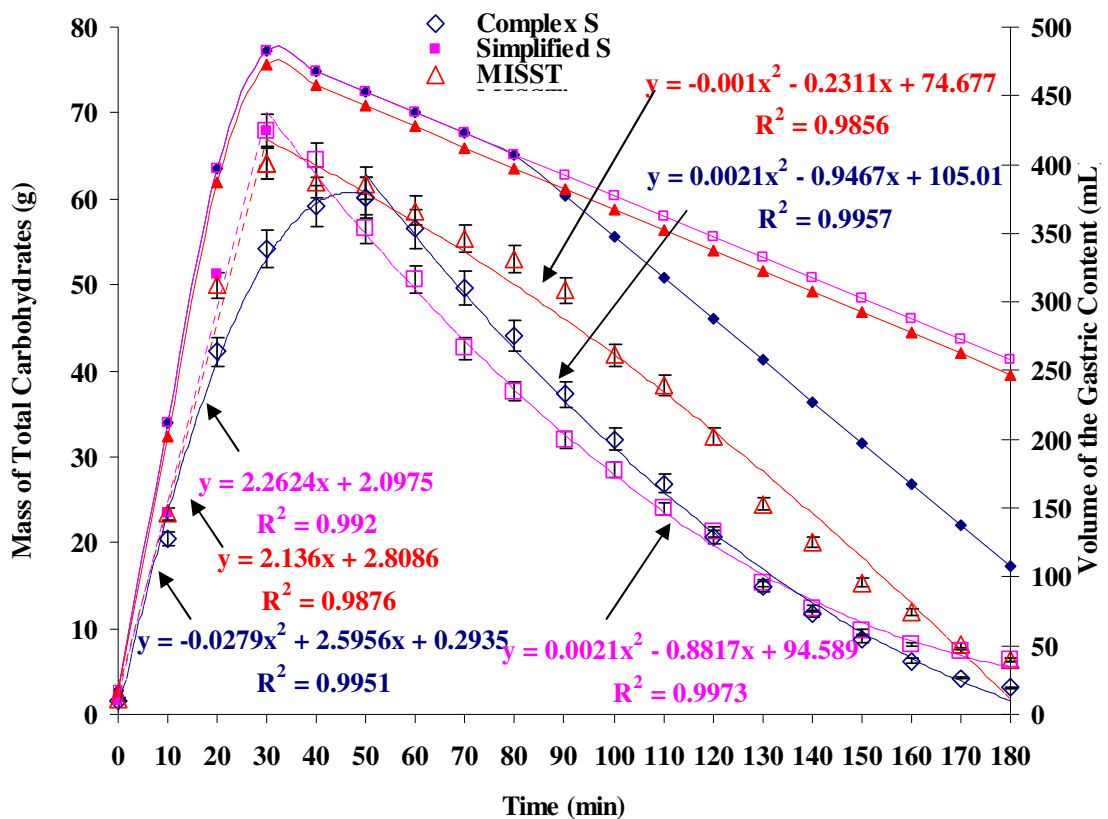


Figure 6-6. A graph showing the concentration of total carbohydrates (g.L^{-1}) during the 3hr digestion time (min). The results obtained from the use of the simplified gastrointestinal (GI) secretions are marked with empty dots in blue, the complex GI compositions in pink and the the simplified GI secretions of the MISST in red. The volumes of the gastric content (mL) for different secretion conditions are shown with filled dots with accordance of color and shape for each condition.

It was expected that the pattern and the rate of digesting the ingested rice meal would be noticeably different between the MISST and the IPUGS as discussed in the previous chapters. However, the values of the MISST are shown in this chapter to evaluate the

overall *in vitro* digestion models in the literature against the new model, IPUGS, including the impact of using different compositions of the secretions. However possible calibration errors from the weight balance when weighing hot cooked rice may have occurred, which seemed to have caused a small difference in the initial total carbohydrates concentrations between the two different compositions used. Although the difference in concentrations of the total carbohydrates in the three conditions varied considerably throughout the experiments, when the masses of the total carbohydrates and the unconverted starch present in the samples were calculated, there was not a substantial difference among the three conditions (Figures 6-6 and 6-9). The fluctuation of the initial values seemed to have risen from the use of small gastric volume (17.5ml) and small volume (5ml) of the samples collected from the model. As the main purpose of the study was to determine and compare different rate and compositions of GI secretions for validation purposes, initial total carbohydrates content can only be used as a reference(control) for the latter data, thus it was decided to only collect the amount (volume) required to conduct analyses. As the initial carbohydrate constituent of rice was mainly starch, the values of the mass of unconverted starch (Figure 6-9) and the values of the mass of the total water soluble carbohydrates were almost the same. It should be noted that the values of the total carbohydrates concentration (g.L^{-1}) have exceeded the total mass of the rice added (100g) and total possible mass of the carbohydrates in the rice (78.5g) as the collected samples were typically of 50ml for simulating the volume gastric content, which have resulted in an arbitrary phenomenon. The total amount (volume) of GI secretions for the complex secretion condition of the IPUGS was higher than the other 2 conditions due to mucosal secretion up to 90min mark, however smaller from 90min to 180min, where the feed-back control was used to simulate the human conditions.

During the ingestion period of up to 30min, there was not a remarkable difference in both the concentrations and the masses of total carbohydrates among the three conditions. They all showed a very sharp and constant increase along with the increase in the volume of the gastric content. All of the models reached their maximal gastric volume by end of the ingestion period, 30min mark, and maximal total carbohydrates concentrations and masses of $139.6 \pm 6.32 \text{g.L}^{-1}$ and $61.8 \pm 3.01 \text{g}$ (MISST), $140 \pm 0.52 \text{g.L}^{-1}$ and $67.9 \pm 1.83 \text{g}$ (simplified composition), $133.0 \pm 0.67 \text{g.L}^{-1}$ and $60.2 \pm 1.67 \text{g}$ (complex composition). However for the complex composition condition, the maximal content of the total carbohydrates was at 50min mark. Physiologically under the normal condition (without any disorders) in the humans, there is not much of the chyme passing from the stomach to the duodenum during the ingestion period and if there is, it would only be liquids (e.g.

water). The samples obtained from the MISST showed a gradient between the solid rice particles and liquid part, whereas the samples obtained from the IPUGS contained no visible solid materials in the samples collected during the ingestion period. It is assumed that the greater curvature of the stomach in the IPUGS allowed the solid particles to be deposited for further digestion. The samples were opaque white in color but not viscous as there was no mucosal secretions for the MISST and the IPUGS with the use of simple composition secretions. However with the complex compositions with the use of mucus, the samples were visibly darker in color, with yellowish green and somewhat light brownish color.

As soon as the meal ingestion ceased, the volume of the gastric content as well as the concentration and the mass of total carbohydrates in the stomach compartment of the MISST and the simple secretion condition of the IPUGS started to decrease. The decrease in the amounts of total carbohydrates was also due to dilution by simulated gastric secretion and gastric emptying (Castela-Papin *et al*, 1999).

The concentration of the MISST showed a slight increase from 30min to 50min, however when considering the volume of the gastric content and the mass of the total carbohydrates, it decreased. For the complex secretion condition, both the concentration and the mass of the total carbohydrates showed a small increase from 30min to 50min interval as well. Despite a sharp linear increase of the total carbohydrates shown in the MISST and the simple secretion condition with the rate of $2.136\text{g}\cdot\text{min}^{-1}$ ($R^2=0.9876$) and $2.2624\text{g}\cdot\text{min}^{-1}$ ($R^2=0.992$), respectively, the complex condition fitted a parabolic function instead, with R^2 value of 0.9951. The gastric secretions were delivered to the stomach constantly, the chyme samples, which were of greater volumes than the volume of the gastric secretion, were also withdrawn at the same time. Thus the volume of the gastric content has decreased over time, and therefore the concentration and the mass of starch in the stomach also decreased over time. At about 45min mark, the values of the concentration and the mass of total carbohydrates for both conditions in the IPUGS showed very similar values, however the trends of decrease were well fitted with parabolic function. When differentiated, both conditions of the IPUGS showed equal gradient of 0.0042. Both of these trends were also able to be fitted with linear function with less R^2 value of about 0.95, referring to the linear trend of gastric emptying which matches with the human clinical studies in the literatures (Schwartz *et al*, 1982; McCallum, 1980 and 1981; Ruby *et al*, 1996). However Yu and Amidon (1998 and 1999) suggested that the gastric emptying can also be described as the first order process.

Around 135min mark, the values of the mass of the total carbohydrates in both IPUGS conditions again coincided. Despite the overall higher range of total carbohydrates mass in the complex secretions when compared to that of the simple secretions, from 135min, the rate of decrease in mass for the simple secretions exceeded that of the complex secretions. This seemed to be due to the reduced rate of complex secretions from the 90min mark, where the rates of chyme removed from the stomach compartment were greater in terms of volumes, thus resulted in a faster drop of the total carbohydrates mass. The overall rate of change in the total carbohydrates during the gastric emptying period, from 30min to 180min, the MISST showed the slowest rate compared to the other conditions in the IPUGS. This seemed to be due to the curvature of the stomach compartment in the IPUGS which allowed the undigested solid rice particles to be deposited for further digestion and let the liquid part to be existed first. The end values of the total carbohydrates for the MISST and the IPUGS were relatively similar to each other, showing a small amount, up to 10g, of carbohydrates left in the stomach. Therefore the complex composition of the GI secretions used in the IPUGS did not significantly affect the transit of the rice meal throughout the experiments. Whitehouse and Temple (1977) reported that the total gastric emptying time for normal healthy subjects took 192 ± 12 min when a balanced meal constituted of carbohydrates, proteins and fat, were fed. The overall rate of gastric emptying seemed to be in accordance with such findings in the literatures.

6.3.2. Somogyi-Nelson Method

The concentration (g.L^{-1}) and the mass of maltose (g) in the stomach compartment of the IPUGS varied considerably from 1 to 18g.L^{-1} and 0 to 16g, respectively, throughout the experiment as illustrated by the Figures 6-7, 6-8 and 6-13. Maltose is a reducing sugar which is a byproduct released during the conversion of amylopectin to amylose and/or amylose converted to a shorter chain of carbohydrate in the process of starch hydrolysis. Hence observing the trend of the concentrations and the masses of maltose in the collected chyme samples over the 3hr digestion period facilitates evaluation of whether the results obtained from the IPUGS are compatible to that of the human conditions. The effect of having different compositions in the digestion processes, in this case, rice starch hydrolysis, can also be investigated and compared to the digestive patterns of the MISST which is representative of the *in vitro* digestion models in the literature. Therefore an

overall evaluation of the IPUGS, in terms of producing more compatible results to human conditions, can be made.

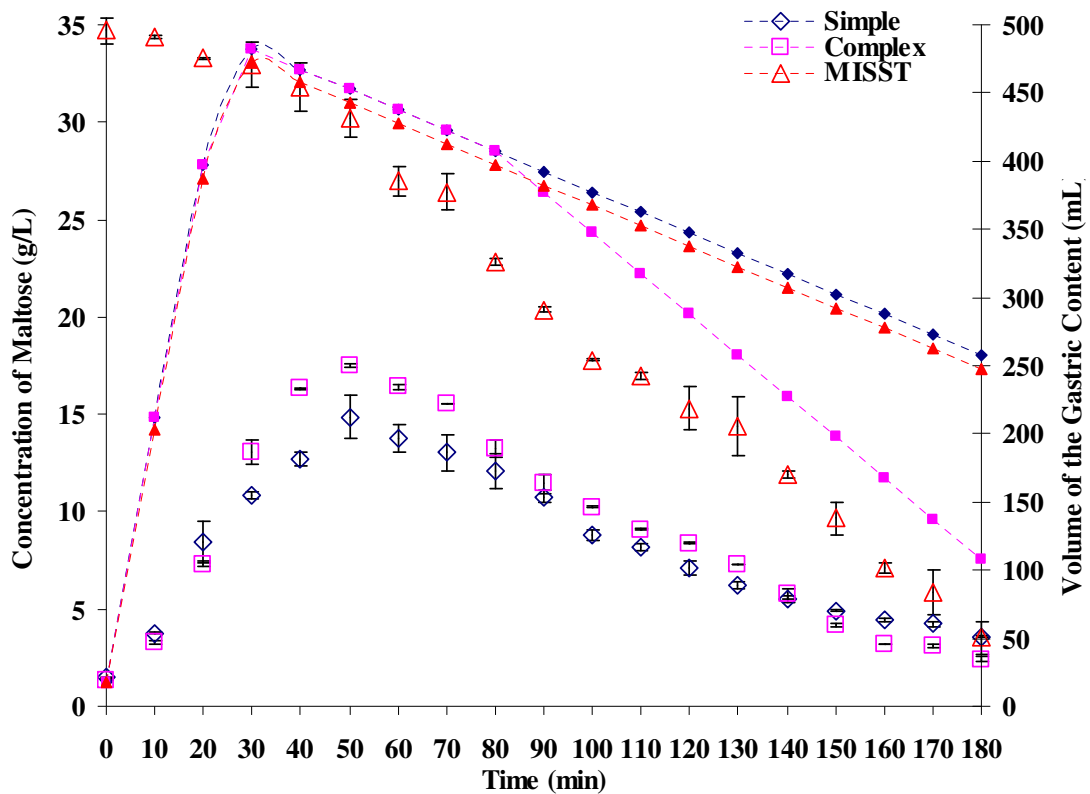


Figure 6-7. A graph showing the concentration of maltose (g.L^{-1}) during the 3hr digestion time (min). The results obtained from the use of the simplified gastrointestinal (GI) secretions are marked with empty dots in blue, the complex GI compositions in pink and the the simplified GI secretions of the MISST in red. The volumes of the gastric content (mL) for different secretion conditions are shown with filled dots with accordance of color and shape for each condition.

Initially, the concentrations of maltose in both simple and complex secretions of the IPUGS showed similar values, $1.47 \pm 0.02 \text{g.L}^{-1}$ and $0.026 \pm 0.001 \text{g}$ and $1.34 \pm 0.02 \text{g.L}^{-1}$ and $0.023 \pm 0.001 \text{g}$, respectively. It should be noted that from 0min mark, salivary amylase secretion began in the mouth compartment for the IPUGS. Thus the rate of rice starch hydrolysis was much slower compared to the MISST, where 5min of pre-digestion period with the use of finely grinded homogenized rice meal facilitated the starch hydrolysis to release maltose in a much faster rate. The initial values of the MISST were $34.7 \pm 0.7 \text{g.L}^{-1}$ and $0.61 \pm 0.02 \text{g}$. The initial mass of maltose in the MISST was more than 20 folds higher than that of the both conditions of the IPUGS. The values of the concentrations and the masses of maltose detected for both of the conditions of the IPUGS were very similar to

the blank (distilled water) when analysed by the UV-photospectrometer and the HPLC (Figures 6-13).

During the ingestion period of up to 30min, the concentrations and the masses of maltose in the simple and complex secretions of the IPUGS conditions showed increasing trend (Krishnakumari and Thayumanavan, 1995) with a cubic function of R^2 values greater than 0.98 for both conditions. The increasing trend must have resulted from the increasing availability of soluble carbohydrates in the stomach compartment which are susceptible to either enzymatic (salivary amylase) or acidic (gastric juice) hydrolysis to produce maltose. Initial rapid increase in the release of maltose could be due to the multiple repetitive random attack mechanism of the amylase where α -1, 4-linkages are randomly attacked and then a number of linkages in the immediate vicinity of the first point of attack are broken down, releasing maltose and maltotriose as observed by Krishnakumari and Thayumanavan (1995). Up to 20min mark, the values of the concentrations and the masses of maltose for both conditions were almost indistinguishable. However the values have started to diverge since 20min, with higher values of both concentrations and the masses for the complex secretions compared to the simple secretions. Unlike the MISST which reached its maximal mass of maltose in the stomach compartment by end of the ingestion period, 30min mark, which was also when the volume of the gastric content was the highest, both of the conditions in the IPUGS reached their maximum values of $14.9 \pm 1.1 \text{g.L}^{-1}$ and $6.7 \pm 0.4 \text{g}$ (simple) and $17.5 \pm 0.1 \text{g.L}^{-1}$ and $7.9 \pm 0.2 \text{g}$ (complex) by 50min mark. It would seem that the greater curvature of the stomach in the IPUGS held back the undigested solid particles for further digestion as the hydrolysis of rice starch carried on even after the gastric emptying initiated. In the MISST, the collected samples contained very fine rice particles and the proportion of the solid to liquid of the collected samples was somewhat greater than that compared to the samples from the IPUGS. The rates of decrease in the concentration and the mass of maltose were much faster for the MISST due to the premature emptying of the undigested solid materials via sampling. When the equations obtained from fitting the cubic function (Figure 6-8) to the mass of maltose with respect to time were differentiated, complex secretions showed a lower gradient value of $-0.0006x^2$ and simple secretions showed a higher value, $-0.00054x^2$, where x refers to time (min). However when the cubic functions are differentiated twice, the rate of change of maltose with respect to time was greater for complex secretions than for simple secretions.

From 50min mark, the concentrations and the masses of maltose started to decrease slowly, and converged to nearly the same value of $9.10 \pm 0.03 \text{g.L}^{-1}$ and $2.89 \pm 0.08 \text{g}$ for complex secretions and $8.15 \pm 0.16 \text{g.L}^{-1}$ and $2.96 \pm 0.11 \text{g}$ for simple secretions by 110min mark. Along with constantly decreasing starch and the gastric volume, it would seem that the amount of maltose decreased together. Also, dilution by the simulated secretions as well as gastric emptying also seemed to play a key role in decreasing trend of maltose in the stomach compartment of both the IPUGS and the MISST (Castela-Papin *et al*, 1999). From 115min, the masses of maltose in both IPUGS conditions started to diverge again, however this time, the masses of maltose in simple secretion condition showed higher values compared to that of the complex conditions.

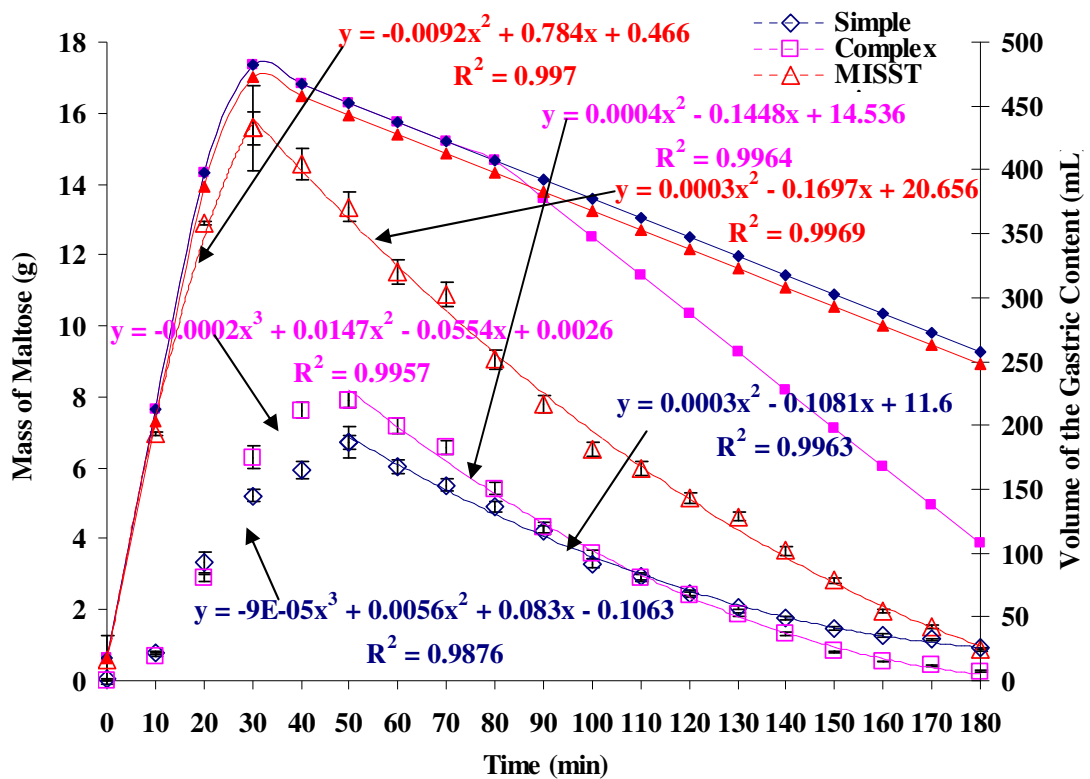


Figure 6-8. A graph showing the mass of maltose (g) during the 3hr digestion time (min). The results obtained from the use of the simplified gastrointestinal (GI) secretions are marked with empty dots in blue, the complex GI compositions in pink and the the simplified GI secretions of the MISST in red. The volumes of the gastric content (mL) for different secretion conditions are shown with filled dots with accordance of color and shape for each condition.

Some literatures argued that as the rice is rich in carbohydrates and carbohydrate portion of the ingested meal is always the fastest to be processed to the next part (duodenum), the transit time of rice can be as short as 2hr. Some literatures also argued that in some cases,

where meat is ingested with the rice (as in most cases of meal consumption, a balanced meal was fed for clinical studies and gastric scintigraphy), the overall digestion took up to 4hr. In order to fully exhibit the effect of all the rice being properly digested, the digestion time of 3hr was chosen. However with the control of secretion and the rate of gastric emptying used for such study, $250\pm 3\text{ml}$ of the fluid remained in the stomach for the MISST and the IPUGS simple secretion, even after the 3hr digestion period. This is due to the absence of feed back control, where the rate of gastric secretion was once set at 3.5ml, which is more representative of the secretion rates at stimulated state, and kept at the same rate till the end of the experiments. This was why the samples collected toward the end of the experiment were very dilute. However with the use of feed-back control for the complex secretion, the final volume of the gastric content was nearly half that of the MISST and the simple secretion condition, $105\pm 3\text{ml}$. This may have biased the value of the maltose mass to be smaller. The change in between the two conditions of the IPUGS was insignificantly different from one another and accounting for the margin of errors in taking measurements, the values of both the concentrations and the masses of maltose in the stomach compartment of the IPUGS were almost the same to one another, throughout the 3hr digestion period. The overall rate of decrease in maltose mass for the complex secretions was somewhat steadier than the simple secretions. The end values of the maltose mass were $0.87\pm 0.14\text{g}$ (MISST), $0.92\pm 0.03\text{g}$ (simple), and $0.26\pm 0.01\text{g}$ (complex). As the conditions and controls of the MISST were more of the ideal situations, where everything was set constant and mechanical, the values obtained seemed to be constant throughout the experiments which are in disagreement with the clinical studies in the literatures (McCallum, 1980 and 1981; Yu and Amidon, 1998).

As illustrated by the Figure 6-9, the trend of unconverted starch mass (g) over time seemed very similar to that of the total carbohydrates (Figures 6-6). The unconverted starch includes unconverted amylopectin and amylose from the rice meal, partially hydrolyzed long and mid chain carbohydrates such as dextrans, maltohexose, maltopentose and maltotetraose. The simple secretions of the IPUGS reached peak unconverted mass value of $59.1\pm 0.5\text{g}$ at 30min which was the time of maximal mass of total carbohydrates and the volume of the gastric content. However for the complex secretions of the IPUGS, the peak value was obtained at 50min mark, with was when the mass of total carbohydrates was at maximum but the volume of the gastric content has started to decrease. The values of the MISST especially during the ingestion period were much smaller compared to both of the conditions in the IPUGS. This seemed to be caused

by the use of homogenized rice meal where the rate of rice starch hydrolysis was expected to be higher.

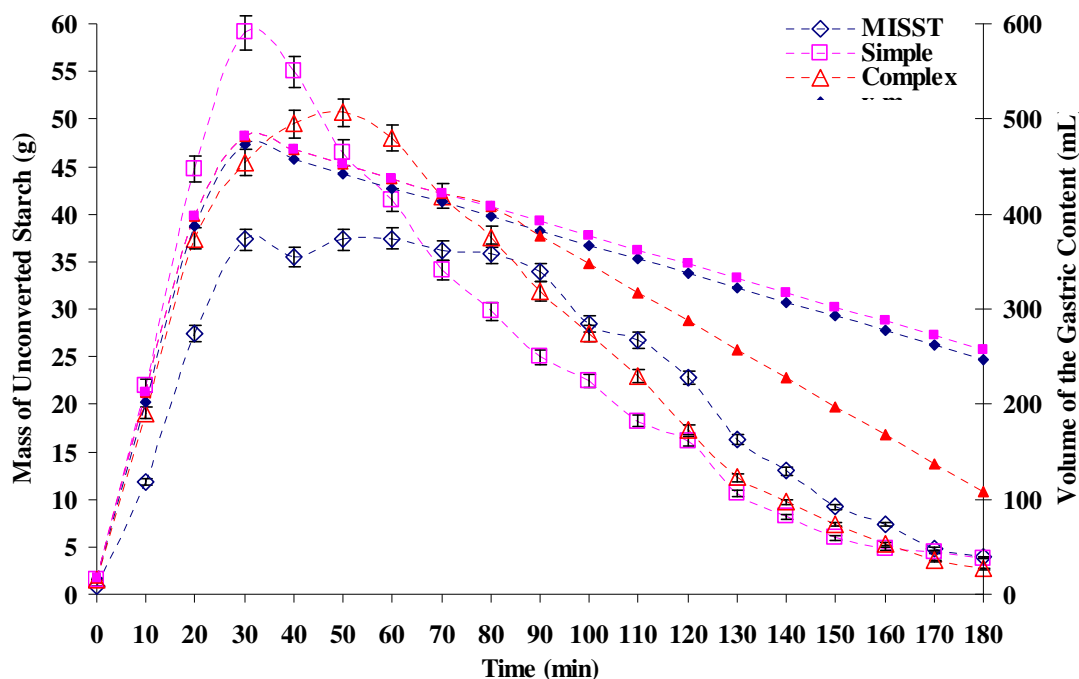


Figure 6-9. A graph showing the mass of unconverted starch (g) during the 3hr digestion time (min). The results obtained from the use of the simplified gastrointestinal (GI) secretions with the MISST are marked with empty dots in blue, the simple GI compositions of the IPUGS in pink and the the complex GI secretions in red. The volumes of the gastric content (mL) for different secretion conditions are shown with filled dots with accordance of color and shape for each condition.

Although the differences in the amounts of the total carbohydrates, unconverted starch and maltose have shown clear differences, a better understanding of the rice starch hydrolysis was attained when the ratio of the mass of maltose to the mass of unconverted starch, was plotted (Figure 6-10). The ratio of maltose to unconverted starch is an important indication to how much of amylopectin and amylose were hydrolyzed to release the reducing sugar, maltose. As the initial mass and concentration of maltose were nearly zero, and larger than the initial mass and concentration of unconverted starch, the ratio was also nearly zero. The ratio of maltose to unconverted starch showed increasing trend, with indistinguishable values between the two conditions up to 20min mark. However from 30min mark, the ratio of maltose to unconverted starch of the complex secretion condition exceeded that of the simple secretion condition. From 50 to 70min, the values of the ratio were nearly the same again. Between 80 and 180min, the values of the ratios for both conditions in the IPUGS fluctuated noticeably, with increasing values of the ratio for the simple secretions and decreasing values of the ratio for the complex

secretion. Thus, the values of the ratio were higher in the simple secretion condition compared to that of the complex condition, with end values of 0.24 and 0.10, respectively. The pattern of the ratio of maltose to unconverted starch in the MISST was totally different to that of the IPUGS. The initial value of the ratio started from 0.7, and decreased rapidly during the first 60min. From 60min to 120min, the ratio decreased as well, but at a slower rate. From 120min to 170min, the ratio increased slightly from 0.23 to 0.32, followed by a sudden drop to 0.22 at 180min. The results indicate that using of comprehensive secretions did not affect the efficiency of starch hydrolysis significantly.

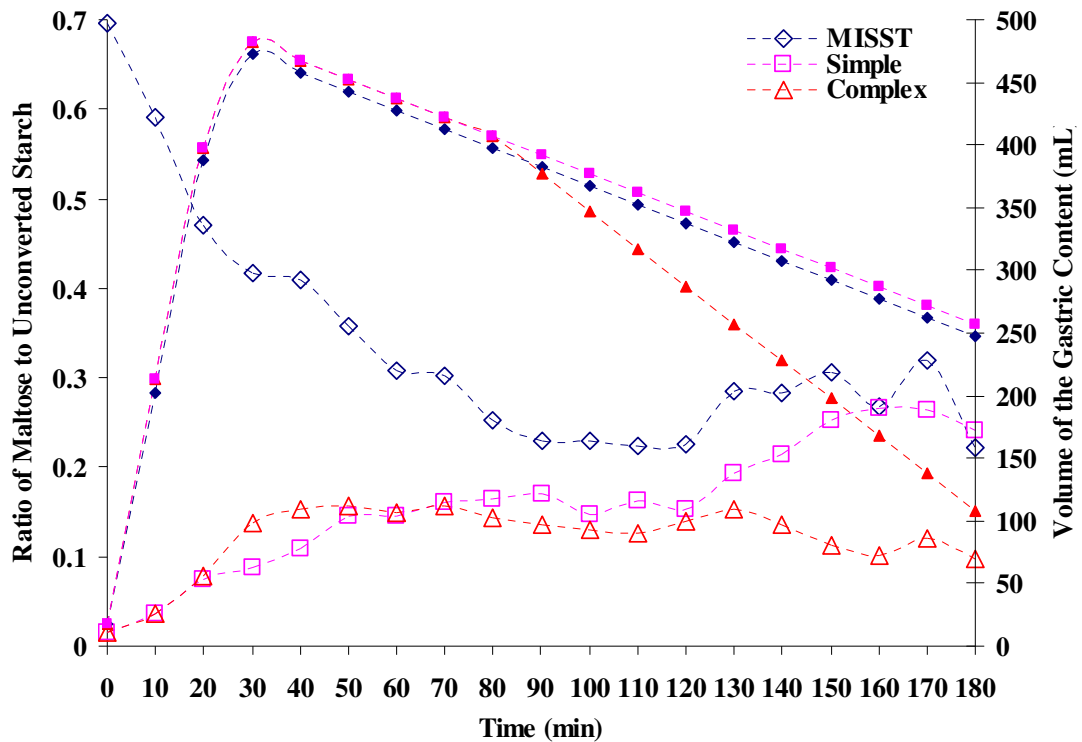


Figure 6-10. A graph showing the ratio of the mass of maltose to the mass of the unconverted starch during the 3hr digestion time (min). The results obtained from the use of the simplified gastrointestinal (GI) secretions of the MISST are marked with empty dots in blue, the simplified GI compositions of the IPUGS in pink and the the complex GI secretions of the IPUGS in red. The volumes of the gastric content (mL) for different secretion conditions are shown with filled dots with accordance of color and shape for each condition.

Gastric pH after ingestion of the cooked rice decreases slowly. The meal is gradually delivered from the stomach and thus portions of the meal escape exposure to low pH and consequently to amylase, acidification and peptic activity. The gradual delivery of the meal can be described by mathematical equations to calculate the cumulative amount of meal delivered in time, expressed as a percentage of intake (Decuyper *et al*, 1986;

Elashoff *et al*, 1982). Liquids and semi-liquids show an exponential gastric delivery pattern, while solids have a more linear pattern of gastric delivery (Novitol *et al*, 1984). To obtain a realistic gastric delivery of the meal, especially when there are particles in the meal, the sieving activity of the pylorus should be simulated well.

6.3.3. High Performance Liquid Chromatography (HPLC)

Using the HPLC, an overall screening of the collected samples was made to clarify the presence of maltose and to identify the possible byproducts of the rice starch hydrolysis. As a result, maltose (Figure 6-11) and maltotriose (Figure 6-12) were detected. The starch hydrolysis in the normal human subjects usually do not result in glucose, as the partially unconverted starch as well as maltose are further digested by pancreatic α -amylase in the small intestines.

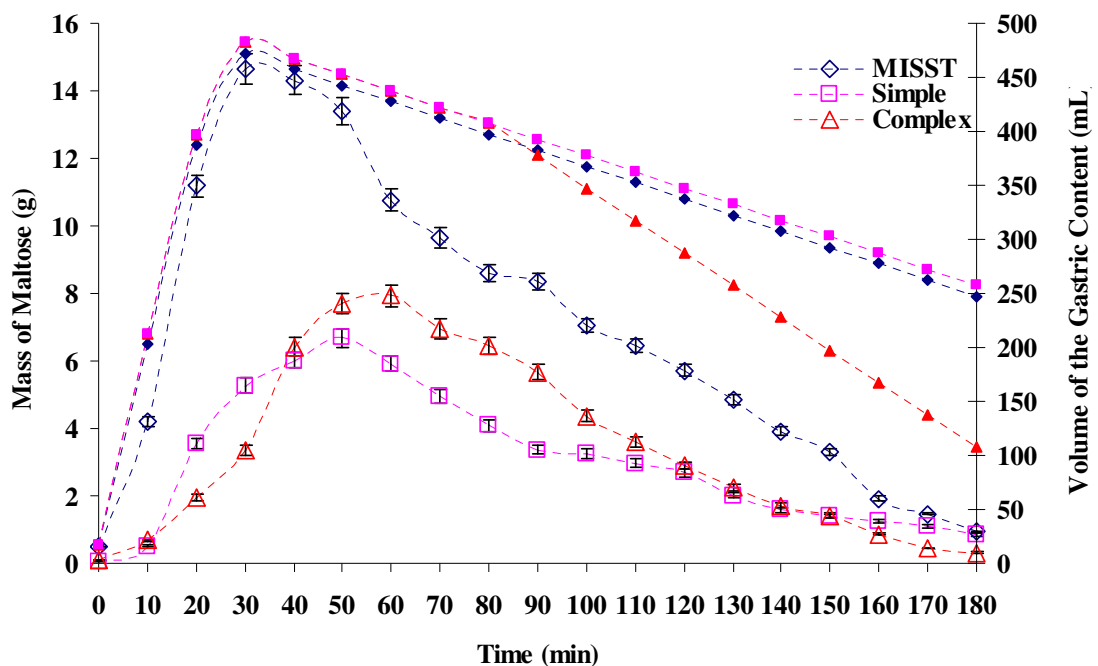


Figure 6-11. A graph showing the mass of maltose measured by HPLC. The results obtained from the use of the simplified gastrointestinal (GI) secretions of the MISST are marked with empty dots in blue, the simplified GI compositions of the IPUGS in pink and the the complex GI secretions of the IPUGS in red. The volumes of the gastric content (mL) for different secretion conditions are shown with filled dots with accordance of color and shape for each condition.

In general, the mass of maltose analyzed from the HPLC showed slightly lower values compared to that of the UV-spectrophotometer for the simple secretion of the IPUGS and the MISST. For the complex secretion of the IPUGS, the values of maltose mass were slightly higher since the ingestion period. The variations in between the two measurements seemed to be caused by the waiting period of the samples collected from the models until the analysis. Although the samples were kept in an ice water bath, and diluted accordingly to a factor of 40, some samples had to wait over 10hrs until the analysis began. However the standing time at room temperature for the UV-spectrophotometric measurements was much shorter when compared to that of the HPLC. Also after dilutions, the samples were chemically treated with arseno and Somogyi reagents, where there were no treatments for the HPLC samples. Even with the use of the shortest column to examine the sample in the HPLC, it took 15-30min, as the HPLC column requires cleaning time to avoid any blockage and accumulation of carbohydrate molecules which may cause interference amongst the samples for analyses. As many of the samples were kept in the auto-sampler at room temperature overnight, it might have caused a further digestion, most likely to be acidic hydrolysis, during the waiting period to be analyzed. In spite of this, the overall trend of the maltose mass was very similar to that found using the UV-spectrophotometer.

Maltotriose concentration was detected by the HPLC. In order to avoid any arbitrary confusions, the obtained values of the concentration (g.L^{-1}) were converted to the mass of maltotriose present (g) (Figure 6-12) by multiplying the gastric content volume to the concentration. The highest mass of maltotriose was again, resulted by the MISST, $9.67 \pm 0.03\text{g}$, due to the use of finely ground rice meals. The mass of maltotriose with both types of secretions increased exponentially during the ingestion period of up to 30min. The maximum mass was $3.58 \pm 0.02\text{g}$ at 40min. However with the use of the complex secretions, the maximum mass of maltotriose was reached at 30min mark, with lesser amount, $2.42 \pm 0.02\text{g}$. A gradual decrease in the mass of maltotriose for both types of secretions was observed, with slightly faster rate with the use of the complex secretions. The end values of the MISST and the simplified secretion condition were almost undistinguishable, $1.55 \pm 0.02\text{g}$ and $1.65 \pm 0.02\text{g}$, respectively. However with the use of complex secretion, the end value was much lower, $0.14 \pm 0.02\text{g}$, which seemed to be caused by smaller volume of the gastric content present in the stomach compartment at the end of the experiments. Overall, the trend of the mass of maltotriose over time was not similar to that of the mass of maltose and the difference in mass between both types of secretion conditions used was relatively small.

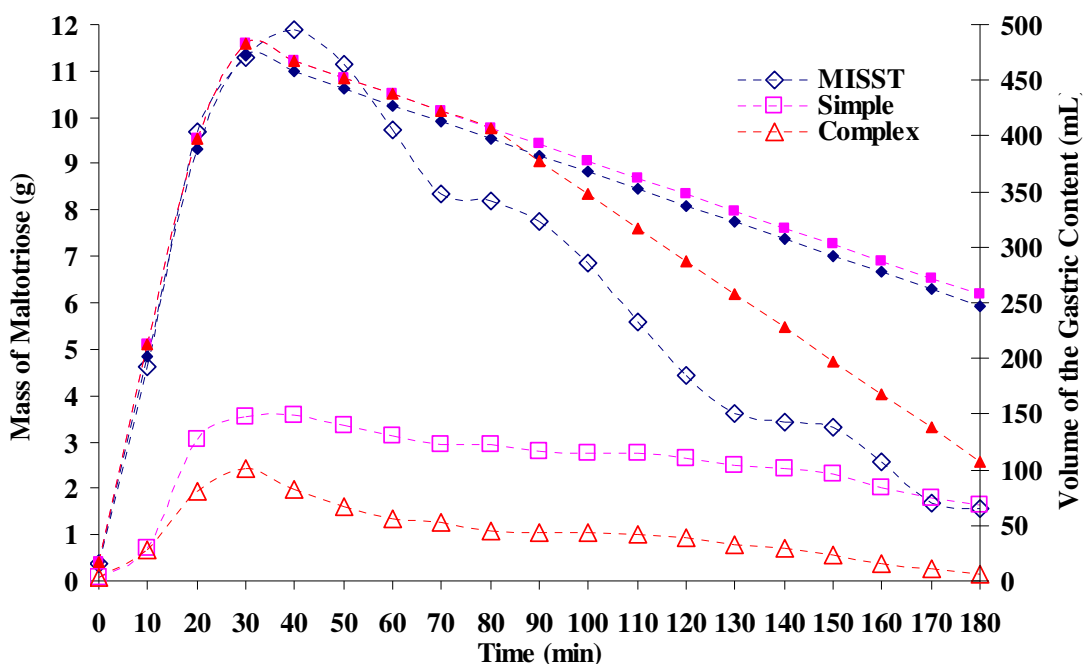


Figure 6-12. A graph showing the mass of maltotriose measured by HPLC. The results obtained from the use of the simplified gastrointestinal (GI) secretions of the MISST are marked with empty dots in blue, the simplified GI compositions of the IPUGS in pink and the the complex GI secretions of the IPUGS in red. The volumes of the gastric content (mL) for different secretion conditions are shown with filled dots with accordance of color and shape for each condition.

6.3.4. Recording of pH profile

The overall trend of the pH profile over the 3hr digestion period was similar to one another for the simple and comprehensive compositions of the GI secretions used by the IPUGS. The measure of the pH profile is one of the simplest analyses which directly indicate the conditions of the stomach and it is of extreme importance as it is able to detect even minor changes of the gastric conditions which may not have been seen via the analyses through the UV-photospectrometer and the HPLC. The pH profile is one of the widely used tools to indicate the feasibility of an *in vitro* testing method, especially for clinical studies such as the interaction of drug and the gastric secretions, disintegration of coating materials and capsules, and possible interference of more than one type of drug taken at the same time. The pH profile is able to emphasize the overall control of motility as well as secretions applied, and in conjunction with results from the Phenol-Sulfuric acid assay, the Somogyi-Nelson method and the HPLC, a better understanding of the

effect of motility can be perceived. The initial pH values of the both secretion conditions largely reflect the pH of the gastric secretion, which fell in the range of 1.03 ± 0.01 . Two probes were used for measuring the pH of the stomach compartment of the IPUGS. Figure 6-13 shows the pH profile of the fundus (probe 1) of the stomach compartment which is the site of major acidic gastric juice delivery, whereas Figure 6-14 shows the pH profile of the antrum (probe 2) of the stomach compartment where mucosal secretions take place. Theoretically, the pH profile of the probe 1 should be slightly more acidic than the probe 2, which corresponded well with the obtained results. A rapid increase in pH during the ingestion period of up to 25min was seen for both of the conditions in the IPUGS as illustrated by Figure 6-11. Buffering capacity of the ingested rice meal was clearly shown in both conditions, where additional mucosal secretion of the comprehensive secretion composition produced a higher buffering capacity with the peak pH of 3.43 ± 0.22 around 25min. With simplified composition of the GI secretions, the pH reached maximum of 3.04 ± 0.06 around 25min. Compared to both of the secretion conditions of the IPUGS, the maximal pH reached by the MISST was only 2.12 ± 0.02 which did not demonstrate a good buffering capacity. The rate of increase in pH during the ingestion period was about 0.2 over the first 10min, which was noticeably lower than that of the results of the IPUGS. It would seem that the grater curvature of the IPUGS was able to hold the non-digested rice grains from slipping through the pylorus and due to this geometrical enhancement of the model, the buffering capacity of the ingested meal has prolonged a bit longer compared to the MISST.

However the values of the gastric pH of the MISST and both of the conditions in the IPUGS have started to decrease immediately after the meal delivery has stopped. The rate of decrease in pH was the fastest for the comprehensive composition of GI secretions used by the IPUGS, which showed pH decrease of 0.044 per min, from 25min to 50min. With the simplified composition of the IPUGS, the rate of decrease was slower, $0.034 \cdot \text{min}^{-1}$ between 30min and 60min, and the MISST showed the slowest rate of $0.017 \cdot \text{min}^{-1}$ between 30min and 60min. By the end of the first hr of digestion, the pH values of the fundus were 2.10 ± 0.14 (comprehensive) and 1.93 ± 0.10 (simplified) and 1.63 ± 0.03 for the overall gastric pH of the MISST. Up to 120min, a gradual decreasing trend of pH in the fundus of the IPUGS and the gastric pH of the MISST showed constant decrease, with the comprehensive secretion compositions used by the IPUGS showing the highest values of pH, followed by the simplified composition of the IPUGS and the MISST showing the lowest values. As rice is rich in starch but deficient in proteins and fats, the buffering capacity is relatively low compared to other types of foods containing

meat. Along with mucosal secretion from the gastric wall and continuous motility of 3cycles/min performed, the mucus covered around the bolus, enhancing a buffering effect. Thus a prolonged buffering effect was noticeably shown over the ingestion period. The rate of decrease in pH seemed very constant for all three conditions, where the values of $0.0080.\text{min}^{-1}$ for the MISST, $0.0065.\text{min}^{-1}$ for the simple and $0.0087.\text{min}^{-1}$ for the comprehensive secretion of the IPUGS were observed between the first and the second hr of the digestion period. However the rate of decrease slowed down even further for the last one hr of the digestion period to $0.0017.\text{min}^{-1}$ for the MISST, $0.0045.\text{min}^{-1}$ for the simple and $0.0032.\text{min}^{-1}$ for the comprehensive secretion of the IPUGS.

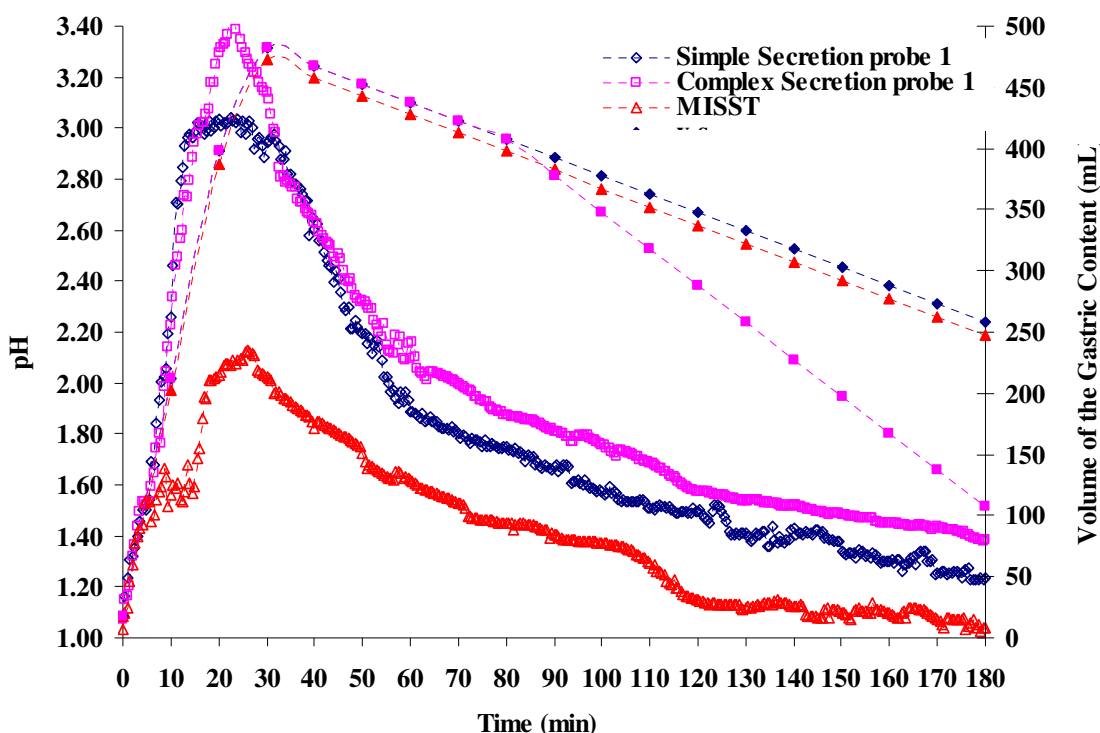


Figure 6-13. The pH profile of the pH probe 1 (fundus) over 3hr digestion period. The results obtained from the use of the simplified gastrointestinal (GI) secretions are marked with empty dots in blue, the complex GI compositions in pink and the the simplified GI secretions of the MISST in red. The volumes of the gastric content (mL) for different secretion conditions are shown with filled dots with accordance of color and shape for each condition.

Small changes in the pH profile of the GI are able to affect dosage form performance, drug dissolution and absorption. Continuous recording of pH by Heidelberg capsule allowed to characterize peaks and fluctuations in pH and to follow the functional form of the rate of return to baseline after a meal (Dressman *et al*, 1990). Dressman *et al* (1990) used a 6oz of hamburger, 2lices of bread, 2oz of hash brown potatoes, 1tbsp each of

ketchup and mayonnaise, 1oz each of tomato and lettuce and 8oz of milk (for a total of 1000Kcal) for a standard meal. A very high buffering effect of the ingested food was shown. The overall median fasting pH was 1.7 with an interquartile range of pH 1.4-2.1. During the meal, the pH increased to a median value of 5.0 with an interquartile range of pH 4.3-5.4. The peak value ranged from 6.4 to 7.0 (Dressman *et al*, 1990). The fasting gastric pH was approximately 2, which was maintained 68% of time, and below pH 3 90% of the time. In young healthy volunteers, pH above 4 was evident about 6% of time. When the standard meal was homogenized, its pH was 5.72. Other meals with lower pH fluids such as coffee, soft drinks, fruit juices may not buffer the gastric pH to as high as a peak pH. During meal ingestion, the pH was above pH 4 73% of time, above pH 5 45% of time and above pH 6 20% of time. The time taken to ingest the meal was between 12min and 30min for all subjects. The peak pH usually occurred within the first 5min of eating. Almost no gender difference in gastric pH was seen (Dressman *et al*, 1990).

After ingestion of a meal, gastric pH is distinctly but briefly elevated in spite of increased gastric acid secretion, which is attributed to the diluting and buffering effect of the ingested food components. After gastric emptying occurs, the gastric pH gradually declines until the fasted state pH has been reestablished. The decline in gastric pH is a function of both the ability of the meal to stimulate gastric acid secretion and the rate at which the meal is emptied from the stomach. Few studies have measured gastric pH after ingestion of relatively normal solid/liquid meals (Malagelada *et al*, 1976; Dressman *et al*, 1990). When a standard meal of ground steak, bread, butter, vanilla ice cream with chocolate syrup and water (458Kcal) (Malagelada *et al*, 1976), the pH of the gastric contents was ~5.0, reflecting both the dilution and buffering effects of the meal. 60min after the meal ingestion, the pH had fallen to less than 3.0, and after 120min, the pH had returned to less than 2.0. In a similar manner, Dressman *et al* (1990) who fed hamburger, bread, hash brown potatoes and milk (1000Kcal), the gastric pH during the meal increased to 5.0 with the highest recorded pH of 6.7 which occurred within the first 5mins of eating. It took 11 ± 10 min to return to pH 5, 28 ± 24 mins to return to pH 4, 56 ± 41 mins to return to pH 3 and 107 ± 70 min to return to pH 2. Similar pH profiles were observed in healthy elderly subjects, with median pH during the meal of 4.9, with a peak pH of 6.2. However the time required for gastric pH to return to 2.0 was significantly longer when compared with the younger subjects (Charman *et al*, 1997).

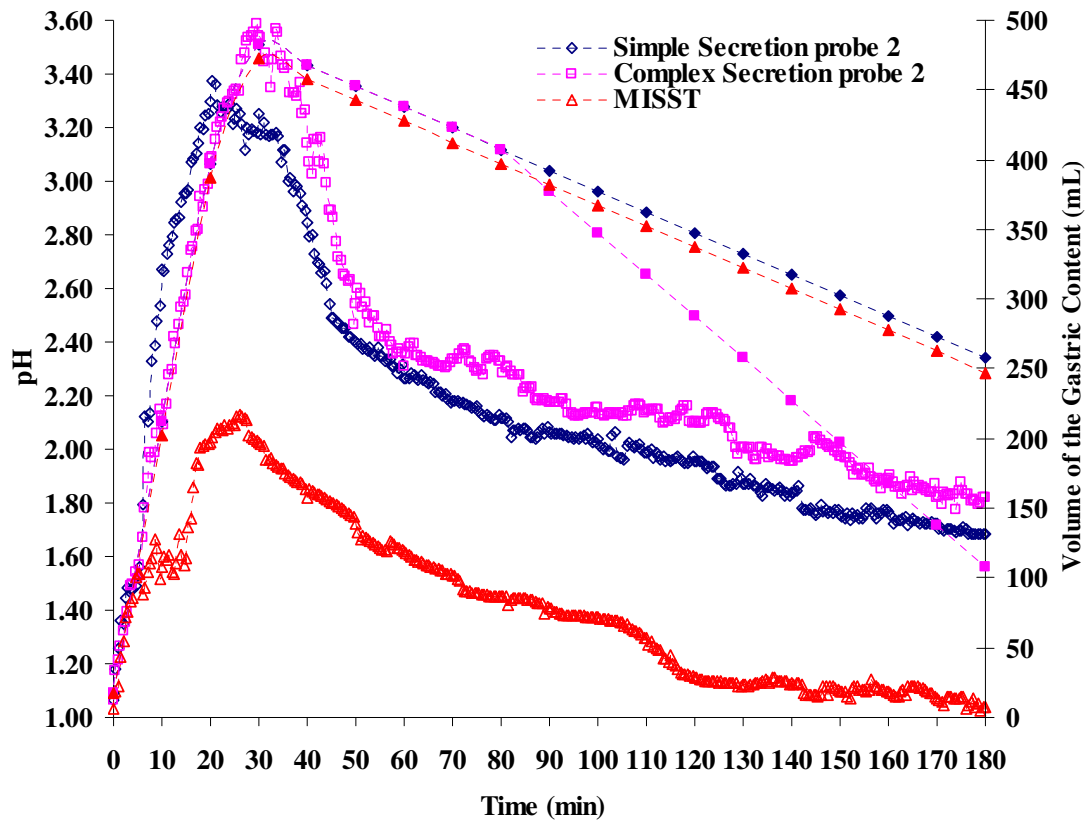


Figure 6-14. The pH profile of the pH probe 2 (antrum) over 3hr digestion period. The results obtained from the use of the simplified gastrointestinal (GI) secretions are marked with empty dots in blue, the complex GI compositions in pink and the the simplified GI secretions of the MISST in red. The volumes of the gastric content (mL) for different secretion conditions are shown with filled dots with accordance of color and shape for each condition.

The pH profiles of the MISST and the IPUGS from the pH probe 2, which was implanted in the wall of the antrum of the IPUGS, are illustrated in the Figure 6-12. The trend in change of pH over time was very similar to that of what was found in the fundus of the stomach by the probe 1 (Figure 6-13). As the antrum is where mucosal secretion is largely taking place and the ingested meal is temporarily held for further digestion with the gastric juice. Thus, slightly elevated level of the pH resulted over the 3hr digestion period compared to that of the probe 1 in the fundus. Only one pH probe was used for the MISST as the space was limited.

Rapid increase in pH values was observed in both conditions of the IPUGS. However the time taken to reach the peak pH values differed from one another. For the use of the simplified composition of the IPUGS, the peak value was $\text{pH } 3.37 \pm 0.08$ at 20min, which was before the ingestion period had ceased. The use of comprehensive composition

showed the peak pH of 3.59 ± 0.08 at 25min, which corresponded with the time of the maximal pH in the probe 1. Up to 50min, the comprehensive composition showed the highest pH range compared to the other two conditions, demonstrating higher pH values for longer period of time due to the buffering capacity of the meal as well as the mucosal secretion. The shape of the pH profile was found to be different to some extent when compared to the probe 1. The range of pH values for the complex secretion showed small fluctuations throughout the experiments, although the values remained the highest among the three conditions. The values of the pH for the complex condition was slightly larger than that of the simple condition, and the values obtained from the MISST showed distinctively lower values of pH when compared to the IPUGS. The end pH values of 1.82 ± 0.06 and 1.68 ± 0.04 were seen for the complex and the simple secretion compositions, respectively.

6.4. Conclusions

In this chapter, the effect of varying the constituents of the GI secretions was studied using the IPUGS. The complex secretion containing the digestive enzymes of non-human sources, which was supplemented with ionic constituents, did not demonstrate a significantly different outcome in terms of rice starch hydrolysis and pH change during the 3hr digestion period. It would seem that as the main constituent of the rice is starch, which has up to 78.5wt% of carbohydrates in total, the other digestive enzymes used, such as lipases and pepsins, did not affect the starch hydrolysis process significantly enough. However slightly faster rate of starch conversion may have resulted from either lipases or pepsins, which digested the macronutrients other than the carbohydrates to make the partially digested rice more susceptible to the action of salivary amylase and hydrochloric acid in the gastric secretion. This may have resulted from ionic interactions between the organic and inorganic salts in the secretions. Mucosal secretions played a key role in providing an elevated level of buffering effect to the stomach compartment of the IPUGS throughout the experiment. As shown in chapter 4, motility patterns applied to the IPUGS and the MISST resulted in a prominent change between the two models. Together with the effect of secretions and the motility, the results obtained from the MISST were incompatible with the IPUGS. The MISST, which is an integrated version of the existing *in vitro* digestion models in the literature, was unable to reproduce the pH profile, gastric emptying pattern as well as the appropriate pattern and rate of rice starch hydrolysis when compared to the *in vivo*/clinical data obtained from humans in the literature. With the use

of enzyme sources from the humans, closer mimicking of the human digestive processes is possible with the IPUGS, however the cost of operation should also be noted as these enzymes cost at least 10 times more per each type of the digestive enzymes when compared to non-human sources such as animal, fungal or bacterial. With the use of enzyme sources from the humans, closer mimicking of the human digestive processes would be possible with the IPUGS. In the future, a variety of balanced meals should be tested to fully examine the key role and efficiency of each type of digestive enzymes as this would clarify whether the constituents of the GI secretions do not affect the extent and the rate of digestion significantly.

6.5. References

www.biochem.ucl.ac.uk/bsm/enzymes/ec3/ec01/ec01/ec0003.html

- Abrams, C. K., Hamosh, M., Hubbard, V. S., Dutta, S. K., Hamosh, P. (1984) Lingual lipase in cystic fibrosis. *J. Clin. Invest.*, 73, 374-382
- Akin, A. (1998) Non-invasive detection of spike activity of the stomach from cutaneous EGG. PhD Thesis Drexel University, Philadelphia
- Alexandropoulou, I., Komaitis, M., Kapsokefalou, M. (2006) Effects of iron ascorbate, meat and casein on the antioxidant capacity of green tea under conditions of in vitro digestion. *Food Chemistry*, 94, 359-365
- Allen, A., Pain, R. H., Robson, T. R. (1976). Model for the structure of the gastric mucous gel. *Nature*, 264, 88-89
- Allen, A. (1989). *Handbook of Physiology - The Gastrointestinal Physiology. Salivary, Gastric and Hepatobiliary Secretions, Section 6, Vol. III* (Forte, J. G. ed.), pg. 359-382, American Physiological Society, Bethesda, MD
- Allerscher, H. D., Abraham-Fuchs, K., Dunkel, R. E., Classen, M. (1998) Biomagnetic 3-Dimensional spatial and temporal characterization of electrical activity of human stomach. *Digestive diseases and sciences*, 43 (4), 683-693
- Al-Zaben, A., Chandrasekar, V. (2005). Effect of esophagus status and catheter configuration on multiple intraluminal impedance measurements. *Physiol. Meas.*, 26, 229-238
- Armand, M., Pasquier, B., André, M., Borel, P., Senft, M., Peyrot, J., Salducci, J., Portugal, H., Jaussan, V., Lairon, D. (1999) Digestion and absorption of 2 fat emulsions with different droplet sizes in the human digestive tract. *Am. J. Clin. Nutr.*, 70, 1096-1106
- Atuma, C., Strugala, V., Allen, A., Holm, L. (2001). The adherent gastrointestinal mucus gel layer: thickness and physical state in vivo. *Am. J. Physiol. Gastrointest. Liver Physiol.*, 280, G922-G929
- Avantaggiato, G., Havenaar, R., Visconti, A. (2003) Assessing the zearalenone-binding activity of adsorbent materials during passage through a dynamic in vitro gastrointestinal model. *Food and Chemical Toxicology*, 41, 1283-1290
- Bansil, R., Stanley, H. E., La Mont, J. T. (1995). Mucin Biophysics. *Annu. Rev. Physiol.*, 57, 635-657
- Bansil, R., Turner, B. S. (2006). Mucin structure, aggregation, physiological function and biomedical applications. *Current Opinion in Colloid & Interface Science*, 11, 164-170
- Barker, M. C., Cobden, I., Axon, A. T. (1979). Proximal stomach and antrum in stomach emptying. *Gut*, 20, 309-311
- Bell, A. E., Allen, A., Morris, E. R., Ross-Murphy, E. R. (1984). Functional interactions of gastric mucus glycoprotein. *Int. J. Macromol.*, 6, 309-315

- Bell, A. E., Sellers, L. A., Allen, A., Cunliffe, J., Morris, E. R., Ross-Murphy, S. B. (1985). Properties of duodenal mucus: effect of proteolysis, disulfide reduction, bile acid, ethanol and hypertonicity on mucus gel structure. *Gastroenterology*, 88, 269-280
- Bhaskar, K. R., Gong, D., Bansil, R., Pajevic, S., Hamilton, J. A., Turner, B. S., La Mont, J. T. (1991). Profound increase in viscosity and aggregation of pig gastric mucin at low pH. *Am. J. Physiol.*, 261, G827-G832
- Bhaskar, K. R., Garik, P., Turner, B. S., Bradley, J. D., Bansil, R., Stanley, H. E., La Mont, J. T. (1992). Viscous fingering of HCl through gastric mucin. *Nature*, 360, 458-461
- Björck, I., Granfeldt, Y., Liljeberg, H., Tovar, J., Asp, N. G. (1994) Food properties affecting the digestion and absorption of carbohydrates. *Am. J. Clin. Nutr.*, 59 (Suppl.), 699S-705S
- Blanquet, S., Zeijdner, E., Beyssac, E., Meunier, J. P., Denis, S., Havenaar, R., Alric, M. (2004) A dynamic artificial gastrointestinal system for studying the behavior of orally administered drug dosage forms under various physiological conditions. *Pharma. Res.*, 21 (4), 585-591
- Carlsen, M., Spohr, A. B., Nielsen, J., Villadsen, J. (1996) Morphology and physiology of an α -amylase producing strain of *aspergillus oryzae* during batch cultivations. *Biotechnol. Bioengineering*, 49, 266-276
- Cao, X., Bansil, R., Bhaskar, K. R., Turner, B. S., LaMont, J. T., Niu, N., Afdhal, N. (1999). pH-dependent conformational change of gastric mucin leads to sol-gel transition. *Biophysical Journal*, 76, 1250-1258
- Castela-Papin, N., Cai, S., Vatier, J., Keller, F., Souleau, C.H., Farinotti, R. (1999) Drug interactions with diosmectite: a study using the artificial stomach-duodenum model. *International Journal of Pharmaceutics*, 182, 111-119
- Chahinian, H., Snabe, T., Attias, C., Fojan, P., Petersen, S. B., Carrière, F. (2006) How gastric lipase, an interfacial enzyme with a Ser-His-Asp catalytic triad, acts optimally at acidic pH. *Biochemistry*, 45 (3), 993-1001
- Charman, W. N., Porter, C. J. H., Mithani, S., Dressman, J. B. (1997). Physicochemical and physiological mechanisms for the effects of food on drug absorption: The role of lipids and pH. *J. Pharmaceutical Sciences*, 86 (3), 269-282
- Charteris, W., Kelly, P. M., Morelli, L., Collins, J. K. (1998) Ingredient selection criteria for probiotic microorganisms in functional dairy foods. *Int. J. Dairy Technol.*, 51 (4), 123-136
- Coles, L. T., Moughan, P. J., Darragh, A. J. (2005) In vitro digestion and fermentation methods, including gas production techniques, as applied to nutritive evaluation of foods in the hindgut of humans and other simple-stomached animals. *Animal Feed Science and Technology*, 123/124, 421-444
- Decuypere, J. A., Denhooven, R. M., Henderickx, H. K. 1986. Stomach emptying of milk diets in pigs. A mathematical model allowing description and comparison of the emptying pattern. *Archives of Animal Nutrition*, 36, 679-696
- Desai, M. A., Vadgama, P. (1991). Estimation of effective diffusion coefficients of model solutes through gastric mucus: assessment of a diffusion chamber technique based on spectrophotometric analysis. *Analysis*, 116, 1113-1116
- DeSesso, J. M., Jacobson, C. F. (2001). Review: Anatomical and physiological parameters affecting gastrointestinal absorption in humans and rats. *Food & Chem. Toxicology*, 39, 209-228
- De Zwart, I. M., Mearadji, B., Lamb, H. J., Eilers, P. H. C., Masclee, A. A. M., De Roos, A., Kunz, P. (2002). Gastric motility: comparison of assessment with real-time MR imaging or barostat measurement - initial experience. *Radiology*, 224, 592-597
- Dominy, N.J., Davoust, E., Minekus, M. (2004) Adaptive function of soil consumption: an in vitro study modeling the human stomach and small intestine. *The Journal of Experimental Biology*, 207, 319-324
- Dressman, J. B., Berardi, R. R., Dermentzoglou, L. C., Russel, T. L., Schmaltz, S. P., Barnett, J. L., Jarvenpaa, K. M. (1990). Upper gastrointestinal (GI) pH in young, healthy men and women. *Pharmaceutical Research*, 7 (7), 756-761
- Dubois, M., Gilles, K., Hamilton, J. K., Rebers, P. A., Smith, F. (1951). A colorimetric method for the determination of sugars. *Nature*, 168, 167
- Dubois, M., Gilles, K., Hamilton, J. K., Rebers, P. A., Smith, F. (1956). Colorimetric method for the determination of sugars and related substances, *Anal. Chem.*, 28, 350-356
- Edgar, W. M. (1990). Saliva and dental health. *British Dental Journal*, 169 (3-4), 96-98
- Elashoff, J. D., Reedy, T. J., Meyer, J. H. (1982). Analysis of gastric emptying data. *Gastroenterology*, 83, 1306-1312

- Fatouros, D. G., Bergenstahl, B., Mullertz, A. (2007). Morphological observations on a lipid-based drug delivery system during in vitro digestion. *European J. Pharm. Sci.*, 31, 85-94
- Fleming, A., Allison, V. D. (1922) Observations on a bacteriolytic substance (lysozyme) found in secretions and tissues. *Br. J. Exp. Pathol.*, 252-260
- Flemström, G. (1987). Gastric and duodenal mucin bicarbonate secretion. In physiology of the gastrointestinal tract, 2nd ed. L. R. Johnson, editor. Raven press, New York. 1011-1029
- Flemström, G., Hällgren, A., Nylander, O., Engstrand, L., Wilander, E., Allen, A. (1999). Adherent surface mucus gel restricts diffusion of macromolecules in rat duodenum in vivo. *Am. J. Physiol.*, 277 (Gastrointest. Liver Physiol., 40), G375-G382
- Franco, C. M. L., Preto, S. J. R., Ciacco, C. F. (1992) Factors that affect the enzymatic degradation of natural starch granules: effect of the size of the granules. *Starch*, 44, 422-426
- Frazier, P. J., Richmond, P., Donald, A. M. (1997). *Starch: Structure and Functionality*. The Royal Society of Chemistry.
- Gal, J-Y, Fovet, Y, Adib-Yadzi, M. (2001). Review: About a synthetic saliva for in vitro studies. *Talanta*, 53, 1103-1115
- Galia, E., Nicolaidis, E., Horter, D., Lobenberg, R., Reppas, C., Dressman, J. B. (1998) Evaluation of various dissolution media for predicting in vivo performance of class I and II drugs. *Pharm. Res.*, 15, 698-705
- Galia, E., Horton, J., Dressman, J. B. (1999) Albendazole generics - a comparative in vivo study. *Pharm. Res.*, 16, 1871-1875
- Griffin, S. M., Alderson, D., Farndon, J. R. (1989) Acid resistant lipase as replacement therapy in chronic pancreatic exocrine insufficiency: a study in dogs. *Gut*, 30, 1012-1015
- Haber, P. S., Gentry, R. T., Mal, K. M., Mirmiran-Yazdy, S. A. A., Greenstein, R. J., Lieber, C. S. (1996). Metabolism of alcohol by human gastric cells: Relation to first-pass metabolism. *Gastroenterology*, 111, 863-870
- Hamosh, M., Klaeveman, H. L., Wolf, R. O., Scow, R. O. (1975) Pharyngeal lipase and digestion of dietary triglyceride in man. *J. Clin. Investigation.*, 55, 908-913
- Haraldsson, A-K., Rimsten, L., Alminger, M., Andersson, R., Aman, P., Sandberg, A-S. (2005). Digestion of barley malt porridges in a gastrointestinal model: Iron dialysability, iron uptake by Caco-2 cells and degradation of β -glucan. *J. Cereal Sci.*, 42, 243-254
- Harding S. E., Rowe, A. J., Creeth, J. M. (1983). Further evidence for a flexible and highly expanded spheroidal model for mucus glycoproteins in solution. *Biochem. J.*, 209, 893-896
- Havenaar, R., Minekus, M. (1996) Simulated Assimilation. *Dairy Industries International* 61(9), 17-20
- Hills, B. A. (1985). Gastric mucosal barrier: stabilization of hydrophobic lining to the stomach by mucus. *Am. J. Physiol.*, 249 (Gastrointest. Liver Physiol., 12), G342-G349
- Ho, S. B., Takamura, K., Anway, R., Shekels, L. L., Toribara, N. W., Ota, H. (2004). The adherent gastric mucous layer is composed of alternating layers of MUC5AC and MUC6 mucin proteins. *Digestive Diseases and Sciences*, 49 (10), 1598-1606
- Hollander, F. (1954). Two component mucous barrier: its activity in protecting gastroduodenal mucosa against peptic ulceration. *Arch. Intern. Med.*, 93, 107-120
- Holm, L., Flemström, G. (1990). Microscopy of acid transport at the gastric surface in vivo. *J. Int. Med.*, 228; 91-95
- Holzappel, W. H., Haberer, P., Snel, J., Schillinger, U., Huis in't Veld, J. H. J. (1998) Overview of gut flora and probiotics. *Int. J. Food Microbiol.*, 41, 85-101
- Humphrey, S. P., Williamson, R. (2001). A review of saliva: Normal composition, flow and function. *The Journal of Prosthetic Dentistry*, 85 (2), 162-169
- Jodál, I., Kandra, L., Harangi, J., Nanasi, P., Debrecen, Szejtli, J. (1984) Hydrolysis of cyclodextrin by *Aspergillus oryzae* α -amylase. *Starch*, 36 (4), 140-143
- Joseph, I. M. P., Zavros, Y., Merchant, J. L., Kirschner, D. (2003) A model for integrative study of human gastric acid secretion. *J. Appl. Physiol.*, 94, 1602-1618
- Kapsokefalou, M., Alexandropoulou, I., Komaitis, M., Politis, I. (2005) In vitro evaluation of iron solubility and dialyzability of various iron fortificants and of iron-fortified milk products targeted for infants and toddlers. *Int. J. Food Sci. Nutr.*, 56 (4), 293-302
- Kararli, T. T. (1995). Review article: Comparison of the gastrointestinal anatomy, physiology and biochemistry of humans and commonly used laboratory animals. *Pharmaceutics & Drug Disposition*, 16, 351-380
- Kelly, K. A. (1974) Gastric motility after gastric operations. *Surgery Annual.*, 6, 103-123

- Kim, J. C., Kim, J. I., Kong, B. W., Kang, M. J., Kim, M. J., Cha, I. J. (2004) Influence of the physical form of processed rice products on the enzymatic hydrolysis of rice starch in vitro and on the postprandial glucose and insulin response in patients with Type 2 Diabetes Mellitus. *Biosci. Biotechnol. Biochem.*, 68 (9), 1831-1836
- Klein, S., Butler, J., Hempenstall, J. M., Reppas, C., Dressman, J. B. (2004) Media to simulate the postprandial stomach I. Matching the physicochemical characteristics of standard breakfasts. *J. Pharma. Pharmacol.*, 56, 605-610
- Kočevar-Nared, J., Kristl, J., Šmid-Korbar, J. (1997). Comparative rheological investigation of crude gastric mucin and natural gastric mucus. *Biomaterials*, 18, 677-681
- Krishnakumari, S., Thayumanavan, B. (1995). Content of starch and sugars and in vitro digestion of starch by α -amylase in five minor millets. *Plant Foods for Human Nutrition*, 48, 327-333
- Krul, C., Luiten-Schuite, A., Baan, R., Verhagen, H., Mohn, G., Feron, V., Havenaar, R. (2000) Research Section: Application of a dynamic in vitro gastrointestinal tract model to study the availability of food mutagens, using heterocyclic aromatic amines as model compounds. *Food and Chemical Toxicology* 38, 783-792
- Krul, C. A. M., Zeilmaker, M. J., Schothorst, R. C., Havenaar, R. (2004) Intragastric formation and modulation of N-nitrosodimethylamine in a dynamic in vitro gastrointestinal model under human physiological conditions. *Food and Chemical Toxicology*, 42, 51-63
- Laurent, C., Besancon, P., Caporiccio, B. (2007) Flavonoids from a grape seed extract interact with digestive secretions and intestinal cells as assessed in an in vitro digestion/Caco-2 cell culture model. *Food Chemistry*, 100, 1704-1712
- Lee, K.Y., Heo, T.R. (2000) Survival of *Bifidobacterium longum* immobilized in calcium alginate beads in simulated gastric juices and bile salt solution. *Applied and Environmental Microbiology*, 66 (2), 869-873
- Lichtenberger, L. M. (1995). The hydrophobic barrier properties of gastrointestinal mucus. *Ann. Rev. Physiol.*, 57, 565-583
- Lock, S., Bender, A. E. (1980) Measurement of chemically available iron in foods by incubation with human gastric juice in vitro. *Br. J. Nutr.*, 43, 413-420
- Lohse, P., Lohse, P., Chahrokh-Zadeh, S., Seidel, D. (1997a) Human lysosomal acid lipase/cholesterol ester hydrolase and human gastric lipase: site-directed mutagenesis of Cys227 and Cys236 results in substrate-dependent reduction of enzymatic activity. *J. Lipid Res.*, 38, 1896-1905
- Lohse, P., Chahrokh-Zadeh, S., Lohse, P., Seidel, D. (1997b) Human lysosomal acid lipase/cholesterol ester hydrolase and human gastric lipase: identification of the catalytically active serine, aspartic acid and histidine residues. *J. Lipid Res.*, 38, 892-903
- Longland, R. C., Shilling, W. H., Gangolli, S. D. (1977) The hydrolysis of flavoring esters by artificial gastrointestinal juices and rat tissue preparations. *Toxicology*, 8, 197-204
- Luiking, Y. C., Peeters, T. L., Stolk, M. F., Nieuwenhuijs, V. B., Portincasa, P., Depoortere, I., van Berge Henegouwen, G. P., Akkermans, L. M. A. (1998). Motilin induces gall bladder emptying and antral contractions in the fasted state in humans. *Gut*, 42, 830-835
- Mainville, I., Arcand, Y., Farnworth, E.R. (2005) A dynamic model that simulates the human upper gastrointestinal tract for the study of probiotics. *International Journal of Food Microbiology*, 99, 287-296
- Malagelada, J. R., Longstreth, G. F., Summerskill, W. H. J., Go, V. L. W. (1976) Measurement of gastric functions during digestion of ordinary solid meals in man. *Gastroenterology*, 70, 203-210
- Marciani, L., Gouwland, P. A., Spiller, R. C., Manoj, P., Moore, R. J., Young, P., Fillery-Travis, A. J. (2001) Effect of meal viscosity and nutrients on satiety, intragastric dilution and emptying assessed by MRI. *Am. J. Physiol. Gastrointest. Liver Physiol.*, 280, G1227-1233
- Marteau, P., Minekus, M., Havenaar, R., Huis in't Veld, J.H.J. (1997) Survival of Lactic Acid Bacteria in a dynamic model of the stomach and small intestine: validation and the effects of bile. *J. Dairy Science* 80, 1031-1037
- McAdam, A. (1993). The effects of gastrointestinal mucus on drug adsorption. *Adv. Drug. Deliv. Rev.*, 11, 201-220
- McArthur, K., Hogan, D., Isenberg, J. (1982) Relative stimulatory effects of commonly ingested beverages on gastric acid secretions in humans. *Gastroenterology*, 83, 199-203
- McCallum, R. W., Saladino, T., Lange, R. (1980) Comparison of gastric emptying rates of intracellular and surface labeled chicken liver in normal subjects. *J. Nuc. Med.*, 21, P67

- McCallum, R. W., Berkowitz, D. M., Lerner, E. (1981) Gastric emptying in patients with gastroesophageal reflux. *Gastroenterology*, 80, 281-291
- Miller, D. D., Schricker, B. R., Rasmussen, R. R., Van Campen, D. (1981). An *in vitro* method for the estimation of iron from meals. *Am. J. Clin. Nutr.*, 34, 2248-2256
- Minekus, M., Marteau, P., Havenaar, R., Huis in't Veld, J. H. J. (1995). A multicompartmental dynamic computer-controlled model simulating the stomach and small intestine. *Alternatives to Laboratory Animals*, 23, 197-209
- Minekus, M., Smeets-Peeters, M., Bernalier, A., Marol-Bonnin, S., Havenaar, R., Marteau, P., Alric, M., Fonty, G., Huis in't Veld, J.H.J. (1999) A computer-controlled system to simulate conditions of the large intestine with peristaltic mixing, water absorption and absorption of fermentation products. *Appl. Microbiol. Biotechnol.* 53, 108-114
- Masuko, T., Minami, A., Iwasaki, N., Majima, T., Nishimura, S-I., Lee, Y. C. (2005) Carbohydrate analysis by a phenol-sulfuric acid method in microplate format. *Analytical Biochemistry*, 339, 69-72
- Molly, K., Woestyne, M. V., Verstraete, W. (1993) Development of a 5-step multi-chamber reactor as a simulation of the human intestinal microbial ecosystem. *Appl. Microbiol. Biotechnol.*, 39, 254-258
- Mossi, S., Meyer-Wyss, B., Beglinger, C., Schwizer, W., Fried, M., Ajami, A., Brignoli, R. (1994). Gastric emptying of liquid meals measured noninvasively in humans with [¹³C] acetate breath test. *Digestive Diseases and Sciences*, 39(12), 107S-109S
- Mun, S, Decker, E. A., McClements, J. D. (2007) Influence of emulsifier type on its *in vitro* digestibility of lipid droplets by pancreatic lipase. *Food Research International*, 40, 770-781
- Nelson, N. (1944) A photometric adaption of the Somogyi method for the determination of glucose. *J. Biol. Chem.*, 153, 375-380
- Nguyen, H. N., Silny, J., Matern, S. (1999). Multiple intraluminal electrical impedancometry for recording of upper gastrointestinal motility: current results and further implications. *Am. J. Gastroenterology*, 94 (2), 306-317
- Norris, D.A., Puri, N, Sinko, P.J. (1998) The effect of physical barriers and properties on the oral absorption of particulates. *Advanced Drug Delivery Reviews* 34, 135-154
- Novitol, R., Carrio, I., Cano, L., Estorch, M., Vilardell, F. (1984) Gastric emptying of solid and liquid meals in healthy young subjects. *Scand. J. Gastroenterol.*, 19, 1107-1113
- Pade, V., Aluri, J., Manning, L., Stavchansky, S. (1995) Bioavailability of pseudoephedrine from controlled release formulations in the presence of guaifenesin in human volunteers. *Biopharmaceutics & Drug Disposition*, 16, 381-391
- PDB sum database <http://www.ebi.ac.uk/pdbsum/>
- Pehlivanov, N., Liu, J., Kassab, G. S., Beaumont, C., Mital, R. K. (2002). Relationship between esophageal muscle thickness and intraluminal pressure in patients with esophageal spasm. *Am. J. Physiol. Gastrointest. Liver Physiol.*, 282, 1016-1023
- Peppas, N. A., Huang, Y. (2004). Nanoscale technology of mucoadhesive interactions. *Advanced Drug Delivery Reviews*, 56, 1675-1687
- Preetha, A., Banerjee, R. (2005). Comparison of artificial saliva substitutes. *Trends Biomater. Artif. Organs*, 18 (2), 178-186
- Rao, P., Pattabiraman, T. N. (1989). Reevaluation of the phenol-sulfuric acid reaction for the estimation of hexoses and pentoses. *Anal. Biochem.*, 181, 18-22
- Rao, B. S., Prabhavathi, T. (1978) An *in vitro* method for predicting the bioavailability of iron from foods. *Am. J. Clin. Nutr.*, 31, 169-175
- Rees, W. D. W., Botham, D., Turnberg, L. A. (1982) A demonstration of bicarbonate production by the normal human stomach *in vivo*. *Digestive Diseases and Sciences*, 27 (11), 961-966
- Roussel, A., Canaan, S., Egloff, M. P., Riviere, M., Dupuis, L., Verger, R., Cambillau, C. (1999) Crystal structure of human gastric lipase and model of lysosomal acid lipase, two lipolytic enzymes of medical interest. *J. Biol. Chem.*, 274 (24), 16995-17002
- Ruby, M. V., Davis, A., Schoof, R., Eberle, S., Sellstone, C. M. (1996) Estimation of lead and arsenic bioavailability using a physiologically based extraction test. *Environ. Sci. Technol.*, 30, 422-430
- Sarosiek, J., McCallum, R. W. (2000) Mechanisms of oesophageal mucosal defence. *Best Practice & Research Clinical Gastroenterology*, 14 (5), 701-717
- Schenkels, L. C. P. M., Veerman, E. C. I., Amerongen, A. V. N. (1995) Biochemical composition of human saliva in relation to other mucosal fluids. *Crit. Rev. Oral Biol. Med.*, 6 (2), 161-175

Schwartz, S. E., Levine, R. A., Singh, A., Scheidecker, J. R., Track, N. S. (1982). Sustained pectin ingestion delays gastric emptying. *Gastroenterology*, 83 (4), 812-817

Schwizer, W., Frazer, R., Borovicka, J., Crelier, G., Boesiger, P., Fried, M. (1994). Measurement of gastric emptying and gastric motility by magnetic resonance imaging (MRI). *Digestive Diseases and Sciences*, 39 (12), 101S-103S

Sheehan, J. K., Carstedt, I. (1989). *Dynamic Properties of Biomolecular Assemblies* (Harding, S. E., and Rowe, A. J., eds.), pg. 256-275, Royal Society of Chemistry, Cambridge

Shellis, R. P. (1978). A synthetic saliva for cultural studies of dental plaque. *Archs. Oral Biol.*, 23, 485-489

Somogyi, M. (1926) Notes on sugars determination. *J. Biol. Chem.*, 79, 599-613

Somogyi, M. (1937) A reagent for the copper iodometric determination of vary small amounts of sugar. *J. Biol. Chem.*, 117, 771-776

Somogyi, M. (1945) A new reagent for the determination of sugars. *J. Biol. Chem.*, 160, 61- 68

Souliman, S., Blanquet, S., Beyssac, E., Cardot, J.M. (2006) A level A in vitro/in vivo correlation in fasted and fed states using different methods: Applied to solid immediate release oral dosage form. *European Journal of Pharmaceutical Sciences*, 27, 72-79

Spencer, J. (1982) The rat isolated stomach sheet; an in vitro model for the study of the physiology and pharmacology of gastric acid secretion. *J. Pharmacol. Methods.*, 8, 197-212

Strous, G. J., Dekker, J. (1992). Mucin-type glycoproteins. *Crit. Rev. Biochem. Mol. Biol.*, 27, 57-92

Suzuki, S. (1987) Experimental studies on the presumption of the time after food intake from stomach contents. *Forensic Science International*, 35, 83-117

Talwar, G. P., Srivastava, L. M. (2004) *Textbook of biochemistry and human biology*. 3rd Edition. Gastrointestinal system section, pg. 603, table 46-5

Tasman-Jones, C., Morrison, G., Thomsen, L., Vanderwee, M. (1989) Sucralfate interactions with gastric mucus. *The American Journal of Medicine*, 86 (S6A), 5-9

Taylor, A. J., Linfoth, R. S. T. (1996) Flavour release in the mouth. *Trends in Food Science and Technology*, 7, 444-448

Tortora, G. J., Grabowski, S. R. (2000) *Principles of anatomy and physiology*. 9th Edition. John Wiley and Sons, Inc., Chapter 24, The Digestive System. pp.818-870

Turnbull, C. M., Baxter, A. L., Johnson, S. K. (2005) Water-binding capacity and viscosity of Australian sweet lupin kernel fibre under in vitro conditions simulating the human upper gastrointestinal tract. *International Journal of Food Sciences and Nutrition*, 56 (2), 87-94

Van Ruth, S. M., Roozen, J. P. (2000). Influence of mastication and saliva on aroma release in a model mouth system. *Food Chemistry*, 71, 339-345

Ville, E., Carriere, F., Renou, C., Laugier, R. (2002) Physiological study of pH stability and sensitivity to pepsin of human gastric lipase. *Digestion*, 65 (2), 73-81

Wicker-Planquart, C., Canaan, S., Rivière, M., Dupuis, L. (1999) Site-directed removal of N-glycosylation sites in human gastric lipase. *Eur. J. Biochem.*, 262, 644-651

Williamson, G., Belshaw, N. J., Sief, D. J., Noel, T. R., Rings, S. G., Cairns, P., Morris, V. J., Clark, S. A., Parker, M. L. (1992) Hydrolysis of A and B type crystalline polymorphs of starch by α -amylase, β -amylase and glucoamylase. *Carbohydr. Polym.*, 18, 179-187

Wong, L., Sissions, C. H. (2001). A comparison of human dental plaque microcosm biofilms grown in an undefined medium and a chemically defined artificial saliva. *Archives of Oral Biology*, 46, 477-486

Wrolstad, R. E., Acree, T. E., Decker, E. A., Penner, M. H., Reid, D. S., Schwartz, S. J., Schoemaker, C. F., Smith, D. M., Sporns, P. (2005) *Handbook of food analytical chemistry*. Water, proteins, enzymes, lipids and carbohydrates. Hoboken, N. J. Wiley.

Yu, L. X., Amidon, G. L. (1998) Saturable small intestinal drug absorption in humans: modeling and interpretation of cefatrizine data. *Euro. J. Pharma. Biopharma.*, 45, 199-203

Yu, L. X., Amidon, G. L. (1999) Compartmental absorption and transit model for estimating oral absorption. *Int. J. Pharm.*, 186, 119-125

Zimmermann, E., Müller, R. H. (2001). Electrolyte and pH stabilities of aqueous solid lipid nanoparticles (SLNTM) dispersions in artificial gastrointestinal media. *Eur. J. Pharm. Biopharm.*, 52, 203-210

Chapter 7

Clinical Application of the IPUGS to Study Secretory Disorders

In this chapter, a short review of disorders related to the gastric secretion of humans is discussed. Using the IPUGS, the conditions of such disorders were simulated and the results were compared with that of the clinical data in the literature.

7.1. Introduction

Secretions of the upper gastrointestinal tract (GIT) are dynamic processes regulated via hormonal and/or neural signals to optimize the digestion of the ingested foods and to maintain the homeostasis of the gastrointestinal (GI) pH of the lumen within a strict range (Freston *et al*, 1995; Joseph *et al*, 2003). The production of HCl in the gastric juice is very important to maintain the acidic pH of the stomach in order to facilitate the unfolding tertiary and secondary structures of proteins, optimization of the gastric pH to initialize the digestion of fats and proteins with the gastric lipases and pepsins, conversion of enzymes to its active form (e.g. pepsinogen to pepsin), killing of the ingested microorganisms, solubilisation of nutrients such as calcium and vitamin B12 (Tortora and Grabowski, 2000; Arthur and Gruner, 2007). The rate of the gastric secretion is variable among individuals, which can be deficit or excess to cause secretory disorders such as gastric hyposecretion and gastric hypersecretion states, respectively.

Gastric hypersecretion is an increase of gastric hydrochloric acid secretion in patients with disordered control of gastrin release, resulting in very high levels of plasma gastrin (Kwiecień and Konturek, 2003). Such disorder is known as Zollinger-Ellison syndrome, which consists of a fulminating ulcer diathesis and gastric acid hypersecretion occurring in association with esophageal disease, gastric and duodenal ulcer, abdominal pain, diarrhea and non-beta non-insulin-producing islet cell tumors of the pancreas (Ellison *et al*, 1963; Passaro *et al*, 1970; Collen and Jensen, 1994; Ellison *et al*, 2003). Zollinger-Ellison syndrome is relatively rare, with less than 1% of the patients with gastric acid hypersecretion are diagnosed to have Zollinger-Ellison syndrome while the majority of other patients have no apparent etiology for their gastric acid hypersecretory states and

often referred to as having idiopathic gastric acid secretion (Collen and Jensen, 1994). The clinical diagnosis of the syndrome depends largely on various measurements of gastric secretion such as the basal acid output, stimulated acid output (Winship and Ellison, 1967). When the gastric secretion rate exceeds $15\text{mEq}\cdot\text{hr}^{-1}$, the condition is diagnosed as the Zollinger-Ellison syndrome. In previous clinical studies, basal acid output of $29.2 - 42.6\text{mEq}\cdot\text{hr}^{-1}$ with peak acid output of $33.2 - 40.2\text{mEq}\cdot\text{hr}^{-1}$, with the ratio of the basal acid output over the ratio of the peak acid output of 80-106% have been observed by Winship and Ellison (1967) and Harford *et al* (2000). Approximately 20-25% of the patients with Zollinger-Ellison syndrome were found to have multiple endocrine neoplasia type 1 (Cadiot *et al*, 1999) and have reduced absorptive capacity of the small bowel caused by hypersecretion of the gastric acid, inhibiting the small bowel absorption of electrolytes and water (Wright *et al*, 1970).

Diminished gastric secretion, called hypochlorhydria, or no gastric acid secretion (achlorhydria) results from the gastritis in the body of the stomach with consequently developed mucosal atrophy of the gastric body, which may in turn develop into gastric cancer (Cater, 1992a and 1992b; Iijima *et al*, 2004). Hypochlorhydria is diagnosed when reduction of the peak gastric acid output is greater or equal to 75% of the normal state (Arthur and Gruner, 2007). Causes of hypochlorhydria have been expected to rise from the ageing process, atrophic gastritis (which results from *Helicobacter pylori* or abdominal radiotherapy), gastritis (which results from acute inflammation of the stomach lining as well as *Helicobacter pylori* infection), stress, gastroesophageal reflux disorder and diabetes mellitus (Arthur and Gruner, 2007). Hypochlorhydria also contributes to the malabsorption of iron, calcium and essential amino acids as well as abnormal protein digestion (Cater, 1992a and b) as well as facilitation of the infections by *Helicobacter pylori*, *Salmonellae*, *Vibrio cholerae*, Rotaviruses, *Escherichia coli* and non-enteric organisms such as Mycobacterium tuberculosis (De Martel *et al*, 2006). *Helicobacter pylori* is able to digest and metabolize the gastric mucin with its protease enzyme (Cater, 1992a), causing direct inhibition of parietal cell acid production by the attachment of the organism to the parietal cell and/or by a toxic product of the bacterium (Feldman and Barnett, 1991) and thereby associate inflammation to progress from the antrum into the adjacent body of the stomach, resulting in injury with a reduction in acid secretion, loss and severe damage of parietal cells (El-Zimaity, 2007). However, drugs and surgeries are able to decrease the gastric acid secretion, thereby increasing the plasma gastrin concentrations (Freston *et al*, 1995). With hypochlorhydria patients, the mean basal acid output was $0.02\pm 0.02\text{mmol}\cdot\text{hr}^{-1}$, with average basal pH of 7.44 ± 0.11 and the mean peak

acid output of $3.30 \pm 0.3 \text{ mmol} \cdot \text{hr}^{-1}$, which have been observed by Feldman and Barnett (1991) and Charman *et al* (1997).

In vitro Physicochemical Upper Gastrointestinal System (IPUGS) has been, in the current study, used to mimic the conditions of such impaired secretions, Zollinger-Ellison syndrome and hypochlorhydria, by varying the rates of the gastric secretions applied, in order to distinguish feasibility of the IPUGS to be used as a clinical tool. As a test material, white short grain rice (Sun Rice Japanese style Sushi Rice, Koshihikari and Opus type) was used as the constituent of the macronutrients is relatively simple (up to 78.5wt% of total carbohydrates) compared to other balanced test meals composed of a mixture of carbohydrates, proteins and fats, thus analyses of carbohydrates would be of the main concern and complications emerging from having to analyze all the nutrients as well as intra and inter-actions of nutrients can be avoided. Studies of starch (including rice starch) have underscored no significant differences between the *in vitro* enzymatic hydrolysis and *in vivo* digestion of starch (Williamson *et al*, 1992; Franco *et al*, 1992; Björck *et al*, 1994; Kim *et al*, 2004). Yet, rice is one of the most abundant staple food worldwide (Frazier *et al*, 1997), where intensive research related to the postprandial glucose and insulin responses, diabetes, coronary heart disease, cancer and ageing are being conducted (Frazier *et al*, 1997; Kim *et al*, 2004). By comparing the results obtained from the IPUGS with the available data collected from patients with secretory disorders in the literature, evaluation of the IPUGS as a clinical tool to be used with or without *in vivo* studies can be determined.

7.2 Materials and Methods

7.2.1. *In vitro* Physicochemical Upper Gastrointestinal System (IPUGS)

The IPUGS consists of three consecutive compartments simulating the conditions of the upper GI organs in humans. The first compartment simulates the food ingestion in mouth, which is composed of a denture set with manually controlled mastication and continuous secretion of artificial saliva of $37 \pm 0.5^\circ\text{C}$ which is transferred via a peristaltic pump at rate of $7.0 \text{ ml} \cdot \text{min}^{-1}$ (Edgar 1990; Humphrey and Williamson, 2001). White short grain rice (Sun Rice Japanese style Sushi Rice) was cooked in a conventional rice cooker with 1:1 volumetric ratio of rice grains to water. 100g of the cooked rice was transferred to the

mouth reactor with 250ml of drinking water to be used as the feed material. As the cooked rice is relatively small in size which can be swallowed without much of mastication, it can be regarded as simpler foods for testing. 5min of gentle manual mastication was applied with the denture set with 20chewings.min⁻¹ to remove large clusters of rice into smaller pieces to aid the swallowing process. The feed material was spoon fed to the next compartment, esophagus at a rate of 8.5ml.30s⁻¹ (equivalent to ½ Tablespoon (tbsp).30s⁻¹).

The next two compartments simulating the conditions of the esophagus and the stomach were built with platinum cure silicon rubber composed of 75-85wt% polyorganosiloxanes, 20-25wt% of amorphous silica and 0.1wt% of platinum-siloxane for part A and 65-70 wt% of polyorganosiloxanes and 20-25wt% of amorphous silica for part B. 1:1 ratio of the parts A and B were mixed and coated to the plastic anatomy model of the stomach which resembles the average human stomach size at unfed state (20cm x 15cm x 8cm, Kararli, 1995; Pade *et al*, 1995) as well as its geometry of J-shaped curve. The coatings were repeated until the thickness of the stomach wall reached 0.50±0.01cm in average. The material is translucent in color thus by adding of food coloring agents to the feed mixture may help clearer view of the reactions in the inner stomach compartment. It offers negligible shrinkage and able to stretch and rebound to its original size and shape without distortion. For the esophagus, paper roll of 1.5cm diameter and 20cm in length was made, and coatings of the silicon rubber were repeatedly made until the wall thickness reached 0.30±0.01cm in average (Al-Zaben and Chandrasekar, 2005). The paper roll and the plastic anatomic model were removed after coatings. In order to deliver the gastric secretions to the wall of the stomach, a large number of Tygon ® Microbore tubings (n=200) with inner diameter of 0.25mm were implanted, with the tips of these tubings pierced into the stomach wall to create a gradual dampening of the wall (Chapter 6, Figure 6-1), secreting 3.5ml.min⁻¹ (Mainville *et al*, 2005) throughout the 3hr digestion period. These tubings are designed for precision injection and dispensing in laboratory applications with flexible and bendable resin. The tubings have a very smooth inner bore surface which reduces the risk of particulate build-up during sensitive fluid transfer and minimal extractable helps to assure fluid purity. Also, these tubings are transparent, thus the gastric secretions passing into the stomach wall can be seen clearly. For mucosal secretions in the esophagus compartment, slightly larger diameter of tubing was used. Micro-Line™ tubing (Thermoplastic Scientifics, Inc.) made of cross-linked ethyl vinyl acetate. These tubings are translucent, flexible and elastic with inner diameter of 0.51mm. One ends of these implanted tubings in both esophagus and the stomach were planted into

the wall of each compartment to create gradual dampening effect from the wall to simulate the opening and closing of the pores in the gastric wall for secretion delivery. The other ends were gathered and squashed into a larger diameter Tygon peristaltic tubings (inner diameter of 1.5cm), which are subsequently connected to the smallest possible peristaltic tubing (inner diameter of 0.80mm). Though the flow rate of the peristaltic pumps can be controlled, changing the peristaltic tubing size also helped to control the flow rate more accurately. For validation of motility experiments, only one peristaltic pump (Autoclude® Peristaltic Pump - 54505) was used to deliver the artificial gastric juice to the stomach compartment.

For mucosal secretions in the esophagus compartment, slightly larger diameter of tubing was used. Micro-Line™ tubing (Thermoplastic Scientifics, Inc.) made of cross-linked ethyl vinyl acetate. These tubings are translucent, flexible and elastic with inner diameter of 0.51mm. One ends of these implanted tubings in both esophagus and the stomach were planted into the wall of each compartment to create gradual dampening effect from the wall to simulate the opening and closing of the pores in the gastric wall for secretion delivery. The other ends were gathered and squashed into a larger diameter Tygon peristaltic tubings (inner diameter of 1.5cm), which are subsequently connected to the smallest possible peristaltic tubing (inner diameter of 0.80mm). Though the flow rate of the peristaltic pumps can be controlled, changing the peristaltic tubing size also helped to control the flow rate more accurately. For validation of motility experiments, only one peristaltic pump (Autoclude® Peristaltic Pump - 54505) was used to deliver the artificial gastric juice to the stomach compartment.

The esophagus and the stomach compartments were placed in an anaerobic chamber with continuous nitrogen gas flow ($1.0\text{L}\cdot\text{hr}^{-1}$) and the temperature inside the chamber was maintained at $37\pm 1^\circ\text{C}$ with a hot plate placed inside the chamber.

The esophagus and the stomach compartments were manually pressed with my hands to mimic the peristaltic waves. For the esophagus, coordinated contractions and relaxations of the peristaltic propulsions were simulated to push the ingested feed material (bolus) towards the stomach with the rate of 5 contractions per 30s. The wall of the esophageal compartment was squeezed both horizontally and vertically by gripping the esophagus using both hands, one on top of each other and in between a thumb and an index finger, squeezed gently to push down the bolus (Chapter 6, Figure 6-2).

The upper esophageal sphincter (UES) controlled the entrance of the feed mixture and the lower esophageal sphincter (LES) controlled the exit of the feed mixture into the stomach compartment. Each cycle of esophageal peristalsis lasted up to 6s (Pehlivanov *et al*, 2002). Apart from mucosal secretions, there are neither digestive secretions nor absorption take place in the esophagus (Tortora and Grabowski, 2000) thus these features were excluded.

Hand squeezed actions to simulate the peristaltic waves of the human stomach was used in the stomach compartment as well. This is a novel approach which reduces the high cost of a robotic motion mechanism whilst examining the feasibility. The first peristaltic wave was initiated from squeezing the proximal part of the stomach compartment (the fundus and upper body). This was to generate a pressure gradient from the stomach to the pylorus, resulting an opening of the pyloric sphincter and emptying of fractions of the stored bolus towards and mix with the gastric secretions, which resembles the action of a contractile grinder, crushing the small chunks of the bolus as described in the literature (Akin 1998; Luiking *et al*, 1998; Nguyen *et al*, 1999; Tortora and Grabowski, 2000) (Chapter 6, Figure 6-3).

The second peristaltic wave with closed cardiac and pyloric sphincters was initiated from the distal stomach (lower body and the antrum), squeezing the wall of the stomach towards the proximal direction (toward the fundus) (Figure Chapter 6, Figure 6-4). Sequential contractions of the antrum crushed the small chunks of the bolus against the closed pyloric sphincter with a large fraction of the remaining bolus squeezed back toward the proximal part for further digestion (Kelly, 1974; Barker *et al*, 1979; Tortora and Grabowski, 2000; De Zwart *et al*, 2002), causing distention of the stomach compartment to accommodate more space for the incoming food which was facilitated by the elastic and stretchy nature of the building material (platinum cure silicon rubber). The overall gastric motility in the proximal stomach compartment remained relatively constant, but for the distal part, stronger contractions with higher depth and amplitudes (Schwizer *et al*, 1994), were used. The first and the second peristaltic waves constitute one wave cycle of the gastric motility. To simulate the normal condition at fed state, $3\text{cycle}\cdot\text{min}^{-1}$ with average duration of wave cycle of $21.5\pm 3.8\text{s}$ (Allescher *et al*, 1998) was used.

The digestion period of 3hrs was set as carbohydrates typically take 2-4hrs to be emptied into the small intestine (Suzuki, 1987; Mossi *et al*, 1994). Initially, 5ml of the samples were taken from the mouth compartment to check the consistency of each batch. From

10min to 30min, 20ml of samples were collected every 10min from the pylorus. From 30min to 180min where the gastric emptying was to be more active, 6.8ml of the chyme mixture was pumped out of the IPUGS per minute (Marciani *et al*, 2001; Mainville *et al*, 2005), collected and stored in sampling bottles with closed lids and placed in an ice water bath (0-2°C) while the experiment was running. Then the samples were centrifuged at 3000rpm for 30min (Holm, 1988; Klein *et al*, 2004) at 2°C. The supernatants were diluted accordingly for each of the analytical methods used. The experiments via the IPUGS were conducted triplicate.

7.2.2. Compositions of the GI secretions used in the IPUGS

7.2.2.1. Saliva

Artificial saliva was made from the list of compositions stated by Shellis (1978) (Table 7-1) as it is the closest possible chemically defined synthetic saliva in the literature (Wong and Sessions, 2001), which contain numerous ions, amino acids, vitamins, growth factors and mucin of appropriate amounts in accordance to the humans. All the chemicals were purchased from Sigma-Aldrich with reagent plus® grade. For the salivary α -amylase, fungal source, *Aspergillus oryzae* (Grindamyl™ A5000, 5000U/g, Danisco 071314), has been used by mixing 2.00 ± 0.02 g of α -amylase powder was with 200ml deionized distilled water with the electrolytes from the Shellis synthetic saliva and 0.10 ± 0.02 g of lingual lipase from *Candida rugosa* (fungal source) with greater or equal to 700U/mg (Sigma-Aldrich, L1754).

In order to simulate the non-Newtonian shear-thinning characteristics of the natural human saliva, which is essential to provide lubrication and proper mixing of the ingested foods (Preetha and Banerjee, 2005), $2500\text{mg}\cdot\text{L}^{-1}$ of mucus (Sigma-Aldrich, M2378) which is classified as glycoproteins, have been added to the artificial saliva mixture (Chapter 6, Table 6-1). Yet, no other *in vitro* digestion models have attempted to simulate the viscous nature of the human saliva although the viscosity is able to influence the diffusion rates of solutes and overall reaction rates which may have an effect in overall digestive processes (Gal *et al*, 2001). The artificial saliva mixture was made prior to each experiment and kept at 37°C until use as the temperature changes may influence the digestive processes in the mouth (Taylor and Linforth, 1996). However, the solutions of

mixed amino acids (Table Chapter 6, 6-2) and mixed vitamins (Chapter 6, Table 6-3) from the Shellis synthetic saliva (Shellis, 1978) were made concentrated (x1000) as numerous kinds of chemicals were required in trace amounts, and diluted accordingly per each experiment.

7.2.2.2. Mucosal secretions for the compartments of esophagus and stomach of the IPUGS

Porcine gastric mucin powder (Sigma-Aldrich, M2378) was dispersed in phosphate buffer solution (pH 6.7) to make 30w/v% mucus solution by stirring at room temperature for 30min at 500rpm to be used as a replacement to the human mucus, which has been widely used by other *in vitro* studies due to its similar structures and functions (Allen *et al*, 1976; Bell *et al*, 1985; Hills, 1985). The mucosal secretions for the esophagus and the stomach compartments of the IPUGS were kept the same in terms of composition. The secretion was delivered to the walls of the esophagus at a rate of $1\text{ml}\cdot\text{min}^{-1}$ to barely cover the walls of the esophagus compartment to aid the movement of the bolus during the ingestion period of up to 30min. As soon as the ingestion period ceased, the mucosal secretion in the esophagus was stopped. For the gastric mucosal secretions, the secretion channels were implanted mostly on the antrum and fewer to the fundus of the IPUGS (Rees *et al*, 1982) to create a pH gradient across the surface of the mucus gel layer. The mucosal secretion was delivered to the walls of the stomach to barely cover the walls of the stomach compartment to create a thin layer to simulate protection against the pepsin and the acidic gastric juice. For normal state, a rate of $2\text{ml}\cdot\text{min}^{-1}$ has been used from 0min to 90min, then reduced to $1\text{ml}\cdot\text{min}^{-1}$ for 90min to 180min. To simulate Zollinger-Ellison syndrome and hypochlorhydria conditions, mucosal secretion rates of $2\text{ml}\cdot\text{min}^{-1}$ and $1\text{ml}\cdot\text{min}^{-1}$ have been used, respectively.

7.2.2.3. Gastric Secretion

The composition of the complex gastric juice used in the IPUGS is shown in Chapter 6, Table 6-4, which contains KCl, HCl, NaCl, CaCl_2 and NaHCO_3 (Minekus *et al*, 1995) for ionic part and pepsin and gastric lipase for the enzyme part. The mean basal acid output in normal humans is 1.56mM of HCl (McArthur *et al*, 1982), thus 0.15N HCl was used.

Lipase from porcine pancreas (Sigma-Aldrich, L3126) containing 100-400U.mg⁻¹ was used to replace the human gastric lipase. 500kU.L⁻¹ was used, as stated by Minekus *et al* (1995). The combined solution containing the electrolytes with 150mM HCl, pepsin and lipase were mixed at 1000rpm at 37°C for 10min prior to experiments, and delivered at 3.5ml.min⁻¹ up to 90min, and 2ml.min⁻¹ from 90min to 180min for the normal condition. For the Zollinger-Ellison syndrome condition, 3.5ml.min⁻¹ was used throughout the experiment, and for the hypochlorhydria condition, 2.0ml.min⁻¹ was used.

7.2.3. Phenol-Sulfuric Acid Assay

Phenol-Sulfuric acid assay is one of the most widely used analytical methods in measuring neutral sugars in oligosaccharides, proteoglycans, glycoproteins and glycolipids. It is a simple, fast, reliable and sensitive method which has been developed by Dubois *et al* (1951) and (1956). Rao and Pattabiraman (1989) reported that phenol underwent sulfonation in situ and the phenol-sulfuric acid complex decreased the color intensity for many hexoses and pentoses. Similar results were seen by Masuko *et al* (2005) whom modified the original method by Dubois *et al* (1951) and (1956) by adding concentrated sulfuric acid to the sample followed by phenol. Instead of using microplate proposed by Masuko *et al* (2005), larger volumes were reconstituted following the ratio of sample to conc. sulfuric acid to phenol. The method was used to determine the concentration of total water soluble carbohydrates from the obtained samples.

3ml of concentrated sulfuric acid was added to 1ml of diluted (factor of 100) sample in a test tube followed by vigorous shaking at high speed in a vortex mixer. 600µL of 5% (w/v) phenol was pipetted into the mixed solution and placed in a water bath at 90°C for 10min. The prepared samples were vortexed at high speed for 30s and left at room temperature for 5mins cooling before reading the absorbance via the UV spectrophotometer (Agilent 8453, UV G1103A) at 490nm.

7.2.4. Somogyi-Nelson Method

Somogyi-Nelson method (Somogyi, 1926; Somogyi, 1937, Somogyi, 1945; Nelson, 1944; Wrolstad *et al*, 2005) is an extensively used highly accurate method for determining the amount of reducing sugars (e.g. maltose). Low alkalinity copper reagent and arsenomolybdate reagent were prepared as follows.

12g of sodium potassium tartate and 24g of anhydrous sodium carbonate with 250ml of distilled water were mixed. 4g of copper sulfate pentahydrate and 16g of sodium bicarbonate were added to 200ml of distilled water. 180g of anhydrous sodium sulfate in 500ml of boiling distilled water was separately prepared. Three mixtures were combined and diluted to 1L to make the low alkalinity copper reagent. The arsenomolybdate reagent was made by mixing 25g ammonium molybdate to 450ml of distilled water. 21ml of concentrated sulfuric acid and 25ml of distilled water containing 3g of disodium hydrogen arsenate heptahydrate were added to the ammonium molybdate solution with stirring. The mixture was continuously stirred for 24hrs at 37°C and kept in brown glass stopped bottle until use.

1ml of the diluted (factor of 100) sample and 1ml of the low alkalinity copper reagent were placed in a test tube and vigorously mixed by a vortex mixer at a high speed for 30s. The test tube was placed in a boiling water bath (100°C) for 10mins, and cooled at room temperature for 5mins. 1ml of the arsenomolybdate reagent was then added and the mixture was vortexed at a high speed for 30s. Absorbance at 500nm was read via the UV spectrophotometer (Agilent 8453, UV G1103A). Blanks for the absorbance were prepared by replacing the sample with 1ml distilled water.

Blue color of the low alkalinity copper reagent and green color of the arsenomolybdate reagent gave a greenish blue color in all the samples. The samples which contained less maltose showed a light green solution, but as the concentration of maltose increased, the color of the sample became darker and bluish. As the arseno reagent is extremely toxic and may cause cancer, particular cares were taken to avoid inhalation and contacts at all times.

7.2.5. High Performance Liquid Chromatography (HPLC)

HPLC is able to provide both qualitative and quantitative analyses with a small amount of diluted sample. As HPLC requires a prestigious level of accuracy, it was used to ensure the compatibility of results from the phenol-sulfuric acid assay and the Somogyi-Nelson method, as well as to screen for any unexpected components (e.g. glucose) in the collected samples.

A carbohydrate ES column (Prevail™ Carbohydrate ES Column-W 150x4.6mm, 5 µm (Alltech Part No. 35102)) was used to specifically analyze maltose, maltotriose and other undigested starch in the samples. A mixture of degassed (Elite™ Degassing System) acetonitrile (Merck, HPLC grade) and deionized water was used as mobile phase and was pumped into the column via a quaternary gradient pump (Alltech, 726) at 1.0ml.min. Isocratic gradient was used for a better separation of carbohydrates – initially 65% to 35% of acetonitrile to water and then from 15mins onwards, 50% to 50%, respectively. Collected samples were diluted (X40) with deionized water, followed by syringe filtration with nylon membranes and automatically injected (Alltech Autosampler 570) into the column with 30mins of analysis time per sample. Evaporative Light Scattering Detector (ELSD) and EZStart software were used to detect and record the findings.

7.2.6. Recording of pH

The measure of the pH profile is one of the simplest analyses which directly indicates the conditions of the stomach and it is of extreme importance as it is able to detect even minor changes of the gastric conditions. For the IPUGS, two pH probes and one temperature probe were pierced into the wall of the stomach compartment in the IPUGS to record the pH in the fundus (probe 1) and the antrum (probe 2). The temperature probe was placed in the middle of the body of the stomach to measure the changes with respect to time. For the MISST, a pH probe and a temperature probe were placed in the middle of the stomach reactor. A pH meter from Hanna Instrument (HI 4212) was used with auto-logging mode of 30s for 3hr.

7.3. Results and Discussions

7.3.1. Phenol-Sulfuric Acid Assay

As shown in the Figure 7-1, the concentration of total water soluble carbohydrates varied noticeably depending on the rate of the applied gastric secretion rate over the 3hr digestion period. The concentration and the mass of total water soluble carbohydrates over time (Figures 7-1 and 7-2) indicate the available amount of rice carbohydrates (mainly starch initially) in the stomach compartment of the IPUGS at given times, which signifies the rate of ingestion as well as the rate of gastric emptying. By examining the amount (both concentration and mass) of the total carbohydrates as well as the amount of maltose and maltotriose (Figures 7-3, 7-4, 7-7 and 7-8) in the stomach compartment, the amount of undigested (unconverted) rice starch (Figure 7-5) can be determined (i.e. Undigested starch = Total carbohydrates – Maltose – Maltotriose). The ratio of maltose to unconverted starch can then be calculated to observe the effect of varying the rate of the gastric secretion applied to the pattern of the rice starch hydrolysis, which can be used as a screening tool to simulate the conditions of the patients as well as used with clinical *in vivo* studies for assistance. The effectiveness of the hormonal control of the gastric secretions throughout the experiments can also be evaluated and by using the normal motility of 3 cycles.min⁻¹ as a control, comparison to the different rates of the secretions can be made.

As it has been proposed by Elashoff *et al* (1982) that for uniformity, time 0 was defined as the point at which the meal ingestion began. Therefore the collected samples at time 0min can be referred to as the bolus from the mouth compartment which was about to be swallowed. These samples were taken before they were ingested into the esophagus. Initially, the values of the total carbohydrate concentration for the three cases were very similar to each other, with average values of 82.5±3.9g.L⁻¹ and 1.44±0.07g for simulation of Zollinger-Ellison syndrome (fast secretion rate of 3.5ml.min⁻¹), 93.8±1.1g.L⁻¹ and 1.64±0.05g for normal hormonal controlled conditions, and 93.2±0.8g.L⁻¹ and 1.63±0.05g for the hypochlorhydria (slow secretion rate of 2ml.min⁻¹). This indicates that a good control of preparing the feed mixture was maintained throughout the experiments, as the procedures for preparing the feed mixture and the rate of mastication applied in the mouth compartment were the same.

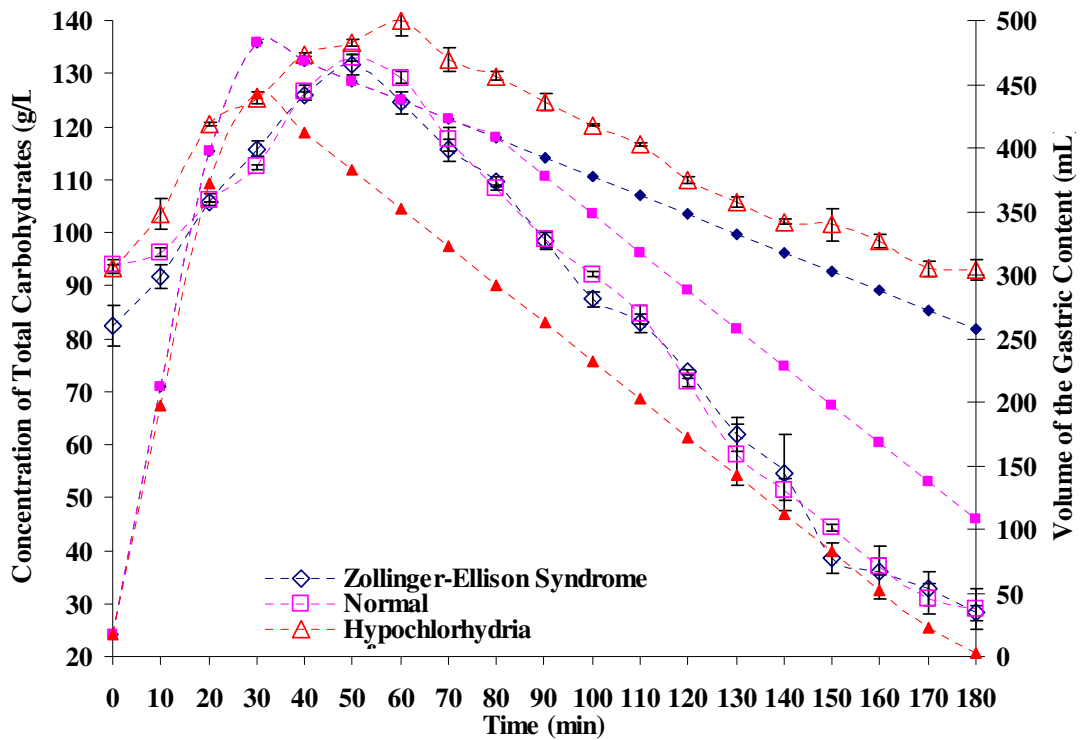


Figure 7-1. A graph showing the concentration of total carbohydrates ($\text{g}\cdot\text{L}^{-1}$) during the 3hr digestion time (min). The results obtained from simulating the secretory conditions of Zollinger-Ellison Syndrome are marked with empty dots in blue, the normal state in pink and the Hypochlorhydria condition in red. The volumes of the gastric content (mL) for different secretory conditions are shown with filled dots with accordance of color and shape for each condition.

Calibration errors from the weight balance when weighing hot cooked rice may have occurred, which seemed to have caused a small difference in the initial starch concentrations. Although the difference in concentrations of the total carbohydrates and unconverted starch in the three cases varied noticeably, when the masses of total carbohydrates and the unconverted starch present in the samples were calculated, there was near to none difference between the three cases (Figures 7-5, 7-6 and 7-9). This was due to the small gastric volume (17.5ml) and small volume (5ml) of the samples collected from the model. As the main purpose of the study was to determine and compare different rate of gastric motility cycles used to simulate the conditions of the motility disorders, initial starch content can only be used as a reference(control) for the latter data, thus it was decided to only collect the amount (volume) required to conduct analyses. As the initial carbohydrate constituent of rice was mainly starch, the values of the mass of unconverted starch and the values of the mass of the total water soluble carbohydrates were almost the same.

Gastric emptying time refers to when only a trace of the meal remained among the gastric rugae (Whitehouse and Temple, 1977). Whitehouse and Temple (1977) reported that the total gastric emptying time for normal healthy subjects took 192 ± 12 min when a balanced meal constituted of carbohydrates, proteins and fats, were fed. Although 180 min of digestion was allowed with normal emptying rate of $5.0 \text{ ml} \cdot \text{min}^{-1}$, due to the different secretion rate, the change in the volume of the gastric content (ml) was different among the three conditions throughout the experiments. The change of volume for each condition is illustrated in each figure to aid the analysis of the starch hydrolysis. During the ingestion period, rapid increase in both the concentration and the mass of total carbohydrates follow that of the volume of the gastric content. Thus it can be concluded that during the ingestion period, the volume of the gastric content largely influences the rate and the pattern of increase in the amounts of total carbohydrates. Not only for the total carbohydrates, but similar trends have been observed by maltose, maltotriose and unconverted starch in subsequent figures. However during the gastric emptying period, the rate and the pattern of decrease did not follow that of the volume of the gastric content, which was linear.

As the ingestion had initiated, the feed mixture was delivered through the esophagus and deposited predominantly in the proximal stomach with progressive distribution into the distal stomach as the gastric emptying progressed. This was also seen by Lee *et al* (2004) in the human stomach. Sharp increases in the concentrations and the masses of the total carbohydrates were observed during the ingestion period of the three different secretion rates examined. Only the hypochlorhydria condition reached its peak mass value of 55.5 ± 1.7 g by the end of the ingestion period of 30 min mark. With Zollinger-Ellison syndrome and the normal state where exactly the same secretion rate of $3.5 \text{ ml} \cdot \text{min}^{-1}$ was applied for up to 90 min, the difference between the two conditions was indistinguishable. The maximum amounts of carbohydrates were reached by 50 min mark with the values of $131.6 \pm 1.9 \text{ g} \cdot \text{L}^{-1}$ and 59.6 ± 1.9 g for the Zollinger-Ellison syndrome and $133.0 \pm 0.7 \text{ g} \cdot \text{L}^{-1}$ and 60.2 ± 1.7 g for the normal condition. The values of masses of total carbohydrates in both conditions were similar to one another until they reached their maximum. However, hypochlorhydria condition showed considerably higher values of concentration of total carbohydrates but lower values of mass of total carbohydrates. This seemed to be due to the slower rate of gastric secretion, resulting in a generally lower range of the volume of the gastric content.

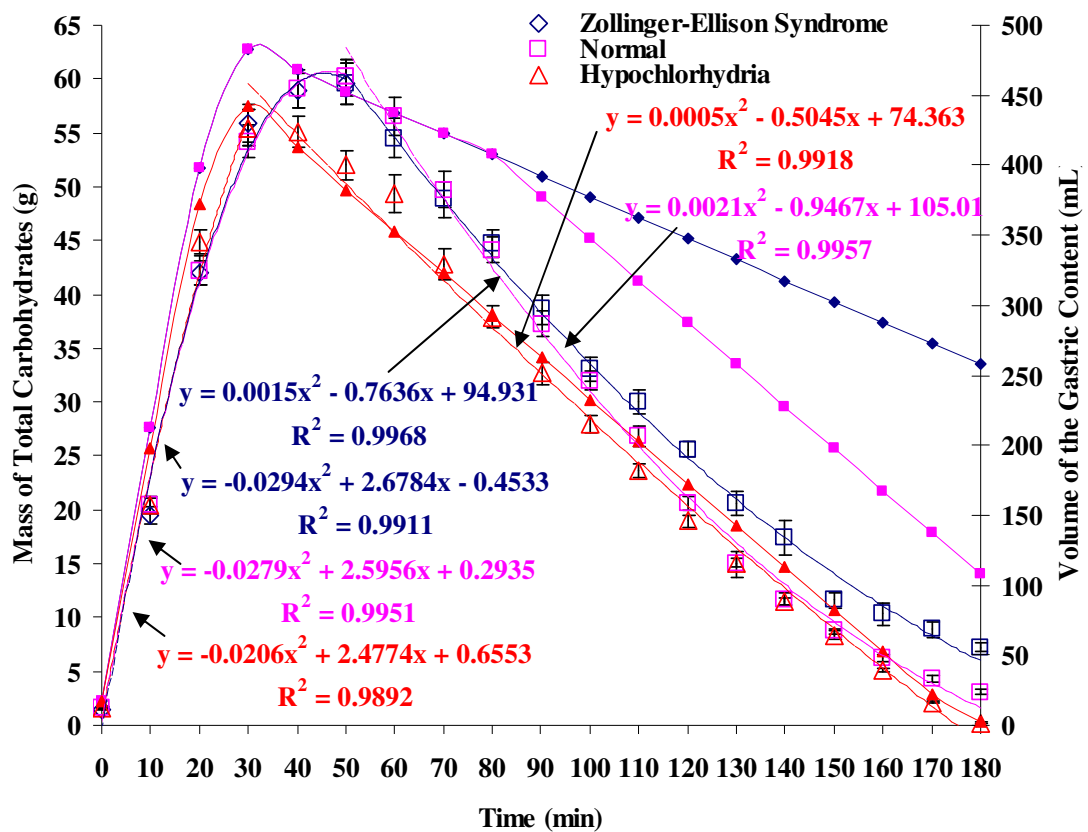


Figure 7-2. A graph showing the mass of total carbohydrates (g) during the 3hr digestion time (min). The results obtained from simulating the secretory conditions of Zollinger-Ellison Syndrome are marked with empty dots in blue, the normal state in pink and the Hypochlorhydria condition in red. The volumes of the gastric content (mL) for different secretory conditions are shown with filled dots with accordance of color and shape for each condition.

The maximum volume of the gastric content of 482.5ml for both the Zollinger-Ellison syndrome and the normal state, whereas for the hypochlorhydria condition, the maximum volume reached was 442.5ml only. As the mass of the total carbohydrates was calculated by multiplication of the gastric volume with the concentration of the total carbohydrates and the rate of gastric emptying was kept the same for all the conditions, the lower volume range of the hypochlorhydria condition consequently resulted in lower values of the mass of the total carbohydrates. The increases in the mass of the total carbohydrates were fitted with parabolic function ($R^2 \geq 0.9892$) for all of the conditions tested.

Since the meal ingestion has ceased, the volume of the gastric content has started to decrease gradually until the end of the digestion period. It is an arbitrary phenomenon that the stated numerical values of the total carbohydrates concentration exceeded the total mass of rice added (100g). Although the gastric secretions (2.0 and $3.5 \text{ mL} \cdot \text{min}^{-1}$) were

delivered to the stomach compartment constantly, the chyme samples, which were of greater volumes than the volume of the gastric secretion, were also withdrawn at the same time. Thus the volume of the gastric content has decreased over time, and therefore the concentration and the mass of total carbohydrates and unconverted starch in the stomach also decreased over time. However for the hypochlorhydria condition, the amount of sample withdrawn exceeded that of the gastric secretions in 10min basis, thus the volume of the gastric content decreased more rapidly over time compared to the other two conditions.

A square function fitted well ($R^2 \geq 0.9918$) for the gastric emptying period from 30min to 180min for all of the conditions tested. From 90min mark, which is considered to be the time at which half of the gastric contents are expected to be emptied under the normal conditions, the rate of gastric secretion for the normal state changed from $3.5\text{ml}\cdot\text{min}^{-1}$ of maximal output to $2.0\text{ml}\cdot\text{min}^{-1}$ to simulate hormonal control of the gastric secretions. Therefore up to 90min mark, the values of the mass of the total carbohydrates were very similar to that of the Zollinger-Ellison syndrome, whereas since 90min mark, the values transient to that of the hypochlorhydria condition. Similar trends were seen with the mass of the unconverted starch with respect to time, as starch is the main constituent of the rice where limited hydrolysis via salivary amylase and HCl took place.

The difference among the three different rates of the gastric secretions tested did not result in a completely different trend or values. Throughout the 3hr digestion period, the values of the three conditions were similar to each other, with overall smaller values obtained by the simulation of the hypochlorhydria condition. At the end of the experiments, the amounts of total carbohydrates remaining in the stomach compartment were $28.2 \pm 1.6\text{g}\cdot\text{L}^{-1}$ and $7.3 \pm 0.4\text{g}$ for the Zollinger-Ellison syndrome, $28.8 \pm 3.8\text{g}\cdot\text{L}^{-1}$ and $3.1 \pm 0.3\text{g}$ for the normal condition and $92.9 \pm 1.9\text{g}\cdot\text{L}^{-1}$ and $0.20 \pm 0.01\text{g}$ for the hypochlorhydria condition. In terms of concentration, the initial total carbohydrate concentration was smaller than that of the final value for the hypochlorhydria condition. Throughout the experiments, the obtained chyme samples from the hypochlorhydria condition contained large chunks of undigested rice particles unlike the other two conditions. This would seem to be caused by having nearly half of the gastric secretion but of the same rate of gastric emptying. The geometrical advantage of having the greater curvature of the stomach in the IPUGS allowed the solid particles to be deposited and remained in the stomach compartment for further digestion. However with the hypochlorhydria condition, not enough time was allowed for all the reactants to be mixed

thoroughly. All the samples were opaque yellowish in color and slightly viscous due to mucosal secretions.

7.3.2. Somogyi-Nelson Method

The Somogyi-Nelson method was used to analyze the concentration (g.L^{-1}) and the mass of maltose (g) in the stomach compartment which varied considerably from 1.3 to 17.8g.L^{-1} and 0 to 8g, respectively, throughout the experiment as illustrated by the Figures 7-7 and 7-8. Maltose is a reducing sugar which is a byproduct released during the conversion of amylopectin to amylose and/or amylose converted to a shorter chain of carbohydrate in the process of starch hydrolysis (Frazier *et al*, 1997). Hence observing the trend of the concentration and the mass of maltose in the collected chyme samples over the 3hr digestion period facilitates the evaluation of whether the application of different rates of motility in the IPUGS was able to detect a significant difference in the digestion of rice between the normal and the impaired secretory patterns seen in the patients with Zollinger-Ellison syndrome and hypochlorhydria.

The initial values of the maltose concentrations were considerably low but of similar values to one another – $1.33\pm 0.07\text{g.L}^{-1}$ and $0.02\pm 0.01\text{g}$ for the Zollinger-Ellison syndrome, $1.34\pm 0.02\text{g.L}^{-1}$ and $0.02\pm 0.01\text{g}$ for the normal condition and $1.37\pm 0.07\text{g.L}^{-1}$ and $0.02\pm 0.01\text{g}$ for the hypochlorhydria condition. This shows that the initial amounts of maltose for all the conditions were very similar to each other, demonstrating a good control in preparing the feed mixture. Along with the rapid increase of total carbohydrates as seen in the Figures 7-5 and 7-6, the amounts of maltose also increased rapidly up to 40min for the hypochlorhydria condition, with the maximal values of $16.0\pm 0.3\text{g.L}^{-1}$ and $6.6\pm 0.2\text{g}$. However for the Zollinger-Ellison syndrome and the normal condition, the maximal values were $17.9\pm 0.1\text{g.L}^{-1}$ and $7.4\pm 0.2\text{g}$, and $17.5\pm 0.1\text{g.L}^{-1}$ and $7.9\pm 0.2\text{g}$, respectively.

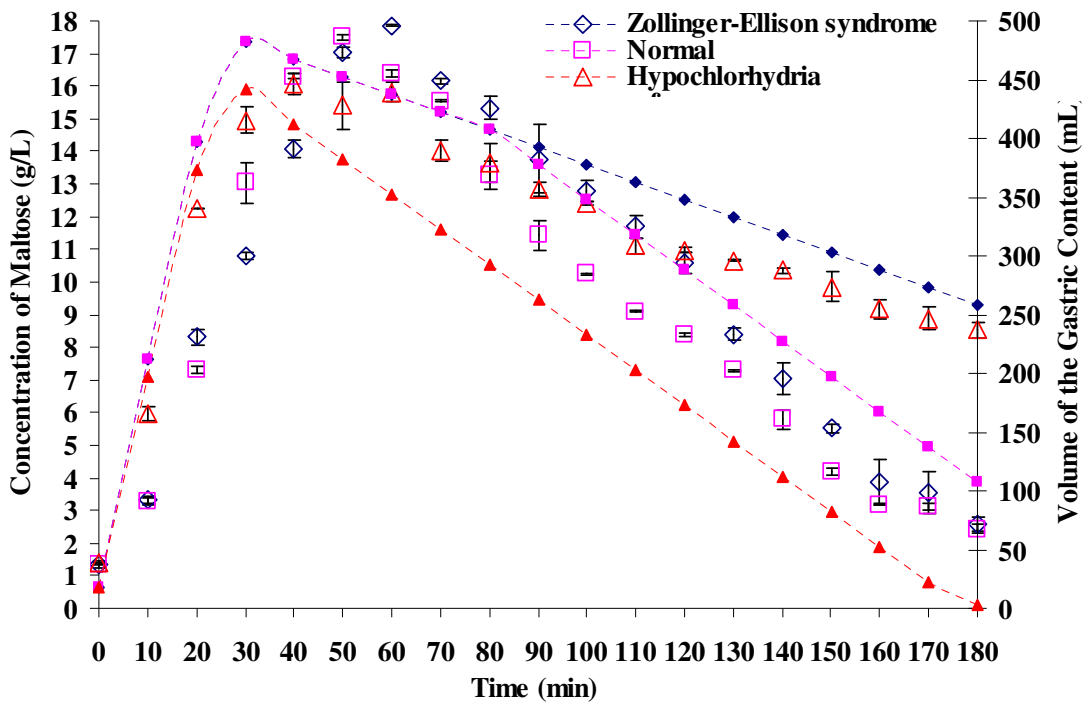


Figure 7-3. A graph showing the concentration of maltose (g) in the stomach compartment during the 3hr digestion time (min). The results obtained from simulating the secretory conditions of Zollinger-Ellison Syndrome are marked with empty dots in blue, the normal state in pink and the Hypochlorhydria condition in red. The volumes of the gastric content (mL) for different secretory conditions are shown with filled dots with accordance of color and shape for each condition.

The faster the rate of the secretion, the faster the hydrolysis of the rice starch, thus the rate of maltose production was faster. Therefore the amounts of maltose in the stomach compartment at any given times were smaller than that of the other two conditions with higher rates of secretions. The increasing and the decreasing trends of maltose mass over time fitted well with parabolic function of R^2 values of greater than 0.9769 and 0.9789, respectively. The overall trend of change in maltose concentration was very similar to that of the maltose mass with respect to time for the conditions of Zollinger-Ellison syndrome and normal state. However with the hypochlorhydria, the change in maltose concentration from 80 to 180min was very small compared to a rapid drop observed in the mass of maltose graph (Figure 7-4). A sharp increase in maltose concentration was seen when the total water soluble carbohydrates and the mass of the unconverted starch in the stomach compartment kept increasing.

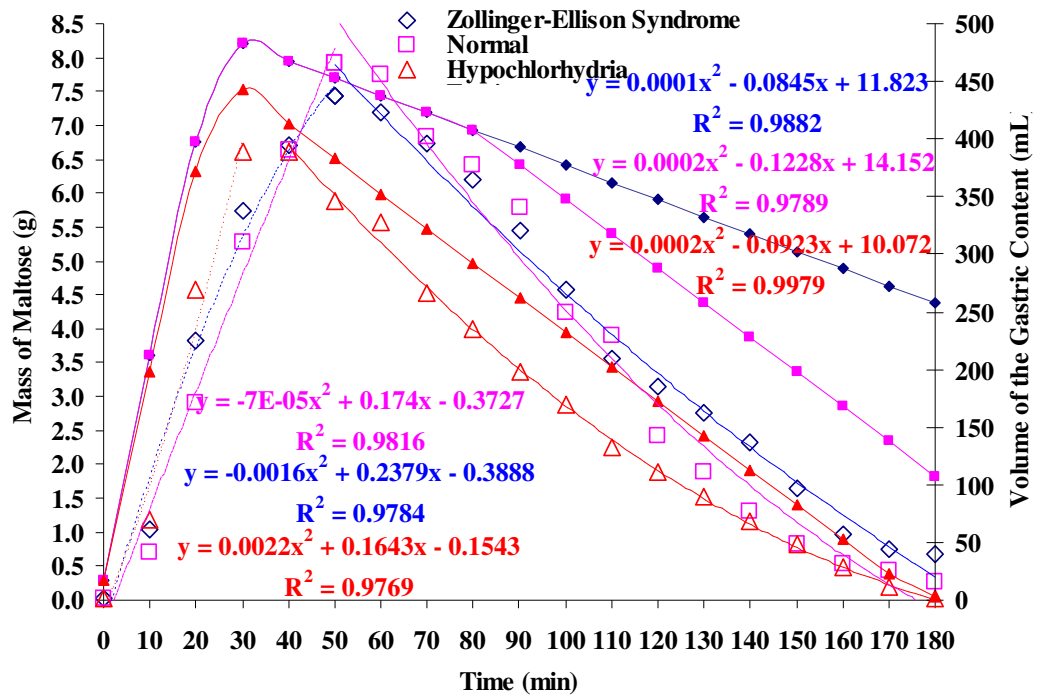


Figure 7-4. A graph showing the mass of maltose (g) during the 3hr digestion time (min). The results obtained from simulating the secretory conditions of Zollinger-Ellison Syndrome are marked with empty dots in blue, the normal state in pink and the Hypochlorhydria condition in red. The volumes of the gastric content (mL) for different secretory conditions are shown with filled dots with accordance of color and shape for each condition.

The change in the mass of the unconverted starch (g) in the stomach compartment of the IPUGS (Figure 7-5) showed very similar overall change compared to that of the mass of the total carbohydrates (Figure 7-1). The increase in the rate and the pattern of the masses of the unconverted starch, total carbohydrates and maltose were similar to each other, which followed the increase in the volume of the gastric content (mL) of the stomach due to the ingestion of the meal. However during the gastric emptying period, the pattern of decrease in the mass of the unconverted starch in the Zollinger-Ellison condition was significantly different to that of the gastric volume change. However with the hypochlorhhdria condition, it would seem that the change in the gastric volume has largely influenced the mass of the unconverted starch with respect to time. It can be speculated that not enough gastric juice was available to carry on the starch hydrolysis in the IPUGS. The conditions of the normal and Zollinger-Ellison state showed less linear trend of decrease during the gastric emptying time.

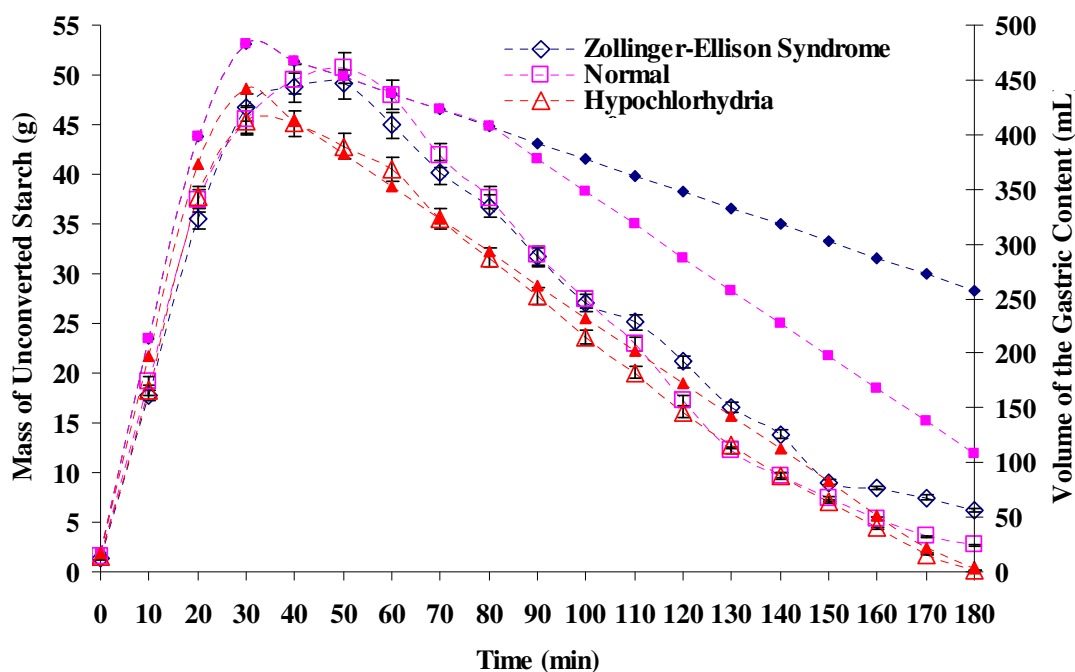


Figure 7-5. A graph showing the mass of unconverted starch (g) in the stomach compartment during the 3hr digestion time (min). The results obtained from simulating the secretory conditions of Zollinger-Ellison Syndrome are marked with empty dots in blue, the normal state in pink and the Hypochlorhydria condition in red. The volumes of the gastric content (mL) for different secretory conditions are shown with accordance of color and shape for each condition.

Although the differences in the amounts of the total carbohydrates, unconverted starch and maltose have been shown clearly, a better understanding of the rice starch hydrolysis was attained when the ratio of maltose to unconverted starch, in terms of mass, was plotted (Figure 7-6). The ratio of maltose to starch is an important indication to how much of amylopectin and amylose were hydrolyzed to release the reducing sugar (maltose). The ratio of maltose to unconverted starch increased rapidly during the ingestion period for all the conditions. From 32min mark, the values of the ratio started to diverge, with the Zollinger-Ellison syndrome showing the highest values and the hypochlorhydria condition showing the lowest values among the three conditions most of the time. At 150min, the Zollinger-Ellison syndrome condition reached the maximum ratio of 0.182, whereas for the normal condition, the maximum ratio of 0.156 was reached at 50min, and the hypochlorhydria condition reached the maximum ratio of 0.147 at 40min. The final values of the ratios were very similar to each other, with 0.10 ± 0.01 as an average value. As the limited amounts of secretions were available to compensate for excessive amount of the food, the interaction of the secretions and the undigested foods seemed to have diminished, showing the lowest range of values for the hypochlorhydria condition.

However for the Zollinger-Ellison syndrome, the newly delivered gastric secretions at higher rate throughout the digestion period have higher chance of reacting with the ingested food materials. The results indicate that provided the same feed materials and the same motility and gastric emptying conditions were supplied, the effect of secretion rates on starch hydrolysis can be perceived.

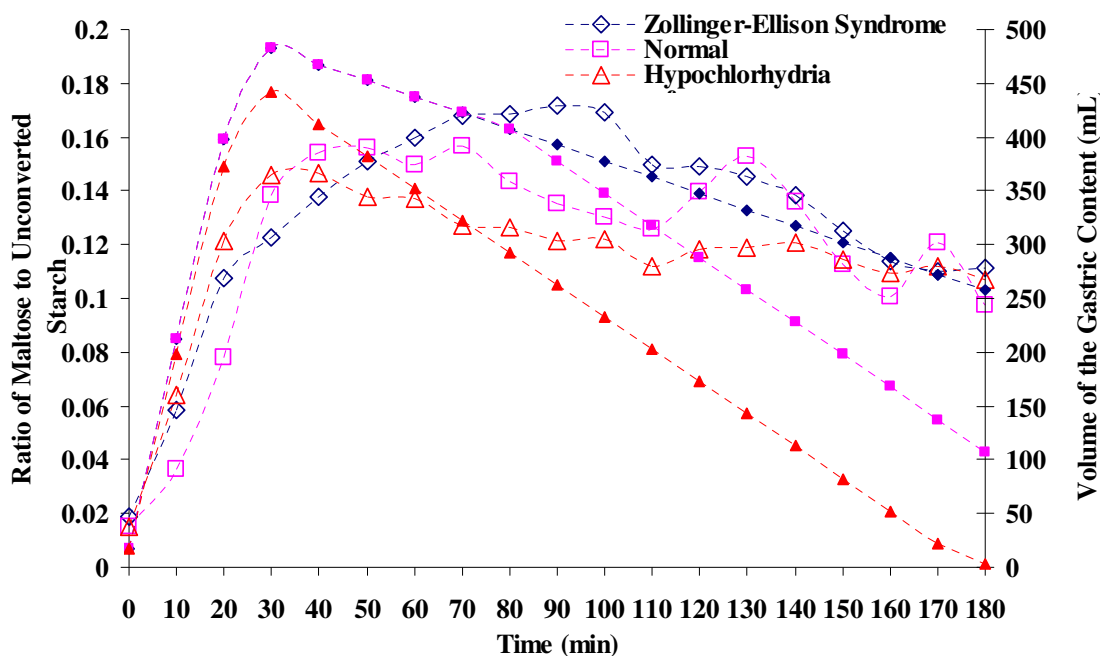


Figure 7-6. A graph showing the ratio of the mass of the maltose to the mass of the unconverted starch with respect to time. The results obtained from simulating the secretory conditions of Zollinger-Ellison Syndrome are marked with empty dots in blue, the normal state in pink and the Hypochlorhydria condition in red. The volumes of the gastric content (mL) for different secretory conditions are shown with filled dots with accordance of color and shape for each condition.

7.3.3. HPLC

Using the HPLC, an overall screening of the collected samples was made to clarify the presence of maltose and to identify the possible byproducts of the rice starch hydrolysis. As a result, maltose and maltotriose were detected. The starch hydrolysis in the normal human subjects usually do not result in glucose, as the partially unconverted starch as well as maltose are further digested by pancreatic α -amylase in the small intestines.

In general, the mass of maltose analyzed from the HPLC showed slightly lower values (Figure 7-7) compared to that of the UV-spectrophotometer. This seemed to be caused by

the waiting period of the samples collected from the models until the analysis. Although the samples were kept in an ice water bath, and diluted accordingly to a factor of 40, some samples had to wait over 10hrs until the analysis began. However the standing time at room temperature for the UV-spectrophotometric measurements was much shorter when compared to that of the HPLC. Also after dilutions, the samples were chemically treated with arseno and somogyi reagents, where there were no treatments for the HPLC samples.

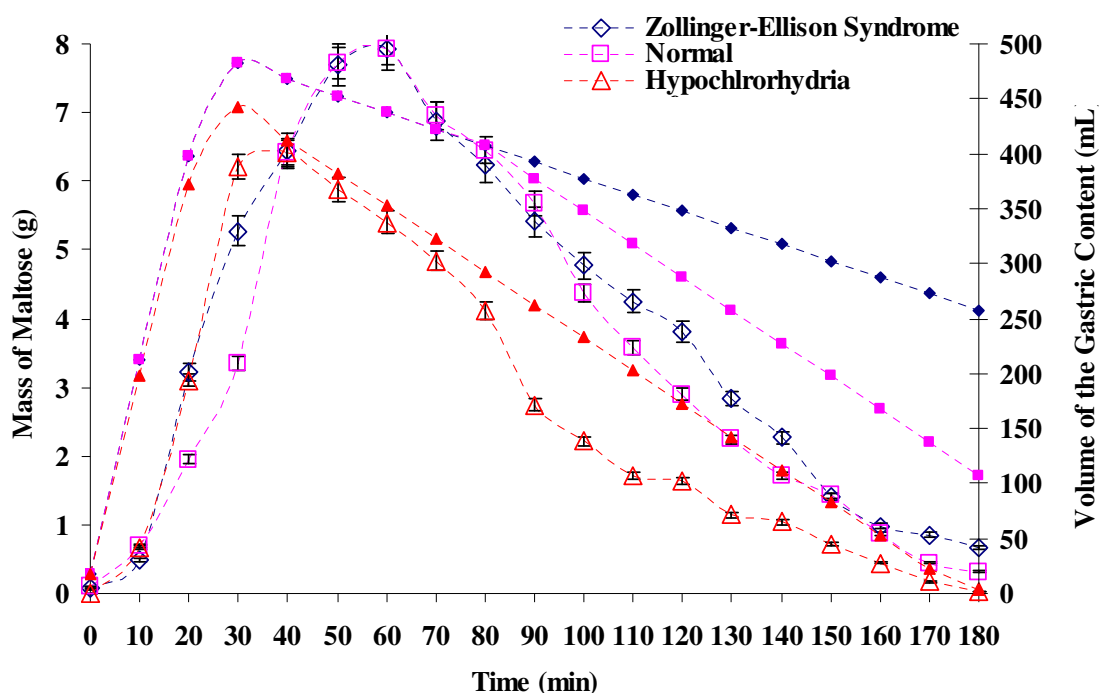


Figure 7-7. A graph showing the mass of maltose (g) in the stomach compartment measured by the HPLC. The results obtained from simulating the secretory conditions of Zollinger-Ellison Syndrome are marked with empty dots in blue, the normal state in pink and the Hypochlorhydria condition in red. The volumes of the gastric content (mL) for different secretory conditions are shown with filled dots with accordance of color and shape for each condition.

Even with the use of the shortest column to examine the sample in the HPLC, it took 15-30min, as the HPLC column requires cleaning time to avoid any blockage and accumulation of carbohydrate molecules which may cause interference amongst the samples for analyses. As many of the samples were kept in the auto-sampler at room temperature overnight, it might have caused a further digestion, most likely to be acidic hydrolysis, during the waiting period to be analyzed. In spite of this, the overall trend of the maltose mass was very similar to that found using the UV-spectrophotometer.

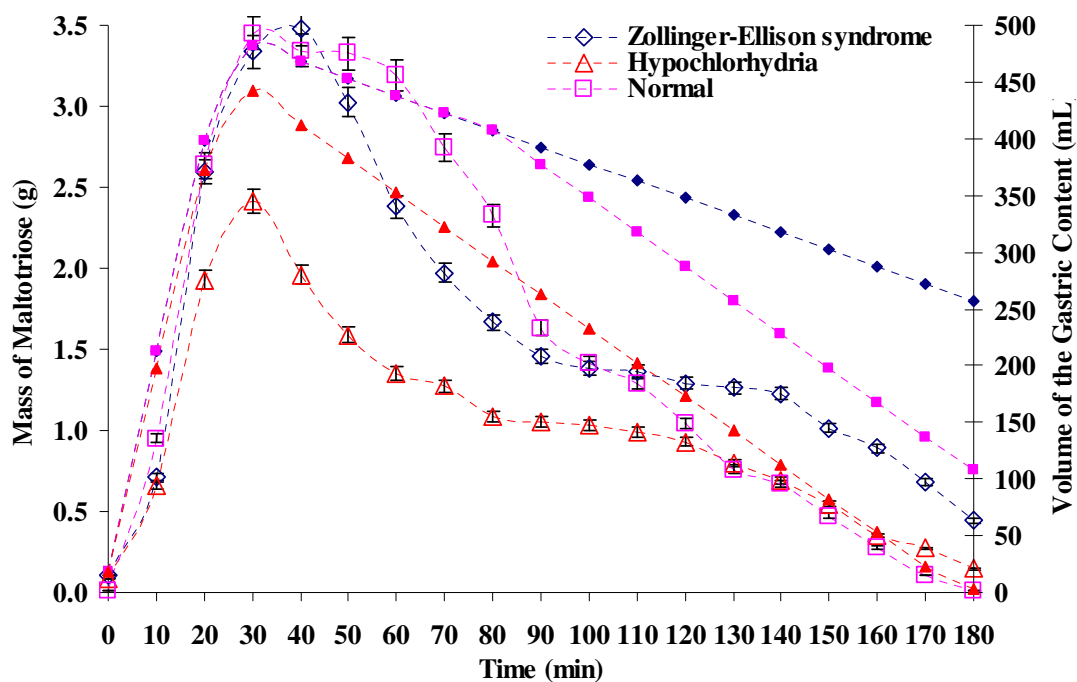


Figure 7-8. A graph showing the mass of maltotriose (g) in the stomach compartment measured by the HPLC. The results obtained from simulating the secretory conditions of Zollinger-Ellison Syndrome are marked with empty dots in blue, the normal state in pink and the Hypochlorhydria condition in red. The volumes of the gastric content (mL) for different secretory conditions are shown with filled dots with accordance of color and shape for each condition.

Maltotriose concentration was detected by the HPLC. In order to avoid any arbitrary confusions, the obtained values of the concentration ($\text{g}\cdot\text{L}^{-1}$) were converted to the mass of maltotriose present (g) by multiplying the gastric content volume (Figure 7-8) to the concentration. Initially, increase in the mass of maltotriose was almost exponential for both the normal and the Zollinger-Ellison syndrome conditions, reaching the maximal values of 3.45g and 3.33g, respectively, at 30min. The hypochlorhydria condition showed the smallest values at all times, reaching the maximum value of 2.41g at 30min. As it has been noticed by the previous graphs, up to 90min mark where there rate of the gastric secretions for both the normal and the Zollinger-Ellison syndrome conditions were kept the same, the values were similar to one another. However from 90min to 180min, the values of the normal condition started to drift, showing similar values to the hypochlorhydria condition of the same secretion rate, especially toward the end of the experiments. Overall, the trend of the mass of maltotriose over time was very similar to that of the mass of maltose, where the lowest values were seen with the hypochlorhydria condition throughout the experiments, followed by the normal and the Zollinger-Ellison syndrome conditions.

7.3.4. Recording of the pH

The pH profile is one of the widely used tools to indicate the feasibility of an *in vitro* testing method, especially for clinical studies such as the interaction of drug and the gastric secretions, disintegration of coating materials and capsules, and possible interference of more than one type of drug taken at the same time (Dressman *et al*, 1990; Hörter and Dressman, 1997; Hörter and Dressman, 2001). The pH profile is able to emphasize the overall control of motility as well as secretions applied, and in conjunction with results from the Phenol-Sulfuric acid assay, the Somogyi-Nelson method and the HPLC, a better understanding of the effect of different frequency of the motility can be perceived. Two probes were used for measuring the pH of the IPUGS. Probe 1 (Figure 7-9) refers to the pH probe which was implanted at the wall of the fundus, where the majority of the acidic gastric secretions took place with mucosal secretions of less extent, and probe 2 (Figure 7-10) was implanted on the wall of the antrum which acts as a temporal reservoir in storing of the ingested foods with mucosal secretions to protect the wall of the stomach.

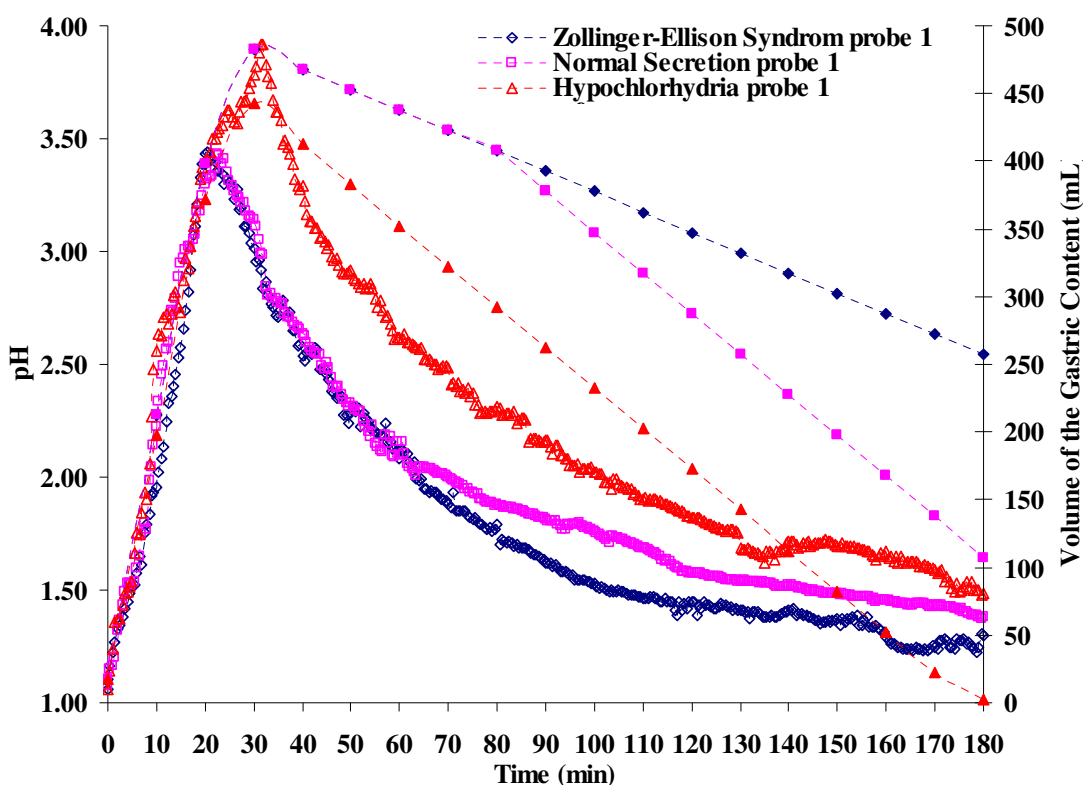


Figure 7-9. The pH profile of the pH probe 1 (fundus) over 3hr digestion period. The results from the simulation of the Zollinger-Ellison Syndrome condition are marked in blank blue dots, the normal state in pink and hypochlorhydria condition in red. The volumes of the gastric content (mL) for different secretion conditions are shown with filled dots with accordance of color and shape for each condition.

Initially the pH values of the three conditions were nearly the same, about 1.03 ± 0.01 , which reflects the pH of the gastric secretion containing 0.15M HCl. The pH profiles of the three conditions were indistinguishable to each other up to 20min. The pH values of the hypochlorhydria condition kept increasing until the end of the ingestion period and reached the peak value of 3.92 ± 0.05 , showing the highest buffering capacity of the ingested meal due to insufficient gastric juice to acidify the ingested meal to aid digestion. For the normal and the Zollinger-Ellison syndrome conditions, the peak pH values of 3.34 ± 0.05 and 3.35 ± 0.05 were reached, respectively. As the ingested feed material was building up in the antrum without being mixed well with the acidic gastric secretion from the fundus, the pH in the antrum as well as in the fundus (Figure 7-10) have kept on increasing. In the antrum, the peak pH reached was 4.16 ± 0.04 with the hypochlorhydria condition, which was the highest amongst the three conditions. The rate of decrease in pH differed noticeably for the hypochlorhydria condition due to the higher maximum pH value.

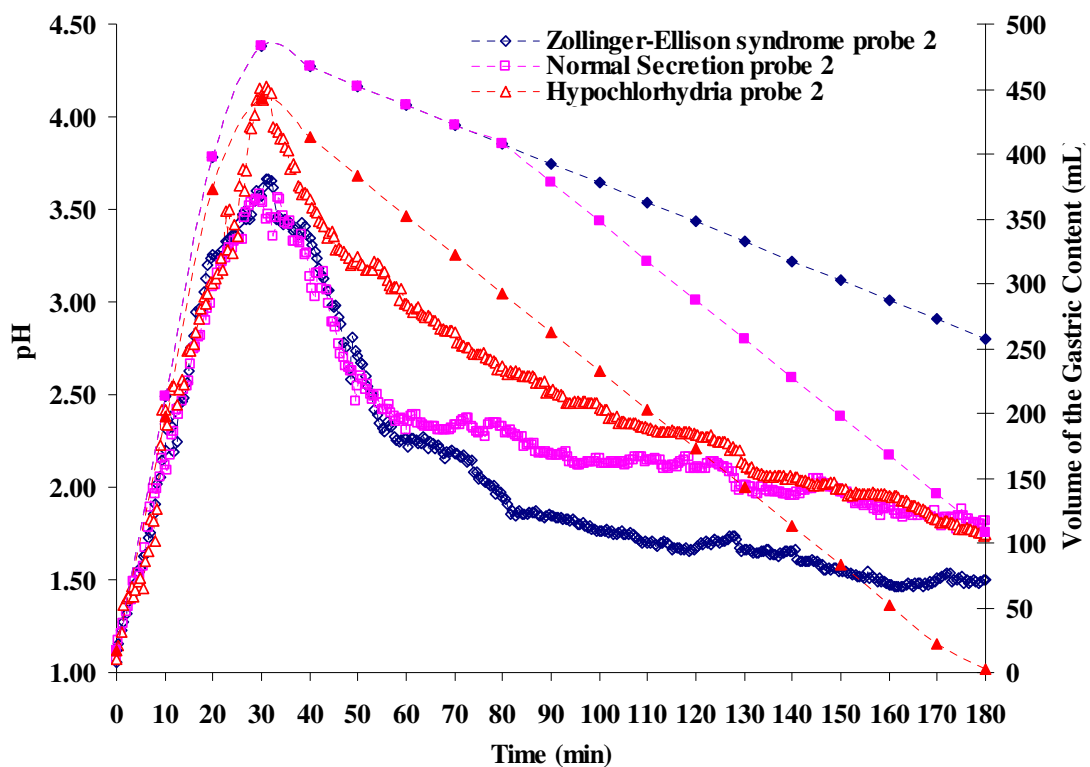


Figure 7-10. The pH profile of the pH probe 2 (antrum) over 3hr digestion period. The results from the simulation of the Zollinger-Ellison Syndrome condition are marked in blank blue dots, the normal state in pink and hypochlorhydria condition in red. The volumes of the gastric content (mL) for different secretion conditions are shown with filled dots with accordance of color and shape for each condition.

The pH profiles of the normal and the Zollinger-Ellison syndrome conditions were nearly the same up to 60min mark for the probe 1 and around 55min mark for the probe 2, and started to diverge since then. It was expected to diverge from the 90min mark, which was the point of change in the gastric secretion rate for the normal condition, however it was perceived earlier. By 90min mark, it was very clear that the pH values of the three conditions differed from one another – the hypochlorhydria condition showing the highest values, the normal condition in the middle and the Zollinger-Ellison syndrome condition showing the lowest values as the high rate of the gastric secretions exceeded the buffering capacity of the ingested meal. The trend of the pH profiles seen in the probe 2 (Figure 7-10) did not show much difference to that of the probe 1 (Figure 7-9). The end values of the probe 2 (antrum) for the normal and the hypochlorhydria conditions were very similar to one another, 1.82 ± 0.04 and 1.74 ± 0.04 , respectively.

7.4. Concluding Remarks and Future Works

The rate of the gastric secretions in the IPUGS was varied to study two common GI secretory disorders, gastroparesis and dumping syndrome. Yet, the study of secretion disorders have never been conducted via *in vitro* digestion models in the literature. Provided a detailed clinical data of such patients, parameters used in the IPUGS can be altered to simulate other uncommon conditions of the GI disorders to understand and predict the digestive processes without the hassle of the ethical constraints with efficiency in time and costs. With the use of slower and faster rates of the gastric secretions, variations in the pattern and the values of the total water soluble carbohydrates, maltose, maltotriose, unconverted rice starch and pH were perceived. Comparison of the ratio of the mass of the maltose to the mass of the unconverted rice starch confirmed a clearer difference between the Zollinger-Ellison syndrome, the hypochlorhydria and the normal conditions once more. The pH profiles among the three conditions also differed noticeably, especially between the Zollinger-Ellison syndrome and the hypochlorhydria conditions. By using the data from many physiological and clinical sources in the literature, the parameters such as the rate of secretions of particular components in the GI secretions, either enzymes or ionic components, can be altered to further study the secretory disorders of not only humans but in animals as well. Provided that the difference in the rate of gastric secretions was bigger than that used in the study, a clearer difference could have been observed by using of the IPUGS. Overall, the IPUGS was able to simulate the conditions of the gastric secretory disorders as described in the literatures

and resulted similar outcomes in many ways. As the research with the secretory disorders has not been conducted as extensively as that of the motility disorders, the results shown in this chapter may seem expository. Nevertheless, the IPUGS can be of a useful tool in predicting of the digestive process and can also be used as a clinical tool with or without *in vivo* studies.

7.5. References

- Akin, A. (1998) Non-invasive detection of spike activity of the stomach from cutaneous EGG. *PhD Thesis* Drexel University, Philadelphia
- Allen, A., Pain, R. H., Robson, T. R. (1976). Model for the structure of the gastric mucous gel. *Nature*, 264, 88-89
- Allerscher, H. D., Abraham-Fuchs, K., Dunkel, R. E., Classen, M. (1998) Biomagnetic 3-Dimensional spatial and temporal characterization of electrical activity of human stomach. *Digestive diseases and sciences*, 43 (4), 683-693
- Al-Zaben, A., Chandrasekar, V. (2005). Effect of esophagus status and catheter configuration on multiple intraluminal impedance measurements. *Physiol. Meas.*, 26, 229-238
- Arthur, R., Gruner, T. (2007) Digestion and enzymes. *Complementary Medicine*, 6 (1), 54-59
- Barker, M. C., Cobden, I., Axon, A. T. (1979). Proximal stomach and antrum in stomach emptying. *Gut*, 20, 309-311
- Bell, A. E., Sellers, L. A., Allen, A., Cunliffe, J., Morris, E. R., Ross-Murphy, S. B. (1985). Properties of duodenal mucus: effect of proteolysis, disulfide reduction, bile acid, ethanol and hypertonicity on mucus gel structure. *Gastroenterology*, 88, 269-280
- Björck, I., Granfeldt, Y., Liljeberg, H., Tovar, J., Asp, N. G. (1994) Food properties affecting the digestion and absorption of carbohydrates. *Am. J. Clin. Nutr.*, 59 (Suppl.), 699S-705S
- Cadiot, G., Vuagnat, A., Doukhan, I., Murat, A., Bonnaud, G., Delemer, B., Thieffin, G., Beckers, A., Veyrac, M., Proye, C., Ruszniewski, P., Mignon, M. (1999) Prognostic factors in patients with Zollinger-Ellison syndrome and multiple endocrine neoplasia type 1. *Gastroenterology*, 116, 286-293
- Cater, R. E. (1992a) The clinical importance of hypochlorhydria (A consequence of chronic Helicobacter infection): Its possible etiological role in mineral and amino acid malabsorption, depression and other syndromes. *Medical Hypotheses*, 39, 375-383
- Cater, R. E. (1992b) Helicobacter (aka Campylobacter) pylori as the major casual factor in chronic hypochlorhydria. *Medical Hypotheses*, 39, 367-374
- Charman, W. N., Porter, C. J. H., Mithani, S., Dressman, J. B. (1997). Physicochemical and physiological mechanisms for the effects of food on drug absorption: The role of lipids and pH. *J. Pharmaceutical Sciences*, 86 (3), 269-282
- Collen, M. J., Jensen, R. T. (1994) Idiopathic gastric acid hypersecretion. Comparison with Zollinger-Ellison syndrome. *Digestive Diseases and Sciences*, 39 (7), 1434-1440
- De Martel, C., Ratanasopa, S., Passaro, D., Parsonnet, J. (2006) Validation of the blood quininium resin test for assessing gastric hypochlorhydria. *Digestive Diseases and Sciences*, 51 (1), 84-88
- De Zwart, I. M., Mearadji, B., Lamb, H. J., Eilers, P. H. C., Masclee, A. A. M., De Roos, A., Kunz, P. (2002). Gastric motility: comparison of assessment with real-time MR imaging or barostat measurement - initial experience. *Radiology*, 224, 592-597
- Dressman, J. B., Berardi, R. R., Dermentzoglou, L. C., Russel, T. L., Schmaltz, S. P., Barnett, J. L., Jarvenpaa, K. M. (1990). Upper gastrointestinal (GI) pH in young, healthy men and women. *Pharmaceutical Research*, 7 (7), 756-761
- Dubois, M., Gilles, K., Hamilton, J. K., Rebers, P. A., Smith, F. (1951). A colorimetric method for the determination of sugars. *Nature*, 168, 167
- Dubois, M., Gilles, K., Hamilton, J. K., Rebers, P. A., Smith, F. (1956). Colorimetric method for the determination of sugars and related substances, *Anal. Chem.*, 28, 350-356

- Edgar, W. M. (1990). Saliva and dental health. *British Dental Journal*, 169 (3-4), 96-98
- Elashoff, J. D., Reedy, T. J., Meyer, J. H. (1982). Analysis of gastric emptying data. *Gastroenterology*, 83, 1306-1312
- Ellison, E. H., Carey, L. (1963) Diagnosis and management of the Zollinger-Ellison syndrome. *The American Journal of Surgery*, 105, 383-387
- Ellison, E. C., Sparks, J. (2003) Zollinger-Ellison syndrome in the era of effective acid suppression: are we unknowingly growing tumors? *The American Journal of Surgery*, 186, 245-248
- El-Zimaity, H. M. T. (2007) Recent advances in the histopathology of gastritis. *Current Diagnostic Pathology*, 13, 340-348
- Feldman, M., Barnett, C. (1991) Fasting gastric pH and its relationship to true hypochlorhydria in humans. *Digestive Diseases and Sciences*, 36 (7), 866-869
- Franco, C. M. L., Preto, S. J. R., Ciacco, C. F. (1992) Factors that affect the enzymatic degradation of natural starch granules: effect of the size of the granules. *Starch*, 44, 422-426
- Frazier, P. J., Richmond, P., Donald, A. M. (1997). *Starch: Structure and Functionality*. The Royal Society of Chemistry.
- Freston, J. W., Borch, K., Brand, S. J., Carlsson, E., Creutzfeldt, W., Håkanson, R., Olbe, L., Solcia, E., Walsh, J. H., Wolfe, M. M. (1995) Effects of hypochlorhydria and hypergastrinemia on structure and function of gastrointestinal cells. *Digestive Diseases and Sciences*, 40 (2), 50S - 62S
- Gal, J-Y, Fovet, Y, Adib-Yadzi, M. (2001). Review: About a synthetic saliva for in vitro studies. *Talanta*, 53, 1103-1115
- Harford, W. V., Barnett, C., Lee, E., Perez-Perez, G., Blaser, M. J., Peterson, W. L. (2000) Acute gastritis with hypochlorhydria: report of 35 cases with long term follow up. *Gut*, 47 (4), 467-472
- Hills, B. A. (1985). Gastric mucosal barrier: stabilization of hydrophobic lining to the stomach by mucus. *Am. J. Physiol.* 249 (Gastrointest. Liver Physiol. 12), G342-G349
- Holm, J., Lundquist, I., Björck, I., Eliasson, A., Asp, N. G. (1988) Degree of starch gelatinization, digestion rate of starch *in vitro* and metabolic response in rats. *Am. J. Clin. Nutri.*, 47, 1010-1016
- Hörter, D., Dressman, J.B. (1997) Influence of physicochemical properties on dissolution of drugs in the gastrointestinal tract. *Advanced Drug Delivery Reviews* 25, 3-14
- Hörter, D., Dressman, J.B. (2001) Influence of physicochemical properties on dissolution of drugs in the gastrointestinal tract. *Advanced Drug Delivery Reviews* 46, 75-87
- Humphrey, S. P., Williamson, R. (2001). A review of saliva: Normal composition, flow and function. *The Journal of Prosthetic Dentistry*, 85 (2), 162-169
- Iijima, K., Sekine, H., Koike, T., Imatani, A., Ohara, S., Shimosegawa, T. (2004) Long-term effect of *Helicobacter pylori* eradication on the reversibility of acid secretion in profound hypochlorhydria. *Aliment. Pharmacol. Ther.*, 19, 1181-1188
- Joseph, I. M. P., Zavros, Y., Merchant, J. L., Kirschner, D. (2003) A model for integrative study of human gastric acid secretion. *J. Appl. Physiol.*, 94, 1602-1618
- Kararli, T. T. (1995). Review article: Comparison of the gastrointestinal anatomy, physiology and biochemistry of humans and commonly used laboratory animals. *Pharmaceutics & Drug Disposition*, 16, 351-380
- Kelly, K. A. (1974) Gastric motility after gastric operations. *Surgery Annual.*, 6, 103-123
- Kim, J. C., Kim, J. I., Kong, B. W., Kang, M. J., Kim, M. J., Cha, I. J. (2004) Influence of the physical form of processed rice products on the enzymatic hydrolysis of rice starch in vitro and on the postprandial glucose and insulin response in patients with Type 2 Diabetes Mellitus. *Biosci. Biotechnol. Biochem.*, 68 (9), 1831-1836
- Klein, S., Butler, J., Hempenstall, J. M., Reppas, C., Dressman, J. B. (2004) Media to simulate the postprandial stomach I. Matching the physicochemical characteristics of standard breakfasts. *J. Pharma. Pharmacol.*, 56, 605-610
- Kwiecień, S., Konturek, S. J. (2003). Gastric analysis with fractional test meals (ethanol, caffeine, and peptone meal), augmented histamine or pentagastrin tests, and gastric pH recording. *Journal of Physiology and Pharmacology*, 54 (S3), 69-82
- Lee, K-J., Vos, R., Janssens, J., Tack, J. (2004). Differences in the sensorimotor response to distension between the proximal and distal stomach in humans. *Gut*, 53, 938-943
- Luiking, Y. C., Peeters, T. L., Stolk, M. F., Nieuwenhuijs, V. B., Portincasa, P., Depoortere, I., van Berge Henegouwen, G. P., Akkermans, L. M. A. (1998). Motilin induces gall bladder emptying and antral contractions in the fasted state in humans. *Gut*, 42, 830-835

- Mainville, I., Arcand, Y., Farnworth, E.R. (2005) A dynamic model that simulates the human upper gastrointestinal tract for the study of probiotics. *International Journal of Food Microbiology*, 99, 287-296
- Marciani, L., Gouwland, P. A., Spiller, R. C., Manoj, P., Moore, R. J., Young, P., Fillery-Travis, A. J. (2001) Effect of meal viscosity and nutrients on satiety, intragastric dilution and emptying assessed by MRI. *Am. J. Physiol. Gastrointest. Liver Physiol.*, 280, G1227-1233
- Masuko, T., Minami, A., Iwasaki, N., Majima, T., Nishimura, S-I., Lee, Y. C. (2005) Carbohydrate analysis by a phenol-sulfuric acid method in microplate format. *Analytical Biochemistry*, 339, 69-72
- McArthur, K., Hogan, D., Isenberg, J. (1982) Relative stimulatory effects of commonly ingested beverages on gastric acid secretions in humans. *Gastroenterology*, 83, 199-203
- Minekus, M., Marteau, P., Havenaar, R., Huis in't Veld, J. H. J. (1995). A multicompartamental dynamic computer-controlled model simulating the stomach and small intestine. *Alternatives to Laboratory Animals*, 23, 197-209
- Mossi, S., Meyer-Wyss, B., Beglinger, C., Schwizer, W., Fried, M., Ajami, A., Brignoli, R. (1994). Gastric emptying of liquid meals measured noninvasively in humans with [¹³C] acetate breath test. *Digestive Diseases and Sciences*, 39(12), 107S-109S
- Nelson, N. (1944) A photometric adaption of the Somogyi method for the determination of glucose. *J. Biol. Chem.*, 153, 375-380
- Nguyen, H. N., Silny, J., Matern, S. (1999). Multiple intraluminal electrical impedancometry for recording of upper gastrointestinal motility: current results and further implications. *Am. J. Gastroenterology*, 94 (2), 306-317
- Pade, V., Aluri, J., Manning, L., Stavchansky, S. (1995) Bioavailability of pseudoephedrine from controlled release formulations in the presence of guaifenesin in human volunteers. *Biopharmaceutics & Drug Disposition*, 16, 381-391
- Passaro, E., Basso, N., Sanchez, R. E., Gordon, H. E. (1970) Newer studies in the Zollinger-Ellison syndrome. *The American Journal of Surgery*, 120, 138-143
- Pehlivanov, N., Liu, J., Kassab, G. S., Beaumont, C., Mital, R. K. (2002). Relationship between esophageal muscle thickness and intraluminal pressure in patients with esophageal spasm. *Am. J. Physiol. Gastrointest. Liver Physiol.*, 282, 1016-1023
- Preetha, A., Banerjee, R. (2005). Comparison of artificial saliva substitutes. *Trends Biomater. Artif. Organs*, 18 (2), 178-186
- Rao, P., Pattabiraman, T. N. (1989). Reevaluation of the phenol-sulfuric acid reaction for the estimation of hexoses and pentoses. *Anal. Biochem.*, 181, 18-22
- Rees, W. D. W., Botham, D., Turnberg, L. A. (1982) A demonstration of bicarbonate production by the normal human stomach in vivo. *Digestive Diseases and Sciences*, 27 (11), 961-966
- Schwizer, W., Frazer, R., Borovicka, J., Crelier, G., Boesiger, P., Fried, M. (1994). Measurement of gastric emptying and gastric motility by magnetic resonance imaging (MRI). *Digestive Diseases and Sciences*, 39 (12), 101S-103S
- Shellis, R. P. (1978). A synthetic saliva for cultural studies of dental plaque. *Archs. Oral Biol.*, 23, 485-489
- Somogyi, M. (1926) Notes on sugars determination. *J. Biol. Chem.*, 79, 599-613
- Somogyi, M. (1937) A reagent for the copper iodometric determination of vary small amounts of sugar. *J. Biol. Chem.*, 117, 771-776
- Somogyi, M. (1945) A new reagent for the determination of sugars. *J. Biol. Chem.*, 160, 61- 68
- Suzuki, S. (1987) Experimental studies on the presumption of the time after food intake from stomach contents. *Forensic Science International*, 35, 83-117
- Taylor, A. J., Linforth, R. S. T. (1996) Flavour release in the mouth. *Trends in Food Science and Technology*, 7, 444-448
- Tortora, G. J., Grabowski, S. R. (2000) Principles of anatomy and physiology. 9th Edition. John Wiley and Sons, Inc., Chapter 24, The Digestive System. pp.818-870
- Whitehouse, G. H., Temple, J. G. (1977) The evaluation of dumping and diarrhoea after gastric surgery using a physiological test meal. *Clin. Radiol.*, 28, 143-149
- Williamson, G., Belshaw, N. J., Sief, D. J., Noel, T. R., Rings, S. G., Cairns, P., Morris, V. J., Clark, S. A., Parker, M. L. (1992) Hydrolysis of A and B type crystalline polymorphs of starch by α -amylase, β -amylase and glucoamylase. *Carbohydr. Polym.*, 18, 179-187
- Winship, D. H., Ellison, E. H. (1967) Variability of gastric secretion in patients with and without the Zollinger-Ellison syndrome. *The Lancet*, 1128-1130

- Wong, L., Sissions, C. H. (2001). A comparison of human dental plaque microcosm biofilms grown in an undefined medium and a chemically defined artificial saliva. *Archives of Oral Biology*, 46, 477-486
- Wright, H. K., Hersh, T., Floch, M. H., Weinstein, L. D. (1970) Impaired intestinal absorption in the Zollinger-Ellison syndrome independent of gastric hypersecretion. *The American Journal of Surgery*, 119, 250-253
- Wrolstad, R. E., Acree, T. E., Decker, E. A., Penner, M. H., Reid, D. S., Schwartz, S. J., Schoemaker, C. F., Smith, D. M., Sporns, P. (2005) *Handbook of food analytical chemistry. Water, proteins, enzymes, lipids and carbohydrates.* Hoboken, N. J. Wiley.

Chapter 8

Mathematical Modeling of the *In vitro* Physicochemical Upper Gastrointestinal System (IPUGS)

8.1. Introduction to mathematical and computational modeling of the human gastrointestinal tract (GIT)

Compared to the infinite research on the *in vitro* digestion models, relatively insignificant number of mathematical and computational models with subject to the human gastrointestinal tract (GIT) has been found in the literature. Numerous softwares simulating the human GIT conditions are available though most of them are focused on pharmaceutical purposes. The mathematical and computational modeling of the *in vitro* digestion models can be divided into five different categories as follows; gastric emptying of nutrients, pharmacokinetics (including gastric emptying and absorption of pharmaceuticals), viability and growth of bacterial strains in the intestinal microflora, gastric secretions and the GI motility. Having such models is useful as these can be applied for both short and long term studies and allow for rapid assessment of global effects (Joseph *et al*, 2003).

One of the most commonly found mathematical equations in the *in vitro* digestion models is the gastric emptying with regards to the fraction of the digested food materials in the stomach compartment with respect to time. Elashoff *et al* (1982) proposed that despite the widely used exponential relationship, power exponential relationship was fitted better with the gastric emptying of the humans. Since then, the power exponential equations describing the gastric and ileal deliveries of foods have been developed with the use of TIM (TNO's gastrointestinal model) by Minekus *et al* (1995), Marteau *et al* (1997) and Blanquet *et al* (2003). Similarly other studies such as $^{13}\text{CO}_2$ breathe test (Meier *et al*, 2006), contractions associated with liquid portion in the gastric content emptying (Pal *et al*, 2007) and optimization of residence times for higher availability of net energy in simple animal tracts (Logan *et al*, 2003) also mathematically modelled the gastric emptying process in relation to nutrients. However, the gastric emptying process in

conjunction with absorption of pharmaceuticals (pharmacokinetics) have been modelled extensively, to study the transport of drugs along the stomach (Pal *et al*, 2007), small intestine (Firmer and Cutler, 1988; Yu and Amidon, 1998; Wu, 1998; Stoll *et al*, 2000), to compute theoretical molecular descriptors of physicochemical properties, for instance, lipophilicity, polarity, polarizability and hydrogen bonding, with MolSurf program and the multivariate Partial Least Squares Projections to Latent Structures (PLS) method (Norinder *et al*, 1999) and to predict the fate of ingested drugs with mechanical simulation (Schmitt and Willmann, 2004).

More comprehensive computational models of physiology-based pharmacokinetics include acs|Extreme™ (aegis Technologies, <http://www.acslextreme.com/>) and Berkeley Madonna™ (University of California Berkeley, <http://www.berkeleymadonna.com/>) which are general simulation softwares with possibility of creating flexible and specific models though simulation expertise is required and no support for model parameterization is given. GastroPlus™ (SimulationsPlus, <http://www.simulationplus.com/>) and IDEA (Lion Bioscience, <http://www.lionbioscience.com/>) are simulations of absorption process which can be useful in discovery phase due to batch modus. However substance properties and input parameters are frequently in need to be determined, although specific simulation expertise is not required. The physiological description is restricted to single absorption, distribution, metabolism and excretion process (Yu and Amidon, 1999; Norris *et al*, 2000). SimCyp® (SimCyp, <http://www.simcyp.com>) is a simulation of metabolism and interactions, where extensive data base with physiological information are included for prediction of population variations without the need of a specific simulation expertise. Physiological description is restricted also limited to single absorption, distribution, metabolism and excretion process and fixed model structure. Whole body simulation with well stirred organs are provided by CloePK™ (Cyprotex, <http://www.cyprotex.com/>) and pkEXPRESS™ (Lion Bioscience, <http://www.lionbioscience.com/>), which describe processes which affect and determine pharmacokinetics. Specific simulation expertise is not required although over-simplification in distribution modelling limits its applicability. Physiological organ model which can simulate the whole body organs such as PK-Sim® (Bayer Technology Services, <http://www.pk-sim.com>), include most important physiological processes with parameters accessible for specific investigations without a specific simulation expertise in need (Willmann *et al*, 2003; Willmann *et al*, 2004).

The bacterial populations in the intestinal microflora, regarding the viability (Spratt *et al*, 2005) and the colonization under limiting nutrient conditions (Ballyk and Smith, 1999

and 2001) and host-microflora interactions (Wilkinson, 2002) has been explored mathematically where over-simplification of the complexity of the GI system and the lack of simulations of the ecological effect resulted in limited extent of predictions.

Mathematical modelling of the bicarbonate secretion release in response to the gastric acid secretion (De Beus *et al*, 1993) and the formation of the gastric acid with translocation of the stored acid into the lumen of the stomach and the storage of the acid (Licko and Ekblad, 1992) provided the concepts of mathematical modeling of the acidic gastric secretions though the regulation of the secretion was ignored (Joseph *et al*, 2003). Simplification of the human gastric secretion and regulation by Joseph *et al* (2003) also neglected many of the complex cellular events which affect the acid secretion, therefore it was unable to precisely reproduce some of the dynamical behaviours in the *in vivo* studies (Joseph *et al*, 2003).

The study of GI motility, in terms of simulating the gastric electrical control activity via bioelectric and biomagnetic fields (Buist *et al*, 2004), dynamics of small intestinal peristaltic propulsions (Lew *et al*, 1971; Miftahof and Akhmadeev, 2007) and numerical simulation of the bolus propulsion by generation and propagation of electro-mechanical waves (Miftahof and Fedotove, 2005), has been mathematically and/or computationally modelled recently. However, these bioelectric and biomeagnetic fields have been further developed to a modelling framework, such as the Physiome project (Hunter, 2003 and 2004), to integrate the knowledge of computational physiology, anatomy and clinical studies of the human GI system (Pullan *et al*, 2004) thus interlinking the biological structure with multiple levels of spatial organization and multiple time scales (Hunter 2004).

8.2. Mathematical modelling of the rice starch hydrolysis

Despite a large number of computational simulations and mathematical modelling of the human digestive system, mathematical modelling of the hydrolysis of rice starch has not yet been studied extensively. Clinical studies of rice starch hydrolysis with respect to the normal subjects and the patients with diabetes mellitus in order to investigate glycemic index (Araya *et al*, 2002; Frei *et al*, 2003), postprandial glucose and insulin responses (Kim *et al*, 2002; Kim *et al*, 2004), effects to the gastric emptying (McIntyre *et al*, 1997) and nutritional studies focusing on rheology (Ahmed *et al*, 2008), processing (Jaisut *et al*,

2008), molecular structure (Hizukuri *et al*, 1989; Reddy *et al*, 1993; Chen *et al*, 2007) and *in vivo* (Beazell *et al*, 1941) and *in vitro* (Zhang *et al*, 1996; Islas-Hernández *et al*, 2006) digestibility of rice, including both brown and white rice, have been conducted by various researchers but the results were not mathematically modelled. In order to study the kinetics of the enzyme (salivary α -amylase) and acid (HCl), and to compare the results obtained from the MISST and the IPUGS with relevance to the reaction kinetics, a series of control experiments were with different digestive solutions composed of either α -amylase, HCl or both, were performed.

8.2.1. Materials and Methods Used for the Control Experiments

For the control experiments to study the kinetics of the enzyme and acid in details, a similar model to the MISST (shown in Chapter 3, 4 and 6) was used. A 1L glass beaker was used as a reactor tank. $100\pm 1\text{g}$ of short grain white rice (Sun Rice Japanese style Sushi Rice) which was cooked in a conventional rice cooker (Breville Advance Rice Duo (Rice Cooker & Steaming, Model RC19) and 250ml of tap water were placed into the reactor and homogenized (Wise Mix Homogenizer, Daihan Scientific HG-15D) at 800rpm for 15min to breakdown the rice grains into very fine particles ($< 500\mu\text{m}$ in diameter) and therefore resulting a smooth blend of thick rice slurry. This was to accomplish near to equilibrium distribution of rice particles in the feed mixture. The reactor with the feed material was then placed on top of a pre-heated (to $40\pm 1^\circ\text{C}$) hot plate magnetic stirrer (Wise Stir® feed back control digital timer function, Daihan Scientific, MSH-20D) (Figure 8-1) and a digestive solution of interest was added.

Five different digestive solutions were made to investigate the compositional efficacy of hydrolysing the rice starch. Considering the upper gastrointestinal secretions, the constituents responsible for the rice starch hydrolysis are α -amylase from the saliva and HCl from the gastric secretion. Unlike the previous experiments of simulating the closest possible human digestive activities (Chapters 3 – 7), all the reactants were placed in the reactor at once, thus focusing on studying the kinetics of the enzyme and the acid rather than simulating the human conditions. $2.00\pm 0.02\text{g}$ of α -amylase (Grindamyl A5000 α -amylase (Danisco 071314)) in 200ml of deionized water, representing the enzymatic concentration of the saliva in normal state (used in the previous studies, shown in the chapters 3-7) and $4.00\pm 0.02\text{g}$ α -amylase (Grindamyl A5000 α -amylase (Danisco 071314)) in 200ml of deionized water, which is doubled the normal concentration, were used to

study the extent of rice starch hydrolysis in absence of the gastric secretion, and to study the effect of high concentration of α -amylase on the rate of rice starch hydrolysis. 0.15N HCl (diluted with a volumetric flask with 1M HCl (Ajax, AF602394) and deionized water) representing the normal concentration of the HCl in the human gastric juice, and 0.30N HCl, which is doubled the concentration of the normal state, were used to investigate the acidic rice starch hydrolysis. The volume of both of the HCl solutions were calculated by multiplying the rate at normal state, $3.5\text{ml}\cdot\text{min}^{-1}$ with the digestion period of 180min, resulting 630ml. 630ml of 0.15N HCl and 2g of α -amylase in 200ml of deionized water were used together to determine the combined effect of the acidic and the enzymatic effects. These digestive solutions were heated to $37.0\pm 0.5^\circ\text{C}$ to avoid large fluctuation of temperature, which may affect the initial kinetics of the starch hydrolysis.

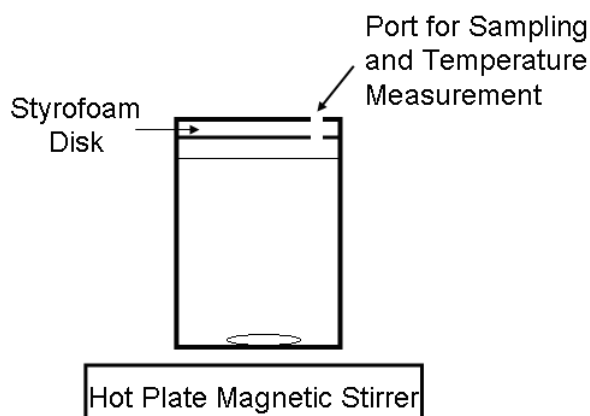


Figure 8-1. Diagram of the apparatus set up for the control experiments

After pouring of the digestive solution into the reactor, the experiment was immediately started with stirring speed of 1000rpm with a magnetic stir bar of 6cm in length and 1cm in diameter. Experiments with stirring speeds of 150rpm and 500rpm have been conducted (refer to Chapter 3), and shown that at 500rpm, the stirring speed was found to be fast enough to well-mix the solutions containing liquid and solid parts. Thus the use of 1000rpm provided a well-mixed condition. The first sample, representing time 0, was taken 30s after placing the digestive solution into the reactor, allowing some time for all the reactants to be mixed and thereby the gradient between the rice slurry and the digestive solution can be avoided. The reactor was then sealed with a styrofoam disk, with the thickness of $2.0\pm 0.1\text{cm}$, to minimize the heat escape through the open top reactor, thereby providing a better temperature control overall. Samples of $100\mu\text{l}$ were withdrawn from the reactor every 10min for 180min of digestion period. The temperature was also

measured every 10min. The withdrawn samples were immediately diluted by a factor of 100 by adding deionized water and placed in an ice water bath (0-2°C). As a control of these experiments, the blended feed mixture of rice and water was also kept at the same conditions. The experiments were conducted in triplicate.

8.2.2. Phenol-Sulfuric Acid Assay

Phenol-Sulfuric acid assay is one of the most widely used analytical methods in measuring neutral sugars in oligosaccharides, proteoglycans, glycoproteins and glycolipids. It is a simple, fast, reliable and sensitive method which has been developed by Dubois *et al*, (1951 and 1956). Rao and Pattabiraman (1989) reported that phenol underwent sulfonation in situ and the phenol-sulfuric acid complex decreased the color intensity for many hexoses and pentoses. Similar results were seen by Masuko *et al* (2005) whom modified the original method by Dubois *et al* by adding concentrated sulfuric acid to the sample followed by phenol. Instead of using microplate proposed by Masuko *et al*, larger volumes were reconstituted following the ratio of sample to conc. sulfuric acid to phenol. The method was used to determine the total concentration of water soluble carbohydrates (Zhang *et al*, 1996), including undigested rice starch, maltose and maltotriose, from the obtained samples.

3ml of concentrated sulfuric acid was added to 1ml of diluted (factor of 100) sample in a test tube followed by vigorous shaking at high speed in a vortex mixer. 600µL of 5% (w/v) phenol was pipetted into the mixed solution and placed in a water bath at 90°C for 10min. The prepared samples were vortexed at high speed for 30s and left at room temperature for 5mins cooling before reading the absorbance via the UV spectrophotometer (Agilent 8453, UV G1103A) at 490nm.

8.2.3. Somogyi-Nelson Method

Somogyi-Nelson method (Somogyi, 1926; Somogyi, 1937, Somogyi, 1945; Nelson, 1944; Wrolstad *et al*, 2005) is an extensively used highly accurate method for determining the amount of reducing sugars (e.g. maltose). Low alkalinity copper reagent and arsenomolybdate reagent were prepared as follows.

12g of sodium potassium tartate and 24g of anhydrous sodium carbonate with 250ml of distilled water were mixed. 4g of copper sulfate pentahydrate and 16g of sodium bicarbonate were added to 200ml of distilled water. 180g of anhydrous sodium sulfate in 500ml of boiling distilled water was separately prepared. Three mixtures were combined and diluted to 1L to make the low alkalinity copper reagent. The arsenomolybdate reagent was made by mixing 25g ammonium molybdate to 450ml of distilled water. 21ml of concentrated sulfuric acid and 25ml of distilled water containing 3g of disodium hydrogen arsenate heptahydrate were added to the ammonium molybdate solution with stirring. The mixture was continuously stirred for 24hrs at 37°C and kept in brown glass stopped bottle until use.

1ml of the diluted (factor of 100) sample and 1ml of the low alkalinity copper reagent were placed in a test tube and vigorously mixed by a vortex mixer at a high speed for 30s. The test tube was placed in a boiling water bath (100°C) for 10mins, and cooled at room temperature for 5mins. 1ml of the arsenomolybdate reagent was then added and the mixture was vortexed at a high speed for 30s. Absorbance at 500nm was read via the UV spectrophotometer (Agilent 8453, UV G1103A). Blanks for the absorbance were prepared by replacing the sample with 1ml distilled water.

Blue color of the low alkalinity copper reagent and green color of the arsenomolybdate reagent gave a greenish blue color in all the samples. The samples which contained less maltose showed a light green solution, but as the concentration of maltose increased, the color of the sample became darker and bluish. As the arseno reagent is extremely toxic and may cause cancer, particular cares were taken to avoid inhalation and contacts at all times.

8.3. Results and Discussion

8.3.1. Phenol-Sulfuric Acid Assay

As shown in the Figure 8-2, the mass of total water soluble carbohydrates (g) from the obtained the samples ranged from 75.2g to 77.8g over the 3hr digestion period for all of the digestive solutions tested. Since only small amounts (100µl per 10min and total of

1.9ml for 180min) of samples were taken, the change of the volume of the reactant mixture seemed negligible over the 3hr digestion period, resulting in negligible changes of the mass of the total carbohydrates over time. Also, the difference among the five different digestive solutions was very small, exhibiting good batch-to-batch controls over the preparation of the feed mixture, the proportion of the carbohydrates in the used rice grains and the overall digestion experiments.

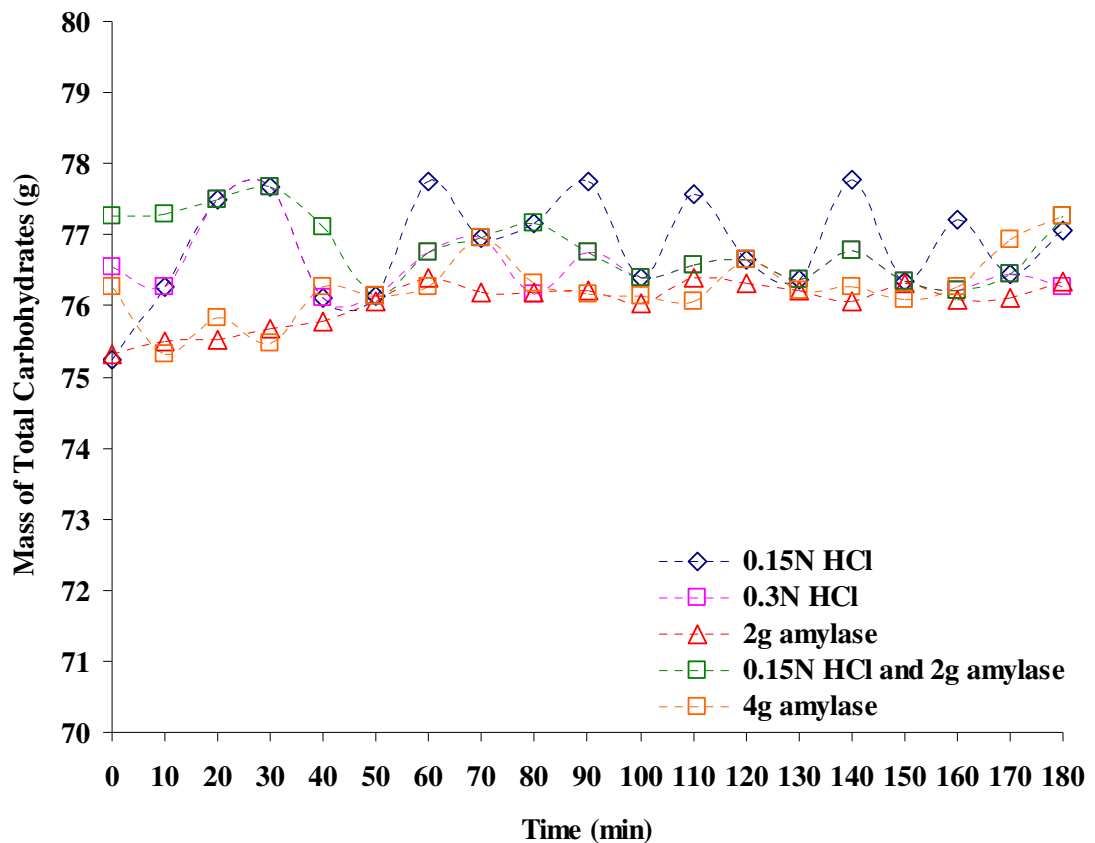


Figure 8-2. A graph showing the mass of total carbohydrates from the obtained chyme samples (g) with respect to time. 5 different conditions of 0.15N HCl, 0.3N HCl, 2g of α -amylase solution, 4g of α -amylase solution and 0.15N HCl with 2g of α -amylase solution are shown.

The average values of the mass of the total carbohydrates over the 3hr digestion period were 76.86 ± 1.26 g for 0.15N HCl, 76.57 ± 0.77 g for 0.30N HCl, 76.04 ± 0.53 g for 2g α -amylase, 76.82 ± 0.76 g for the combined 0.15N HCl and 2g α -amylase, and 76.26 ± 0.97 g for 4g α -amylase. However, the nutrition information displayed on the package showed 78.5g of total carbohydrates per 100g of rice, which is slightly higher than the values obtained via the Phenol-Sulfuric acid assay. Possible loss of the rice slurry may have resulted from the preparation of the feed mixture, where the blade of the homogenizer was surrounded by the rice slurry at the end of the homogenization and the rice slurry

could not be scraped off from the blade completely, causing loss of the feed mixture. Calibration error may also have arisen from the mass balance used. However, a good control of the overall total carbohydrates in the reactor was shown for all experiments.

8.3.2. Somogyi-Nelson Method

The Somogyi-Nelson method was used to analyse the mass of maltose (g) in the reactor which increased almost linearly from near to 0g to 69g as illustrated by the Figure 8-3. Maltose is a reducing sugar which is a by-product released during the conversion of amylopectin to amylose and/or amylose converted to a shorter chain of carbohydrate in the process of starch hydrolysis (Frazier *et al*, 1997). Hence observing the trend of the mass of maltose in the collected sample over the 3hr digestion period facilitates the comparison of the digestive efficiency of the α -amylase, HCl and combined effects.

Initially, all the digestive solutions showed similar values to each other, within the range of 0 to 4g. However, rapid rice starch hydrolyses were seen for α -amylase of both concentrations, with slightly faster release of maltose for the higher concentration (4g of α -amylase) with a gradient of $0.364\text{g}\cdot\text{min}^{-1}$, compared to that of the lower concentration (2g of α -amylase) with a gradient of $0.3547\text{g}\cdot\text{min}^{-1}$. At 180min, the masses of the maltose in the obtained sample were 67.01g and 68.56g for 2g and 4g of α -amylase, respectively. Despite the doubled concentration, the rate of maltose releasing from the rice starch was not doubled that of the lower concentration used. However it can be extrapolated that if the experiments were extended for a longer digestion period with a larger amount of the feed mixture, the trend of the maltose mass over time could be different and it is likely that the higher concentration of the α -amylase used would result in significantly faster hydrolysis compared to that of the lower concentration.

However with HCl, very slow release of maltose was observed with both of the concentrations when compared to that of the enzymatic hydrolysis by the α -amylase. The rates of the maltose release were $0.1524\text{g}\cdot\text{min}^{-1}$ and $0.1396\text{g}\cdot\text{min}^{-1}$ for 0.15N and 0.30N of HCl, respectively, which were very similar to one another. Unexpectedly, the rate of maltose release for the higher concentration of HCl used was slightly lower than the lower HCl concentration. The end values of the mass of maltose were 27.81g and 26.50g for 0.15N and 0.30N HCl, respectively. The combined solution of 0.15N HCl and 2g of α -amylase resulted in a faster rate, $0.1986\text{g}\cdot\text{min}^{-1}$, of maltose release compared to that of the

digestive solutions of HCl, however much slower than that of the digestive solutions of the α -amylase. The final value of the maltose mass for the combined solution was 36.69g, which is nearly half of the final maltose mass of the α -amylase solutions. As the α -amylase and HCl were both poured into the reactor at the same time, the α -amylase, which is non-acidophilic, must have reached lethal level of acidic pH due to the HCl (pH 1.03 ± 0.01), thus the rapid digestibility of the rice starch as demonstrated by the α -amylase solutions could not be seen. However the rice feed mixture showed small buffering effect, increasing the overall pH of the mixture in the reactor to the pH of 1.20. Thus some of the α -amylase may have survived, at least initially, during the experiment.

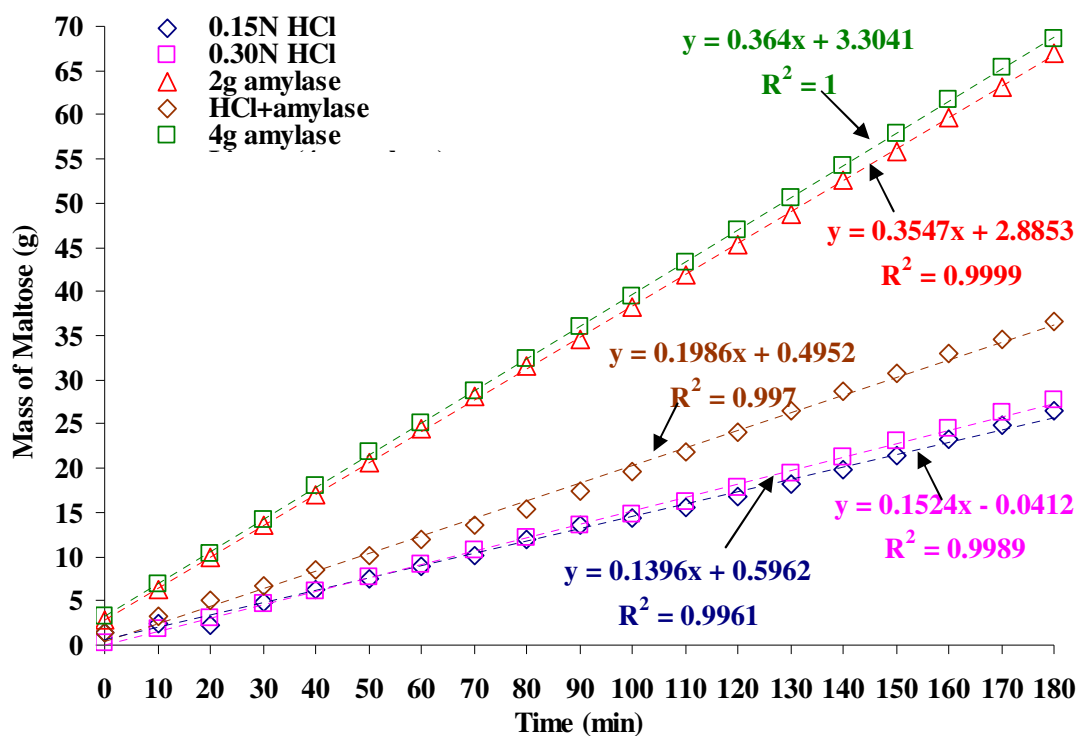


Figure 8-3. A graph showing the mass of maltose (g) of the obtained samples with respect to time, which was analysed by Somogyi-Nelson method. 5 different digestive solutions of 0.15N HCl, 0.3N HCl, 2g of α -amylase, 4g of α -amylase and combined solution of 0.15N HCl and 2g of α -amylase are shown.

The use of the mass of the total carbohydrates (Figure 8-2) and the mass of maltose (Figure 8-3) can be used to calculate the percentage of conversion of the rice starch into maltose (Figure 8-4). Furthermore, the ratio of digested (maltose) to undigested rice starch (Figure 8-5) can be determined, and the fraction of undigested rice starch remaining in the reactor (Figure 8-6) can also be calculated to empirically formulate the rice starch hydrolysis.

Jaisut *et al* (2008) studied the effect of drying temperature and tempering time on starch digestibility of brown fragrant rice which is composed of 12-17wt% of amylose. Instead of the effect of salivary α -amylase, the digestibility of porcine pancreatic α -amylase and HCl-KCl buffer, simulating the gastric digestion of the rice hydrolysis, were observed. 26.3wt%, 25.3wt% and 24.8wt% of the brown rice starch hydrolysis was seen at 30, 60 and 120min of tempering times, respectively, and claimed that these values were lower than the reference starch hydrolysis value of 31wt%. These values correspond well with the findings of the IPUGS as described in previous chapters (chapters 3-7). Jaisut *et al* (2008) also reported that the porcine α -amylase had difficulty to digest the heat-treated rice starch, where 6% of decrease in the maximum brown rice hydrolysis was evident when the tempering time was increased from 30 to 120min. The results from the Jaisut *et al* (2008) seemed similar the results obtained from the current kinetics experiments (Figure 8-4), where the hydrolysis rates of 34.74wt%, 36.09wt% and 47.48wt% were observed from the use of digestive solutions of 0.30N HCl, 0.15N HCl and the combined solution of 0.15N HCl and 2g α -amylase.

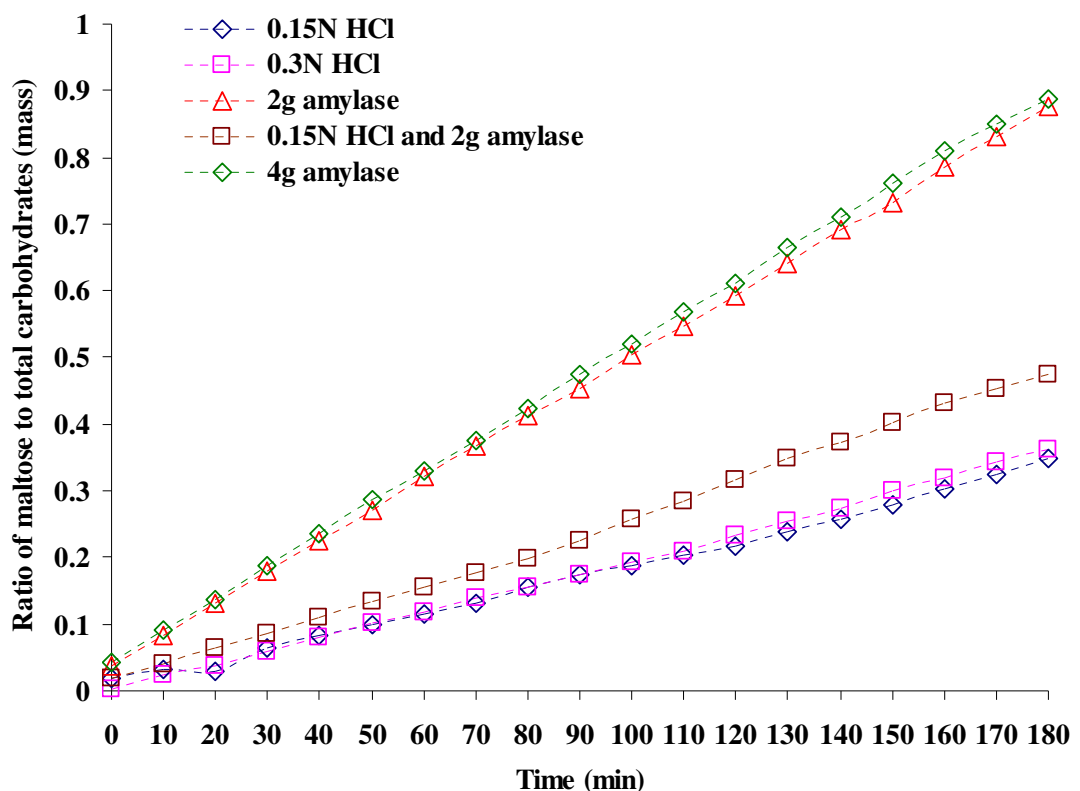


Figure 8-4. A plot of the ratio of the mass of maltose (g) to the mass of total carbohydrates (g) with respect to time (min).

The higher rates of hydrolysis were inevitable as the amylose content of the white short grain rice (Koshihikari) is higher, 19wt%, than that of the brown rice. Also, the absence of salivary α -amylase in Jaisut *et al* (2008) may have contributed to a lower hydrolysis rate. Rapid hydrolyses of rice starch were seen with both of α -amylase concentrations, 87.79wt% and 88.73wt% for 2g and 4g of α -amylase, respectively. The rapid hydrolyses must have resulted from having all the reactants placed all at once. The pH of the rice mixture was 5.40 ± 0.05 throughout the 3hr digestion period, showing a good buffering capacity. However with the results of the IPUGS, where new secretions of salivary α -amylase (during the ingestion period) and acidic gastric juice were constantly supplied and chyme samples of much greater volume (around 65ml) were continuously removed, a dynamic state of digestion process was simulated, thereby exposing of the α -amylase to the acidic HCl in the gastric juice. This would have killed many α -amylase enzymes, especially after the ingestion period where a gradual reduction of pH profile was evident in all types of studies. Hence the rice hydrolysis rate was much lower in the IPUGS than the enzymatic kinetic studies shown in here. However from the obtained results, it would seem that the efficiency in rice hydrolysis was much greater for the α -amylase than that of the HCl.

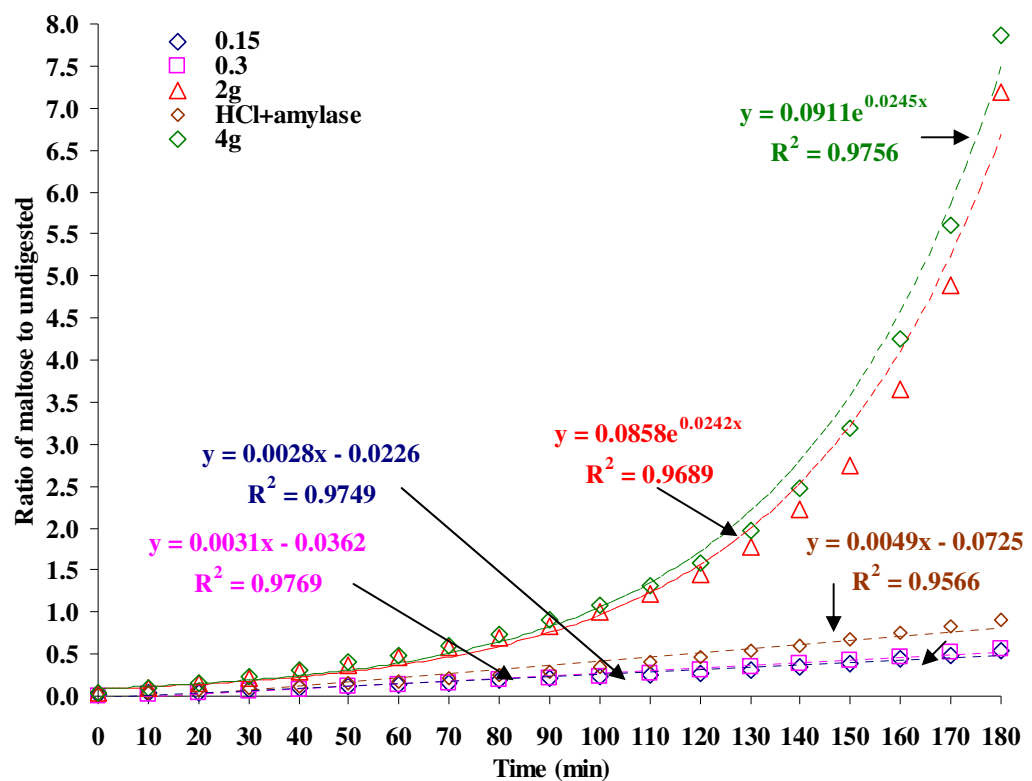


Figure 8-5. A graph illustrating the ratio of the mass of maltose (g) to the mass of undigested starch (g) with respect to time (min). Keys on the graph refer to 0.15N HCl, 0.30N HCl, 2g of α -amylase, 0.15N HCl + 2 g of α -amylase, and 4g of α -amylase.

The ratio of the mass of maltose (digested) to the mass of the undigested rice starch from the obtained samples is illustrated on the Figure 8-5. The mass of undigested starch was calculated by subtracting the mass of maltose (digested) from the mass of the total water soluble carbohydrates. A very small difference between the use of HCl and the combined digestive solution including both HCl and α -amylase was seen. The ratio of maltose to undigested starch increased with respect to time for all the digestive solutions tested, which demonstrated that the digestive solutions were effective to some extent in the rice hydrolysis process.

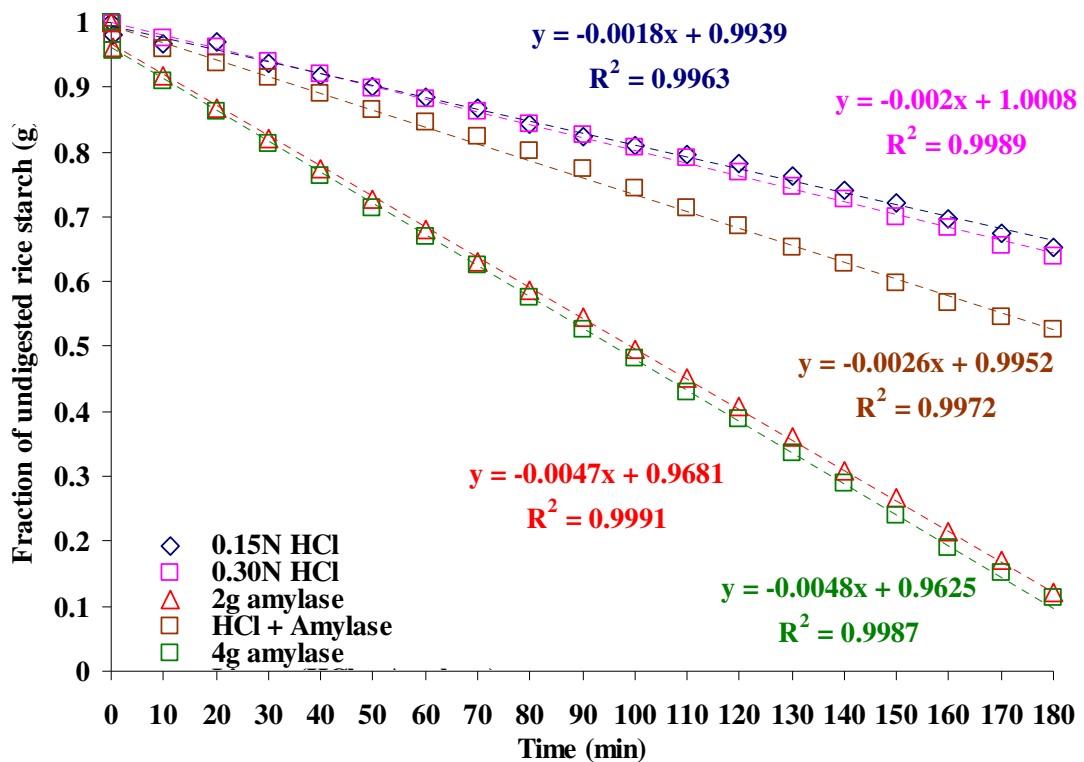


Figure 8-6. A plot of the fractional mass of the undigested rice starch (g) over time.

With the presence of HCl, the ratio showed linear function with respect to time ($R^2 \geq 0.9566$), whereas for the use of α -amylase, the increase in the ratio showed exponential relationship ($R^2 \geq 0.9689$) with time, showing a very high amount of maltose present in the reactor towards the end of the digestion period. Alternatively, the fraction of the undigested rice starch remaining in the reactor (Figure 8-6) was calculated as many of the mathematical equations regarding the gastric emptying showed the fraction of the undigested material remaining in the stomach (Elashoff *et al*, 1982). The five digestive solutions tested all showed negative linear relationship, with initial content of 1:1 ratio of the mass of undigested starch to the mass of total carbohydrates. The fastest decrease of the undigested rice starch in the reactor was shown by the α -amylase solutions once again.

The rate of decrease was slightly faster for the 4g α -amylase ($0.0048\text{g}\cdot\text{min}^{-1}$) compared to that of the 2g α -amylase ($0.0047\text{g}\cdot\text{min}^{-1}$). The combined solution of the HCl and α -amylase was laid between the HCl and α -amylase, with $0.0026\text{g}\cdot\text{min}^{-1}$ of undigested starch converting to maltose. Much lower values of the rate of decrease in the fraction of the undigested rice starch were seen by both concentrations of HCl, $0.002\text{g}\cdot\text{min}^{-1}$ and $0.0018\text{g}\cdot\text{min}^{-1}$ of 0.15N HCl and 0.30N HCl, respectively.

From Figure 8-3, it can be seen that the rate of increase in maltose concentration fits well with linear function, which infers zero-order kinetics for both α -amylase and HCl.

$$\text{i.e. } \frac{d C_{\text{maltose}}}{dt} = k_{\text{maltose}} \cdot C_{\text{maltose}} \quad (1)$$

Therefore,

$$C_{\text{maltose}, t=t} - C_{\text{maltose}, t=0} = k_{\text{maltose}} (t-0) \quad (2)$$

$$k_{\text{maltose}} = f(\alpha\text{-amylase, HCl}) \quad (3)$$

where C_{maltose} refers to the concentration of maltose ($\text{g}\cdot\text{L}^{-1}$) at given times, t (min) and k_{maltose} ($\text{g}\cdot\text{min}^{-1}$) refers to the rate constant of the maltose mass (k_{maltose}) ($\text{g}\cdot\text{min}^{-1}$).

Table 8-1. A table summarizing the rate of change in maltose mass with respect to the digestive conditions

Concentration of α -amylase $C_{\text{maltose}} (\text{g}\cdot\text{L}^{-1})$	Rate of change in maltose mass $k_{\text{maltose}} (\text{g}\cdot\text{min}^{-1})$	Concentration of HCl $C_{\text{maltose}}(\text{N})$	Rate of change in maltose mass $k_{\text{maltose}} (\text{g}\cdot\text{min}^{-1})$
0	0.0073	0	0.0073
10	0.3547	0.15	0.1396
20	0.3640	0.30	0.1524

Note: The values used for the k_{maltose} at time 0 in Table 8-1 refers to the condition of 100g of cooked rice in 250ml of tap water, at 37°C and 1000rpm stirring.

Between the initial and the final volume of the reactants (rice meal and the corresponding amounts of α -amylase and HCl), there has been a change of less than 2ml, which is negligible. Thus the trend of changes in the concentrations ($\text{g}\cdot\text{L}^{-1}$) and the masses (g) of

maltose with respect to time is exactly the same to one another. As the term, concentration, is more widely used in mathematical formulae, the above equations were written in regards to the concentration, rather than mass. However, provided that the volume of the fluids in the reactor does not change significantly, the above equations can be applied. Using the values of the rate of constant of the mass of maltose (k_{maltose}) in the Figure 8-3, the effect of α -amylase and HCl to rice starch hydrolysis can be investigated further.

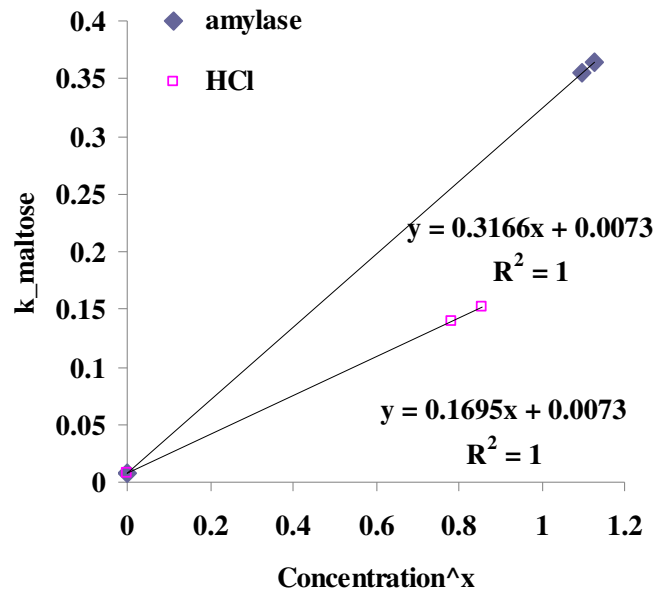


Figure 8-7. A plot of the concentrations of HCl (N) and amylase (g.L^{-1}) raised to the powers of 0.13 and 0.04, respectively, against the rate constant of maltose (k_{maltose}), respectively.

Plotting of the experimental data of C_{maltose} and k_{maltose} showed that power function fitted well (Figure 8-7). Using the equation derived from the gradient of the graph, C_{maltose} against k_{maltose} , the following equations can be deduced.

For α -amylase,

$$k_{\text{maltose}} = k_{0\text{maltose}} + 0.3166 \cdot C_{\text{amylase}}^{0.04} \quad (4)$$

For HCl,

$$k_{\text{maltose}} = k_{0\text{maltose}} + 0.1695 \cdot C_{\text{HCl}}^{0.13} \quad (5)$$

where

$$k_{\text{maltose}} = c \cdot f(\alpha\text{-amylase and HCl}) \quad (6)$$

Therefore when combined,

$$k_{\text{maltose}} = 0.0073 + 0.1695 \cdot C_{\text{HCl}}^{0.13} + 0.3166 \cdot (1 - 1.1705 \cdot C_{\text{HCl}}) \cdot C_{\text{amylase}}^{0.04} \quad (7)$$

By plotting of the experimental data and the mathematical data generated from the equations 4 and 5 in Figures 8-8 and 8-9, it would seemed that a rate-limiting step is involved in the kinetics of amylase and HCl. As the reactants, amylase and HCl, were all placed inside the reactor at the beginning of the experiments without continuously replenishing the used reactants, it reflected the rate-limiting step. However in terms of the values of the k_{maltose} and concentrations of amylase and HCl, the experimental and the mathematical data matched well with one another, except that only 3 values were provided from the experiments. Provided that more k_{maltose} values are generated from the experiments with various concentrations of amylase and HCl, the relevance of the equations, 4, 5 and 7, can be further justified. A more comprehensible analysis on the effect of the concentrations of the amylase and HCl on the rice starch hydrolysis is provided in Figure 8-10.

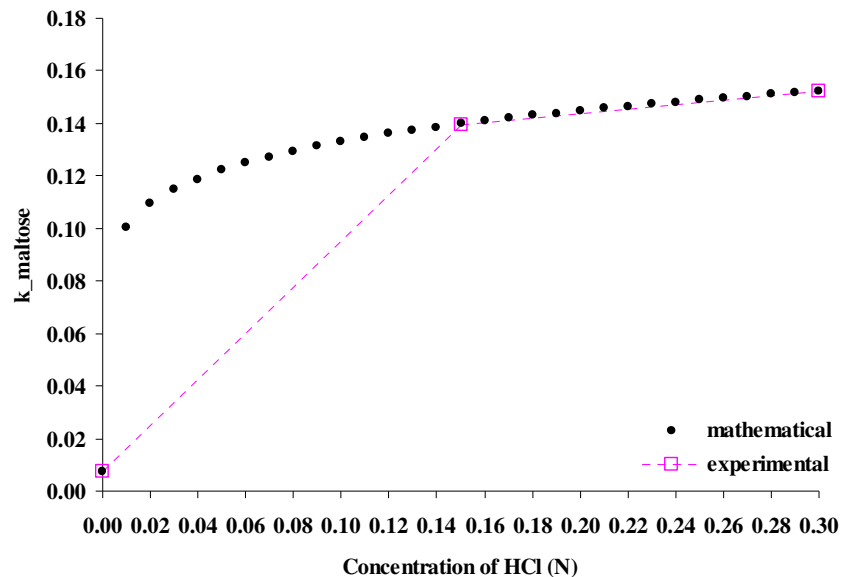


Figure 8-8. A plot of the rate constant of HCl (k_{maltose}) against the concentration of HCl (N). Data from experiments are plotted with empty pink dots, whereas the data calculated from the equation 4 are plotted with filled black dots.

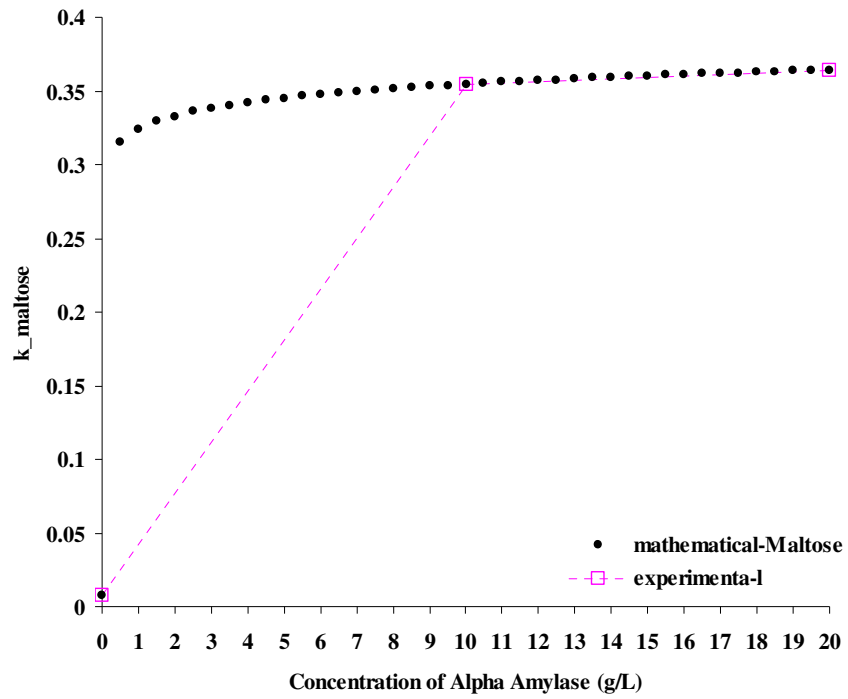


Figure 8-9. A plot of the rate constant of HCl (k_{maltose}) against the concentration of amylase ($\text{g}\cdot\text{L}^{-1}$). Data from experiments are plotted with empty pink dots, whereas the data calculated from the equation 5 are plotted with filled black dots.

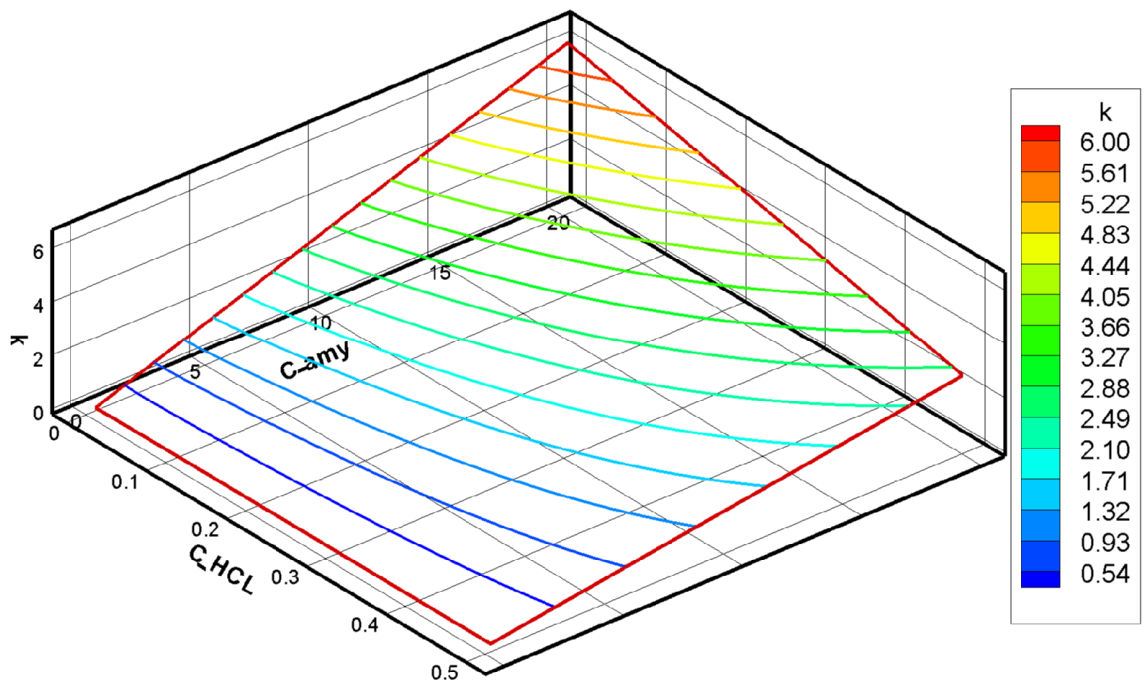


Figure 8-10. A 3-D plot of the k_{maltose} with respect to the concentrations of amylase and HCl, generated by Tecplot.

From the above figures, the following stoichiometric equations can be derived.

100g of rice grains → 78.5g total carbohydrates + 15.0g water + 5.9g proteins + up to 1g of fats and dietary fibres.

78.5g total carbohydrates → 78.5g starch → 14.9g amylose + 63.6g amylopectin

Condition 1. Use of 0.15N HCl with magnetic stirring of 1000rpm at 37°C

78.5g starch $\xrightarrow{1\text{hr digestion}}$ 9.2g maltose + 69.3g undigested starch

78.5g starch $\xrightarrow{90\text{min digestion}}$ 13.5g maltose + 65.0g undigested starch

78.5g starch $\xrightarrow{2\text{hr digestion}}$ 17.8g maltose + 60.7g undigested starch

78.5g starch $\xrightarrow{3\text{hr digestion}}$ 27.8g maltose + 50.7g undigested starch
(Equivalent to 35.4% of hydrolysis of the rice starch to maltose)

Condition 2. Use of 0.15N HCl and 10mg.mL⁻¹ α-amylase solution with magnetic stirring of 1000rpm at 37°C

78.5g starch $\xrightarrow{1\text{hr digestion}}$ 11.9g maltose + 66.6g undigested starch

78.5g starch $\xrightarrow{90\text{min digestion}}$ 17.4g maltose + 61.1g undigested starch

78.5g starch $\xrightarrow{2\text{hr digestion}}$ 24.2g maltose + 54.3g undigested starch

78.5g starch $\xrightarrow{3\text{hr digestion}}$ 36.7g maltose + 41.8g undigested starch
(Equivalent to 46.8% of hydrolysis of the rice starch to maltose)

Condition 3. Use of 10mg.mL⁻¹ α-amylase solution with magnetic stirring of 1000rpm at 37°C

78.5g starch $\xrightarrow{1\text{hr digestion}}$ 24.5g maltose + 54.0g undigested starch

78.5g starch $\xrightarrow{90\text{min digestion}}$ 34.6g maltose + 43.9g undigested starch

78.5g starch $\xrightarrow{\text{2hr digestion}}$ 45.3g maltose + 33.2g undigested starch

78.5g starch $\xrightarrow{\text{3hr digestion}}$ 67.0g maltose + 11.5g undigested starch

(Equivalent to 85.4% of hydrolysis of the rice starch to maltose)

*note that the values of the percentage of rice starch hydrolysis shown in brackets are slightly lower than the values mentioned in the text due to the small amount of loss (up to 3g maximum) of the rice slurry during the process of homogenization as mentioned above, creating $\pm 1.9\text{wt}\%$ error.

8.4. Conclusions

The mathematical model/equations outlined in this chapter would be useful in evaluating the influence of various parameters on the digestion of cooked rice. This model may have an important role in food processing and pharmaceutical preparations and can be used for preliminary testing of rice products and educational purposes. The obtained results of the kinetics of the salivary α -amylase and HCl shown can be further developed using complicated mathematical modelling approaches, such as MatLab or FlexPDE. Various food materials should be tested via the IPUGS and also by the outlined kinetics experiments, thus more parameters can be added to provide more accurate and detailed insights into the *in vitro* digestion modelling.

8.5. References

- Araya, H., Contreras, P., Alvina, M., Vera, G., Pak, N. (2002). A comparison between an *in vitro* method to determine carbohydrate digestion rate and the glycemic response in young men. *Eur. J. Clin. Nutri.*, 56, 735-739
- Ballyk, M., Smith, H. (1999) A model of microbial growth in a plug flow reactor with wall attachment. *Mathematical Biosciences*, 158, 95-126
- Ballyk, M. M., Jones, D.A., Smith, H.L. (2001) Microbial competition in reactors with wall attachment: a mathematical comparison of chemostat and plug flow models. *Microbial Ecology*, 41, 210-221
- Beazell, J. M. (1941) A reexamination of the role of the stomach in the digestion of carbohydrate and protein. *Am J Physiol* 132, 42-50
- Blanquet, S., Meunier, J.P., Minekus, M., Marol-Bonnin, S., Alric, M. (2003) Recombinant *Saccharomyces cerevisiae* expressing P450 in artificial digestive systems: a model for biotransformation in the human digestive environment. *Applied and Environmental Microbiology*, 69(5), 2884-2892

- Buist, M. L., Cheng, L. K., Yassi, R., Bradshaw, L. A., Richards, W. O., Pullan, A. J. (2004) An anatomical model of the gastric system for producing bioelectric and biomagnetic fields. *Physiol. Meas.*, 25, 849-861
- Chen, M. H., Bergman, C. (2007) Method for determining the amylose content, molecular weights, and weight- and molar-based distributions of degree of polymerization of amylose and fine-structure of amylopectin. *Carbohydrate Polymers*, 69, 562-578
- De Beus, A. M. Fabry, T. L., Lacker, H. M. (1993) A gastric acid secretion model. *Biophys. J.*, 65, 362-378
- Dubois, M., Gilles, K., Hamilton, J. K., Rebers, P. A., Smith, F. (1951). A colorimetric method for the determination of sugars. *Nature*, 168, 167
- Dubois, M., Gilles, K., Hamilton, J. K., Rebers, P. A., Smith, F. (1956). Colorimetric method for the determination of sugars and related substances, *Anal. Chem.*, 28, 350-356
- Elashoff, J. D., Reedy, T. J., Meyer, J. H. (1982). Analysis of gastric emptying data. *Gastroenterology*, 83, 1306-1312
- Firmer, S.J., Cutler, D.J. (1988) Simulation of gastrointestinal drug absorption I. Longitudinal transport in the small intestine. *International Journal of Pharmaceutics*, 48, 231-246
- Frazier, P. J., Richmond, P., Donald, A. M. (1997). *Starch: Structure and Functionality*. The Royal Society of Chemistry.
- Frei, M., Siddhuraju, P., Becker, K. (2003) Studies on the in vitro starch digestibility and the glycemic index of six different indigenous rice cultivars from the Philippines. *Food Chemistry*, 83, 395-402
- Hizukuri, S. (1986) Polymodal distribution of the chain lengths of amylopectins, and its significance. *Carbohydr. Res.*, 147 (2), 342-347
- Hunter, P. J. (2004) The IUPS physiome project: a frame work for computational physiology. *Progress in Biophysics & Molecular Biology*, 85, 551-569
- Hunter, P. J., Borg, T. K. (2003) Integration from proteins to organs: the physiome project. *Nature Reviews, Molecular Cell Biology*, 4, 237-243
- Islas-Hernandez, J. J., Rendon-Villalobos, R. R., Agama-Acevedo, E., Gutierrez-Meraz, F., Tovar, J., Arambula-Villa, G., Bello-Perez, L. A. (2006) In vitro digestion rate and resistant starch content of tortillas stored at two different temperatures. *LWT*, 39, 947-951
- Jaisut, D., Prachayawarakorn, S., Varayanond, W., Tungtrakul, P., Soponronnarit, S. (2008) Effects of drying temperature and tempering time on starch digestibility of brown fragrant rice. *J. Food Engineering*, 86, 251-258
- Joseph, I. M. P., Zavros, Y., Merchant, J. L., Kirschner, D. (2003) A model for integrative study of human gastric acid secretion. *J. Appl. Physiol.*, 94, 1602-1618
- Kim, J. I., Kong, B. W., Jung, S. H., Park, S. J., Kwon, T. W., Kim, J. C. (2002) Postprandial glucose and insulin response to processed rice products in normal subjects. *Nutraceuticals & Food*, 7, 174-178
- Kim, J. C., Kim, J. I., Kong, B. W., Kang, M. J., Kim, M. J., Cha, I. J. (2004) Influence of the physical form of processed rice products on the enzymatic hydrolysis of rice starch in vitro and on the postprandial glucose and insulin response in patients with Type 2 Diabetes Mellitus. *Biosci. Biotechnol. Biochem.*, 68 (9), 1831-1836
- Lew, H. S. (1971) Peristaltic carrying and mixing of chyme in the small intestine (an analysis of a mathematical model of peristalsis of the small intestine). *J. Biomechanics*, 4, 297-315
- Licko, V., Ekblad, E. B. (1992) What dual-action agents reveal about acid secretion: a combined experimental and modeling analysis. *Biochim. Biophys. Acta.*, 1137, 19-28
- Logan, J. D., Joern, A., Wolesensky, W. (2003) Chemical reactor models of optimal digestion efficiency with constant foraging costs. *Ecological Modelling*, 168, 25-38
- Marteau, P., Minekus, M., Havenaar, R., Huis in't Veld, J.H.J. (1997) Survival of Lactic Acid Bacteria in a dynamic model of the stomach and small intestine: validation and the effects of bile. *J. Dairy Science*, 80, 1031-1037
- Masuko, T., Minami, A., Iwasaki, N., Majima, T., Nishimura, S-I., Lee, Y. C. (2005) Carbohydrate analysis by a phenol-sulfuric acid method in microplate format. *Analytical Biochemistry*, 339, 69-72
- McIntyre, A., Vincent, R. M., Perkins, A. C., Spiller, R. C. (1997). Effect of bran, ispaghula, and inert plastic particles on gastric emptying and small bowel transit in humans: the role of physical factors. *Gut*, 40, 223-227

- Meier, J. J., Nauck, M. A., Pott, A., Heinze, K., Goetze, O., Bulut, K., Schmidt, W. E., Gallwitz, B., Holst, J. J. (2006) Glucagon-like peptide 2 stimulates glucagon secretion, enhances lipid absorption and inhibits gastric acid secretion in humans. *Gastroenterology*, 130, 44-54
- Miftahof, R., Fedotov, E. (2005) Intestinal propulsion of a solid non-deformable bolus. *J. Theoretical Biology*, 235, 57-70
- Miftahof, R., Akhmadeev, N. (2007) Dynamics of intestinal propulsion. *J. Theoretical Biology*, 246, 377-393
- Minekus, M., Marteau, P., Havenaar, R., Huis in't Veld, J. H. J. (1995). A multicompartamental dynamic computer-controlled model simulating the stomach and small intestine. *Alternatives to Laboratory Animals*, 23, 197-209
- Nelson, N. (1944) A photometric adaption of the Somogyi method for the determination of glucose. *J. Biol. Chem.*, 153, 375-380
- Norinder, U., Österberg, T., Artursson, P. (1999) Theoretical calculation and prediction of intestinal absorption of drugs in humans using MolSurf parametrization and PLS statistics. *Euro. J. Pharma. Sci.*, 8, 49-56
- Norris, D. A., Leesman, G. D., Sinko, P. J., Grass, G. M. (2000) Development of predictive pharmacokinetic simulation models for drug discovery. *J. Control Release*, 65, 55-62
- Pal, A., Bresseur, J. G., Abrahamsson, B. (2007) A stomach road or "Magenstrasse" for gastric emptying. *J. Biomechanics*, 40, 1202-1210
- Pullan, A., Cheng, L., Yassi, R., Buist, M. (2004) Modelling gastrointestinal bioelectric activity. *Progres in Biophysics & Molecular Biology*, 85, 523-550
- Rao, P., Pattabiraman, T. N. (1989). Reevaluation of the phenol-sulfuric acid reaction for the estimation of hexoses and pentoses. *Anal. Biochem.*, 181, 18-22
- Reddy, K., Zakiuddin, S., Bhattacharya, K. R. (1993) The fine structure of rice-starch amylopectin and its relation to the texture of cooked rice. *Carbohydrate Polymers*, 22, 267-275
- Schmitt, W., Willmann, S. (2004) Physiology-based pharmacokinetic modeling: ready to be used. *Drug Discovery Today: Technologies Drug Development*, 1 (4), 449-456
- Somogyi, M. (1926) Notes on sugars determination. *J. Biol. Chem.*, 79, 599-613
- Somogyi, M. (1937) A reagent for the copper iodometric determination of vary small amounts of sugar. *J. Biol. Chem.*, 117, 771-776
- Somogyi, M. (1945) A new reagent for the determination of sugars. *J. Biol. Chem.*, 160, 61- 68
- Spratt, P., Nicolella, C., Pyle, D.L. (2005) An engineering model of the human colon. *Trans IChemE, Part C, Food and Bioproducts Processing*, 83 (C2), 147-157
- Stoll, B. R., Batycky, R. P., Leipold, H. R., Milstein, S., Edwards, D. A. (2000) A theory of molecular absorption from the small intestine. *Chemical Engineering Science*, 55, 473-489
- Wilkinson, M. H. F. (2002) Model intestinal microflora in computer simulation: a simulation and modeling package for host-microflora interactions. *IEEE Transactions on Biomedical Engineering*, 49, 10, 1077-1085
- Willmann, S., Schmitt, W., Keldenich, J., Dressman, J. B. (2003) A physiologic model for simulating gastrointestinal flow and drug absorption in rats. *Pharm. Res.*, 20, 1766-1771
- Willmann, S., Schmitt, W., Keldenich, J., Lippert, J., Dressman, J. B. (2004) A physiological model for the estimation of fraction dose absorbed in humans. *J. Med. Chem.*, 47 (16), 4022-4031
- Wrolstad, R. E., Acree, T. E., Decker, E. A., Penner, M. H., Reid, D. S., Schwartz, S. J., Schoemaker, C. F., Smith, D. M., Sporns, P. (2005) *Handbook of food analytical chemistry. Water, proteins, enzymes, lipids and carbohydrates.* Hoboken, N. J. Wiley.
- Wu, G. (1998) Estimation of drug excretion rate from blood into the gut using a three-compartment closed model. *Pharmacological Research*, 37 (2), 157-164
- Yu, L. X., Amidon, G. L. (1998) Saturable small intestinal drug absorption in humans: modeling and interpretation of cefatrizine data. *Euro. J. Pharma. Biopharma.*, 45, 199-203
- Yu, L. X., Amidon, G. L. (1999) Compartmental absorption and transit model for estimating oral absorption. *Int. J. Pharm.*, 186, 119-125
- Zhang, Q., Abe, T., Takahashi, T., Sasahara, Y. (1996) Variations in in vitro starch digestion of glutinous rice flour. *J. Agric. Food Chem.*, 44, 2672-2674

<http://www.acslextreme.com>

<http://www.berkeleymadonna.com>

<http://www.cyprotex.com>

<http://www.lionbioscience.com>

<http://www.pk-sim.com>
<http://www.simulationplus.com>
<http://www/simcyp.com>

Concluding Remarks and Future Works

The IPUGS was designed to simulate the conditions of the upper GI organs of the normal human subjects as closely as possible in terms of motility, secretion and geometrical properties, in order to study the behaviour of the ingested materials during digestion. Compared to the MISST which represents a typical *in vitro* digestion system in the literature, the IPUGS performed with different patterns of rice starch hydrolysis and achieved improvements in mimicking of the dynamic human conditions as discussed in Chapters 3, 4 and 6. Clinical applications of the IPUGS with the study of the common gastric disorders such as gastroparesis and dumping syndrome regarding different rates of gastric motility (Chapter 5) and hypochlorhydria and Zollinger-Ellison syndrome regarding different rates and amounts of gastric secretions (Chapter 7), have highlighted the key use of the IPUGS as a clinical tool. Yet, the studies of such disorders have never been conducted via *in vitro* digestion models in the literature. Thus the IPUGS should further be developed in studying various disorders of not only humans but in animals as well, to be used as a clinical tool with or without *in vivo* studies. The pattern of rice starch hydrolysis has been simplified for mathematical modelling (Chapter 8), which can be useful in evaluating the influence of various parameters on the digestion. The IPUGS may have an important role in food processing and pharmaceutical preparations and can be used for preliminary testing of food products and educational purposes.

Future works with various food materials/meals should be conducted as this would provide more accurate and detailed insights to the effect of having soft, geometrical resemblance to humans, hand squeezable walls with a unique mechanism of delivering secretions and efficiency of the non-human enzyme replacements used in the IPUGS. Pharmaceutical and probiotic products should also be tested to further validate and apply the IPUGS as a clinical and microecological tool.

The IPUGS should be automated to ease labor. Also, the recorded data should be mathematically modeled with programs such as MatLab or Flex PDE to implicate a better understanding of the overall digestion process. Despite the state-of-art appearance of the IPGUS, the manufacturing process was quite time-consuming with a lot of efforts, thus the first aspect to look at would be the more uniform production of the *in vitro* model devices and the incorporation of the robotic actions to ease labor and time.

In future, more complicated mouth compartment and consequently, the small intestinal compartments should be added, thus the oral texture, bioavailability and absorption of nutrients and drug compounds can be studied.